CHEMICAL REVIEWS

pubs.acs.org/CR

Review

Pulmonary Surfactant: A Mighty Thin Film

Fred Possmayer,* Yi Y. Zuo,* Ruud A. W. Veldhuizen,* and Nils O. Petersen*

Cite This: *Chem. Rev.* 2023, 123, 13209−13290

Read Online

ACCESS | Metrics & More | Article Recommendations

ABSTRACT: Pulmonary surfactant is a critical component of lung function in healthy individuals. It functions in part by lowering surface tension in the alveoli, thereby allowing for breathing with minimal effort. The prevailing thinking is that low surface tension is attained by a compression-driven squeeze-out of unsaturated phospholipids during exhalation, forming a film enriched in saturated phospholipids that achieves surface tensions close to zero. A thorough review of past and recent literature suggests that the compression-driven squeeze-out mechanism may be erroneous. Here, we posit that a surfactant film enriched in saturated lipids is formed shortly after birth by an adsorption-driven sorting process and that its composition does not change during normal breathing. We provide biophysical evidence for the rapid formation of an enriched film at high surfactant concentrations, facilitated by adsorption structures containing hydrophobic surfactant proteins. We examine biophysical evidence for and against the compression-driven squeeze-out mechanism and propose a new model for surfactant function. The proposed model is tested against existing physiological and pathophysiological evidence in neonatal and adult lungs, leading to ideas for biophysical research, that should be addressed to establish the physiological relevance of this new perspective on the function of the mighty thin film that surfactant provides.

CONTENTS

Received: March 12, 2023
Published: October 20, 2023

https://doi.org/10.1021/acs.chemrev.3c00146
Chem. Rev. 2023, 123, 13209−13290

1. INTRODUCTION

Breathing with relatively small muscular efforts, as observed in mammals, is dependent on a thin surface tension (γ) reducing film of lipids and proteins, that lines the aqueous layer covering the alveolar surface of the lung. The existence of this material, pulmonary surfactant, was first postulated by von Neergaard in the 1920s on the basis of differences in pulmonary behavior with air- and water-filled lungs.[1] However, it was not until the 1950s that definitive experimental evidence was obtained by Pattle and Clements for a material that reduced γ in mammalian lungs, including those of humans, to the extremely low near-zero values necessary for lung function.[2−5] It was soon recognized that pulmonary surfactant contained mostly phospholipids (PLs) and that disaturated dipalmitoylphosphatidylcholine (DPPC, 16:0/16:0-PC), was the dominant constituent.[6] Nevertheless, it was not until the 1980s that the full chemical composition of pulmonary surfactant, particularly in terms of the surfactant protein constituents, was determined.[7−11]

Although some variability exists among species, surfactant isolated from lung lavage material generally consists of ∼80%

https://doi.org/10.1021/acs.chemrev.3c00146
Chem. Rev. 2023, 123, 13209−13290

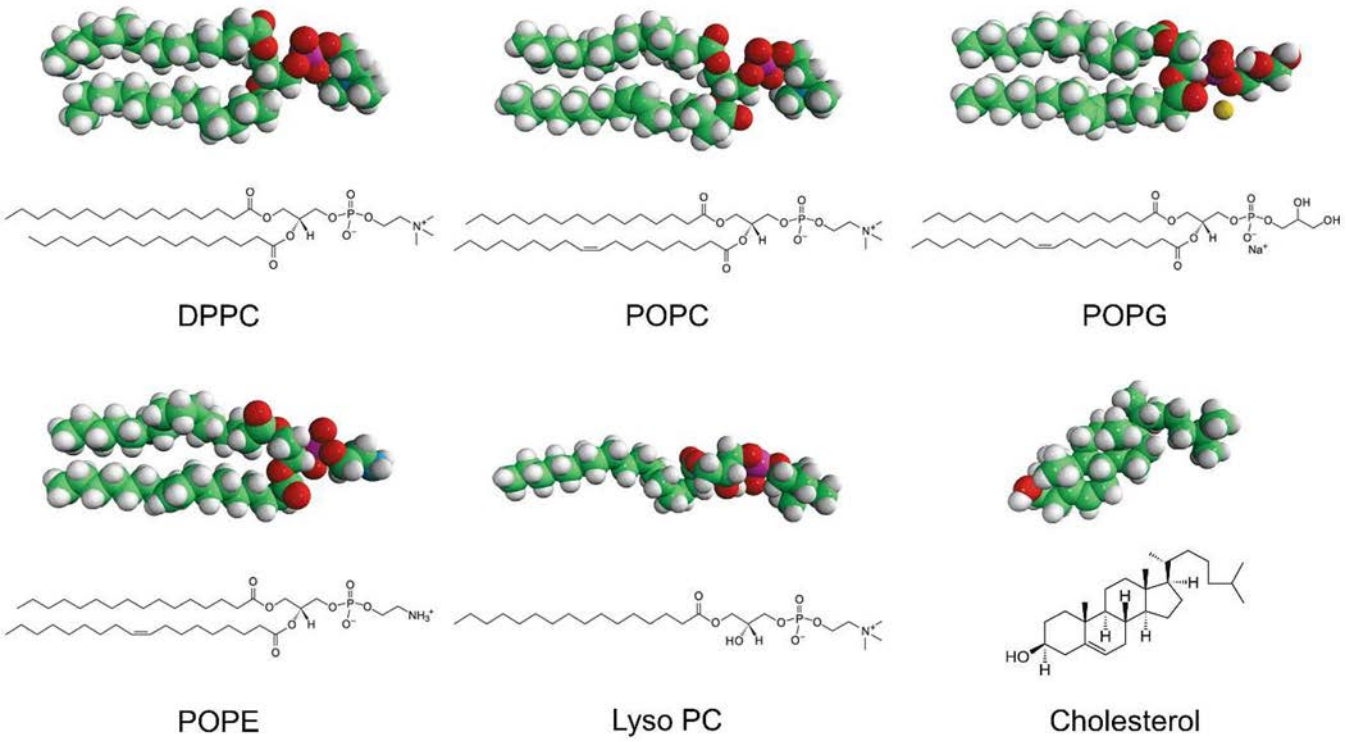

Figure 1. Chemical structures and space-filling models of the most common lipid molecules in pulmonary surfactants. Chemical structures were adapted from Avanti Polar Lipids (https://avantilipids.com/).

PLs, 5−10% neutral lipids (mainly cholesterol), and ∼10% surfactant-associated proteins by weight. The major PL components are phosphatidylcholine (PC) ∼80%, approximately half of which are disaturated, and acidic PL ∼15%, such as phosphatidylglycerol (PG), phosphatidylinositol (PI), and *bis*(monoacylglyero)phosphate, as well as small amounts of phosphatidylethanolamine (PE), sphingomyelin (SM), and lyso-phosphatidylcholine (LPC).[12−15] Small amounts of plasmalogens are also present. Figure 1 shows the structure of some of the most important lipid components of natural surfactant.

The protein components of surfactant consist of surfactant proteins A and D (SP-A and SP-D), which are calcium-dependent, oligomeric collectins with important roles in the innate immune system,[16−22] and surfactant proteins B and C (SP-B and SP-C), which are low molecular weight hydrophobic proteins essential for surfactant's γ reducing functions.[13,20,23−26] Figure 2 shows the schematics of these proteins.

The unusual chemical nature of pulmonary surfactant, its unique physiological functions, and its clinical significance have attracted considerable scientific interest. Hence, it appears somewhat remarkable that a consensus regarding the mechanisms by which pulmonary surfactant stabilizes our alveoli has still not been achieved. It has long been suggested (but not always accepted) that the ability of pulmonary surfactant to stabilize our terminal alveoli depends on a surface lipid monolayer, highly enriched in DPPC. It has further been argued that this DPPC enrichment is achieved by a compression-driven squeeze-out of the other less stable surfactant lipids from the film, during exhalation in normal breathing.

Recent technical advances in pulmonary surfactant research have enabled new approaches to test and extend previous concepts to the molecular level. In particular, the recent development of the constrained drop surfactometer (CDS)[29−31] and the application of fluorescence microscopy,[32] X-ray diffraction techniques,[33] and molecular dynamic simulation approaches[34−37] have provided novel insights into the biophysical mechanisms of surfactant function. Data recently obtained by these, and other new procedures, provide evidence which supports the following updated model of surfactant function:

- Pulmonary surfactant adsorbs rapidly to the air−water surface to *form a monolayer highly enriched in DPPC and cholesterol*. This process is the key aspect of the updated adsorption-driven lipid sorting model.
- During the alveolar surface area reduction induced by exhalation, γ is reduced to low values. This is a consequence of the low compressibility of the DPPC:cholesterol film and occurs with *little or no change* in monolayer composition.
- Deep inhalations and sighs can induce temporary changes in monolayer composition followed by compression-driven lipid sorting to restore the DPPC:cholesterol film.

The purpose of this review is threefold: (1) to provide the foundational knowledge needed to understand the biophysical properties of pulmonary surfactants, (2) to describe the literature that supports the updated model, and (3) to attempt to integrate the manner in which the biophysical activities fit with overall pulmonary function in health and disease. In Sections 2 and 3, we will address why it is important to study the biophysical properties of surfactants and how the properties of surfactant lipids and proteins can lead to low γ in thin films. Section 4 highlights the techniques used to study surfactants. Section 5 describes the structural features of

https://doi.org/10.1021/acs.chemrev.3c00146
Chem. Rev. 2023, 123, 13209−13290

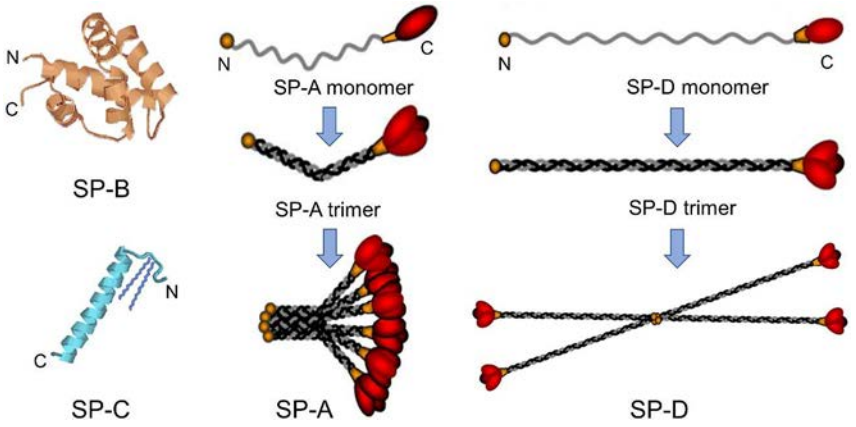

Figure 2. Ribbon diagrams for the surfactant proteins. SP-B is a surface membrane protein of 79 amino acids (4.1 kDa). A monomer is depicted, although in the lung SP-B functions as a disulfide-dependent dimer. The N-terminal insertion sequence and the C-terminal of the SP-B monomer are indicated. SP-C is a transmembrane protein of 35 amino acids (3.7 kDa), although some N-terminal amino acids are sometimes deleted. The N-terminal, which possesses bilayer disrupting properties, and the C-terminal, which terminates in an α-helix, are indicated. The N-terminal contains two adjacent palmitoylated cysteines. The length of the α-helix approximates that of a DPPC bilayer. SP-A and SP-D are complex calcium-dependent, collagen-containing lectins, i.e., collectins, which bind certain sugars and lipids. For SP-A, the upper panel shows a ~30 kDa SP-A monomer that contains a short N-terminal of ~10 amino acids with two cysteines involved in interchain linkage, followed by a collagen-like region containing 24 Gly-Xaa-Yaa repeats, including six hydroxyprolines or prolines. The collagen-like region is interrupted after 12 repeats by an additional cysteine, introducing a ~60° bend. This is followed by a hydrophobic α-helical neck region of ~40 amino acids that terminates in the C-terminal carbohydrate-recognition domain (CRD) of ~115 amino acids. The middle panel shows that three SP-A monomers fold together to form a compact trimer. The trimer is stabilized by disulfide bridges in the N-terminal segment, by the triple helical collagen-like segment, and by hydrophobic interactions creating a coiled-coil region through the tight binding of the three helical neck segments. The three CRD segments fold together to form a tulip-like formation. The lower panel shows that six SP-A trimers coalesce to form the mature SP-A octadecamer. This complex of ~650 kDa has the appearance of a bouquet of tulips. Normally there is variable length glycosylation of the extra cysteine in the collagen-like region and the CRD, resulting in a range of molecular weights. For SP-D, the upper panel shows the N-terminal region of a ~40 kDa SP-D monomer that contains ~21 amino acids and 2 cysteines. The collagen-like domain is continuous with no bend and is longer than that of SP-A, containing ~120 amino acids. The coiled-coil neck and CRD regions have an overall structural similarity to SP-A. The middle panel shows that SP-D forms trimers in a manner much like SP-A, except that the collagen-like region is straight. The lower panel shows that in contrast to SP-A, SP-D trimers are bound with each other via the N-terminal segments in an end-to-end manner. Here four trimers are linked to form an overall X or cruciform shape. SP-D complexes containing 6 or 8 trimers are also present. The latter have been termed "fuzzy balls". Schematics of SP-B and SP-C were adapted with permission from ref 27. Copyright 2012 Elsevier. Schematics of SP-A and SP-D were adapted with permission from ref 28. Copyright 2006 Elsevier.

surfactant components that ensure that these surfactants can adsorb rapidly to form a surfactant film. Section 6 discusses how the surfactants reduce γ during exhalation and how the stability of the film is maintained. Additionally, this section introduces the evidence for an updated model of surfactant function, while recognizing that there are alternative models for surfactant function. Section 7 describes the updated model and discusses some of the potential ramifications and caveats associated with this new perspective. Section 8 provides additional insights from physiological and pathophysiology research. Section 9 presents selected challenges for future research, particularly those implied by this updated model.

2. WHY STUDY PULMONARY SURFACTANT?

Under normal circumstances, pulmonary surfactant supports breathing without our awareness of its essential function of keeping the alveolar spaces filled with air rather than liquid. It is only when it is absent or damaged that we encounter complications and decreased lung function, leading to lower levels of oxygenation with possibly fatal consequences. Further, exogenous surfactant therapy is acknowledged as a key contributor to neonatal pulmonary health in premature infants and has a, yet to be realized, potential to help fight adult pulmonary diseases, including those inflicted by severe COVID-19. Past insights into the biophysical properties of surfactants have informed the therapeutic approaches, but better understanding is needed to realize the full potential of future surfactant therapies.

2.1. Neonatal Respiratory Distress Syndrome

Neonatal respiratory distress syndrome (NRDS or RDS) is the prototypic condition that illustrates the importance of pulmonary surfactant for lung function.[4] Characterized by insufficient surfactant levels due to prematurity, neonates with RDS are unable to inflate their lungs, leading to severe lung dysfunction. Avery and Mead's discovery[4] that premature infants suffering from Hyaline Membrane Disease, at that time the major cause of infant morbidity and mortality, were deficient in this substance prompted considerable clinical interest and led to an enormous surge in surfactant research.[5,38−40]

It is not surprising, therefore, that following recognition of the disaturated lecithin DPPC as a major constituent,[6] clinical trials were instituted where DPPC was aerosolized into the lungs of premature infants suffering from RDS.[41,42] Unfortunately, aerosolized DPPC had no effect on survival. Consequently, surfactant as a therapeutic treatment was essentially abandoned. While there were several reasons for this failure, this was clearly the wrong surfactant for the time, and as happens too often, a theoretically valid, practical approach was doomed through a lack of adequate understanding.

https://doi.org/10.1021/acs.chemrev.3c00146
Chem. Rev. 2023, 123, 13209−13290

Table 1. Lipid and Protein Compositions of Several Exogenous Surfactants[a,b,c]

Generic name	Beractant	Poractant alfa	Calfactant	BLES	CHF5633
Trade name	SURVANTA	CUROSURF	INFASURF	BLES	CHF5633
Source	Bovine lung mince	Porcine lung mince	Calf lung lavage	Bovine lung lavage	Synthetic
Phospholipids	84	99	91	96	98.3
PC/DPPC	71/50	69/47	79/43	77/41	49/49
PG	2.4	1.2	4.5	13	49
PE	3.4	4.5−7.4	2.8	2.6	0
PI+PS	1.3	4.5−8.4	4.0	1.0	0
LPC	1.5	1.0−7.0	<1.0	0.9	0
SM	3.4	1.8−7.9	0.8	1.4	0
Neutral Lipids					
Cholesterol	<0.2	0	5−8	2−3	0
Free fatty acids	5.8−14	n/a	0.64	n/a	0
Hydrophilic Proteins	0	0	0	0	0
Hydrophobic Proteins	0.94	1.1	1.6−2.2	2.0	1.7
SP-B	0.04	0.4	0.9	0.5	0.2
SP-C	0.9	0.7	0.7−1.3	1.5	1.5

[a]Adapted with permission from ref 64. Copyright 2011 Elsevier. [b]BLES: Bovine lipid extract surfactant; PC: phosphatidylcholine; DPPC: dipalmitoyl phosphatidylcholine; POPG: palmitoyl-oleoyl phosphatidylglycerol; PG: phosphatidylglycerol; PS: phosphatidylserine; PE: phosphatidylethanol; PI: phosphatidylinositol; LPC: lysophosphatidylcholine; SM: Sphingomyelin; SP: surfactant protein; n/a: no available data. [c]Data shown in this table represent approximate weight percentage of each composition with respect to the total mass of the surfactant preparation.

Fortunately, not everyone gave up on surfactant supplementation for RDS. In the 1970s, Enhörning, with several collaborators, including Forest Adams (Southern California, United States), Bengt Robertson (Sweden), and Fred Possmayer (Canada), developed a prematurely delivered rabbit pup model which demonstrated that instillation of natural pulmonary surfactant promoted lung expansion, gaseous exchange, peripheral circulation, and prolonged life.[43−49] Because of potential immunological risks, natural surfactant could not be employed for clinical use. However, a number of protein-poor lipid extracts of bovine or porcine natural surfactant, which retained the essential properties of natural surfactant *in vitro* and *in vivo*, were developed. These naturally derived surfactants included Surfactant TA (Survanta),[50] BLES,[51] Infasurf,[52] and Curosurf.[53] Two wholly synthetic surfactants, Exosurf and ALEC, were also formulated.[54,55]

Following animal experiments testing proof of principle, pilot trials initially reported in 1980 by Fujiwara in Japan clearly demonstrated clinical potential.[50] Of note, it was soon learned that the sickest premature babies responded most poorly. Surfactant had to be delivered early, before the infant's fragile lungs were damaged.[56,57] Treatment with exogenous surfactant preparations contributed to the well documented >90% reduction in neonatal morbidity and mortality due to RDS during the last few decades of the 20th century.[58−61]

The major exogenous surfactants utilized throughout the world to treat neonates are modified animal-derived surfactants. While there are differences due to their particular modes of manufacture, these preparations have a PL profile like that of natural surfactant and contain the hydrophobic surfactant proteins SP-B and SP-C and variable levels of cholesterol (Table 1). They do not contain SP-A or SP-D, because of their potential immunological effects. There are subtle differences in compositions. For example Survanta and Curosurf lack cholesterol, and Survanta has significant amounts of fatty acids but relatively little SP-B, but they all have a significant proportion of DPPC and contain mostly PL. Infasurf possess a lipid profile identical to the neonatal calf surfactant from which it is derived. BLES also has a similar PL profile as the starting bovine surfactant material but has most of the cholesterol removed during its preparation. Most synthetic surfactants, as exemplified in Table 1 by inclusion of the recently developed CHF5633,[62] include only 2 or 3 lipids and always contain a high percentage of DPPC. All these preparations in Table 1 contain hydrophobic surfactant proteins. Importantly, in comparison to the protein-free synthetic therapeutic surfactants, such as Exosurf and ALEC, the hydrophobic protein-containing preparations perform their therapeutic functions more effectively.[63]

Despite the success of the naturally derived preparations, functional synthetic surfactant preparations are desirable for a multitude of reasons, such as cost, potential variability in natural sources, supply limitations, and social, cultural, and religious concerns. Progress has been made in this area, with the recent development of several synthetic surfactants, which contain synthetic analogues of both SP-B and SP-C.[65,66] More recently it has become possible to express human recombinant SP-A and SP-D in Chinese Hamster Ovary cells and in *E. coli* using advanced molecular biology approaches.[67,68] Further understanding of the biophysical properties of surfactant could lead to the formulation of novel synthetic surfactants with additional improved properties compared to the currently manufactured products.

The history of the discovery, characterization, preparation, and application of exogenous surfactants to treat RDS provides an important lesson in how understanding the biophysical properties of surfactants is essential for clinical success. That ∼25-year quest, leading to successful therapy in the 1980s, has been reviewed, and the reader is encouraged to become familiar with this fascinating story.[38,40,61,69,70]

In addition to surfactant therapy, the detrimental effects of premature birth on pulmonary function can be alleviated by counteracting alveolar collapse at end expiration, for example with continuous positive airway pressure, with the appropriate use of mechanical ventilators, and by antenatal treatment with

https://doi.org/10.1021/acs.chemrev.3c00146
Chem. Rev. 2023, 123, 13209−13290

glucocorticoids.[71] Currently, death due to RDS alone is rare in developed countries.[61]

2.2. Acute Respiratory Distress Syndrome

The clinical significance of pulmonary surfactant is also seen in the deleterious alterations in surfactant in patients with Acute Respiratory Distress Syndrome (ARDS), a connection initially recognized by Ashbaugh and associates in 1967.[72] Experimentally induced respiratory failure in animals is currently designated Acute Lung Injury (ALI).[73−80] This syndrome denotes acute respiratory failure with reduced blood oxygenation and significant pulmonary inflammation.[73] Although ARDS is accompanied by massive atelectasis (alveolar collapse), our lungs normally possess excess capacity for gaseous exchange which can be advantageously enhanced by supportive ventilation. In addition, the lungs possess a remarkable ability for regeneration.[81] There are many causes of ARDS, including direct lung injury (bacterial pneumonia, near drowning, aspirations, and inhalation of smoke and other toxic materials) and indirect systemic insults (sepsis, pancreatitis, burns, and general trauma). Prior to COVID-19, the incidence of ARDS in the USA was estimated as ∼190,000 cases per year, with mortality rates above 35%.[82] Such a high mortality rate, ranging from ∼35% for mild to ∼45% for severe ARDS, was also observed in a more recent large epidemiological study encompassing intensive care units in 50 countries.[83]

Animal studies and clinical observations provide strong evidence for the concept that alterations to the composition and function of the endogenous surfactant system contribute to the pathophysiology of the disease.[76,77,84] Exogenous surfactant therapy has demonstrated improvements in lung function in animal studies.[85] However, this therapy has not yet provided a significant improvement in mortality rate, when tested in clinical trials of patients afflicted with ARDS.[86] Numerous factors may have contributed to this lack of clinical success for surfactant therapy in ARDS, including the diversity of initiating insults, the severity of lung dysfunction at the time of treatment, and specifics related to the implementation of this therapeutic approach.[87−89] Importantly, the mechanisms underlying the biophysical dysfunction of endogenous surfactant in these patients may also impact the efficacy of the exogenously administered therapeutic surfactant.[15,89]

COVID-19, caused by infection with the SARS-CoV-2 coronavirus, can lead to ARDS in some patients. It has dramatically increased the incidence of ARDS-type illnesses and highlights the lack of accepted suitable pharmacological therapies.[90] For the most part, treatment for ARDS has tended to consist largely of supportive measures such as mechanical ventilation.[91,92] COVID-19 could provide a unique opportunity for testing the efficacy of surfactant therapy with severe cases, because it is a single direct form of ARDS.[92,93] Early clinical studies have been initiated with some apparent success.[93,94] Overall, a better understanding of the biophysical and physiological properties of surfactant could contribute to the development of strategies that target surfactant dysfunction in ARDS.

2.3. Other Conditions Related to Surfactant Dysfunction

As pulmonary surfactant continued to be investigated, a surprisingly large number of clinical and subclinical conditions were found to be related, at least in part, to abnormal surfactant metabolism. It was soon discovered that the large complex hydrophilic surfactant proteins, SP-A and SP-D, were intimately involved with the innate host defense systems responsible for maintaining clean alveolar surfaces by limiting microbial invasion. These collectins are also inherently involved with intra-alveolar surfactant metabolism.[17,95−98] Furthermore, while surfactant deficiency is important in RDS and ARDS, the presence of too much surfactant can lead to respiratory dysfunction with pulmonary alveolar proteinosis (PAP), which results from aberrant surfactant metabolism.[99−102] Surfactant abnormalities have also been noted with Chronic Obstructive Pulmonary Disease (COPD), a condition involving restricted air flow due to bronchitis (persistent bronchiolar inflammation) and/or to emphysema.[103] Surfactant dysfunction has also been associated with asthma.[104−106] Additionally, environmental factors as well as genetic mutations can impact pulmonary function, for example by inducing endoplasmic reticulum stress.[107−109]

Specifically, several genetic conditions specifically targeting the surfactant system have been reported. Mutations in SP-A, SP-B, and SP-C have all been reported in the human population.[110,111] Many of the clinical observations are phenocopied in animals, showing, for example, that SP-B expression is essential for surfactant function and hence life[23,110,112] and that SP-C mutations, although not lethal, are often associated with the development of childhood or adult pulmonary fibrosis.[113,114] Other mutations, for example in the gene encoding for thyroid transcription factor-1 (TTF-1), a transcription factor for surfactant proteins, and the ABCA3 transporter, responsible for intracellular transport of surfactant lipids, can impact the surfactant system as well.[111] Mutations in ABCA3 can affect intracellular lamellar body size and content, resulting in Type II cell dysplasia which contributes to pulmonary fibrosis.[115,116] Other mutations, such as those associated with Niemann−Pick Disease and Hermansky−Pudlak Syndrome, also affect surfactant metabolism and lung function.[117−120] These latter two conditions, however, are multisystemic, in which many additional organs are affected.[121,122]

In summary, although this review is mainly dedicated toward understanding the biophysical properties of pulmonary surfactant, and these obviously impact RDS and ARDS, it has become clear that surfactant has other important functions in health and disease. The impact of surfactant, and its individual components, on the lung may either directly or indirectly be associated with its activity at the alveolar interface. As such, the surfactant-related conditions, beyond RDS and ARDS, must also be kept in mind while considering surfactants' primary role in surface tension reduction.

3. HOW DO PULMONARY SURFACTANTS DETERMINE SURFACE TENSION?

The most critical physical property of a surfactant is that it can define the γ of a film. Most of this control derives from the amphipathic (containing both polar and nonpolar functional groups) lipids in a surfactant and depends in detail on the phase behavior of the lipid monolayer film. Here we highlight the fundamental physics of monolayer films.

Pulmonary surfactants contain four surfactant proteins: the lectins, SP-A and SP-D, and the low molecular weight hydrophobic proteins, SP-B and SP-C. The lectins do not contribute directly to the γ properties of the surfactant film. The hydrophobic proteins facilitate formation of the surfactant film but do not directly affect the resulting γ in any significant way. The focus is therefore on the lipid components when we

https://doi.org/10.1021/acs.chemrev.3c00146
Chem. Rev. 2023, 123, 13209−13290

consider the nature of the surface properties of the surfactant film.

3.1. Surface Tension and Surface Pressure

Surface tension, γ, is a measure of the work, or energy (ΔE), needed to increase the area (ΔA) of a surface of a liquid, so $\gamma = (\Delta E/\Delta A)$.[38,47,123] More precisely, γ is the change in free energy when the area is changed at constant temperature and pressure, $\gamma = \left(\frac{\delta G}{\delta A}\right)_{T,P}$. The lower the γ, the less energy is needed to increase the surface area. Hence, in a lung, a low γ allows for easier changes in alveolar surface area, i.e., less work to breathe.

The alveoli in the lung can be approximated as small air bubbles coated with a monolayer of surfactant. The Law of Young and Laplace[47] relates the pressure difference (ΔP) across the film to γ and the radius of the alveolus (R) as

$$\Delta P = 2\gamma/R \quad (1)$$

This shows that at lower γ, less pressure is required to keep the alveolus inflated. However, because ΔP is inversely related to R, the smaller the alveolus, the higher the required pressure.

Whereas the Young and Laplace equation shown in eq 1 applies to a single independent sphere, the lung consists of airways as well as interconnected alveoli and includes a structural extracellular matrix with elastic properties. Therefore, direct application of the Young and Laplace Law as for a single bubble is oversimplified. Each alveolus backs onto several other alveoli by thin septa. The tendency for a single alveolus to collapse will be resisted by the alveoli around it, a property known as interdependence.[124,125] Nevertheless, experimental evidence supports the relevance of γ in lung mechanics. Specifically, the importance of γ during breathing was illustrated by seminal pulmonary pressure−volume experiments, conducted by Radford and co-workers in the 1950s as depicted in Figure 3.[126−128] These curves show the pressure needed to expand the volume of dog lungs when they are filled with either saline or air. The incompressible saline liquid causes expansion of the lung at low pressures, and the lung tissue responds elastically when the pressure is lowered again. In contrast, the opening pressure required for air to enter the lungs and expand them to the total lung capacity (TLC) is significantly higher. When the pressure is reduced, the lungs tend to remain expanded, creating a hysteresis loop that reflects the work done to expand the lungs. When lungs are lavaged, thereby removing surfactant, the pressure to open the lungs is even greater (not shown), demonstrating that it takes more work to expand the lung in the absence of the surfactant. As such, at a given pressure, the lung volume in the absence of the lung surfactant is lower. These early experiments pointed to a substance that reduced the work to expand the lungs through a reduction in γ in the alveolar spaces.

As depicted in Figure 4a, γ originates from an imbalance in the intermolecular forces at an air−water interface. The attractive forces on a molecule in the bulk phase balance each other. The net attractive force is zero. However, water molecules at the surface experience a net attractive force into the bulk phase because the attractive forces in the liquid are greater than in the vapor. Thermodynamically, the chemical potential (the molar free energy) is lower in the bulk than at the surface. Therefore, water molecules will tend to migrate from the surface to the bulk, which will decrease the surface

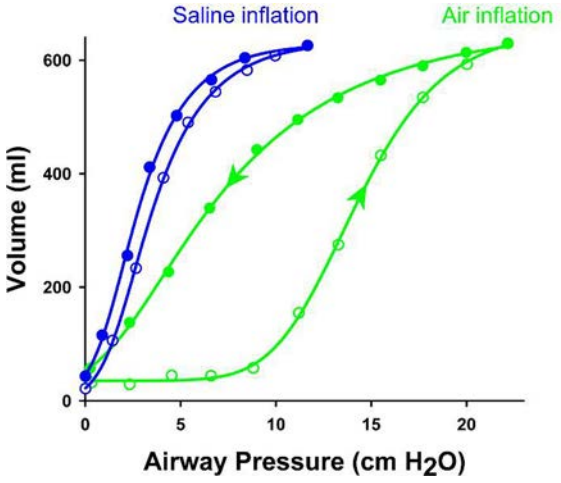

Figure 3. Pressure−volume relationship of an isolated dog lung. The saline-filled lung inflates with minimal pressure and deflates reversibly. This represents a measure of the tissue elasticity in the absence of surface tension effects. The air-filled lung reflects both tissue and surface tension forces. A significant critical opening pressure of ∼9 cm H_2O is required. Even larger pressures are required to initiate inflation of a surfactant-deficient lung (not shown), indicating an even greater work expenditure. Even at higher pressures, surfactant deficient lungs can only achieve very low lung volumes. Adapted with permission from ref 128. Copyright 1957 American Physiological Society.

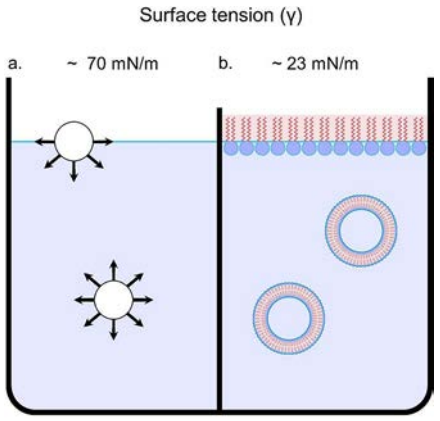

Figure 4. Molecular explanation of surface tension. (a) Surface tension (γ) arises because molecules at the surface of a liquid are subject to different potential forces than molecules in the bulk phase. A water molecule in the bulk phase is attracted equally by those molecules around it, above, below, and to either side. The net attractive force is zero. However, water molecules at the surface are attracted downward and to either side, but not upward. Thus, all molecules at the air−water surface experience a net attraction inward. Should a molecule of water be drawn into the subphase, other surface molecules will fill the vacated space, leading to a tendency to minimize the surface area. Correspondingly, small droplets of liquids with high γ, such as water or mercury, adopt spherical shapes with a minimal surface area. (b) When spread at an air−water interface, normally with an organic solvent, PLs, such as PC, will interact with the water via their charged polar headgroups to anchor the PL at the surface, whereas the nonpolar, hydrocarbon fatty acids extending upward replace the air−water interface with an air−hydrocarbon interface. The water−headgroup interaction will decrease the net attraction inward on the water molecules, decreasing γ from 70 mN/m, which is γ for pure water at 37 °C, to ∼23 mN/m for a surface completely filled with PL. Excess PL would lead to formation of bilayer vesicles in the subphase.

https://doi.org/10.1021/acs.chemrev.3c00146
Chem. Rev. 2023, 123, 13209−13290

area whenever possible. If the area cannot be reduced, this creates a tension (surface tension, γ) or pressure (surface pressure, π) along the plane of the surface.[129]

The γ will be large when intermolecular attractive forces are large, as in water, and small when intermolecular attractive forces are small, as in hydrocarbons. Amphiphilic molecules, such as PL, which have a hydrophilic group at one end and a hydrophobic group at the other end, can lower the γ of water. The hydrophilic group binds to the water at the surface, while the hydrophobic group is exposed to the air as shown in Figure 4b. The amphiphilic molecule will spread to cover the surface, and excess material will accumulate in the subphase, where they can form micelles or bilayer vesicles (Figure 4b). Such molecules are called surface active agents or surfactants.

For a surfactant film on water, the surface pressure (π) is defined as the difference between the γ of a clean air−water surface (γ_0) and that of a surfactant-covered surface (γ).

$$\pi = \gamma_0 - \gamma \tag{2}$$

At physiological temperatures, the γ of pure water is approximately 70 mN/m and π is zero. Correspondingly, the γ of a surfactant-covered surface can vary from 70 to 0 mN/m, with π varying from 0 to 70 mN/m.

Note that π is in the plane of the surface and is a distinct property from the alveolar pressure (ΔP). The latter function denotes the pressure difference across the plane of the surface. Nevertheless, these parameters are related through γ.

A PL, spread at the air−water surface with the aid of a spreading agent, such as chloroform, will form a monolayer that will eventually attain an equilibrium surface tension γ_{eq} of ∼23 mN/m, corresponding to a π_{eq} of ∼47 mN/m. This is also the minimum γ and the maximum π that can be achieved by steady compression of 1-palmitoyl-2-oleoyl-phosphatidylcholine (POPC) monolayers with a barrier (Figure 5b). Further reduction in surface area will lead to removal of the POPC from the surface without a decrease in γ. In contrast, compressing a film of a solid PL, such as DPPC, can reduce the γ to near zero, corresponding to a π of 70 mN/m (Figure 5a). Further reduction in surface area leads to film collapse, i.e, the loss of surface material without any change in π.

The difference in behavior of unsaturated and saturated PL emphasizes the importance of the phase of the surfactant, i.e., a fluid versus a solid film, and shows the need for saturated PL to reach the low γ observed in the lung during normal breathing. Note that such phases are dependent on their composition, the temperature, and the inherent or applied lateral pressure.

Mixtures of PL in monolayers can exhibit separation of different phases into distinct domains. These domains are composed of the more solid phase which arises due to the more efficient packing of DPPC molecules with themselves. This can be seen with fluorescence because the domains exclude bulky fluorescent probes. The size and structure of such domains are in part governed by the line tension, τ. Line tension is the two-dimensional equivalent of γ. Both arise because molecules at interfaces experience different forces than molecules in either phase. Thus, as γ reflects the energy difference between molecules at the air surface and those in the bulk phase, τ reflects the difference in energy of a molecule at a domain edge, compared with molecules in either phase. Thus, τ is a measure of the energy needed (ΔE) to change the perimeter (ΔL) of the domain.

$$\tau = \Delta E/\Delta L \tag{3}$$

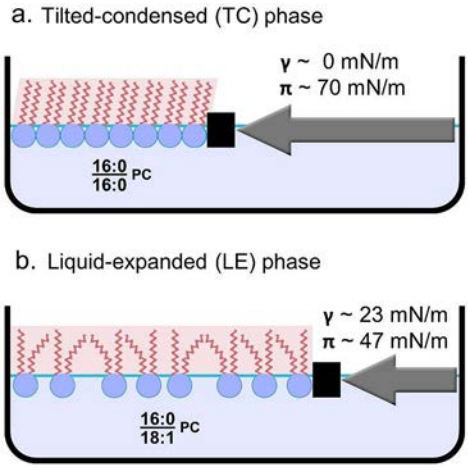

Figure 5. Surface tension and surface pressure. (a) A DPPC film spread on a Langmuir film balance can withstand up to ∼70 mN/m surface pressure (π) before undergoing collapse (material loss). This is equivalent to a near-zero surface tension (γ). This film is considered metastable because γ is below the equilibrium γ of ∼ 23 mN/m. The low γ is possible because DPPC molecules pack together very efficiently, forming a solid-like film. The fatty acid moieties are tilted to best accommodate the difference in size between the two palmitates and the hydrated headgroups. (b) In contrast, a POPC film can only withstand a π of ∼47 mN/m, which corresponds to the equilibrium γ of ∼ 23 mN/m. This occurs because the double bond produces a kink in the oleic acid moieties making the film too fluid to withstand high π.

3.2. Phase Behavior of Pulmonary Surfactant Lipids

Phospholipids can form monolayers at the air−water surface that can exist in different phases at a given temperature, depending on the lipid structure and the π. Within the aqueous phase, PL form bilayers because they have very low critical micellar concentrations (∼10^{-9} M for DPPC).[26] They can form single bilayer vesicles or multilamellar liposomes that can exist in any one of several well-characterized phases, depending on the lipid structure and the temperature.

While the phases in monolayers and bilayers are conceptually similar, there are subtle differences that have led to distinct nomenclatures, as schematically shown in Figure 6 and elaborated on below. In both cases, the manner in which the lipids pack to form different phases depends not only on the composition but also on the temperature. As well, with monolayers phase distribution is highly dependent on the applied lateral pressure.

3.2.1. Bilayers. Bilayers composed of DPPC molecules undergo a phase transition at 41 °C, from a solid-like structure in which the lipids do not diffuse laterally or rotationally and the lipid chains are rigid, to a liquid-like structure in which the lipid chains are fluid and the PL can diffuse freely laterally and rotationally. The bilayer phase above this main transition temperature (T_m) is called the L_α phase (Figure 6). The bilayer phase below this transition can adopt slightly different solid structures depending on the temperature, but the most important structure is the $L_{\beta'}$ phase, in which the palmitic acid chains are tilted relative to the plane of the bilayer. This tilting allows for a tighter packing of the PL, minimizing their surface area, and lessens hydration of the headgroups. This tends to minimize exposure of the acyl groups to water. There is another solid phase, in which the chains are immobile but perpendicular to the plane of the bilayer, called the L_β phase, a

https://doi.org/10.1021/acs.chemrev.3c00146
Chem. Rev. 2023, 123, 13209−13290

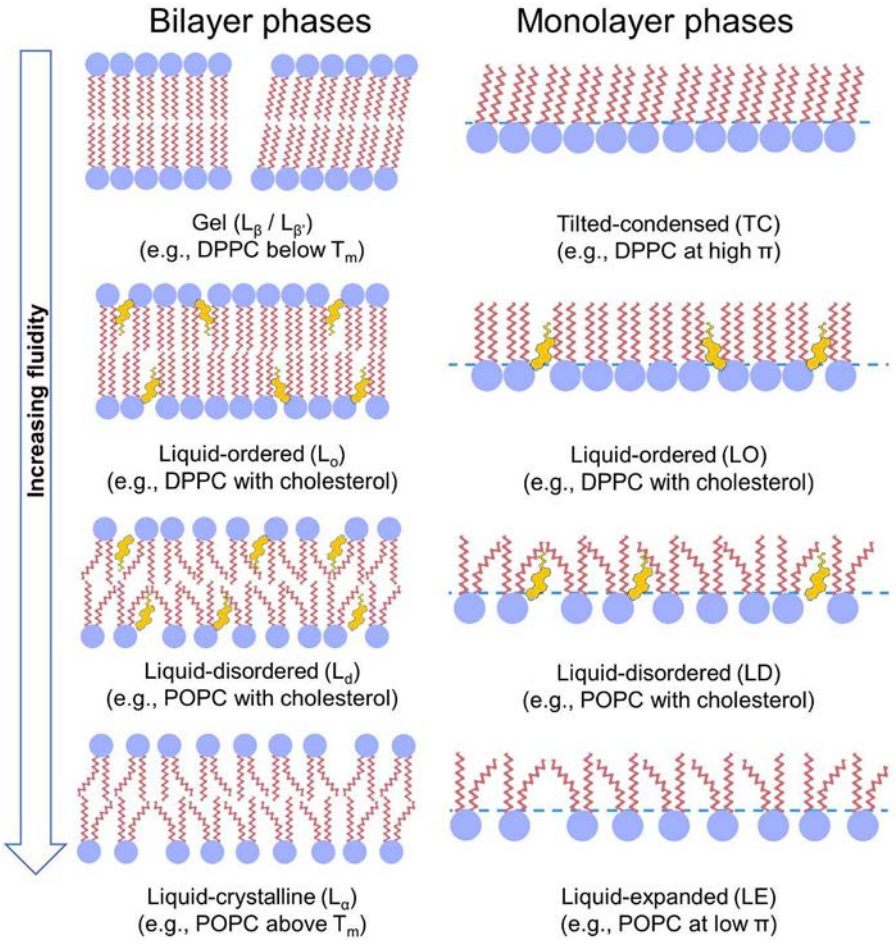

Figure 6. Comparison of the possible lipid phases present in bilayers and monolayers at physiological temperatures arranged by the order of fluidity, which is a measure of the ability of lipids to undergo rotational and translational diffusion. T_m is the melting temperature of the lipid. For DPPC, the tilted chain phases, $L_{\beta'}$ and TC, are the most stable. Unsaturated PLs do not exhibit a tilted phase. Cholesterol tends to fluidize the ordered phase and condense the disordered phase.

terminology used for other similar solid phases. It should be noted that in the older literature the term gel phase encompassed both the $L_{\beta'}$ and the L_β phases and the term liquid crystalline phase referred to the L_α phase.

Bilayers composed of POPC molecules undergo a similar phase transition at −2 °C. The solid-like phase is an L_β phase, and the liquid-like phase is an L_α phase. It should be noted that in the older literature the terms gel and liquid crystalline phases are used for the L_β phase and the L_α phase, respectively.[130−132] Bilayers containing two or more PLs can form a single L_α phase if the temperature is above T_m of all the components. However, the lipids will be partly immiscible at lower temperatures and more than one phase will appear. For example, mixtures of DPPC and POPC form coexisting DPPC-rich L_β phases and POPC-rich L_α phases at physiological temperatures and below.

Addition of small amounts of cholesterol to DPPC at low temperatures creates a new, relatively solid DPPC-rich L_β phase that can contain up to 7 mol % cholesterol.[133] At about 7 mol % cholesterol, a liquid-ordered, or L_o, phase is formed, creating a two-phase coexistence. This L_o phase contains about 22 mol % cholesterol and is fluid in the sense that lateral and rotational diffusion is possible, but there is a long-range order between the palmitic acid chains. Beyond 22 mol %, only the L_o phase exists.

Addition of cholesterol to POPC leads to a single phase at all compositions, which is characterized as a L_o phase at high cholesterol concentrations but a liquid-disordered or L_d phase at low cholesterol concentrations. The L_d phase is also fluid with free lateral and rotational diffusion but with less long-range order.

Ternary mixtures of DPPC, POPC, and cholesterol can form bilayers with a L_d phase and a L_o phase in equilibrium. This occurs with cholesterol concentrations between 10 and 30 mol % and DPPC concentrations between 25 and 75 mol %, with POPC making up the remainder.[133] The relative fluidity (meaning the rate of lipid chain motion as well as rotational and translational diffusion) of these bilayer phases is $L_{\beta'} < L_\beta < L_o < L_d < L_\alpha$.

More detailed discussion of the phase behavior of mixed lipid systems can be found in the work of McConnell and Keller.[134−137]

3.2.2. Monolayers. Somewhat analogous, though not identical, phase transitions can occur in lipid monolayers (Figure 6). The major difference between monolayers and bilayers is that bilayer phase transitions arise when the composition or temperature is changed. This occurs with a constant inherent lateral pressure, estimated to be ∼30 mN/m, arising from the PL:PL intermolecular forces. These intermolecular forces function to limit hydrocarbon−water

https://doi.org/10.1021/acs.chemrev.3c00146
Chem. Rev. 2023, 123, 13209−13290

interactions.[138−140] However, monolayer phase transitions primarily arise when either the composition or the lateral pressure is changed at a constant temperature. Here, there is no "inherent" PL:PL intermolecular lateral pressure. Nevertheless, if the temperature is increased, the molecular fluctuations or motions will increase so that higher pressures are required to maintain the same molecular area.

At low pressures with a complete monolayer of DPPC, the monolayer adopts a liquid phase called the liquid-expanded, or LE phase, somewhat analogous to the L_α phase in bilayers. The fatty acids are mobile within the plane of the monolayer. Decreasing the surface area produces an increase in π, and a tilted-condensed, or TC, phase appears, analogous to the $L_{\beta'}$ phase in bilayers, within which the chains are at an angle of about 27° relative to the normal of the bilayer. It should be noted that in the literature, the TC phase is often referred to as the liquid-condensed (LC) phase. Here we adopt the terminology recommended by Kaganer, Möhwald and Dutta.[141] At $\pi \sim 70$ mN/m, the TC phase collapses, by ejecting DPPC molecules from the monolayer, while maintaining $\gamma \sim 70$ mN/m.

At low lateral pressures, a monolayer of POPC is also in the LE phase. As pressure increases, the LE phase can be compressed to about $\pi \sim 47$ mN/m ($\gamma \sim 23$ mN/m) but not beyond. The POPC remains in a liquid state, and if the compression is continued, material is lost from the surface into the aqueous phase and will form bilayers.

At low π, DPPC and POPC mix completely in the LE phase. At higher pressures, the DPPC, which packs together with itself better than it does with POPC, separates into separate TC phase regions known as "domains".

Cholesterol exhibits strong interactions with the palmitates of adjacent DPPC molecules in monolayers forming complexes in which the surface area at a particular π is less than the sum of the surface areas of the constituents.[142,143] Thus, the addition of cholesterol to DPPC at low π value's causes a condensation of the film. Since cholesterol is very stiff, this effect is due to compacting of the palmitoyl groups.[142] Adding cholesterol to DPPC in the TC phase leads to formation of a liquid-ordered, or LO, phase, in which there is more mobility, in analogy with the cholesterol-induced formation of the L_o phase from the $L_{\beta'}$ phase in bilayers.

Adding cholesterol to POPC at low pressures likewise decreases the mobility of the lipid chains, leading to a condensation of the film. Cholesterol therefore induces a liquid-disordered, or LD, phase from the LE phase, in analogy with the cholesterol-induced formation of the L_d phase from the L_α phase in bilayers.

In ternary mixtures of DPPC, POPC, and cholesterol, it is possible to generate two phase regions, where DPPC-rich LO phases are in equilibrium with POPC-rich LD phases.

The relative fluidity of these monolayer phases is highly influenced by π and varies as follows: TC < LO < LD < LE.[33,142,144−150]

4. WHAT ARE THE TECHNIQUES USED FOR STUDYING PULMONARY SURFACTANT?

A variety of techniques and methods have been developed to understand lipids and pulmonary surfactants in various scientific disciplines, from their biophysical properties to lateral structure and molecular organization, physiological function, and lipid−protein interactions at the molecular level. Some of these methods have played a significant role historically in pulmonary surfactant research but gradually faded out due to their intrinsic limitations, while others are still in the infancy of development. This section will briefly review the main methods for studying the biophysical properties of pulmonary surfactants, organized by the type of information that can be derived from these particular techniques. The focus is to discuss the pros and cons of these methods, as these have guided some of the interpretations and conclusions as discussed in the remainder of this review. Although researchers could use this section as a guideline for selecting suitable procedures for their research, readers will be referred to more detailed descriptions to learn more technical aspects associated with some of these methods.

4.1. Choice of Surfactant Material

A surfactant is a complex mixture of PLs, neutral lipids, and proteins (Table 1), and there are numerous preparations of surfactant analogs with vastly different compositions of these components, ranging from extracts of lung surfactants to pure PLs to single components. It is therefore evident that whatever method is applied to study the surfactant, the outcome will depend on the specific composition of the material used. For example, there are a number of studies on the effect of the surfactant proteins on DPPC and DPPC:DPPG. Such investigations can reveal details on these specific interactions, but interpretation must also consider the fact that the hydrophobic proteins, SP-B and SP-C, reside in the more fluid regions of bilayers and monolayers.

Natural lung derived materials, such as surfactant isolated from lung lavage material, contain all surfactant components but may also be contaminated with other compounds present in the alveolar space during lavage, such as serum proteins. As will be discussed later, most studies using lavage material have used differential centrifugation to obtain the biophysically active subfraction of the surfactant called large aggregates (LAs). Purified lamellar bodies, the intracellular storage organelle of surfactant, contain all surfactant ingredients although they have reduced SP-A content and are usually purified in relatively small quantities. Commercially available exogenous surfactants generally consist of extracts containing surfactant lipids and with SP-B and SP-C (Table 1). These samples will be relatively consistent and abundant but lack SP-A and sometimes other components such as cholesterol. Reconstituted surfactants, as well as studies on individual components of surfactant, are important to dissect individual roles for specific proteins or lipids; however, it can be difficult to extrapolate individual results to behavior in a more complex system.

By systematically using known mixtures of key PLs and neutral lipids, such as DPPC, POPC, POPG, and cholesterol, it has been possible to tease out some of the minimal requirements for mimicking some of the biophysical properties of natural lung surfactant, such as rapid adsorption and low γ. Controlling and varying the compositions have been invaluable tools for the biophysicist but also raise the question of physiological relevance. This is particularly true of reconstituted samples containing only disaturated PLs, such as DPPC:DPPG.

Using natural surfactants or surfactant extracts has provided the benchmarks for characterizing the key properties of surfactants and has raised some interesting questions: How can surfactants with somewhat different compositions behave very similarly in biophysical tests? Is the detailed composition

https://doi.org/10.1021/acs.chemrev.3c00146
Chem. Rev. 2023, 123, 13209−13290

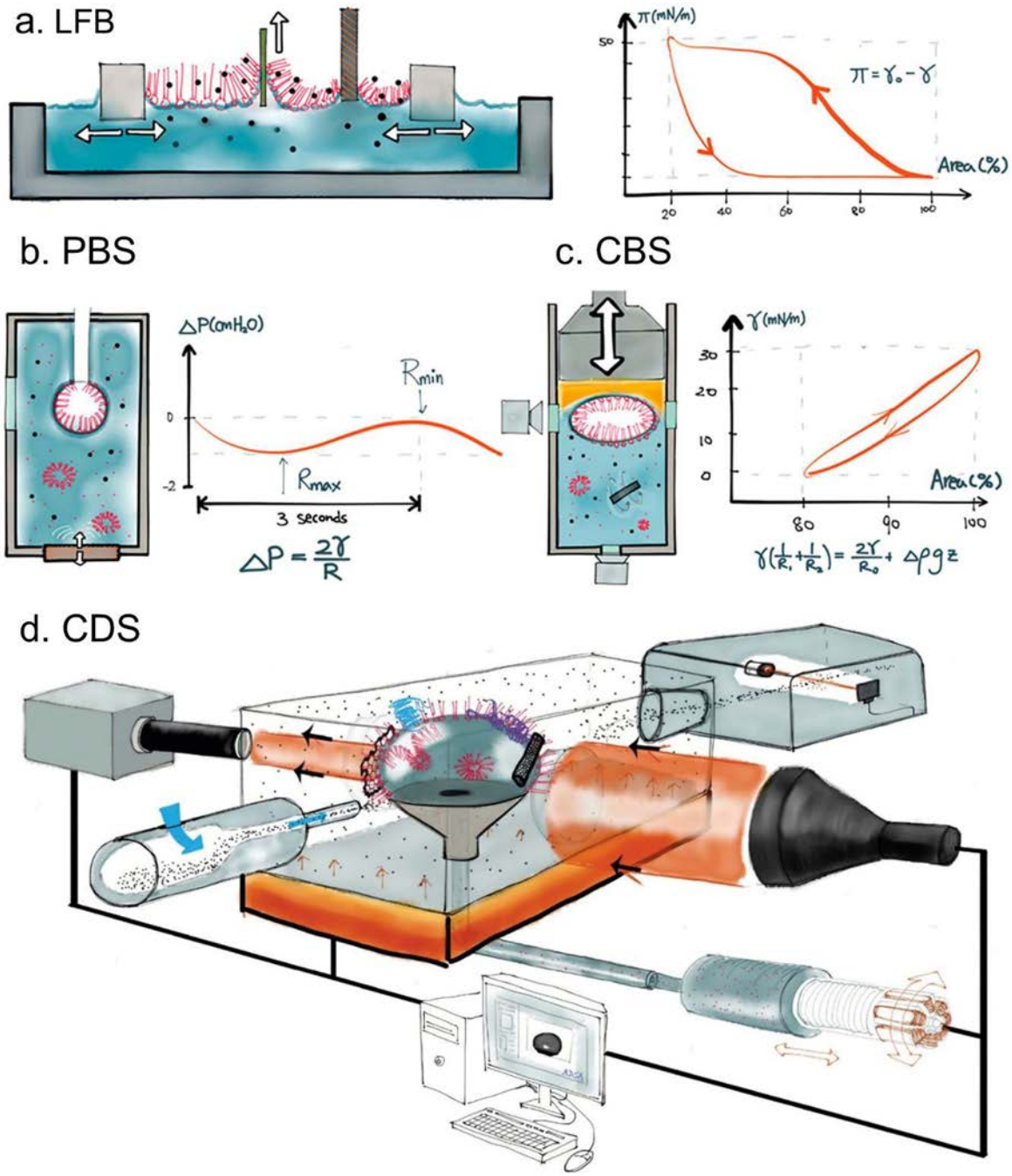

Figure 7. Schematics of *in vitro* methods for studying pulmonary surfactant films. (a) Langmuir film balance (LFB) and a typical compression−expansion isotherm of pulmonary surfactant (surface pressure vs surface area). Due to its large surface area, Langmuir trough experiments are usually performed under ambient environment to avoid local temperature gradients and the effects of evaporation. The surface pressure ($\pi = \gamma_o - \gamma$, where γ_o is the γ of the air−water surface) is determined with a Wilhelmy plate in contact with the air−liquid interface. In practice, the rate of film compression is limited, as quick compression generates waves at the surface, interfering with the π measurement. Due to the very slow changes in surface area imposed by these constraints, the Langmuir trough is incapable of faithfully mimicking the biophysical properties of natural surfactant. In addition, the Langmuir trough is usually only used for studying compression, as the π decreases steeply upon the initial expansion, resulting in a large hysteresis area for the compression−expansion loop. Surfactant films at the air−liquid interface can be Langmuir−Blodgett transferred onto a solid substrate (upward arrow) for microscopy imaging. (b) Pulsating bubble surfactometer (PBS) and a typical result of pulmonary surfactant measurements. A ∼1 mm air bubble, suspended from a capillary tube open to the atmosphere, is oscillated between two fixed radii by drawing air into the bubble, usually at 20 cycles/min with a maximum 50% variation in its surface area. The γ is estimated from the negative pressure caused by the pulsator, i.e., the pressure difference across the bubble surface (ΔP), using the Laplace equation for a spherical surface, $\Delta P = 2\gamma/R$. (c) Captive bubble surfactometer (CBS) and a typical result of dynamic cycling experiments (surface tension vs surface area) of pulmonary surfactant. An air bubble of ∼5 mm in diameter floats against a hydrophilic ceiling usually made of 1% agarose gel. The hydrophilic ceiling adsorbs a thin aqueous wetting film that prevents the bubble from physically touching the solid surface, thus maintaining the integrity of the "captive" bubble completely at the air−water surface. The surfactant subphase is normally stirred to maintain an evenly controlled environment. Temperature is maintained by immersion in a bath. The bubble is oscillated by varying the hydraulic pressure of the subphase with tunable rates of cycling and amounts of compression. The γ is determined by analyzing the shape of the captive bubble, e.g., numerically solving the Laplace equation of capillarity, as

https://doi.org/10.1021/acs.chemrev.3c00146
Chem. Rev. 2023, 123, 13209−13290

Figure 7. continued

indicated in the figure, in which R_1 and R_2 are the two principal radii of curvature at any point of the bubble surface; R_0 is the radius of curvature at the bubble apex; and $\Delta\rho$ is the density difference across the bubble surface. The CBS has been proven to be a benchmark apparatus for simulating the biophysical properties of a natural pulmonary surfactant, such as rapid adsorption, low film compressibility upon compression, and rapid readsorption upon expansion. (d) Constrained drop surfactometer (CDS). A surfactant droplet is formed on a 3 mm hydrophilic knife-sharp pedestal using a programmable motorized syringe. This droplet is enclosed in an environmental control chamber, where core body temperature is maintained with a thermoelectric heater. The drop profile is illuminated with a monochromic parallel backlight and is recorded continuously with a high-definition camera. The profile images are sent directly to the axisymmetric drop shape analysis (ADSA) software and processed to yield real-time γ measurements. Also shown in this schematic are a particle insufflator and a particle counter based on laser diffraction spectroscopy, which can be used to study nano−bio interactions in the sample. Adapted with permission from ref 29. Copyright 2015 American Chemical Society.

important, or are only a few key components essential for function *in vitro* and *in vivo*? It has therefore been instructive to study lung surfactants from a variety of species of animals.

4.2. Biophysical Simulations of Surfactant Films

Methods in this category are used for *in vitro* biophysical simulations of pulmonary surfactant films. These methods need to satisfy at least three basic requirements.[151] They should be able to study adsorbed pulmonary surfactant films.[152] They should be able to determine the γ−surface area correlation that mimics the dynamic γ variation during normal tidal breathing. Dynamic γ of a pulmonary surfactant film is a function of both the compression rate (i.e., how fast the film is compressed) and compression ratio (i.e., how much the film is compressed). A healthy adult breathes approximately 20 times per minute, while the area of the alveolar surface varies less than 20%, during normal tidal breathing.[153,154] They should be able to control the experimental conditions to simulate the intra-alveolar environment of the lungs, including the core body temperature of 37 °C and 100% relative humidity. As shown in Figure 7, there are four established *in vitro* methods for studying pulmonary surfactants, i.e., the Langmuir film balance, pulsating bubble surfactometer, captive bubble surfactometer, and constrained drop surfactometer. While few of these methods are able to completely satisfy the above three fundamental requirements for biophysical simulations of pulmonary surfactant films, they have provided significant insights when they were used.

4.2.1. Langmuir Film Balance. The Langmuir film balance, also called the Langmuir trough, was first utilized to study pulmonary surfactant by John Clements in the 1950s.[126,155−157] The so-called classical model of pulmonary surfactant was largely established with the Langmuir trough, which provided a means of studying the π variations corresponding to the changing surface area of a spread pulmonary surfactant monolayer. In addition, the Langmuir trough can easily be coupled with optical and fluorescence microscopy. The Langmuir−Blodgett technique allows the surface film to be transferred to a flat surface on a disc, such as mica, by drawing the submerged disc vertically through the surfactant film (Figure 7a). This film can then be studied by a variety of analytical techniques, such as atomic force microscopy, time-of-flight secondary ion mass spectrometry, and X-ray scattering techniques, to study the phase behavior, lateral structure, and chemical composition of the surfactant monolayers.

The Langmuir trough has played a central role in early studies of pulmonary surfactant. However, it has a few intrinsic limitations which need to be considered when interpreting data related to pulmonary surfactant films. Due to its large size, the Langmuir trough is usually only applied to the study of spread monolayers rather than studying adsorption. The Langmuir trough may also suffer from film "leakage", which means the loss of surface-active material, such as pulmonary surfactant, onto the barriers and walls of the trough at low γ. Although the extend of leakage may depend on the specific properties of the balance, film leakage makes it difficult to study the complete physiologically relevant γ range of pulmonary surfactants, and it limits studies on the expansion of the pulmonary surfactant film. A second limitation of the Langmuir trough is that it cannot simulate the normal rate of respiration since fast compression−expansion cycles generate waves that interfere with γ measurements. Further, environmental control, such as physiological temperature and humidity, is difficult, although not impossible, to apply when using a Langmuir trough. These constraints in applicability of the Langmuir trough need to be considered when studying pulmonary surfactant.

Nevertheless, despite the limitations, the Langmuir trough has proven useful for many experiments over the years to study the phase behavior of monolayers of pure PLs, mixtures of PLs, surfactant preparations, and natural surfactants.[158] A strength of the Langmuir balance is that a known amount of material can be deposited, and therefore the molecular properties of individual molecules are statistically defined. Such investigations have provided key insights and led in large part to the understanding that low γ can only be achieved with films highly enriched in DPPC.[13,159,160]

4.2.2. Pulsating Bubble Surfactometer. The pulsating bubble surfactometer (PBS) was introduced by Goran Enhörning in the mid-1960s.[161−164] It was the first bubble-based surfactometry technique developed specifically for studying pulmonary surfactants under conditions approaching the physiological situation.[163] A commercial version became available by 1990. The PBS was designed to determine the rate of surfactant adsorption and minimum and maximum γ of pulmonary surfactant during cycling. A small air bubble (~1 mm in diameter) is created in a surfactant suspension. After monitoring adsorption for a minute, the bubble is pulsated with a fixed 50% surface area reduction and a predetermined range of pulsations per minute (Figure 7b). The greatest advantages of the PBS are its low sample volume (~20 μL), relatively short period of operation (<5 min), and minimum requirements in the expertise of operation. The PBS remains the primary surfactometer used in clinical investigations.

The PBS has certain drawbacks. This device is normally designed to trace ΔP with time, from which γ is easily evaluated at minimum and maximum bubble size. The fixed 50% surface area reduction during pulsation has little physiological relevance, since the surface area of the lung varies less than 20% during normal tidal breathing. Similar to the Langmuir trough, film leakage in the PBS, mostly by material coating the capillary tube to which the air bubble is suspended, hinders the rate at which the film reaches low γ.

https://doi.org/10.1021/acs.chemrev.3c00146
Chem. Rev. 2023, 123, 13209−13290

This problem was particularly apparent with the commercially available chambers. Consequently, the PBS can require up to 100 pulsations, i.e., up to 5 min, before showing meaningfully low γ. The low γ value output by the PBS is not completely reliable because the γ is determined by assuming a spherical bubble so that the simplified Laplace equation (eq 1, $\Delta P = 2\gamma/R$) can be used to calculate γ. At low γ (<5 mN/m), the spherical bubble assumption does not hold true. However, it is obvious that γ is very low. Since the PBS is operated by lowering the pressure to less than atmospheric, at times small air bubbles can be sucked into the surfactant chamber. Once this happens, the experiment needs to be stopped and repeated.

Still, during the early years of investigation the PBS provided a bridge from the Langmuir trough to more realistic surface films and allowed initial studies of the adsorbed rather than spread films, at realistic dynamic cycling rates. This changed the perception of pulmonary surfactant function. Currently, the PBS remains the predominant device used for clinical studies. This is because it is a relatively fast screening technique, with samples being analyzed in ∼10 min. This approach also provided important further support for the need for highly enriched DPPC films to attain low γ (for further details see refs 13, 159, 160, and 165). This device proved instrumental in the development of several of the clinical surfactants.

4.2.3. Captive Bubble Surfactometer. The captive bubble surfactometer (CBS) was invented by Samuel Schürch in 1989.[166] It is the first fully functional *in vitro* biophysical model capable of simulating and evaluating biophysical properties of pulmonary surfactant films under physiologically relevant conditions. Compared to the PBS, the CBS uses a much larger air bubble (2−7 mm in diameter) submerged in a surfactant suspension and floating against a hydrophilic ceiling (Figure 7c). The bubble is separated from the ceiling by a thin wetting film of the surrounding aqueous fluid, in other words, "captured" by the liquid phase, thus eliminating all potential pathways for film leakage. The γ is derived by analyzing the bubble shape using the height-to-diameter ratio of the bubble,[167] or using axisymmetric drop shape analysis (ADSA).[168−170] The CBS is capable of assaying the biophysical properties of pulmonary surfactant films, including their rapid adsorption and near-zero γ during quasi-static or dynamic cycling with extraordinary film stability.[171] In addition to being able to directly assess these surfactant properties, researchers have been able to apply the CBS to obtain novel experimental evidence. For example, the finding that pulmonary surfactant films possessed a multilayered architecture comprising the so-called surfactant reservoir was based on γ measurements using this apparatus.[172]

In spite of its exceptional capability for biophysical studies on pulmonary surfactant, the CBS also has a few limitations. The CBS is designed to study adsorbed surfactant films. Although a spreading technique has been developed for the CBS,[173] it is technically challenging to study spread films, since the bubble is submerged in a liquid phase. The CBS can normally be used only to study low surfactant concentrations, usually no more than 2 mg/mL, because surfactant suspensions become murky or even opaque at higher concentrations, which makes γ measurements from the shape of the bubble challenging. This limitation can be circumvented by spreading a high-concentration surfactant suspension around the bubble surface using a microsyringe.[174] However, to ensure that the surfactant suspension is restricted to the bubble surface efficiently, the saline subphase needs to be modified by increasing its density with 10 wt % sucrose. This precludes stirring, but the aqueous deposit is very thin. Compared to the PBS, operation and data processing of the CBS are much more complicated and time-consuming. The CBS lacks control of environmental factors influencing the gas phase of the bubble. There has been a general concern that the bubble is not saturated with water vapor and, hence, fails to mimic the 100% relative humidity in the lung.[175,176] Compared with the Langmuir trough, the CBS lacks the capacity of being incorporated with microscopy and analytical techniques, since the air−water surface of the bubble is submerged in a liquid phase. In addition, it cannot be used to prepare Langmuir−Blodgett films.

That said, the CBS system allowed for precise evaluation of various factors on surfactant adsorption processes and study of the biophysical properties at various rates and ratios of compression and as a function of temperature. As such it has become the go to apparatus for detailed examination of surfactant properties (for further details, see refs 13, 160, and 177).

4.2.4. Constrained Drop Surfactometer. The current constrained drop surfactometer (CDS) was developed by Yi Zuo in 2015.[29] A key feature of the CDS is a carefully machined droplet pedestal (3−5 mm in diameter), initially designed by Wilhelm Neumann,[178] which uses its knife-sharp edge to maintain the droplet integrity, even at very low γ. The droplet pedestal provides a leakage-proof environment so that the surfactant film is "constrained" at the air−water surface of the droplet without leaking over the pedestal (Figure 7d). The sessile droplet is enclosed in an environmental control chamber that facilitates rigorous control of the experimental conditions, including physiologically relevant temperature, relative humidity, gas composition, and aerosol concentrations.

The CDS constitutes a new generation of droplet-based surfactometry. It has been proven to be an ideal *in vitro* biophysical model for studying pulmonary surfactant films under physiologically relevant conditions. The CDS combines the advantages of the Langmuir trough, PBS, and CBS and removes some of their disadvantages for studying pulmonary surfactants. The CDS can be used to study either adsorbed films or spread films. When studying adsorbed pulmonary surfactant films, the CDS only requires a very small sample (<10 μL per measurement), i.e., the size of a single droplet, considerably smaller than the sample volume for the PBS or CBS. The CDS also eliminates the concentration limitation of the CBS for studying adsorbed films, since the drop shape analysis is not affected by the surfactant concentration. When studying spread surfactant films, the CDS works as a miniaturized Langmuir film balance, as the air−water surface of the droplet can be readily accessed by a microsyringe for spreading.[30] The CDS can be easily incorporated with various microscopy and analytical techniques to study the lateral structure and phase behavior of the pulmonary surfactant films. The air−water surface of the CDS is readily accessible with an upright fluorescence or confocal microscope. An *in situ* Langmuir−Blodgett transfer technique has been developed to transfer the surfactant film from the air−water surface to a solid substrate to allow topographic analysis with atomic force microscopy (AFM).[29,30] A novel subphase replacement technique has been developed for the CDS to allow AFM imaging for adsorbed surfactant films.[31] This subphase replacement technique is capable of washing away excess

https://doi.org/10.1021/acs.chemrev.3c00146
Chem. Rev. 2023, 123, 13209−13290

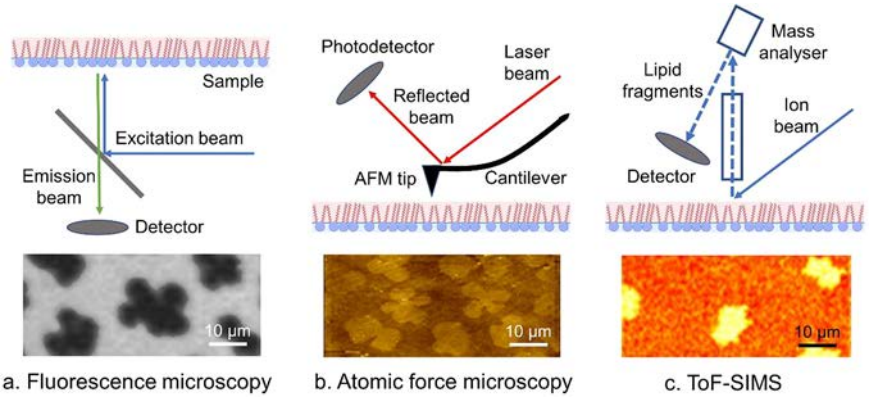

Figure 8. Schematics of and images from (a) fluorescence microscopy, (b) atomic force microscopy, and (c) time-of-flight secondary ion mass spectrometry (ToF-SIMS). The images are from identical monolayers composed of DPPC and DOPG in 3:1 molar ratios, which are compressed on a Langmuir trough to 18 mN/m at 22 °C. The fluorescence image in (a) is from the air−water interface, while the atomic force microscopy and ToF-SIMS images in (b) and (c) are from Langmuir−Blodgett films deposited on a mica surface. It is important to note that the Langmuir−Blodgett films are faithful representations of the structures and compositions at the air−water interface. All images are 60 μm wide. Images courtesy of Nils Petersen (unpublished data).

(i.e., unattached) surfactant vesicles in the droplet while maintaining constant volume, surface area, and γ of the pulmonary surfactant droplet. This technical advance provides an important bridge between Langmuir−Blodgett transfer and AFM, thus allowing direct AFM imaging of adsorbed surfactant films. New data obtained with this method have established the foundation for the updated model presented in this review. Very recently, the CDS has extended its application for pulmonary surfactant and PL self-assembly from the air−water surface to the oil−water interface.[179−181]

A fully automatic mechatronic system, called closed-loop axisymmetric drop shape analysis (CL-ADSA), has been developed to control the CDS.[182] CL-ADSA is capable of determining the surface properties of a droplet in real-time, including its γ, surface area, and volume, and thus controlling these properties by a proportional-integral-derivative feedback control loop. The CL-ADSA transforms ADSA from a γ measurement methodology to a single-droplet-based control platform. As a result, the time required to conduct studies is very short, even compared to the PBS. Most importantly, the CL-ADSA enables droplet oscillation to follow well-defined sinusoidal waveforms, thereby allowing for the study of interfacial dilational rheology, which provides novel implications about the viscoelastic properties and chemical composition of the interfacial monolayer.[183] The CDS has evolved into a versatile experimental platform capable of various surfactant and lipid related studies, such as interfacial rheology,[183,184] surface thermodynamics,,[30,185,186] lipid−protein interactions,[187,188] toxicology of nanomaterials,[29,189−195] health impact of e-cigarette aerosols,[196,197] synthesis of biomaterials,[198] and biophysical studies of tear films[199−201] and xylem surfactants.[202,203]

4.3. Lateral Structure and Phase Separation

4.3.1. Fluorescence Microscopy. Fluorescence microscopy was one of the earliest microscopy techniques applied to pulmonary surfactant research.[204] The fluorescence microscope, and its high-resolution variant, the confocal microscope, is an optical microscope in which fluorescence dyes, or fluorophores, are excited with an illuminated light and subsequently emit light at a longer wavelength (Figure 8a). When the pulmonary surfactant film is doped with a small amount of fluorescent lipid dye, usually <1%, fluorescence microscopy can be used to determine PL phase separation and lipid−protein interactions. Fluorescent dye-labeled PLs selectively partition into the disordered liquid-expanded (LE) phase, thus setting an optical contrast against the dark dry-excluded tilted-condensed (TC) phase.[205,206] Fluorescence microscopy opens a new horizon for directly visualizing PL phase transition and separation *in situ* at the air−water surface. However, restricted by the diffraction limit of light, it is challenging to detect any feature in the pulmonary surfactant film with a lateral dimension much less than 1 μm using fluorescence microscopy. Moreover, it is known that the addition of fluorescence dye, even at very small levels, can affect the lateral organization of pulmonary surfactant monolayers.[207,208]

4.3.2. Atomic Force Microscopy. Atomic force microscopy is a scanning probe microscopy technique. It determines the lateral structure and topography of a surface by raster-scanning the surface with a nanometer-sized probe mounted on a flexible spring called a cantilever (Figure 8b). While scanning the sample with a piezoelectric scanner, the probe maintains a constant distance from the sample, by deflecting the cantilever to closely track the topography of the surface. The degree of cantilever deflection is determined with a quadrant photodiode detector. Resolution of the AFM can easily extend to the submicron level in the lateral dimension and to the subnanometer level in the vertical dimension. The latter allows the detection of PL phase separation since AFM can easily discern the ∼1 nm height differences between the ordered TC domains and the surrounding disordered LE phase.[64,209] The AFM allowed the discovery of PL nanodomains in pulmonary surfactant monolayers, which are invisible with fluorescence microscopy.[210,211] In addition, since AFM provides structural information of the surfactant film with one more dimension than traditional fluorescence microscopy, it led to experiments proving the existence of multilayered structures with compressed surfactant films.[212,213]

There are some disadvantages of the AFM experiments on these films. Potential artifacts can arise from the Langmuir−Blodgett transfer process, since it cannot image the surfactant film *in situ* at the air−water surface.[214] Therefore, AFM measurements on LB films must be conducted on films without a substantial aqueous subphase and in some cases on

https://doi.org/10.1021/acs.chemrev.3c00146
Chem. Rev. 2023, 123, 13209−13290

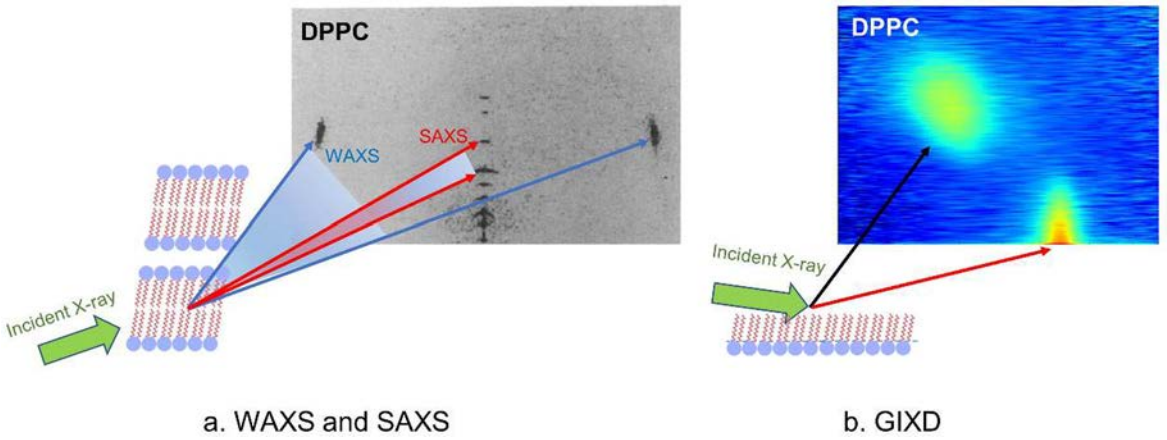

Figure 9. Schematic representations of X-ray scattering techniques for studying bilayer and monolayer structures. (a) Wide-angle X-ray scattering (WAXS) and small-angle X-ray scattering (SAXS). The green arrow represents the incident X-rays on an oriented multilamellar bilayer lipid sample. The blue arrows represent the WAXS scattering in the near-horizontal direction from the periodicity of the lipid chains. The red arrows represent the SAXS, scattering in the vertical direction from the periodicity of the multiple layers of lipid. The image of the X-ray diffraction is from a fully hydrated sample of DPPC at 25 °C. Adapted with permission from ref 221. Copyright 1992 Cell Press. (b) Grazing incidence X-ray diffraction (GIXD). The green arrow shows the incident X-ray at a grazing (very low) angle and the scattering from a monolayer of lipids in the tilted-condensed phase. The black and red arrows represent the scattered X-rays. The image shows the intensities of scattered radiation in the plane of (horizontal axis) and perpendicular to (vertical axis) a deposited monolayer of DPPC on water at a π of 30 mN/m and at 23 °C. Adapted with permission from ref 222. Copyright 2016 American Chemical Society.

"dry" films. However, as seen in Figure 8, the Langmuir–Blodgett transfer technique appears to provide a faithful representation of the structures at the air–water interface, because a very thin layer of water remains bound to the substrate. In comparison to fluorescence microscopy, AFM has a relatively small field-of-view, usually less than 100 × 100 μm^2.

The AFM measurements on Langmuir–Blodgett films of pure lipids, lipid mixtures, and surfactant preparations have provided exquisitely detailed information about the phase and mixing behavior of these lipids and provided evidence for the strong correlation between the phases observed in monolayers and in bilayers, as discussed in Section 3.

4.3.3. Time-of-Flight Secondary Ion Mass Spectrometry. Time-of-flight secondary ion mass spectrometry (ToF-SIMS) is a powerful surface imaging and analytical technique.[215] It operates by bombarding a sharply focused primary ion beam onto the sample surface, which induces a collision cascade among the target atoms (Figure 8c). This leads to desorption of neutral and ionized fragments of the molecules on the surface, which are collected and analyzed by a mass spectrometer to allow identification of these molecules. The high-energy beam is raster scanned across the sample to yield an image for each mass fraction (over 5 million measurements per scan), providing spatially localized, detailed compositional information. The ToF-SIMS technique is superior to fluorescence microscopy and AFM by providing correlated information of the lateral structure and chemical composition of the pulmonary surfactant film.[216,217] This provides a two-dimensional chemical map of the surface. Since many of the fragments from PL are very similar, the use of specifically deuterium labeled lipids has helped in the detailed location of the major lipid species. As with the AFM measurements, there are some drawbacks of the ToF-SIMS measurements. They are also measured on Langmuir–Blodgett films and, thus, may be subject to artifacts from the transfer. The measurements are made in a vacuum. Hence, the films are certainly dry. The spatial resolution is limited to the focus of the ion beam, typically about 1 μm. Mass resolution is limited to about one mass unit, so there can be some ambiguity in the identification of some species, which can be alleviated by using isotopic labeling.

The ToF-SIMS images have provided direct evidence in understanding the mechanisms of lipid–protein interactions and squeeze-out of fluid lipids from the pulmonary surfactant monolayer.[218−220] Such studies have also generated unique insights into PL:PL localization, for example the initial indication that DPPG co-localizes with DPPC in the TC phase of monolayers.[219]

4.4. Bilayer and Monolayer Structures and Dynamics

4.4.1. X-ray Scattering. Scattering of electromagnetic radiation of all wavelengths is deployed extensively to study the chemical, physical, and biological properties of matter. The scattering process, and the information it provides, depends on the wavelength of the incident electromagnetic radiation, but generally it provides structural or dynamic information.

X-ray scattering uses electromagnetic radiation in the range of wavelengths from fractions of nanometers to several nanometers to examine the scatter produced by electrons in the material being studied. If there is any periodicity in the material, such as crystal structures, then the scattered radiation will create patterns of high and low intensities on the detector, which can be interpreted in terms of the underlying periodicity. In the context of lipid membranes, there are three major sources of periodicity: the periodicity within the bilayer created by parallel lipid chains and organization of the headgroups; the periodicity of the bilayer itself, i.e., the pattern of a headgroup layer, two layers of lipid chains, and another headgroup layer that can define the bilayer thickness; and the periodicity of multiple bilayers, which reveals the thickness of hydration between bilayers as well as the bilayer thickness.

The Bragg Law of scattering, or diffraction, relates the periodicity of the structure, described by the parameter, d, to the angle at which the high intensity of the scattered beam is observed, described by the parameter θ and the wavelength, λ, of radiation used, $n\lambda = 2d \sin \theta$, where n is a number describing

https://doi.org/10.1021/acs.chemrev.3c00146
Chem. Rev. 2023, 123, 13209−13290

whether it is the first, second, or higher scattering angle. The high intensity arises from the constructive interference of the scattered radiation at that particular angle. It is evident that there is an inverse relationship between the periodicity of the structure and the angle at which the constructive interference is observed. Thus, small periodicities, such as distances between lipid chains, are observed at wide angles, while large periodicities, such as bilayer thickness, are observed at small angles.

There are two major types of X-ray diffraction commonly used to study lipid systems.[223] First, wide-angle X-ray scattering (WAXS), illustrated by blue arrows in Figure 9a. This reveals detailed information about the structure of the lipids within the bilayer, here the distance between the palmitic acid chains. WAXS has provided the structural details of the L_{α}, L_{β}, and $L_{\beta'}$ phases in bilayers, and by inference of the LE and TC phases in monolayers. Second, small-angle X-ray scattering (SAXS), illustrated by red arrows in Figure 9a.[221] This reveals information about the structure of the bilayers, such as their thickness and their separation, and has led to additional information about the bilayer phase information, as well as the state of hydration. Differences in bilayer thickness in different phases measured by SAXS have been correlated exactly with differences in monolayer heights observed by AFM.

The X-ray diffraction pattern shown in Figure 9a was the first experimental evidence for the $L_{\beta'}$ phase, where the lipid chains are tilted. This is seen by the WAXS diffractions being above the horizontal axis in the image. Nontilted chains would cause these diffraction patterns to be precisely located at the horizontal axis. The angle above the horizon shows that the chains are tilted at about 27°. The distance between the chains at this temperature was measured to be 0.42 nm.

The SAXS diffraction shows multiple spots in the vertical direction which arise from multiple periodicities in the direction perpendicular to the multilayers, for example from headgroup to headgroup within a bilayer (its thickness), or between adjacent bilayers (the thickness of the water layer), or between the top of one bilayer and the top of the next (the lamellar periodicity, or *d*-spacing). In this case, the *d*-spacing was about 5.9 nm.

In most experiments, the WAXS or the SAXS is observed on samples where the incident X-rays pass directly through the sample and are observed on a detector at the other side. Thus, the information is relevant to the bulk of the material. Grazing Incidence X-ray Diffraction (GIXD) is a technique where the X-rays are incident at a small angle and the scattered radiation is observed from the same side (Figure 9b).[224] The low angle of incidence ensures that the scattering is confined to the structures close to the surface, so this is a surface sensitive technique and only the periodicities at the surface are detected. It is therefore ideal for studying monolayers at the air−water surface.

The GIXD of the image shown in Figure 9b was used to show that the tilt angle of the palmitic acid chains in the monolayer was about 27° and the thickness of the monolayer was close to 2.5 nm.[222,225] The chain-to-chain separation varied between nearest neighbor and next to nearest neighbor from 0.43 to 0.46 nm.

X-ray diffraction tools are incredibly powerful tools, since they provide extraordinarily detailed structural information about all types of materials, from nanomaterials, to proteins, to membranes. With the advent of high-intensity X-ray sources in synchrotrons, the information can now be collected so quickly that it is even possible to study dynamic changes in the structures. Synchrotron radiation sources can also be focused on smaller samples, so sample size is less critical. The limitation with X-ray diffraction is often in the preparation of the sample. It needs highly ordered samples to provide good diffraction patterns. The analysis and interpretation of diffraction data are complex. They usually require a mathematical model, which is used to fit the data iteratively until the best match between model and data is found. Fast computational tools have, however, made this a less cumbersome aspect of the technique.

4.4.2. Spectroscopic Techniques. Over the years a number of spectroscopy techniques have been applied to study the structure and dynamics of lipid membranes in particular, but to a lesser extent to study monolayers.[226] Of these, nuclear magnetic resonance (NMR) has been particularly useful.[227,228] NMR probes the environment of nuclei with magnetic spin, such as hydrogen, phosphorus, and deuterium, in several ways: (1) by the energy needed to cause spin transitions, also known as the NMR spectrum, which reveals information about the electronic environment; (2) by the coupling between nuclear spins, which reveals information about the bonding and spatial connection between nuclear spins or their relative positions in space; and (3) through the rates of relaxation when the nuclei are transiently put into an excited state, from which they can decay by spin−spin relaxation mechanisms, or spin−lattice relaxation mechanisms, which provide important information about the dynamics of the part of the molecule that is detected.

In the context of lipid membranes, hydrogen NMR has been very useful at determining the degree of order—measured by an order parameter—of the lipid chains in various phases. It has also been very useful in establishing the rates of motion of segments of lipid chains as well as the rotational rates of whole lipid molecules. For example, it has been shown that in the L_{α} phase there are rapid motions of the segments of lipid chains at the time scale of nanoseconds and that there are oscillations of the whole chains at the time scale of microseconds.[229,230] NMR of lipids specifically substituting deuterium isotopes for hydrogen has been instrumental in determining the phase behavior of lipid systems. In this case, the spectrum of the deuterium signals can show which phase the lipid membrane assumes. This is a complex analysis but has led to determination of the entire ternary phase diagram of DPPC:POPC:cholesterol.[133,134]

Phosphorus NMR has likewise been an invaluable tool in determining the structural organization and dynamics of the headgroups of PL bilayers. The spectrum is sensitive to orientation, dynamics, and environment, including the state of hydration of the lipid.

The disadvantages of NMR include the lack of sensitivity—it requires relatively large samples. It is also a measure of the bulk of any sample and is therefore an averaging technique. It cannot be applied to monolayers. It also requires that there be NMR active nuclei in the material of interest. Nonetheless, a lot of structural and dynamic information has been provided by NMR and it remains a viable tool for studying membrane systems.

4.5. Molecular Dynamics Simulations

Molecular dynamics (MD) is a computer simulation method in which physical motion and collision of atoms and molecules are simulated by following Newton's laws of motion. By

https://doi.org/10.1021/acs.chemrev.3c00146
Chem. Rev. 2023, 123, 13209−13290

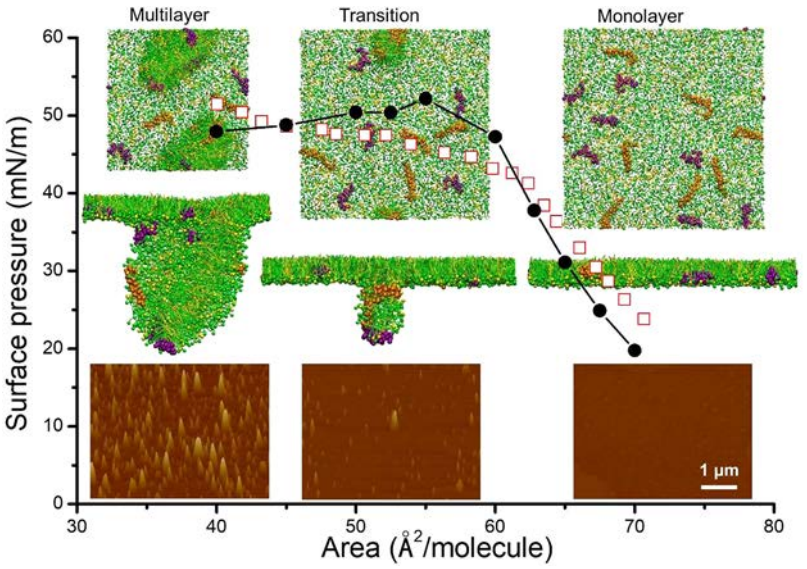

Figure 10. Comparison of computer simulated and experimentally obtained molecular organization and lateral structure of a pulmonary surfactant monolayer upon compression. The model pulmonary surfactant monolayer is constructed with 1,120 coarse-grained (CG) DPPC (green) and 480 CG POPG (yellow) molecules (7:3), doped with 7 CG SP-B[1−25] (purple) and 7 CG SP-C (orange) molecules. The solid circles indicate the computer simulated compression isotherm, while the open squares indicate the experimentally measured compression isotherm using a Langmuir trough. The insets show the lateral structures of the pulmonary surfactant film throughout the plateau region of the compression isotherms. At each compression stage (monolayer, transition, and multilayer), both the top view and side view of the computer simulated film and AFM images of an Infasurf film are shown in a column. The lateral dimension of the computer simulated film is 31 × 31 nm^2. The scan area of the AFM images is 5 × 3.75 μm^2; and the full z-range is 20 nm. Results from the computer simulation and the experimental methods demonstrate good agreement. Both methods are qualitatively consistent in showing a pressure-driven monolayer-to-multilayer transition during the plateau region of the compression isotherm. Adapted with permission from ref 231. Copyright 2013 American Chemical Society.

applying molecular mechanics potentials, a preset number of molecules, from a few hundreds to millions, are allowed to interact with each other, with certain initial positions and velocities, in a computer-simulated virtual space for a certain period of time until an equilibrium is reached. Thermodynamic and kinetic properties of the system can be estimated by analyzing the simulation configurations and trajectories with statistical mechanical theories. MD simulations have been applied to pulmonary surfactant research.[36] They are particularly useful for studying the molecular mechanisms responsible for lipid−lipid, lipid−protein, and lipid−protein-nanoparticle interactions. To date, MD simulations have been used to study the collapse mechanism of pulmonary surfactant monolayers,[34,35] adsorption of PL vesicles,[37] and nanoparticle interactions with pulmonary surfactants.[231−233] A major limitation of the MD simulation technique is its restriction in the length scale and time scale of simulations. Restricted by the computational power, most MD simulations are currently limited to a length scale of no more than a few nanometers and a time scale of only a few nanoseconds to milliseconds. Coarse-grained (CG) modeling omits less critical features, such as hydrogen atoms, in order to more efficiently utilize computer storage capacity. Consequently, CG modeling is able to extend the simulated length and time scales, but not yet to an extent directly comparable to experimental observations. Figure 10 shows a qualitative comparison of the MD simulated and experimentally obtained results of a pulmonary surfactant film. The lack of direct quantitative experimental verification puts a general caveat on MD simulations.

4.6. Physiological Assays

There are two important and general limitations to almost all of the biophysical methodologies described above. The first is that most surfactometers and other methods use area compressions that range from 20 to 50%. Although accurate *in vivo* values are difficult to obtain, these experimental values are considered higher than the surface area change that occurs in the lung, at least during regular breathing.[125,153,234,235] A second limitation is that the biophysical studies are usually performed using a clean interface as a starting point. With the possible exception of the formation of the surfactant film at birth in which the interface may be relatively clean, such clean interfaces do generally not exist under physiological conditions. These limitations should be considered when interpreting the results utilizing the various biophysical methodologies. Furthermore, physiological assessment, linking or correlating the biophysical approaches, is of critical importance. In fact, the physiological role of surfactant is a constant thread throughout all studies into the biophysics of surfactant function. The discovery and clear importance of surfactant in the *in vivo* lung initiated this field of study; investigations into the biophysical properties of surfactant in health and disease have helped to establish the physiological and clinical significance; and developing new exogenous surfactant treatment strategies for various clinical conditions remains an important future goal.

From this methodological perspective, we will focus solely on models of surfactant deficiency to test the function of exogenously administered surfactants, since this approach specifically addresses the properties of surfactant *in vivo*. A second, surfactant-specific approach, the microdroplet method, to measure γ in the intact lung *in situ*, has been reported. To date, this sophisticated approach, which utilizes the shape of a water immiscible liquid with known γ on top of the surface film to estimate γ, represents the only direct assessment of γ within the lung. This technically difficult technique has not been

https://doi.org/10.1021/acs.chemrev.3c00146
Chem. Rev. 2023, 123, 13209−13290

further utilized beyond the original landmark findings (for more details, see refs 234−237).

It is also appreciated that many other physiological studies have made significant contributions to our understanding of surfactant function. However, the methodology for these is more generic rather than surfactant focused. These include characterization of, and experimentation with, genetically modified mice, studies on the physiological processes associated with pregnancy, birth, aging, sex, exercise, and other life-style choices, and animal models of specific lung injuries and other pulmonary challenges.

The most straightforward method to test the efficacy of a surfactant preparation *in vivo* is to intratracheally administer the material to surfactant-deficient animals and observe the physiological response (i.e., blood oxygenation and lung compliance). Surfactant deficiency can be obtained either by using premature animals or by removing the surfactant from the lungs of adult animals by full lung lavage. In addition to testing a surfactant's biophysical function, both models can be utilized to study multiple aspects of surfactant administration such as delivery method, ventilation mode, surfactant distribution throughout the lung, metabolism of the exogenously administered material, and others.

Testing surfactant function in premature animals has been performed mainly in rabbits and lambs. Fetuses are delivered prematurely at a time-point during gestation at which the lungs are still surfactant-deficient and are connected to a mechanical ventilator. Surfactant is usually instilled directly into the lung *via* a bolus injection of a suspension through the trachea. The main outcome monitored in fetal rabbit experiments is lung compliance during ventilation, whereas in lambs, blood oxygenation is also easily measured. The advantages of these premature models for assessing surfactant function are (1) its clinical significance, since they reflect infants with surfactant deficiency, and (2) its reproducibility in terms of surfactant deficiency and responses. Disadvantages include (1) the technical expertise required, the expense, and the time-consuming nature of experiments involving timed pregnancies and caesarean sections and (2) that outcomes can be affected by other factors than those associated with the biophysical properties of the exogenous surfactant, such as dosing (concentration and volume), the mechanical ventilation technique utilized, the metabolism of the exogenous surfactant, and the method of surfactant administration.

The lavage model of surfactant deficiency has been employed using rats, rabbits, sheep, and pigs. In these experiments, healthy animals are connected to a mechanical ventilator and are instrumented with arterial lines to monitor blood gases. Following baseline measurements, animals are disconnected from the ventilator and the lungs are lavaged with 37 °C saline. This washing procedure is repeated several times until the animals display low oxygenation values, which are used as a surrogate for surfactant deficiency. Subsequently, animals can be administered exogenous surfactant and monitoring includes blood gases and compliance during mechanical ventilation. Advantages of the lavage models of surfactant deficiency are (1) the procedures are relatively straightforward, (2) these models are less expensive than those involving premature animals, (3) baseline measures prior to surfactant deficiency are obtained as a reference point for responses, and (4) they can be performed on a diverse set of mammals. Disadvantages are that (1) the lavage procedure may cause lung injury and inflammation beyond surfactant deficiency, (2) similar to the prematurity models, outcomes can be affected by other factors beyond just surfactant biophysics, and (3) there is variability in the number of lavages required to generate surfactant deficiency, leading to different lengths of time the animal is on the ventilator.

Overall, models of surfactant deficiency have contributed to our understanding of surfactant function and provide an essential approach to validate biophysical *in vitro* observations. They also provide an essential preclinical test for the development of new clinical exogenous surfactants.

4.7. Brief Synopsis of Methods Used to Study Pulmonary Surfactants

While the individual methods discussed in this segment have provided detailed insights into the biophysical properties of surfactant films, it is the combination of outcomes from multiple techniques that has provided our current state of knowledge as presented in this review. Just as the surfactant is a complex material, the information about its function presents a complex picture that needs systematic and detailed assessment.

One of the most promising tools for future research, the constrained drop surfactometer (CDS), was recently redesigned to study the structure of adsorbed films. It probably provides the closest *in vitro* mimic of the *in vivo* surfactant film and will begin to narrow the current gap between the biophysical measurements and their importance to physiological applicability. As the quest for understanding continues, there will probably be new and elegant techniques that can be applied to further illuminate the mighty thin film that surfactants provide in the lung.

5. HOW DOES PULMONARY SURFACTANT ADSORB RAPIDLY?

The ability of pulmonary surfactant to adsorb rapidly to form a surface-active film has long been considered a hallmark of pulmonary surfactant function. Physiologically, this property is essential for newborns to rapidly establish air breathing. In this scenario, the endogenous pulmonary surfactant, present within alveolar Type II epithelial cells as lamellar inclusion bodies, fuses with the plasma membrane during secretion.[238,239] Secreted surfactant forms large multilamellar structures that can rapidly adsorb to the air−water surface to form a film that reduces γ.[9,240−242] Isolated natural and clinical surfactants primarily consist of large bilayer vesicles that are structurally comparable to, and display similar overall properties as, multilamellar particles formed *via* exocytosis of lamellar bodies.[241,243] Significant progress has been made in deciphering the potential roles of specific surfactant constituents.

5.1. Role of Surfactant Lipid Structures in Adsorption

The inherent problem faced by the lungs is that disaturated PLs, such as DPPC, the major single molecular species (35−50%) in pulmonary surfactants, adsorb extremely slowly and incompletely.[37] Unsaturated PLs adsorb much more quickly, but are incapable of sustaining the high compressions necessary to achieve high π. Furthermore, this adsorption is still much too slow to sustain life. As will be described below, the hydrophobic proteins, SP-B and SP-C, have been shown to facilitate adsorption, both individually and together. However, there have also been suggestions that some of the minor lipid components of surfactants contribute to PL adsorption. The premise of this theory is that PL adsorption shares several characteristics with the fusion of bilayer membranes, a process

https://doi.org/10.1021/acs.chemrev.3c00146
Chem. Rev. 2023, 123, 13209−13290

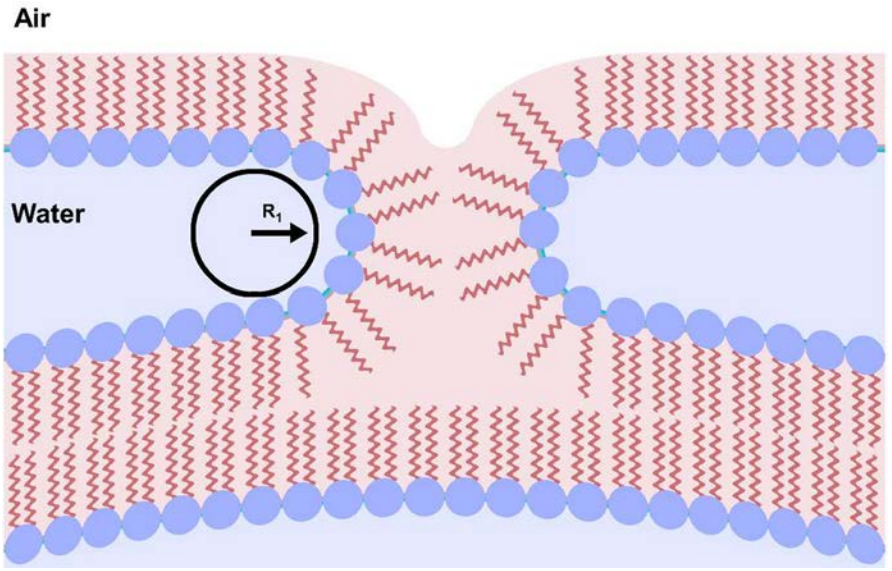

Figure 11. Model depicting the role of negative curvature in a bilayer−monolayer transition. Adsorption corresponds to a hemifusion that occurs at the air−water interface to form an attached monolayer. It illustrates the advantage of a smaller headgroup in the PL or other molecular entities that can facilitate the formation of neck-like hemifusion structures. R_1 designates the negative curvature at the level of the PL phosphates. Adapted with permission from ref 26. Copyright 2008 Elsevier.

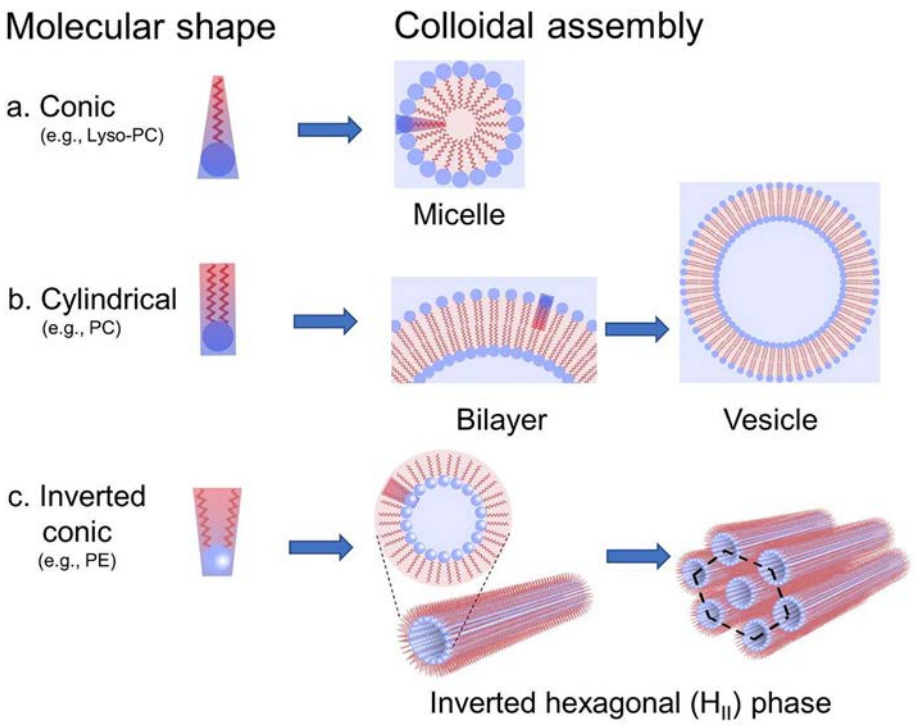

Figure 12. Schematic representation of the relation between the molecular shape of the lipids in surfactants and the membranous structures they can form. (a) Conic: Lyso-PC and many detergents are inverted cone shaped and can form micelles, where the polar, usually ionic, headgroups are larger that the hydrophobic tails. The headgroups of the lipids protect the hydrophobic tails from contact with water. Micelle centers are filled by the hydrophobic tails. Such structures are relatively stable but can easily transfer molecules to the air−water interface. (b) Cylindrical: Most PLs, such as PC and PG, have a cylinder-like shape. These lipids form bilayers with the headgroups of both leaflets facing the water and the lipid chains facing each other. The headgroups tend to be hydrated and shield the lipids from exposure to water, although water can transiently cross the bilayer. While flat bilayers are more stable, these structures normally form enclosed vesicles to limit hydrocarbon−water interactions. These possess curved bilayers, where smaller vesicles are more strained, because greater curvature induces greater strain. These lipids can form multilamellar vesicles, structures with multiple concentric bilayers. (c) Inverted conic: Some PLs such as PE, with smaller headgroups and larger lipid tails, are inverted cone shaped and can form inverse micellar structures. At higher temperatures and low water content, they can form an inverted hexagonal phase (H_{II} phase) which contains cylindrical structures enclosing a water core. In order to limit water interactions, these cylinders can arrange in a hexagonal pattern.

https://doi.org/10.1021/acs.chemrev.3c00146
Chem. Rev. 2023, 123, 13209−13290

facilitated by the presence of surfaces with negative curvature (Figure 11).[26] This section examines the structural features of surfactant lipids, including the minor components, and then, more specifically, the manner in which these structures could influence surfactant adsorption. Considering the role of the hydrophobic proteins in adsorption, the ways that the lipid structures are affected by these proteins are also discussed.

The ease by which individual PL species adsorb to the air−water surface is related to their molecular shapes (Figure 12). Lipids aggregate to form structures that minimize exposure of the hydrophobic groups to water because of the hydrophobic effect.[244] These structures also tend to maximize hydrophilic group−water interactions.

Lysophospholipids, including lyso-PC, *bis*(monoacylglyero)-phosphate, and short chained PC (diC2−diC6) have headgroups that are larger in area than the hydrophobic tails, creating a "cone shape" allowing them to form micelles (Figure 12a). Most detergents can also form micelles. Micelles can spontaneously adsorb to the air−water interface to form so-called "Gibbs soluble films". This likely occurs because the shielding of the water-repelling regions is incomplete, facilitating the formation of monolayers. With these films, the monolayers do not expose the hydrophobic chains to water and are stable. However, they remain in equilibrium with the subphase micelles. Therefore, soluble films reversibly form micelles when subject to lateral compression, without significant further reduction of γ.[13,126,157]

Most of the PLs in surfactants, such as saturated and unsaturated PC and PG, have headgroups and lipid chains of comparable cross-sectional areas. They are shaped like cylinders and readily form bilayers (Figure 12b). Single unilamellar and multilamellar bilayer vesicles are relatively stable, because the exterior charged polar groups effectively exclude water from interacting with the internal nonpolar constituents. Consequently, these lipids are ill fitted to accommodate the spatial requirements for such adsorption structures and adsorb relatively slowly. When spread at an air−liquid interface they form "Langmuir insoluble films" that lower γ during monolayer compression and rapidly increase γ during film expansion, thereby generating hysteresis loops.

Some of the minor components of surfactants, such as PE and plasmalogens, have headgroups that are smaller than the lipid chains and are shaped like an inverse cone. They can form non-bilayer structures such as the hexagonal II (H_{II}) phase, composed of cylinders with the headgroups lining an aqueous cylinder, with the fatty acids extending outward. These cylinders align to form extended lipid−water complexes (Figure 12c).[13,245,246] When mixed with PC bilayers, they can support negative curvatures as illustrated in Figure 11.

At low temperatures, PE forms bilayers. As temperature is increased, PE bilayers convert from the $L_{\beta'}$ to the L_{α} phase and then, as the acyl chains become very mobile, transition into the H_{II} phase (Figure 12c). When in the H_{II} configuration, PE rapidly adsorbs to equilibrium γ. Mixtures of POPE (16:0/18:1-PE):DPPC (1:1 mol/mol) and POPE:DPPC:POPG (10:8:1 mol/mol) also rapidly adsorb to equilibrium, as do mixtures of DOPE:DPPC:cholesterol (7:3:5 mol/mol).[247,248]

Addition of SP-B at low levels lowers the temperature at which POPE undergoes the lamellar-to-inverse hexagonal phase transition.[249,250] Moreover, addition of the hydrophobic proteins at low concentrations to DOPE:POPG (9:1 wt/wt) reduces the diameters of the H_{II} phase cylinders, providing clear evidence for enhanced negative curvature.[251] Whether this effect is specifically related to pulmonary surfactant function is unclear. Addition of amphipathic proteins, like Gramicidin A, also promotes formation of dioleoyl-PC bilayers to the H_{II} phase and their adsorption to equilibrium.[252]

In addition to the H_{II} phase, PE can also generate cubic phases, such as the inverse bicontinuous cubic phase. These structures comprise a group of structurally similar isotropic lipid structures, which typically present as viscous, optically transparent gels. The entire formation is composed of bilayers with a saddle shaped, continuous negative curvature. These cubic phases possess fusogenic properties,[253−256] and so could also be involved in PL adsorption. Evidence exists for such structures in pulmonary surfactant.[250] For example, when cooled from the high-temperature H_{II} state, in the absence of SP-B, POPE can form inverse continuous cubic phases.[249,250] With ∼1% SP-B, wt/wt, cubic phase but no H_{II} phase is detected. This conversion is detected at lower temperatures than with the pure lipid. SP-C on the other hand did not promote cubic phase formation. These findings are consistent with SP-B either promoting the formation or stabilizing the presence of the hypothetical adsorption structures.[249,250,257]

Addition of the cone shaped lyso-PC to total surfactant lipids should induce positive curvature. This can disturb the normal lamellar structure sufficiently to produce a slight increase in adsorption, but this enhancement does not attain equilibrium. In contrast, when added to the clinical surfactant Infasurf, lyso-PC inhibits adsorption.[258] This latter effect can be explained by incorporation of the lyso-lipid into the neck region of the adsorption structure model depicted in Figure 11. Thus, insertion of lyso-PL counters the negative curvature, resulting in prolonged adsorption times.

In addition to PL, the presence or absence of neutral lipids, mainly cholesterol, can also affect lipid structures and fluidity, thus potentially impacting adsorption. It has long been known that cholesterol has profound influences on the behavior of biological membranes, effects that are primarily related to the interactions of this sterol with saturated and unsaturated PLs.[259−261] With monolayers at physiological temperature, cholesterol induces the conversion of TC to LO phase, with increased fluidity relative to pure DPPC monolayers. This can enhance adsorption of DPPC:cholesterol mixtures.[261,262] In keeping with this, the total lipid constituents of porcine surfactant (minus the proteins) adsorb to a greater extent than these extracts without cholesterol, but not to equilibrium. When the hydrophobic proteins were included, essentially identical adsorption to equilibrium was observed with and without cholesterol included.[263] In contrast, experiments employing the CBS demonstrated that addition of 5, 10, or 20 wt % cholesterol has little effect on the adsorption of the cholesterol-poor BLES[218] and that 5 wt % cholesterol does not enhance adsorption of surfactant-like PL mixtures supplemented with SP-C.[264] This questions the need for cholesterol to enhance surfactant adsorption.

5.2. SP-B and SP-C Are Important for Rapid Surfactant Adsorption

5.2.1. Properties of SP-B and SP-C. There is overwhelming evidence demonstrating that the hydrophobic surfactant proteins, SP-B and SP-C, contribute essential properties to pulmonary surfactants by causing rapid adsorption.[26,149,172] These small hydrophobic proteins display remarkable stability in organic solvents and at high temperatures, especially in the presence of lipids. In fact, the

https://doi.org/10.1021/acs.chemrev.3c00146
Chem. Rev. 2023, 123, 13209−13290

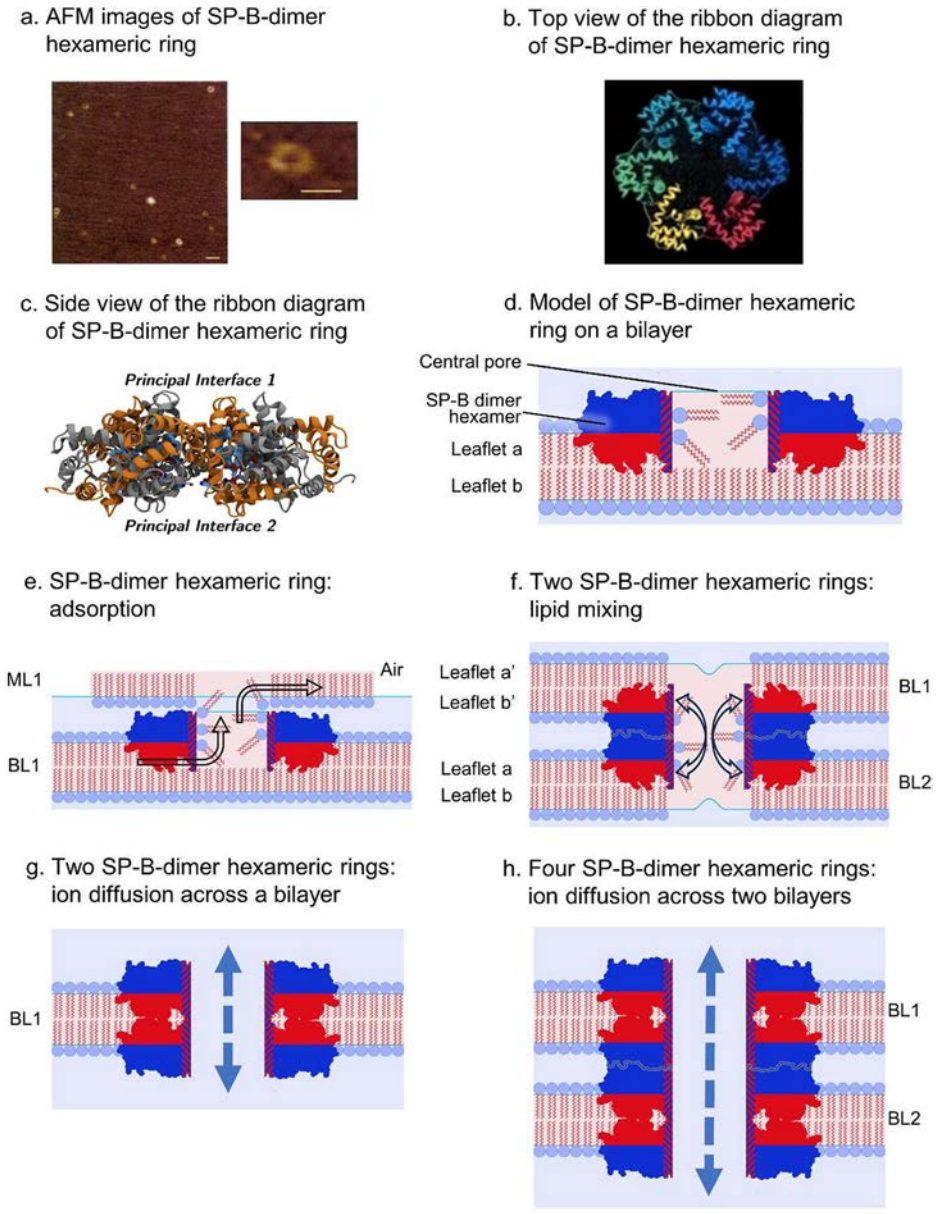

Figure 13. Proposed structures for SP-B dimeric ring structures and schematic models explaining how such rings could perform the various functions attributed to SP-B. (a) Low- and high-magnification AFM images of SP-B rings isolated by detergent purification of porcine surfactant. The individual rings are ∼10.5 nm across with a ∼4.5 nm pore. The inserted bar is 10 nm. Adapted with permission from ref 311. Copyright 2020 Elsevier. (b) Proposed model of an SP-B ring (top view). Six SP-B dimers are assembled to create the 3D model. Each dimer is based on the saponin motif. Adapted with permission from ref 305. Copyright 2015 Wiley. (c) Ribbon diagram of a cross section of an SP-B ring (side view). Principal interface 1 is more hydrophilic than principal interface 2. The more hydrophobic interface can, in principle, penetrate into the outer leaflet of a bilayer. Schematic representation of a SP-B dimer hexameric ring embedded in a lipid bilayer. Phospholipids from the upper, leaflet a, can flow into the central pore, where they interact primarily *via* their headgroups. (d) Schematic representation of a SP-B dimer hexameric ring partially embedded in a lipid bilayer from the side. The hydrophilic interface 1 is depicted as blue while the hydrophobic interface is depicted as red and is partly in the membrane. Phospholipids from the upper, leaflet a, can flow into the central pore, where they interact primarily *via* their headgroups. This shields the interior bilayer from the water. (e) Schematic diagram of the possible action of the SP-B ring in the adsorption of a monolayer—the adsorption structure. The SP-B ring is partially inserted in the bilayer as in part d and the hydrophilic interface 1 is associated with the headgroups of the monolayer. The lipids can transition between the upper leaflet of the bilayer and the monolayer through the central pore. (f) A schematic diagram of the possible action of the SP-B ring in lipid mixing between bilayers. Two SP-B rings are interacting *via* their hydrophilic interfaces while the hydrophobic interfaces are partially inserted in the abutting bilayers. Lipids can transfer from the lower leaflet *b′* of bilayer 1 to the upper leaflet *a* of bilayer 2 and vice versa through the central pore. (g) A schematic diagram of the possible action of the SP-B ring in bilayer leakage. Two SP-B rings are interacting via their hydrophobic interfaces within the bilayer. The central pore acts as a conduit for water, ions, and small molecules to transit between the aqueous compartments. (h) A schematic diagram of the possible action of the SP-B ring in multilayer leakage. Four SP-B rings interact respectively *via* their hydrophobic interfaces within each of the abutting bilayers and *via* the hydrophilic interfaces in the aqueous space between the bilayers. The aligned central cores act as conduits for water, ions, and small molecules to transit across both bilayers.

https://doi.org/10.1021/acs.chemrev.3c00146
Chem. Rev. 2023, 123, 13209−13290

realization that organic solvent extracts, containing these proteins, retained the essential ability of natural pulmonary surfactant to adsorb rapidly and reduce γ to low values was key to the introduction of surfactant treatment for RDS.[7,265−275] Natural and clinical surfactants containing the hydrophobic surfactant apoproteins, SP-B and/or SP-C adsorb very rapidly.[37,171,238] Furthermore, reconstitution studies of simple surfactant-like lipid mixtures with purified SP-B and/or SP-C demonstrate a rapid reduction in γ.

Surfactant protein B is a highly hydrophobic protein that is a member of the saposin family, which comprises a number of mainly water-soluble proteins, that interact with lipids.[10,276−278] Surfactant Protein B, encoded by the *SFTPB* gene, is synthesized as a 381 amino acid preproprotein in the alveolar epithelial Type II and the bronchiolar Clara secretory cells.[279] The preproprotein is only fully processed in the Type II cells, and its function in the secretory Clara cells is unclear.[280] The mature SP-B of 78 amino acids contains three circularized ring sections, stabilized through three intramolecular disulfide bridges (Figure 2). A third, intermolecular disulfide bridge generates a 17 kDa dimer. SP-B dimers are critical for its biological functions.[277,279,281,282] The SP-B dimer is highly cationic, containing 18 positive and four negatively charged residues,[10] consistent with its functional interactions with the acidic PL PG.[7,283−285] The five amphipathic (hydrophobic and hydrophilic) helices in each monomer direct its function as a membrane surface protein.[277,286] This protein is capable of binding, lysing (i.e., inducing bilayer leakage), and fusing PL membranes.[10]

The second hydrophobic surfactant protein, SP-C, is synthesized in Type II cells and in epithelial progenitor cells.[287] In addition to being one of, if not the most, highly hydrophobic proteins known, it appears to be a unique protein in that it does not possess any known family members.[288,289] The SP-C preproprotein, encoded by the *SFTPC* gene, contains 197 amino acids.[279] The mature SP-C consists of an approximately 12 amino acid N-terminal region, containing two adjacent palmitoylated cysteines, and a 23-amino acid, valine rich, carboxyl terminus, that forms an extremely hydrophobic transmembrane helix, for a molecular mass of 4.2 kDa (Figure 2).[290] The mature protein possesses a ragged N-terminal, due to variable proteolytic processing.[290,291] It appears that the cysteine-associated palmitates can remain associated with the same membrane or form a transmembrane helix or bridge into adjacent bilayer membranes or with the surface monolayer.[145,213,264,290,292]

The extremely hydrophobic C-terminal helix is just long enough to span the acyl group section of a fluid DPPC bilayer.[290] With an ordered DPPC bilayer the helix adopts an ∼24° tilt, with respect to the norm of the bilayer.[293] This would be roughly parallel to the ordered acyl chains giving tight packing. The SP-C helix may also align in the acyl region in an orientation parallel to the bilayer.[294] As such, it appears possible that this peptide can generate a packing defect, which promotes adsorption to create a monolayer. It is known that hydrophobic peptides such as polyleucine or polyphenylalanine can promote PL adsorption.[295] Interestingly, although the C-terminus of SP-C contains high amounts of valine, polyvaline peptides did not promote this activity.

Considerable evidence demonstrates that the N-terminal region interacts dynamically with DPPC and DPPG bilayer surfaces at the level of the glycerol-palmitoyl ester, but less so in the absence of the cystine-linked palmitates.[296−298] Both N-terminal forms are capable of disrupting acyl chain packing in lipid bilayers, and currently this is considered to play a major role in promoting monolayer formation (see Serrano[292] for a review). The N-terminal is involved in promoting the aggregation of anionic PL vesicles, inducing leakage of PL vesicles, as well as perturbing the mobility of PL acyl chains in bilayers.[297,299] When both TC and LE are present, the peptide will preferentially reside in the more fluid phase.[294,300] Recent MD simulations suggest that with a surfactant-like PL monolayer, the SP-C helix tends to reside within the acyl region, where it adopts an orientation parallel to the surface.[301]

SP-B knockout (KO) mice succumb at birth from respiratory failure, and infants bearing mutations in the *SFTPB* gene require pulmonary transplantation for survival.[23,279,281] Importantly, SP-B plays a critical role in the formation of lamellar bodies in Type II cells, and these organelles are required for SP-C proprotein processing.[23,281] Thus, SP-B deletion results in a double KO, and the respiratory failure in mice and infants reflects the critical nature of both SP-B and SP-C. Clearly, understanding the manner whereby these low-molecular-weight hydrophobic proteins contribute to the biophysical properties of pulmonary surfactant continues to be a key issue.

There is evidence indicating that SP-B dimers can span the gap between two adjacent bilayers.[231,302,303] Likewise, SP-C could be associated with the outer leaflet of an adjacent bilayer *via* its covalently bound palmitic acids.[20,24,25,231,264] Such connections would exist within natural lamellar bodies and in processed clinical pulmonary surfactant vesicles. These observations support the suggestion that SP-B and SP-C can form specific "adsorption structures" that facilitate spreading of surfactant PLs from vesicular bilayers onto the air−water surface.[26,249] The nature of these structures is still being investigated, but it may involve pores, rings, stalks, or necks with a high curvature containing non-bilayer PL phases.[250,251,285,304−306]

5.2.2. Role of SP-B in Adsorption. Very strong evidence supports the critical role of SP-B in rapid adsorption. For example, reconstitution studies of purified SP-B with lipid mixtures clearly indicate the ability of this protein to accelerate PL adsorption and γ reduction. These studies also demonstrated that the presence of the anionic PL PG allowed for superior activity.[283,284,307] The N-terminal nine amino acids of SP-B, and in particular the tryptophan at position 9, are critical for promoting PL adsorption.[303,308] Residues 1−37, which include the nonhelical N-terminal plus helices 1 and 2, are sufficient to promote rapid liposome fusion.[309]

In addition to promoting adsorption, reconstitution studies, using giant unilamellar vesicles (GUVs), demonstrated that SP-B promoted the formation of pores, that facilitated penetration of water-soluble polar fluorescent-labeled dextrin probes of up to 40 kDa (∼4.5 nm in diameter) into the GUV interiors.[310,311] Both permeation and surface activity processes are inhibited by anti-SP-B antibodies.[310]

Recent studies have provided a possible mechanistic insight into the biophysical properties of SP-B. Surfactant protein B containing supramolecular complexes can be prepared using nondenaturing detergent extraction.[20,305,310] Electron microscopy (EM) and AFM reveal that these preparations contained ring-like structures, consisting of SP-B multimers forming amphipathic assemblies with a central pore (Figure 13a and b).

These observations were supported by MD simulations.[285] Assuming a hexamer of SP-B dimers, these simulations predict

https://doi.org/10.1021/acs.chemrev.3c00146
Chem. Rev. 2023, 123, 13209−13290

a flat disc ∼10.5 nm wide with a central hydrophobic pore ∼4.5 nm wide. As shown in Figure 13c, the resolved structure is amphipathic, with more hydrophilic residues on the outer "principal interface 1" side, while the somewhat more hydrophobic, inner "principal interface 2" side can penetrate into the bilayer membrane. Potential binding sites, favoring PG and cholesterol, exist on both flat surfaces. The interacting nanoring central pore is amphipathic, containing both hydrophobic and hydrophobic residues. Presumably PL and cholesterol molecules, binding to the ring *via* the inner side of the oligomeric complex, can migrate into the pore and associate with the pore sides *via* their polar heads (Figure 13d). The fatty acyl chains would extend toward the pore center, virtually filling the available space. Thus, these SP-B ring structures, alone or by interacting with one another through their principal 1 or 2 faces, can rationally explain the functional properties of SP-B (Figure 13). These include the following: monolayer formation (Figure 13e), lipid mixing between the outer leaflets of two bilayer vesicles (Figure 13f), pore formation through a bilayer in a GUV (Figure 13g), and pore formation connecting the contents of two bilayers GUV (Figure 13h).[20,302,304,305,310,311]

5.2.3. Role of SP-C in Adsorption. As with SP-B, reconstitution studies of SP-C with surfactant-like lipids demonstrate the ability of this protein to enhance PL adsorption[25,149,160,290] (see Serrano[292] and Zuo[13] for reviews). As with SP-B, SP-C catalyzes lipid mixing, but with SP-C, anionic PLs can lessen the process.[312,313] However, mechanistic interpretations into SP-C molecular functions are still vague. Not surprisingly, neither SP-B nor SP-C fits well in the DPPC or DPPC:DPPG monolayer TC phase, and so they reside in the fluid areas.[300,301,314,315] The emergence of multilayer structures during surfactant monolayer compression appears to commence at TC:LE interfaces, and presumably adsorption could also initiate at these junctures.[220] The chain packing perturbations induced in DPPC and DPPG bilayers by the C-terminal helix could induce temporary exposure of the acyl chains, thereby accelerating adsorption.[316] However, monolayer and bilayer disruption has more often been attributed to N-terminal SP-C charge interactions that interfere with acyl chain packing.[297,298,316,317] It has also been suggested that the penetrating N-terminal segment of SP-C could generate an interdigitated phase in bilayers, where the fatty acyl groups from opposing bilayer leaflets line up, side by side rather than end to end, which could resolve by transferring PLs to the aqueous surface.[316,318]

Furthermore, as shown in Figure 14, SP-C could transfer PLs from the perturbed fluid area of the outer leaflet of an underlying bilayer to the air surface. A PL inversion mechanism has been proposed for the creation of very small 2-dimensional (2D) to 3-dimensional (3D) lipid structures during monolayer compression. This would involve PL molecular flip-flop generated by rotation of the charged N-terminus with respect to the hydrophobic C-terminal helix imbedded in the underlying bilayer.[314,319,320] It appears feasible that the reverse process might occur during PL adsorption, thereby promoting transfer of outer leaflet bilayer PLs to the surface, next to the air-associated palmitates. Upon completion of adsorption, the palmitates associated with the N-terminal region would remain in the transferred monolayer, providing a monolayer-to-bilayer attachment (Figure 14).

There is considerable evidence for extensive functional interactions between cholesterol and SP-C.[306,318,321−323] In addition, PC and especially PG headgroups associate with the positively charged arginine and lysine in the N-terminal.[301,314] There are also indications of the existence of SP-C C-terminal associated dimerization and possibly further self-assembly.[321,324,325] Taken together, these could provide a basis, at least theoretically, for potential SP-C-based ring-like clusters.[324] Although extensive experimental evidence is still lacking, this suggestion is supported by the ability of SP-C to promote diffusion of polar dextrin molecules of up to 40 kDa through bilayers into GUVs.[326]

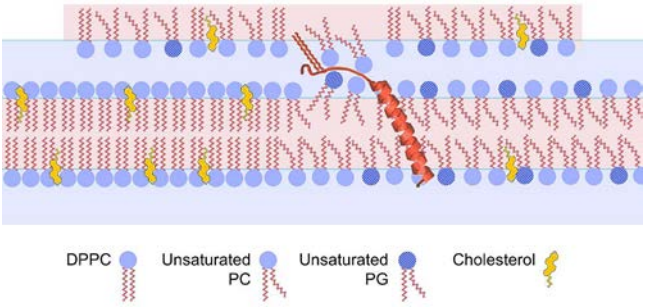

Figure 14. Schematic representation of a potential model for the ability of SP-C to catalyze the formation of a surfactant monolayer from a bilayer vesicle at the air−water interface. By extending outward from a bilayer, the N-terminal section of SP-C could provide a defect promoting the release of PL molecules to the air interface by the N-terminal-induced flip-flop of PL molecules, particularly PG from the outer leaflet of the vesicle. In this scenario, the cystine-associated palmitates would extend into the air, thereby escaping the energetically expensive interaction with water and facilitating N-terminal bound lipids' access to the surface. Presumably the defect created in the underlying bilayer could enhance further loss from the upper PL leaflet. At a certain point, this lipid donating leaflet would become unstable, allowing collapse of the remaining vesicle onto the surface. At the end of adsorption, once equilibrium is attained, the N-terminal palmitates would remain encased in the adsorbed monolayer. This provides a functional connection between the surface monolayer and the underlying PL bilayer. Note the above model does not take into consideration the reported suggestion that SP-C can be present as dimers due to interactions at the N- or C-terminal. Adapted with permission from ref 292. Copyright 2006 Elsevier.

Considerable effort has been made to examining the role of the N-terminal palmitates. Surfactant protein C lacking these hydrophobic modifications has a diminished α-helical content,[290,327,328] although this has been contested[299] (see Castillo-Sánchez[240] and Johansson[290] for reviews). Nevertheless, it is evident that depalmitoylated SP-C can enhance surfactant lipid adsorption. Some investigators have reported that this occurs to a lesser extent than with the intact lipoprotein,[290,329,330] but this observation is not consistent.[264] More recent data has shown that SP-C analogues, where the adjacent cysteines are replaced with phenylalanines, are as active with various surfactant-like lipid mixtures as the native protein.[331] The aromatic amino acids were used because a single phenylalanine replaces a cystine in canine and mink pulmonary surfactants.[332,333]

It is evident that palmitoylated SP-C can link lipid multilayers together, a function that helps explain why this hydrophobic protein greatly enhances surfactant lipid respreading when the surface area is rapidly increased.[264,330,334]

In contrast to its ability to form connected multilayers, SP-C can also catalyze fragmentation of lipid bilayers to form small unilamellar vesicles (∼25 nm diameter), which appear to be

https://doi.org/10.1021/acs.chemrev.3c00146
Chem. Rev. 2023, 123, 13209−13290

unstable.[306,318,321,335] The manner by which these apparently discordant properties influence surfactant biophysical activity is not yet clear.

The mechanistic understanding of the SP-C properties has been somewhat complicated by the tendency of purified and synthetic peptides of SP-C to form β-sheets, which generate irreversible aggregates.[290,336−340] This molecular transformation could interfere with appropriate interpretation of many of the *in vivo* and *in vitro* observations.[87] Since this oligomerization is promoted by depalmitoylation, the earlier results must be carefully considered.[333]

5.2.4. Cooperative Activities of SP-B and SP-C in Adsorption. Considering the conserved nature of both SP-B and SP-C in mammalian lungs, and their tight association with the surfactant lipids, it is clear that both play a role in surfactant function. A combined role for both proteins is supported by numerous reconstitution and synthetic pulmonary surfactant preparation studies, demonstrating that superior *in vitro* activities occur with the combined proteins.[310,334,341−346] Similarly, optimal physiological responses to exogenous surfactant in premature rabbits require the presence of both proteins.[23,341,342] It has been suggested that the fusogenic properties of SP-B both compliment and counteract the membrane destabilizing effects of SP-C, observed with small vesicles.[306,326] A notable indication of the cooperative roles of these two proteins is that including physiological amounts of cholesterol inhibits the ability of surfactant-like mixtures (DPPC:POPC:POPG) containing SP-B to attain low γ during compression. Mixtures containing SP-C alone have very high γ_{max} values. These deficits are normalized by the inclusion of both SP-B and SP-C.[264,322,323]

It has been further suggested that these biophysical and physiological observations indicate that these hydrophobic proteins not only have complementary functions but also coexist in a combined SP-B:SP-C supramolecular complex.[160,304,310,344,347] Evidence includes the observation that either anti-SP-B or anti-SP-C antibodies can block the adsorption of isolated lamellar bodies, the natural form of pulmonary surfactant *in vivo*.[238,310] The abilities of SP-B and SP-C to promote the diffusion of water-soluble materials between GUV interiors is modified by the combination of both proteins.[326] Some,[304] but not all,[348] fluorescence studies with labeled SP-B and SP-C indicate similar locations in reconstituted samples. However, this suggestion is not supported by X-ray diffuse scattering or MD analysis.[294]

Supramolecular complexes containing both SP-B and SP-C may be important. However, a specific stoichiometry has not yet been observed. The molar ratio of SP-C to SP-B in natural and clinical surfactants as determined by UV absorption varies greatly: Alveofact, 11:1; native bovine, 13:1; Survanta, 55:1; native porcine, 9:1; Curosurf, 14:1.[243] Colorimetric assays indicate the SP-C:SP-B molar ratios for the bovine clinical surfactants are BLES, 6:1 and CLSE (Infasurf), 5:1.[349,350] This data indicates that SP-C is normally considerably more abundant, particularly if it is assumed that most of the SP-B is localized in hexamers composed of SP-B dimers. Although direct evidence is lacking, it should be considered that SP-C could also form multimer structures.

Despite the excess of SP-C, it has not been detected in the SP-B-containing nanoring complexes and it is not easy to envisage how all the SP-C would be localized in such structures. It could be that SP-B:SP-C interactions are transitory, requiring a greater abundance of SP-C, or that the hetero-oligomeric complexes present in native surfactant membranes do not readily reassemble when mixed *in vitro*.[160,302,304,310,351] However, while the evidence points at cooperative functions of the two proteins, there is no clear indication how structural interactions could occur.

It is clear that except for certain specific strains, such as 129/Sv, SP-C-deficient mice not only survive at birth but lead apparently normal lives and have intact lung morphology. However, other null SP-C strains are more susceptible to prolonged inflammation, for example by *P. aeruginosa*, syncytial virus, bleomycin, or lipopolysaccharide (see Sehlmeyer[351] for a review). Interestingly, clinical and experimental surfactants containing only SP-C have obvious physiological benefit with ALI, although not as beneficial as with the combined proteins (see Curstedt[352] and Curstedt[353] for reviews).

5.2.5. Surfactant Adsorption during Film Re-expansion. Once a surfactant film is formed at the air−liquid interface in the alveoli, it undergoes breathing engendered repetitive compression:expansion cycles. With pure lipid mixtures, unsaturated PL must be ejected in order to attain low γ.[354−357] During inspiration from low lung volumes, additional material is required to maintain γ near equilibrium. A process known as respreading is used to mimic the effects of inspiration from a low lung volume. Experimentally this involves a rapid increase in the surface area of an established film at low γ in a CBS. It is thought that after cycling of an adsorbed film, the established surfactant film can support a very rapid uptake of surfactant into the expanding monolayer. Experiments with either bovine or porcine extracts or with reconstituted preparations reveal that even with a ∼9-fold increase in surface area, equilibrium is rapidly reattained with similar kinetics to the initial adsorption event.[25,264,322,334,358] In reconstitution studies, SP-B exhibited the better performance, but the combined proteins tended to show marked improvement.[264,334]

5.2.6. Brief Summary of the Roles of SP-B and SP-C in Surfactant Adsorption. The larger hydrophobic protein, SP-B, is a surface membrane protein, while SP-C appears to normally act as a transmembrane protein. These surfactant proteins exhibit both similar and different, but complementary, effects on surfactant-like lipid mixtures. Both hydrophobic proteins enhance adsorption to equilibrium. Especially with SP-B, this property is improved when PG is present. It appears that SP-B initiates surfactant lipid adsorption by forming or stabilizing a neck-like fusion structure with high curvature. SP-C may initiate adsorption by disrupting the packing of PL in the outer leaflet of bilayers, that approach the air−water interface. In contrast to SP-B, SP-C has only a limited affinity to the anionic PG. Phospholipid interdigitation structures with SP-C may be involved in adsorption. SP-B dimers form hexameric rings which are capable, at least theoretically, of performing all of the basic functions attributed to this protein. Whether SP-C forms large complexes is not clear, but there is evidence for SP-C dimers. It has been suggested that SP-C may form functional complexes with the SP-B rings.

Additionally, both hydrophobic proteins support the stabilization of surfactant PL to attain very low γ during dynamic compression. With SP-B, this property is impeded by physiological amounts of cholesterol. While SP-C alone can support the ability of lipids to attain low γ, with cholesterol present, γ values at maximal areas are high. Both problematic situations can be resolved by including both proteins.

https://doi.org/10.1021/acs.chemrev.3c00146
Chem. Rev. 2023, 123, 13209−13290

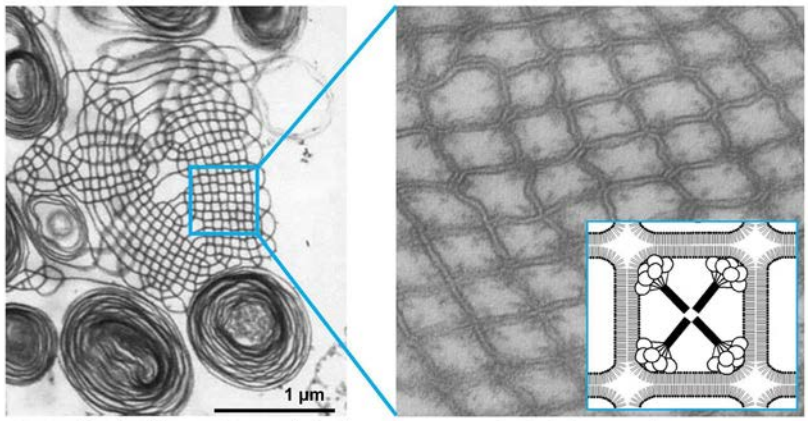

Figure 15. Tubular myelin is formed by the interaction of separately secreted SP-A and calcium with the material secreted from lamellar bodies. It is composed of long parallel bilayer tubes that are fused at the corners. (a) Electron microscopic view of tubular myelin being formed by PL bilayers peeling off multilamellar structures. Adapted with permission from ref 359. Copyright 1992 Taylor & Francis. (b) Enlarged electron microscopic view of a tubular myelin cross section. The image is 0.6 μm wide. The small bars projecting from the corners are SP-A oligomeric molecules. Adapted with permission from ref 360. Copyright 1980 Elsevier. The inset shows a schematic model that represents the cross-sectional view of the tubular myelin showing SP-A oligomers interacting with the corners of the bilayer squares *via* their carbohydrate recognition domains. It has been proposed that the corners of the lattice are fused by SP-B. Adapted with permission from ref 361. Copyright 2001 Elsevier.

5.3. Surfactant Features That Enhance the Rate of Adsorption

5.3.1. Lamellar Bodies. Recent reports have indicated that multilamellar structures (Figure 15a), the extracellular vesicular forms produced by intracellular lamellar inclusion body secretion, have extraordinary surfactant properties, relative to natural surfactants isolated by lavage.[116,238,240,242,362,363] Adsorption of multilamellar particles proceeds more rapidly than similar PL concentrations of isolated natural surfactant, except when the latter are at high concentrations.[242,364]

Despite the above, note that isolated lamellar bodies are remarkably stable, existing in aqueous medium for many hours.[363] Yet they spontaneously collapse onto a clean air surface. However, as π increases to above ~25 mN/m ($\gamma \sim 45$ mN/m), adsorption declines, and these particles simply line the interface.[363] The manner by which interaction with air at low π triggers unravelling remains unknown. However, insights into adsorption have arisen through investigations with reconstituted surfactants containing DPPC:PG (7:3) and the hydrophobic surfactant proteins. With preformed PL monolayers at $\pi \sim 20$ mN/m, added DPPC:PG vesicles do not adsorb. When SP-B and SP-C are present in either monolayer or vesicles or both, there is rapid adsorption to equilibrium.[343,365] Note, subphase ions are required and divalent cations were superior to monovalent. This is consistent with the many studies demonstrating the contribution of calcium to surfactant function.[267,319,366,367] When the hydrophobic proteins were present in the monolayer only, small unilamellar vesicles adsorbed better than large unilamellar vesicles, which were better than multilamellar vesicles, suggesting an effect of curvature. This difference was not seen when the proteins were present in both monolayer and vesicles. In contrast to isolated lamellar bodies, this "pull-up" mechanism performed better at higher π. This reveals an obvious difference between reconstituted surfactants and the mechanisms controlling lamellar body insertion.

The precise basis for the more rapid adsorption of isolated lamellar bodies is not completely clear. It has been suggested that in lamellar bodies, SP-B and SP-C are oriented on the "outer facing leaflets" of the bilayers, while in reconstituted surfactants and surfactant lipid extracts these proteins would reside in both interfaces.[238] An additional important factor is likely to be related to the hydration status of the lipids in the lamellar body. Differential scanning calorimetry, fluorescence emission measurements, and ^{31}P-nuclear magnetic resonance all indicate greater PL headgroup dehydration in the lamellar bodies.[362] These observations suggest that the ABCA3 PL transporter within the Type II cell can pack dehydrated PL into lamellar inclusion bodies, producing very highly energized lipid structures allowing for rapid adsorption.[116,240,242,364] In addition, lamellar bodies are modified lysosomes and a pH lower than that of the aqueous media would also promote PL adsorption.[329] An additional possibility is that the SP-B- or SP-C-containing adsorption structures, abutting against the lipid domains within the lamellar body, somehow create a nucleation site.[368] This nucleation site would grow as the monolayer experiences the compaction that arises from colliding individual lipid patches, as more material gains the surface. Possibly the generation of these large, fused domains at a surface locus can facilitate liquid-crystalline monolayer collapse, thereby ejecting the fluid PL (which possess weaker PL–PL association forces), into the subphase.[26,369] Such extruded material would tend to spontaneously form bilayers to minimize fatty acid–water interactions. Another possibility is that the still undefined adsorption structures would not only catalyze monolayer nucleation formation but also act as fusogens for the nascent bilayers.[10]

The observation that antibodies against either SP-B or SP-C block adsorption of isolated lamellar bodies could indicate that these proteins are combined during lamellar body formation and thus act cooperatively during the adsorption process, but not necessarily in the same manner during subsequent surfactant functions.[242] Nevertheless, these subsequent activities where SP-B functions to create surface films, enhances the

https://doi.org/10.1021/acs.chemrev.3c00146
Chem. Rev. 2023, 123, 13209–13290

ability of surfactant lipids to achieve low γ during compression, and promotes respreading during film expansion compliment the ability of SP-C to counteract the deleterious effects of cholesterol and to induce membrane fragmentation for surfactant transport to Type II cells for recycling and to macrophages for degradation.

5.3.2. Role of SP-A. Whereas the discussion on adsorption mainly focused on the role of lipids and the hydrophobic surfactant proteins, natural surfactant also contains significant amounts of the hydrophilic, oligomeric glycoprotein SP-A. Although SP-A knockout animals breathe normally, it is clear that SP-A modifies surfactant *in vivo*. Thus, separately secreted SP-A interacts with secreted lamellar body contents to generate a novel extracellular surfactant arrangement known as tubular myelin (Figure 15). Recent electron tomography studies, utilizing serial sectioning, describe a lattice-like structure of parallel tubes with a marked heterogeneity especially at the intersections with other structures.[370]

The role of tubular myelin in adsorption *in vivo* is unclear, although early investigations led to the suggestion that tubular myelin functioned as an obligatory intermediate between secreted lamellar bodies and the surface film.[9,371−373] Certainly, tubular myelin that is reconstituted by combining DPPC, PG, SP-A, and calcium[371,374] is quite surface active. However, the tubular myelin content of these mixtures is too low to make definitive conclusions. Furthermore, isolated lamellar bodies lacking tubular myelin possess excellent surface activity even at low concentrations[242] and transgenic animals lacking SP-A expression, or tubular myelin, have normal lung function, demonstrating tubular myelin is not essential.[375]

5.3.3. Impact of Surfactant Concentration on Adsorption. In addition to structure and composition, the ability of a surfactant to adsorb rapidly and reduce γ to low values is highly affected by its concentration. At low (<250 μg/mL) and intermediate (~750 μg/mL) concentrations, lamellar body particles adsorb faster than natural pulmonary surfactants, which adsorb faster than either organic solvent lipid extract surfactants or natural surfactant-derived clinical surfactants. These adsorption rates increase rapidly with increasing concentrations, such that at high concentrations (~2 mg/mL or more) these differences between surfactant preparations become small and almost nondetectable.[159,171,242,267,367,376]

5.3.4. Other Factors Influencing Phospholipid Adsorption. The initial step in surfactant lipid absorption, the interaction with the surface, proceeds more rapidly when anionic PLs such as DPPG or PG are included and, as indicated above, as the PL concentration is increased.[366] This first step is dependent on the hydrophobic proteins, but surprisingly, the PL saturation state has little effect. The subsequent step, spreading at the interface, proceeds more efficiently when unsaturated lipids are included and with higher PL surface concentrations, i.e., with higher π. With low surfactant concentrations, an acceleration during the late stage of adsorption can be discerned.[377] This contrasts with detergents such as sodium dodecyl sulfate, which adsorb to equilibrium with first-order kinetics.

Additional information on potential mechanisms involved in PL adsorption has been derived from investigations on the formation of supported lipid bilayers. With this procedure, lipid vesicles adsorb and spontaneously rupture onto a substrate of glass, mica, silicone, or other materials. Attractive forces between the vesicle lipids and the substrate, such as van der Waals and electrostatic, will induce vesicle deformation, which can result in rupture due to vesicle−substrate or vesicle−vesicle interactions.[378,379] The circumferences of the adsorbed ruptured vesicle will have very high curvature and so will be unstable. This instability assists deformed vesicle−vesicle fusion generating large, flattened supported membranes. Fusion of additional vesicles to the initial bilayer engenders multilamellar bilayers.[380]

The major mechanism described for the formation of supported PL bilayers involves adsorption on a substrate to generate a semidome.[380,381] The creation of a membrane pore then allows escape of the vesicle's contents, thus permitting the formation of two closely opposed bilayers. This results in a double-bilayer patch approximating a heart shape, due to the effects of accommodating the membrane pore. The speed with which collapse happens, milliseconds, suggests that there are driving forces inherent within the vesicles.[380−382]

Some of the collapsing forces involved in monolayer formation may derive from the tendency of bilayers to form flattened shapes to minimize the bending energies required to form a sphere, for example collapsing CLSE and DPPC:cholesterol monolayers form flattened disks at the surface.[383] Yet, the greatest bending energy would be inherent in very small vesicles. However, isolated lamellar bodies and lipid extract surfactant vesicles, which are quite large, adsorb most readily. Also, it has been suggested that the positive curvature of the outer leaflet of a bilayer is compensated by the negative curvature associated with the inner leaflet.[26] Consequently, the contribution of forces derived from curvature may be limited. With supported lipid bilayers, pore formation can contribute to bilayer rupture, and this appears linked to high-curvature necks or "worm-hole" formation[380,384,385] (see Katsaras[386] and Lind[382] for reviews). However, in practice, the adsorption mechanism for surfactant vesicles does not require such a curvature-induced bilayer pore, because both SP-B and SP-C readily induce vesicle leakage, presumably *via* such transmembrane neck-like structures.[10,26,290,326]

5.4. Structural Features of Adsorbed Surfactant Films

Whereas the above section focuses on the rapid adsorption of surfactant lipids to form films at the air−water surface, it does not address the structural features of those films. Several lines of evidence suggest that the adsorbed film is not simply a monolayer but contains a surface-associated surfactant reservoir (SASR).

The first suggestion for a SASR stemmed from observations using the CBS and BLES. In these experiments the excess, nonadsorbed BLES vesicles in the subphase were washed out, leaving only the adsorbed film. When this remaining film was expanded beyond its original size near equilibrium γ, subsequent compressions led to an increased surface area at $\gamma \sim 0$ mN/m. Repetition of these overexpansion/compression cycles progressively increased the surface area such that the final compressed film contained over three times the surface area of the initial adsorbed film. These observations were interpreted as indicating that, during expansion, additional highly surface active material, namely DPPC, must be incorporated from a SASR that was functionally associated with the interfacial monolayer.[25,172,358] This SASR presumably represented excess material remaining in the partially adsorbed vesicles. Similar observations were made with adsorbed Curosurf, a clinical surfactant produced from porcine lungs, but not with protein-free synthetic lipids.[234,387] While the

https://doi.org/10.1021/acs.chemrev.3c00146
Chem. Rev. 2023, 123, 13209−13290

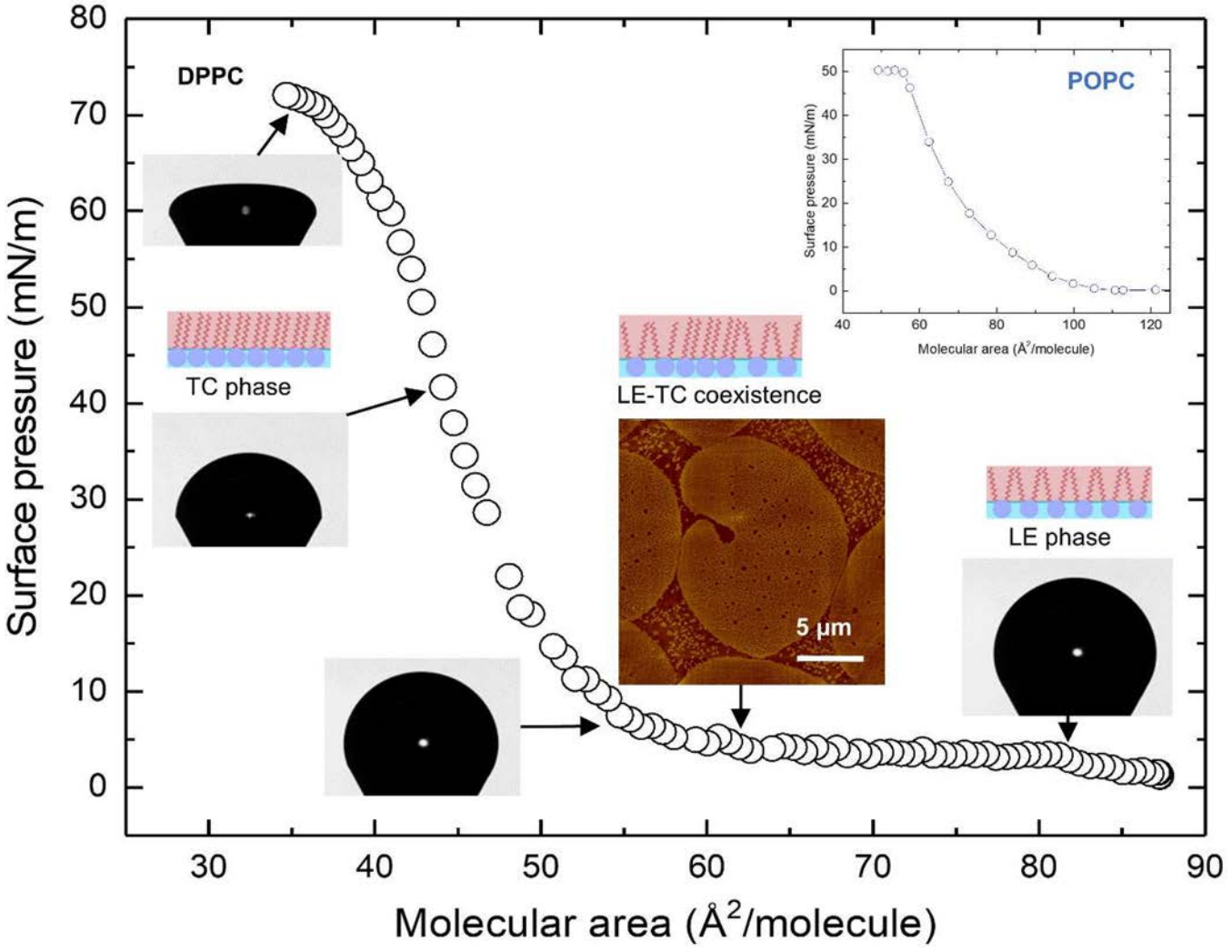

Figure 16. A typical compression isotherm of the DPPC monolayer at 20 °C, produced with a constrained drop surfactometer (CDS). Insets are images of the constrained sessile drop that demonstrate correlations between the drop shape and the corresponding π determined with axisymmetric drop shape analysis (ADSA). The AFM image (20 × 20 μm^2) shows the LE-TC phase transition in the DPPC monolayer. The TC domains demonstrate the typical shape of a kidney bean due to the intermediate line tension. Adapted with permission from ref 30. Copyright 2016 American Chemical Society. The monolayer schematics illustrate the presence of the LE phase at low pressures, the coexistence of the LE and TC phases at pressures corresponding to the AFM, and the presence of the TC phase at high pressures. Also shown in this figure is a compression isotherm of POPC, produced with a Langmuir film balance at room temperature. Adapted with permission from ref 32. Copyright 2011 Elsevier. Comparison of the compression isotherms of DPPC and POPC at room temperature shows that only disaturated PLs, like DPPC, can be quasi-statically compressed to a high surface pressure of 70 mN/m, while the fluid PLs, like POPC, collapse at 50 mN/m.

deduction that a functionally attached SASR existed was entirely based on γ and area measurements, it aligned well with EM observations that demonstrated the presence of stacked bilayers with adsorbed films and at the alveolar surface in fixed lung slices.[234,358,388]

Overall, these results therefore indicate that the *de novo* adsorbed surfactant film at γ_{eq} cannot be just a monolayer but is a multilayer consisting of an interfacial monolayer at the air−water surface with functionally attached vesicular structures.[172,234,389] The formation of such functional structures apparently requires the hydrophobic surfactant proteins SP-B and/or SP-C.[26,334,390] It should be noted that another feature of these adsorbed films is the potential compositional difference between the monolayer and attached bilayers in the SASR. This aspect is highly relevant for γ reduction and will be discussed in Sections 6 and 7.

It should also be noted that another form of surfactant reservoir can be formed by the compression-driven squeeze-out of PL from spread monolayers.[213,220,391] This sort of reservoir is often referred to in the literature as SASR as well. It is considered that the latter form of reservoir should be considered distinct, not only because of its method of formation, but importantly because such structures are highly enriched in unsaturated lipids. Thus, they are compositionally different as well. This raises the possibility that both kinds of reservoir could exist in the same film.

5.5. Brief Synopsis of Surfactant Adsorption

Taken together, a multitude of experimental approaches have provided overwhelming evidence for essential roles for SP-B and SP-C in promoting the adsorption of pulmonary surfactant lipids. While either of these hydrophobic proteins can promote the bilayer-to-monolayer transition, their mechanisms appear distinct. SP-B induces bilayer instability leading to a

https://doi.org/10.1021/acs.chemrev.3c00146
Chem. Rev. 2023, 123, 13209−13290

monolayer−bilayer fused complex, and this process functions optimally when PG is present. SP-C induces PL bilayer instability which can lead to vesiculation. These functions appear to complement each other. With isolated lamellar bodies, adsorption is further enhanced by the unique properties of these organelles, particularly extensive dehydration of PL headgroups. In general, the process of adsorption is thought to involve specific adsorption structures which generate a monolayer with attached bilayers. It should be noted that the information about adsorption, described above, focused on the speed of forming a surface film, independent of the specific lipid composition of the adsorbed film. Compositional aspects are discussed below ,as they directly impact γ reduction during compression.

6. HOW DOES PULMONARY SURFACTANT REDUCE SURFACE TENSION TO LOW VALUES?

Adsorption is necessary for the initial formation of a surfactant film. Once formed, the film composition must permit reduction of γ to near 0 mN/m during expiration *in vivo* or during compression *in vitro*. In this section, we first examine the evidence that this requires a monolayer highly enriched in DPPC or DPPC and cholesterol, described as Postulate I of the classical model. We second examine the evidence that the enriched membrane arises from a compression-driven squeeze-out of unsaturated lipids during compression, which is considered as Postulate II of the classical model. We third examine evidence against the occurrence of compression-driven squeeze-out during normal quiet breathing and present evidence in favor of an adsorption-driven lipid sorting during the initial film formation, in support of our updated model. We also recognize that there are other mechanisms proposed in the literature, as well as processes that interfere with surfactant function; these are discussed at the end of this section.

6.1. The Classical Model of Pulmonary Surfactant Function

The information on the composition of surfactant, the concept of γ, and the phase behavior of lipids, together with some initial experimental evidence, provided the basis for what is known as the classical model of surfactant function.[26,145,392,405] Specifically, the discovery of PLs as the primary components and DPPC as the major single constituent of pulmonary surfactant provided a potential explanation for surfactant function.[6,155,393,394] Experimentally, it was observed that films of pulmonary surfactant extracts, or bubbles squeezed out of excised lungs, displayed the ability to attain very low γ, indicating the formation of gel−solid films at the air−water surface.[2,3] Since DPPC can readily be compressed to γ near zero, whereas films containing unsaturated fatty acids were only capable of reducing γ to ∼23 mN/m, it was concluded that during exhalation, lung alveoli are protected from collapse by a surface monolayer composed of DPPC (or highly enriched in DPPC).[355,356,393,394] We will refer to this conclusion as Postulate I of the classical model for surfactant function.[26,392,395] Since that time, it has become evident that surfactant contains other disaturated PLs other than DPPC. In addition, pulmonary surfactant contains cholesterol, which has a strong affinity to DPPC and so is clearly present in the monolayer. For simplicity, these considerations will be largely ignored in this review.

Postulate I immediately prompted an important second question, namely, how does pulmonary surfactant, which is approximately half unsaturated PLs, generate a monolayer enriched in DPPC? Early considerations suggested that such DPPC enrichment could arise from a squeeze-out mechanism, whereby, the more fluid constituents of the interfacial monolayer, the unsaturated PLs, are ejected from the surface during surface area reduction.[355,356,393,394] The remaining disaturated PLs would then be able to reduce γ to near zero. The squeezed-out unsaturated PL species would spontaneously form lipid bilayers in the subphase. We will refer to the concept that monolayer enrichment in disaturated PC results from a squeeze-out mechanism during surface area reduction as Postulate II of the classical model. Note, this postulate implies that the composition of the original adsorbed monolayer resembles that of the applied surfactant.

The classical model has informed much of the experimental design of the last several decades, and there is considerable data to support it. More recent data has raised questions about the veracity of Postulate II, while adding further support for Postulate I.

6.2. Evidence for a Surface Film Enriched in DPPC at Low Surface Tension

The first experimental data in support of a DPPC-enriched film is the observation that spread DPPC monolayers, for example on a Langmuir surface balance, can reach near-zero γ when compressed.[354,355,393,394] As shown in Figure 16, this occurs because as dilute DPPC films are compressed, surface monolayers undergo two first-order phase transitions, initially at $\pi \sim 0$ mN/m, from a gas-like phase to the liquid-expanded (LE) phase, and at $\pi \sim 7$ mN/m, from the LE to the tilted-condensed (TC) phase. The first transition is difficult to observe experimentally, but the second is visible, as the isotherm exhibits a broad compliant plateau representing two-phase coexistence. Within this plateau, increasing amounts of the TC phase arise. Upon further compression, the saturated palmitates pack closely together, forcing them to extend higher into the air.[30,33,210] This continues up to $\pi \sim 70$ mN/m ($\gamma \sim 0$ mN/m) and reflects the compressibility of the TC phase, where the isothermal film compressibility is defined as $\kappa = -\frac{1}{A}\left(\frac{\partial A}{\partial \pi}\right)_T$. Decreasing the surface area further will eventually produce "collapse", where DPPC material corresponding to the area decrease is forced from the monolayer, while γ remains unchanged.[26,392,396] The depicted isotherm is fully reversible below 70 mN/m.[186] However, DPPC ejected by collapse during overcompression is lost.[397]

Compression of dilute POPC, the most abundant unsaturated molecular species in most animal surfactants, can only reduce γ down to the γ_{eq} of ∼23 mN/m, but no further (see inset in Figure 16).[354,398] This occurs because the double bond in the oleic acid (18:1) produces a kink, making the PL film fluid, so that it remains in the LE expanded phase and cannot form the solid-like TC phases at room or physiological temperatures. Further compression of the monolayer simply forces material out of the monolayer without significantly reducing γ. In other words, POPC has a significantly lower collapse pressure than DPPC (∼47 vs ∼70 mN/m).

It is important to note that under lateral compression, the π of DPPC monolayers and surfactant films can be higher (γ can be lower) than the initial equilibrium spreading π of PL. Some have argued that these monolayers appear to be in a metastable state.[26,398] Indeed, these high π are only attained with continuous external compression and should, at least theoretically, eventually return to the equilibrium pressure.

https://doi.org/10.1021/acs.chemrev.3c00146
Chem. Rev. 2023, 123, 13209−13290

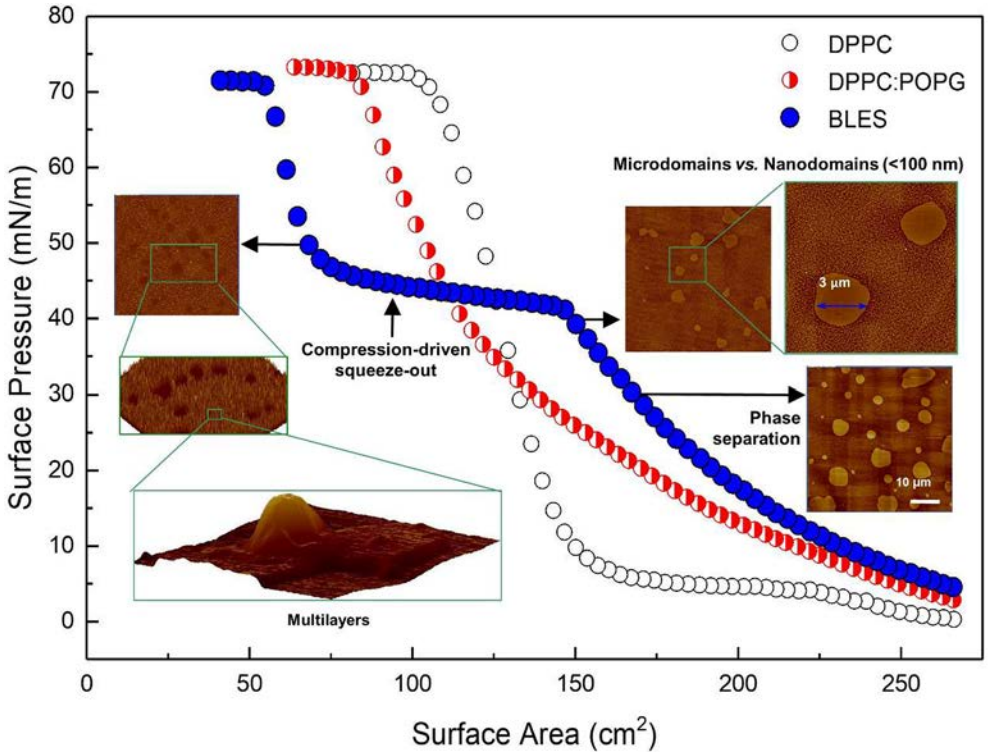

Figure 17. Comparison of the compression isotherms of BLES (blue circles), DPPC:POPG (7:3 wt/wt) (red circles), and a pure DPPC monolayer (open circles), measured with a Langmuir surface balance at room temperature. The area is that of the Langmuir film balance during film compression. AFM images of the BLES film are shown at selected surface pressures. The DPPC:POPG monolayer does not exhibit the same first-order phase transition observed in DPPC. Rather it shows a steadily decreasing compressibility as the surface area is reduced to the point where it approached the compressibility of pure DPPC at high π. This change in compressibility is interpreted as a steady loss of the fluid POPG during compression, presumably into the aqueous subphase. This interpretation is consistent with the observation that while the DPPC isotherm is reversible, the isotherm of the mixture is not. The BLES isotherm is different from both of the others. At large surface area, the BLES film is less compressible than either the pure DPPC in the LE phase or the binary DPPC:POPG film. Nevertheless, there is a segregation of phases during this compression, as seen in the AFM images, which show formation of both microscale and nanoscale solid-like domains rising about 1 nm above the surrounding phase. These are interpreted as being domains that contain mostly disaturated PLs. Since BLES is a complex mixture of many components, this is not a first-order phase transition and occurs continuously while the pressure is increasing. As the pressure reaches about 40 mN/m, corresponding to the equilibrium π for unsaturated lipids, the surface area is reduced significantly with only a small change in π. This plateau is interpreted as the "squeeze-out" region during which the unsaturated lipids are removed from the monolayer into a PL reservoir containing PLs attached to the monolayer *via* an adsorption structure. This is consistent with the observation that the surface area changes by about 40%, corresponding roughly to the percentage of unsaturated lipids in the BLES mixture. At the end of this plateau, the AFM reveals a significant number of structures corresponding to one or a few bilayer thicknesses, also consistent with the concept of a reservoir which can be reincorporated into the monolayer on expansion. Further area reduction leads to a sharp increase in π with a compressibility very similar to that of pure DPPC, also consistent with the film being highly enriched in DPPC. Isotherms were adapted with permission from ref 64. Copyright 2011 Elsevier. AFM images were adapted with permission from ref 210. Copyright 2008 Cell Press.

Nevertheless, such films can remain sufficiently stable for far longer than is necessary to stabilize our lungs during expiration.

In addition to the Langmuir balance studies, experiments conducted with excised animal lungs have shown that the deflation pressure–volume curves are also consistent with a surface monolayer that is highly enriched with DPPC.[237,399−401] Schürch and colleagues devised a novel fluorocarbon microdroplet technique to access γ at the alveolar surface *in situ*. This method relies on the principle that an inert insoluble oil placed on a film will adopt an equilibrium state dependent upon the differences in γ of the substrate, the fluorocarbon, and air (see Schürch[234] for further description). Applying this fluorocarbon microdroplet approach showed that the γ of deflated lungs was ∼2 mN/m, but this rose to ∼30 mN/m at TLC.[125,234] These observations suggest that the surfactant film is sorted or purified to generate a monolayer highly enriched in disaturated PL.

Whereas the above discussion primarily focuses on DPPC monolayers, DPPC containing up to 10 wt % cholesterol can also attain near-zero γ, although with a somewhat increased compressibility.[357] Fluorescence studies on the compression of spread surfactant films on the Langmuir apparatus reveal that during compression, small circular probe-excluding areas in the micron range (i.e., microdomains) are generated. These represent DPPC or DPPC:cholesterol-enriched areas, that form because these lipids pack together more efficiently than they do with unsaturated PLs (see Figure 17). However, these probe-excluding microdomains, which are evident at $\pi \sim 30$ mN/m, disappear at higher pressures and in the presence of cholesterol. It has thus been argued, on the basis of such fluorescence studies, that the physiological levels of cholesterol are important for preserving the essential phase distributions of surfactant.[263,264,306,322,402−405] However, in practice, this effect is due to the conversion of microdomains to nanodomains, which are difficult to detect by fluorescence but are evident

https://doi.org/10.1021/acs.chemrev.3c00146
Chem. Rev. 2023, 123, 13209−13290

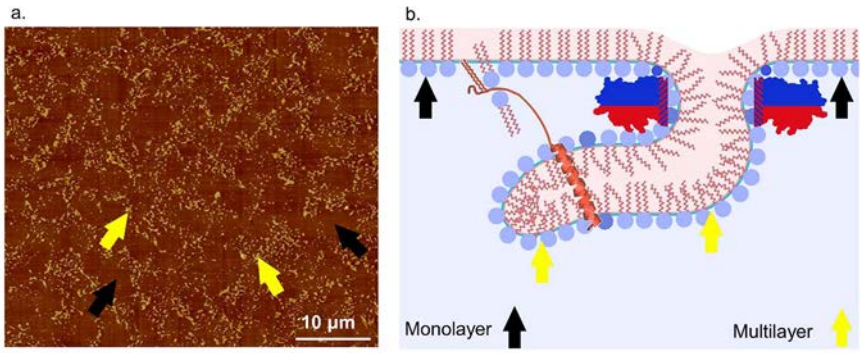

Figure 18. AFM evidence for the three-dimensional structure of a Survanta film and the corresponding model. (a) AFM image of a spread Survanta film compressed to 50 mN/m using a Langmuir film balance. The black arrows point to the surface monolayer, and the yellow arrows point to multilayers. (b) Schematic model showing the putative bilayer structure (yellow arrows) containing primarily unsaturated PL and the monolayer enriched in DPPC (black arrows). The transition from monolayer to the bilayer structure is presumed to involve the SP-B and SP-C adsorption structures. Note that while this schematic model depicts the evolving bilayer as extending downward into the aqueous subphase, it could also protrude above the water plane.[364,392,407] AFM image was adapted with permission from ref 209. Copyright 2011 American Chemical Society.

with AFM. Therefore some of these interpretations may need to be revisited.[13] Overall, films of either DPPC or DPPC:cholesterol are capable of reaching near-zero γ upon compression. It thus remains unclear if the phase distributions due to cholesterol serve a specific function in pulmonary surfactant.

6.3. Evidence for Compression-Driven Squeeze-out of Non-DPPC Components

The compression-driven squeeze-out mechanism is the predominantly proposed mechanism by which pulmonary surfactant, which is more than half unsaturated PLs, forms a DPPC-enriched film. The premise of this mechanism is that all the surfactant lipids adsorb to the interface, forming a film with a composition similar to that of the bulk. The less stable, more fluid constituents of this interfacial monolayer are then eliminated from the surface during surface area reduction,[355,356,393,394] so the remaining, mostly disaturated PLs would be able to reduce γ to near zero. The squeezed-out unsaturated PL species of surfactant would spontaneously form lipid bilayers.[354] This interpretation is consistent with experiments conducted with excised animal lungs, which show that the deflation pressure−volume curves are consistent with a surface monolayer that is highly enriched with DPPC.[237,399,400] Since film compression corresponds to lung deflation, this compression-driven squeeze-out mechanism was therefore thought to occur during the exhalation process.[234] During the inhalation process, this process is then reversed in a respreading process.

Insights into the molecular interactions occurring at the air−liquid interface of PL and surfactant monolayers have been derived from studies using the Langmuir balance in combination with fluorescence microscopy.[204,206−208,392,404−406] Fluorescence microscopy can detect the segregation of the lipids into domains that exclude the fluorescent probes and the more fluid areas that include the probes (see Section 4.3.1 for technical details). As explained earlier, this occurs because DPPC molecules pack together well and so tend to exclude the bulky fluorescent probes. Compression of porcine or calf surfactant extract monolayers on the Langmuir balance generates probe-excluding DPPC-enriched areas with diameters of ∼5 μm, i.e., microdomains.[206,392,404−406] Such domains can be thought of as an example of two-dimensional crystallization. Importantly, these domains grow as the pressure is increased, but only up to a point. We speculate that the limit on the domain size is controlled by competing forces: the line tension, which will seek to minimize the periphery of the domains; the pressure difference between the two phases, which will tend to increase the size of the domains; and the electrostatic repulsive forces between lipid headgroups, which will tend to increase the domain periphery (see Figure 8).

As mentioned earlier, fluorescence microscopy is limited to the detection of microdomains because of the optical resolution. At high π the microdomains seem to disappear.[405] However, this occurs because the compact domains break up into the much smaller nanodomains, which can no longer be detected by fluorescence. Additional insight has been obtained using AFM and ToF-SIMS[210,219] (see Sections 4.3.2 and 4.3.3 for details). Compressing a BLES film from high γ leads to a continuous decrease in γ (increase in π), until the equilibrium pressure is approached (Figure 17). At this point, there is a rising plateau, where decreasing the surface area only minimally decreases γ. While this plateau looks like a phase transition, it represents a change in the overall distribution of the components, causing enrichment of DPPC in the LD domains and depletion of the unsaturated PL in the LO regions. Following this plateau, long known as the squeeze-out plateau, further area decrease lead to a rapid reduction in γ to near zero.

AFM examination of such spread BLES films at different γ values provides insight into the different lipid phases during this compression. At low π, the film reveals large circular LO domains, apparently arising above the surrounding LD phase (Figure 17). With further area reduction, π increases and the number of large domains decreases, but these are replaced by nanodomains. This transformation is related to the presence of neutral lipids, such as cholesterol, and the hydrophobic proteins, which alter the balance of forces at the domain peripheries and promotes the formation of nanodomains[405] (see Piknova[392] for further details). Interestingly, during compression the proportion of the total surface area covered by microdomains and nanodomains increases to near 40%, which is similar to the percentage of DPPC plus cholesterol in BLES.[13] This would imply that the remaining more fluid LD regions could become somewhat depleted of cholesterol.

https://doi.org/10.1021/acs.chemrev.3c00146
Chem. Rev. 2023, 123, 13209−13290

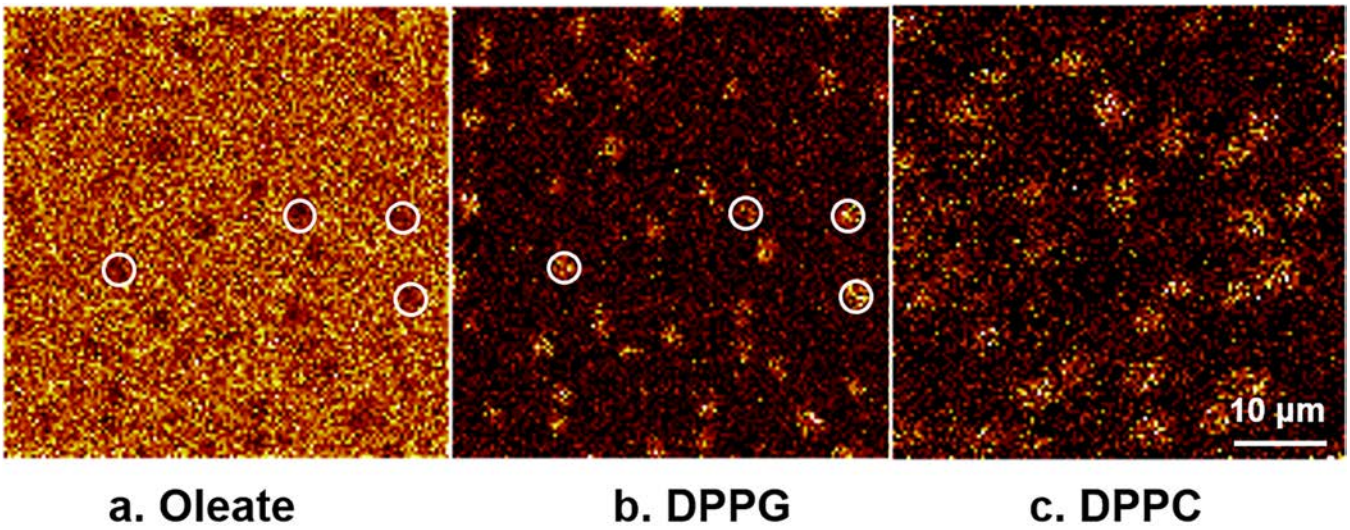

Figure 19. Time of flight secondary ion mass spectrometry (ToF-SIMS) images of BLES films compressed to about 50 mN/m at room temperature. (a) Image of the negative ions of mass 281 representing oleate from unsaturated PLs such as POPC and POPG. These lipids are excluded from small regions of the surface as indicated in selected areas by circles drawn on the image. (b) Image of the negative ions of mass 721 representing DPPG. This lipid is seen to be concentrated in small regions of the surface as indicated by the circles. This image is from the same area of the film as the image in (a), showing that the DPPG is enriched in the same areas that are depleted in unsaturated lipids. (c) Image of the positive ions of mass 735 representing DPPC. This lipid is also seen to be concentrated in small regions on the surface. This image is not from the same image as in (a) and (b), but the number of regions is comparable, although slightly larger than that of the DPPG-containing regions, presumably because of the higher concentration and perhaps an increased flight propensity. The implication is that the DPPC and DPPG exist in the same domains, and these mostly exclude the unsaturated lipids. It is interesting to note that AFM images of comparable films show regions that are 4 nm deeper than the surroundings, which may mean that these regions correspond to monolayers and the surroundings are mostly bilayers on top of the monolayers, consistent with the picture in Figure 18. Adapted with permission from ref 220. Copyright 2012 Elsevier.

Further compression results in the formation of multiple protrusions in the LE region. These increase in height until they start to flow over the LO microdomains. Conversion of most of the fluid LE phase to the bilayer protrusions would leave a monolayer highly enriched in disaturated PL species, which, as observed in Figures 17, can achieve γ near 0 mN/m ($\pi \sim 70$). Thus, compression of surfactant films leads to the generation of a compression-driven surfactant reservoir, apparently containing mainly unsaturated PL.

Spread DPPC monolayers require 12−15% surface area reduction to reduce γ from equilibrium to near zero. It is important to note that the compressibility of the BLES film at π between 50 and 70 mN/m is very similar to that of pure DPPC, lending further support to the notion of squeeze-out of the unsaturated lipid components and the formation of a TC-like phase. Comparing the compressibility of the BLES film and the DPPC film in this pressure regime to that of a 7:3 mixture of DPPC and POPG (Figure 17), it is evident that the latter is more compressible since it still contains POPG.

An AFM topographical image of a Survanta film compressed to π = 50 mN/m, i.e., above equilibrium, is shown in Figure 18a. In AFM images the higher regions are lighter in color. Thus, much of the film is composed of multilayers, indicated by the yellow arrows. The black arrows point to the remaining monolayer, which appear as holes or "wells" underlying the multilayers in this orientation (Figure 18a). Figure 18b presents a schematic representation of a PL compression-driven surfactant reservoir formed during the surface area reduction of a surfactant film just above equilibrium π and just below equilibrium γ.

Complementing the topographic measurements of AFM are ToF-SIMS studies on the chemical analysis of surfactant films. With ToF-SIMS, a strong gallium beam is scanned across a Langmuir−Blodgett deposited film, causing fragmentation of the surfactant molecules to yield positive, negative, and neutral products (see Section 4.3.3 for technical details). The charged fragments can then be analyzed by mass spectroscopy to produce a two-dimensional chemical compositional map of the pulmonary surfactant film.[145] As shown in Figure 19, at $\pi \sim$50 mN/m, i.e., $\gamma \sim$ 20 mN/m, just below γ_{eq}, the interfacial monolayer of a spread BLES is highly enriched in disaturated PLs, such as DPPC and DPPG, while the squeezed-out multilayers (i.e., the compression-driven surfactant reservoir) are enriched in unsaturated oleate-containing species.[219,220] It should be noted that this provides direct analytical evidence for chemical purification in a compressed modified natural pulmonary surfactant film. It is evident that such a chemical purification by selective squeeze-out of non-DPPC components is facilitated by the presence of the proposed adsorption structures stabilized by SP-B and/or SP-C, leading to buckled, elevated regions.[26]

These observations led to the following proposed compression-driven squeeze-out model. As a pulmonary surfactant spread monolayer is compressed toward equilibrium, DPPC TC or DPPC: cholesterol-containing LO micro- and nanodomains, corresponding to two-dimensional crystals, are generated. Initially the microdomains gradually grow in size within the surrounding more fluid surface. With further compression, the microdomains fragment into nanodomains. As compression proceeds toward γ_{eq}, the surfactant monolayer reaches a critical minimum surface area at which a true monolayer is no longer stable, requiring that some of the PL molecules be ejected from the surface, i.e., a 2D-to-3D transition occurs (Figure 18). In contrast to the large and relatively stiff DPPC or DPPC:cholesterol-containing microdomains and nanodomains, the fluid unsaturated PL species

https://doi.org/10.1021/acs.chemrev.3c00146
Chem. Rev. 2023, 123, 13209−13290

can readily migrate through the SP-B- and/or SP-C-containing adsorption structures into the subphase to form bilayers. This results in a DPPC- or DPPC:cholesterol-enriched monolayer above the attached unsaturated PL-enriched stacks of bilayers. This squeeze-out process further clarifies the requirement for hydrophobic surfactant proteins SP-B and/or SP-C[25,145,408] (see Zuo[13] for a review). Importantly, these transitions are reversible, demonstrating that the squeezed-out unsaturated lipids stored in the compression-driven surfactant reservoir can return to the monolayer through the adsorption structures as the surface area is increased again. This process is selective for fluid PLs.

6.4. Evidence against Compression-Driven Squeeze-out of Non-DPPC Components

The experimental observations derived using the combined fluorescence, AFM, and ToF-SIMS methodologies appear to support the compression-driven squeeze-out model. In addition, the increase in ordered domains in monolayers near γ_{eq} has recently been confirmed with X-ray diffraction.[33,403] However, several experimental limitations should be noted:

- These experiments were conducted with compressed Langmuir films deposited at room temperature. It is well-known that PL monolayer phase behavior is highly dependent on temperature.[185,263,356]
- These studies were conducted on slowly compressed spread films, whereas in the lung natural pulmonary surfactant is adsorbed at high concentrations and compression−expansion is usually continuous and highly dynamic.
- This proposed compression-driven squeeze-out mechanism was mostly derived using the Langmuir monolayer model, in which the surfactant film is formed at the air−water surface by spreading using a microsyringe, usually with an organic solvent, rather than the adsorption of surfactant vesicles from the subphase.

More important than technical limitations, there is also experimental data that is inconsistent with the compression-driven squeeze-out model. Specifically, experiments using the CBS, at physiological temperatures and using adsorbed films, have revealed data incompatible with the above model. These experiments examined the bubble surface area reduction required to reduce the γ of adsorbed BLES films from γ_{eq} to near-zero. BLES contains ∼38% DPPC, ∼10% other disaturated PC, ∼2.5% disaturated PG, ∼2.5% sphingomyelin, and ∼2.5% cholesterol, equivalent to ∼55% total nonfluid, stable lipid components by weight (Table 1). Consequently, a perfect squeeze-out process would theoretically require a minimum of 45% surface area reduction to remove the fluid constituents of a BLES monolayer containing all lipid components. Furthermore, spread DPPC monolayers require ∼15% area compression to reduce γ from equilibrium (∼23 mN/m) to near-zero (Figure 17).[30,37] Applying this compressibility factor adds an additional area of ∼7%, resulting in a theoretical total surface area reduction of at least 52% to reduce an adsorbed BLES film, containing all lipid components, from γ_{eq} to near-zero.[25,172,358] However, the CBS studies demonstrated that BLES films adsorbed at 1 mg/mL required only 20−25% surface area reductions to achieve γ ∼ 2 mN/m.[25,172] These observations strongly imply that if Postulate I, which suggests that a film of DPPC (or DPPC:cholesterol) is responsible for reaching low γ, is correct, the monolayer must already be enriched in DPPC *prior to* compression, i.e., during adsorption. This phenomenon conflicts with the implication of Postulate II, that all of the surfactant components adsorb to the interfacial surface.[172]

The rate of adsorption of a surfactant preparation increases with increasing concentrations. Interestingly, in general this rate of adsorption also correlates with its ability to attain low γ with low compression ratios.[25,159,171,267,367,376] Surfactants adsorbed at relatively low concentrations, as well as spread surfactant monolayers, normally require surface area reductions well over 30% from equilibrium. This is seen with natural porcine surfactant and with Curosurf, Infasurf and BLES films adsorbed on the CBS and CDS.[25,31,159,358,409] At intermediate concentrations of ∼750 μg/mL and higher, a 25% area reduction is often sufficient to attain low γ during the first compression. In both cases, subsequent compression−relaxation cycles exhibit hysteresis loops with surface area reductions decreasing to about 20% needed to attain low γ. At concentrations higher than about 1 mg/mL, the initial hysteresis loops tend to disappear and the film cycling exhibits hysteresis loops with surface area reductions between 25 and 2.5 mN/m of about 15%, the same reduction that is required for pure DPPC and DPPC:cholesterol mixtures.[31,159] These observations are in agreement with numerous studies showing that continuous dynamic surface cycling manifests in highly superior surface activity compared to quasistatic compressions−expansions.[240,322,334,358]

These experiments suggest that at low concentrations, the originally adsorbed monolayer contains components other than DPPC and cholesterol. These are likely unsaturated PG and PC and perhaps some cubic phase inducers, such as PE and *bis*(monoacylglyero)phosphate, which are then reduced in concentration by compression-driven squeeze-out during the repeated cycling, leaving mainly DPPC and cholesterol. However, as the applied concentration increases, less and less of these other components are adsorbed initially, due to the more efficient adsorption-driven lipid sorting at the higher concentrations. For example, isolated lamellar bodies and natural porcine surfactant adsorbed at 15 mg/mL exhibit identical biophysical properties where γ immediately oscillates between ∼27 and ∼2 mN/m with area variations of ∼15%.[242]

Interestingly, reconstituted DPPC:DPPG:SP-B:SP-C (63:33:2:2) mixtures adsorb quite rapidly.[159] Furthermore, once established, such films display dynamic cycling behavior comparable to that of porcine surfactant. This suggests that the hydrophobic proteins may sufficiently fluidize small peripheral areas of the DPPC:DPPG domains to allow attachment of the adsorption structures, eliminating the requirement for large LD or LE pools.[301] There is evidence indicating these hydrophobic proteins can adhere to the edges of the dense domains.[220,410]

These biophysical observations indicate that at concentrations above 1 mg/mL surfactants can form monolayers enriched in DPPC and cholesterol during *de novo* adsorption. As we shall show later, concentrations in neonatal lungs likely exceed this concentration, making this physiologically relevant.

6.5. Evidence for Adsorption-Driven Lipid Sorting

The observed initial area compression required to reach low γ with surfactant is about half of what would be expected if the composition of the adsorbed film had the composition of the bulk surfactant.[25] This strongly implied the possibility of a mechanism by which the monolayer can be enriched in DPPC during adsorption.

https://doi.org/10.1021/acs.chemrev.3c00146
Chem. Rev. 2023, 123, 13209−13290

Significant new evidence has been obtained using the CDS, with its recent adaption that allows for subphase replacement under physiological conditions.[31] With 1 mg/mL Infasurf, γ_{eq} is attained within a few seconds. The γ of washed Infasurf films at 37 °C varies between ∼30 and ∼2.5 mN/m during dynamic compression−expansion at 20 cycles per min with a compression ratio < 25%. Significantly, the initial compression, immediately after *de novo* adsorption, was able to attain γ < 5 mN/m with subphase-replaced films and ∼20% compression.[31]

Washing the subphase to remove free vesicles with up to 4 replacement volumes had no discernible effect on the dynamic surface properties, indicating the surface film is relatively stable. However, after 10 washes, the film behavior deteriorated considerably. This not only demonstrates that the adsorption-driven surfactant reservoir is sufficient to support surface cycling loops but also shows that these membranes are somewhat, but not strongly, resistant to disturbance by washing.

More importantly, surface dilational rheology measurements, performed on the freshly adsorbed films, demonstrated they have physical properties similar to those of pure DPPC monolayers.[31] These interfacial rheological studies imply that the DPPC or DPPC:cholesterol sorting process, i.e., chemical purification of the monolayer, is largely completed during *de novo* adsorption, *prior to* the initial compression. These results are interpreted to mean not that DPPC is selectively adsorbed[234] but rather that considerable DPPC:cholesterol (Infasurf), or DPPC (Curosurf), enrichment occurs during the adsorption process, by a mechanism involving an adsorption-driven lipid sorting. Formation of gel phases during adsorption has also been suggested by studies with isolated lamellar bodies.[364] These conclusions further emphasize the difference between spread and adsorbed films and provide the rationale for updating the model.

Recent GIXD investigations on spread DPPC, spread DPPC:cholesterol, and spread or adsorbed CLSE (Infasurf) films provide further strong evidence supporting these overall conclusions.[33] The GIXD experiments confirmed that spread DPPC monolayers at π ∼47 mN/m contain highly ordered TC structures where individual tilted DPPC molecules are packed into small, hexagonal units. Incorporating 25 mol % cholesterol changes the ordered structures from TC to the more fluid LO phase. The 3:1 DPPC:cholesterol (mol:mol) (approximately the ratio in CLSE) monolayer contains packed hexagonal unit structures with minimal acyl chain tilt. Spread CLSE monolayers likewise possessed the hexagonal unit structures as ordered regions with untilted chains, resembling the LO rather than the TC phase This is consistent with the presence of the anticipated DPPC:cholesterol unit structures (Figure 20). Not surprisingly, such ordered LO phases were also noted with adsorbed films created by infusion of CLSE vesicles. Interestingly, the proportion of the hexagonal ordered phase in the adsorbed monolayers increased substantially as the surfactant vesicle concentration was doubled to ∼1.1 mg/mL. This was interpreted as representing monolayer DPPC:cholesterol unit structure enrichment,[33] in agreement with the above CDS experiments.[31] The authors concluded that their GIXD data indicated a compositional change of the monolayer by selective insertion but did not propose a mechanism. It is suggested that these results can also be explained by an adsorption-driven sorting process.

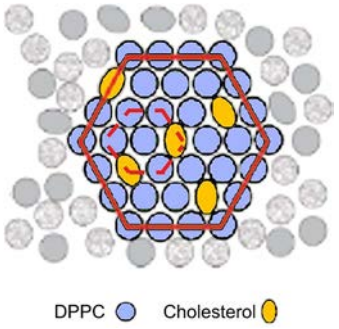

Figure 20. Hexagonal structures of DPPC-cholesterol complexes at the water surface, as determined by grazing incident X-ray diffraction. The large hexagon contains 32 DPPC and 5 cholesterol molecules. Note there is a small, seven molecule-containing smaller unit structure within the large hexagon. With high bulk concentrations of adsorbing surfactant, the proportion of organized unit structures at the surface increases. Adapted with permission from ref 33. Copyright 2020 American Chemical Society.

A difficulty with these GIXD studies is that, as with the ToF-SIMS investigations cited above,[220] experimental constraints limited the studies to room temperature. Nevertheless, when considered together with the CDS results, these observations provide powerful evidence indicating the creation of a DPPC:cholesterol-enriched monolayer during adsorption.

6.6. Other Potential Models for Surface Tension Reduction to Low Values

It should be noted that several other models have been proposed in addition to the classical model.

6.6.1. Surfactant as a Glass-like Amorphous Film. It has been reported that very rapid compression, with the CBS, of monolayers composed of surfactant lipid mixtures or even a spread monolayer of pure POPC generates a film, which is capable of supporting the high π required to reduce γ to near zero.[392,398,411,412] The proposed explanation is that such very rapid monolayer compression results in coalescence into an amorphous structure so quickly that the PL molecules lack sufficient time to form the normal liquid-crystalline phase and so are trapped in a glass-like amorphous state. This would suggest that the only role for SP-B and SP-C is to promote adsorption. However, whether alveolar surface area reductions attain sufficient speed to generate such situations has not been established. It may be that the rapid adsorption occurring with high surfactant concentrations can produce such monolayer structures in the lung. Nevertheless, the numerous observations demonstrating that relatively slow compressions of surfactant adsorbed at high bulk concentrations readily support high π and that quasi-static inflation:deflation maneuvers of immature lungs treated with surfactant or of mature lungs achieve very low γ would suggest that glass-like structures might help but are not essential.

6.6.2. Film Stability via Multilayers. As noted earlier, EM has demonstrated the presence of multilayered surfactant stacks at the air−water interface of the alveoli.[234] EM and AFM studies have revealed bilayer stacks, which could represent surfactant reservoirs, with adsorbed and compressed monolayers.[31,64,209,210] It has been suggested that compression of such underlying structures could generate resistance to collapse, not only due to the interfacial monolayer but also through lateral forces on the combined underlying bilayers.[149,160,264,292,403] In other words, each underlying bilayer

https://doi.org/10.1021/acs.chemrev.3c00146
Chem. Rev. 2023, 123, 13209−13290

provides some further resistance and, when added together, sufficient force is generated to attain π near 70 mN/m. The underlying vesicular structures thus constitute a kind of exoskeleton or scaffold, which deters shrinkage. While it is difficult to disprove such a suggestion, there is no real experimental evidence known to support it.[33,358]

Single spread monolayers of clinical surfactant extracts can reduce γ to low values. Infusion of lipid extract surfactant vesicles under a preformed surfactant monolayer at equilibrium does not result in a change in the proportion of the DPPC:cholesterol basic unit structures thought responsible for reducing γ to low values during compression.[33] Nor was there any evidence for the view that PL multilayer structures provide additional monolayer stability. As previously stated, the monolayer-associated bilayers of the adsorbed film (i.e., the SASR) would contain physiological levels of SP-B and SP-C. Any compressive forces on these underlying layers would tend to induce further subphase budding. Thus, the tendency would be to generate additional bilayers, rather than providing significant further resistance to collapse. It is observed that compressed surfactant Langmuir films initially produce long silo-like structures extending from the monolayer rather than closely packed bilayer sheets.[209,368,383,413,414] EM studies of adult lungs indicate that a large proportion of the alveolar hypophase is covered by a trilayer consisting of a monolayer lying above a PL bilayer. While there are sections of stacked multilayers, these only lie under portions of the surface monolayer.[358,388,415]

Another way that underlying bilayers could provide additional support to the overlying PL monolayer has been investigated using Langmuir trough, AFM, CBS, and computer modeling of monolayer behavior.[416] These studies revealed that the presence of underlying bilayer patches, equivalent to ∼20% of the monolayer area, approximately doubled the resistance to film buckling with low compression. However, this support was dependent on structural pinning involving the hydrophobic surfactant proteins. The presence of these proteins in monolayer:bilayer complexes provided physical resistance to scraping by AFM tips. These observations were interpreted as indicating that the "pinned" bilayer patches act as a kind of strapping, which breaks up long-range lateral forces, thereby providing support for the overall monolayer against buckling. The existence of SP-B-dependent bilayer contacts within vesicles has been observed with EM, and it has been suggested that such connectivity could be involved in promoting high π in monolayers.[302] Note that this model differs from the model in the previous paragraph by only requiring small "patches" rather than extending over the entire compressed region.

The process of film collapse into a multilayer structure at high pressures has been extensively studied using fluorescence microscopy and atomic force microscopy.[407] It appears that the composition of the monolayer determines the inextensibility (or rigidity) of the monolayer and that the larger this is, the more likely the film is to allow folding of the membrane. Furthermore, this inextensibility can be modulated significantly by small molecules, such as glycerol, binding to the interface.[417] These findings clearly have a direct bearing on how the monolayer film may collapse at high pressures and may provide a better understanding of how the monolayer can, or cannot, sustain high pressures.

6.6.3. The Role of Curvature. The human alveolus, with an average radius of ∼50 μm, has very high curvature compared to the droplets studied with the CDS, i.e., 3−5 mm.[31] It has been shown by fluorescence microscopy that there is a marked alteration in the morphology of the TC domains of adsorbed films of the clinical surfactant Survanta when the radius of bubbles is decreased to ∼100 μm.[418] The normally observed circular domains, that exclude the bulky fluorescent probes, increase in size and form roughly linear arrays. At radii larger than 100 μm, the monolayers are dominated by the LE phase surrounding the small, dark DPPC-rich TC domains. Compression isotherms of such films would be dominated by the fluid areas. However, with a radius of ∼100 μm, or smaller, the TC phase becomes predominant and surrounds pools of LE phase. These films would represent an example of percolation. Percolation refers to the concept where a fluid LE film with "islands" of TC phase offers little resistance to compression: the fluid phase will dominate the behavior. In contrast, a film with continuous TC phase containing small "pools" of fluid LE phase will be less compressible, because π will tend to reflect the continuous TC phase. Thus, the more continuous phase is known as the percolation phase and this governs the properties of the film.[398,418]

Survanta differs from Infasurf, BLES, and Curosurf in having added DPPC and free palmitic acid.[64] It also lacks cholesterol, so it forms TC domains rather than LO domains. Furthermore, Survanta has very limited amounts of SP-B (Table 1).[64,243] It was argued that the tilting of the DPPC chains creates an anisotropic film that will be prone to form elongated structures. Of note here, in contrast to Survanta, Infasurf and Curosurf do not exhibit high levels of the linear arrays of TC or LO phase on highly curved bubbles.[418] This may be related to compositional differences; Survanta contains ∼10 wt % palmitic acid and high (∼50%) levels of DPPC relative to the other surfactants. This could augment the tendency of the DPPC and palmitic acid (together comprising over 60% of Survanta) to localize in large TC-containing areas rather than nanodomains. This would automatically relegate the LE phase into small pools. It was also indicated that TC domain edges possess electrical charge, which promotes nanodomain formation, but this was overcome with high curvature.[418] The ability of natural and clinical surfactants, such as Infasurf and Curosurf, to attain low γ on more slightly curved bubbles or even flat Langmuir films would suggest that this mechanism could contribute but is not essential.

6.6.4. Asymmetric Bilayers. It has been speculated that the bilayers that compose lamellar bodies could be asymmetric, as occurs with the plasma membranes of cells.[149,419] In this context, recent observations, using wide-angle X-ray scattering (WAXS) (see Section 4.4.1 for technical details), have discovered that stacked bilayers of surfactant PL can form a L_γ phase, where a unit cell consists of two adjacent bilayers with similar asymmetric leaflet orientations (Figure 21).[420] Thus, the two inner facing leaflets of a bilayer pair of the unit structure are composed of crystalline, i.e., DPPC-enriched, PL, while the outer facing leaflets of each bilayer pair are enriched in acidic, anionic lipids such as PG. Such unit structures could feasibly be involved in spontaneously generating DPPC-enriched monolayers by somehow selectively delivering different leaflets to the surface. However, how this could occur remains uncertain. In addition, this L_γ phase is lost when surfactant neutral lipids and/or hydrophobic proteins are included in the mixture. Consequently, this cannot be considered a viable surfactant model. Nevertheless, the

https://doi.org/10.1021/acs.chemrev.3c00146
Chem. Rev. 2023, 123, 13209−13290

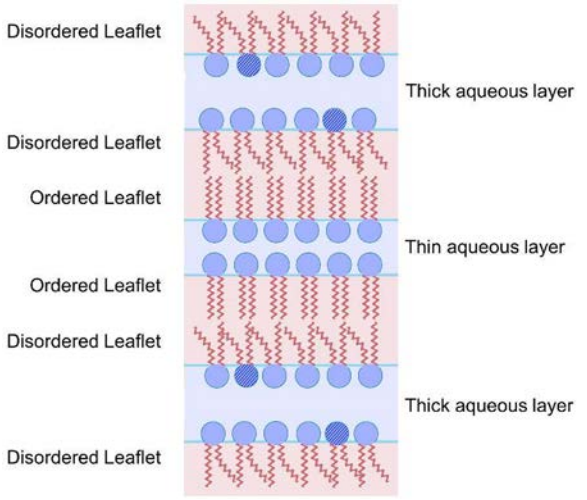

Figure 21. Schematic representation of the L_γ phase of pulmonary surfactant. The lipid fraction of Infasurf (CLSE) can spontaneously form bilayers in the L_γ phase, which contains asymmetric bilayers in which the one leaflet contains mostly unsaturated PL, including PG (purple), while the other contains mostly disaturated PLs in altering layers. As shown, the ordered leaflets face each other across a thin layer of water while the disordered leaflets face each other across a thick layer of water. Adapted with permission from ref 420. Copyright 2018 American Chemical Society.

observation that lipid mixtures can self-assemble into such nonhomogeneous asymmetric structures is intriguing. However, whether such counterintuitive, asymmetric behavior could contribute to DPPC enrichment during adsorption must still be investigated.

6.6.5. Surfactant Monolayers as Composites. The assumption that monolayers composed of ~50% LE fluid phase lipids are incapable of resisting a π of ~70 mN/m may not be entirely valid. High lateral resistance could arise through the principles governing the behavior of composites. Composites gain strength by dividing up large forces into a series of miniforces. The pressurized surface monolayer can thus be considered as a matrix composed of an LE phase enveloping the uniformly distributed LO nanodomains.[210,211] These nanodomains, which with BLES comprise close to half of the monolayer surface area at room temperature, could contribute strength by dividing up the large lateral pressure, as in composites or alloys.[13,24,210,211,421] Nanodomains should strengthen a film more than the larger microdomains because they partition the forces into smaller parcels. Composites gain strength through the fact that a fracture line through the weaker regions must travel around the solid elements to circumvent the structure.

This model is similar in concept to the pinned bilayer model.[416] Both interpretations involve the introduction of something, either stiff bilayer strapping or hard gel-like nanodomains, that serves to break up the overall long-range structural forces that can generate buckling or fracture. The resulting smaller dispersed forces can then be more readily accommodated. Consequently, a thin surfactant monolayer, fortified through the presence of embedded LO nanodomains, could generate significant resistance to collapse. However, increasing the temperature to the physiological range would decrease the number of gel phase domains in monolayers. With Infasurf bilayers, WAXS studies document that the nanodomains almost disappear at 37 °C.[349] The presence of SP-B plus SP-C accelerates this loss. Small angle X-ray scattering (SAXS) analyses (see Section 4.4.1 for technical details) of porcine natural and lipid extract surfactant bilayers find no evidence for the LO phase when heated to 40 °C, although this thicker lamellar phase is still detected with the total porcine surfactant PL fraction.[403] However, the lateral compressive forces in monolayers at π_{eq}, and more so at $\pi \sim 70$ mN/m, are considerably higher that the inherent ~30 mN/m membrane intermolecular pressure demonstrated for PL bilayers.[138−140] Nevertheless, whether these pressures generate sufficient nanodomains to provide adequate composite properties in monolayers at 37 °C is unknown.

6.7. Inhibition of Pulmonary Surfactant and Approaches to Counteract This Inhibition

Although usually studied in the context of lung injury, another approach to explore the mechanisms by which surfactant reduces γ is by examining compounds and enzymes that lead to inhibition of the material, as well as approaches to counteract this dysfunction. These studies often investigated inhibition of exogenous surfactant preparation by serum proteins, excess cholesterol, reactive oxygen species, phospholipases, and proteases, among others. The counteraction of inhibition has been demonstrated for polymer additives as well as SP-A.

The most frequently studied example of surfactant inhibition is by the addition of serum proteins. Mixed with exogenous surfactant, these proteins interfere with adsorption and γ reduction when analyzed on various surfactometers. Certain proteins such as fibrinogen, C-Reactive Protein, and hemoglobin are particularly inhibitory,[422,423] while the effect of albumin, although extensively studied, is relatively weak. The main mechanism for inhibition that has been suggested is that serum proteins interfere with surfactant adsorption by competing for the interface. Inhibition by phospholipases and proteases simply occurs due to altering lipid and protein content. Lysophospholipid generated *via* phospholipase A2 activity not only inhibits surfactant function, but it also makes surfactant more susceptible to inhibition by serum proteins. Finally, exposing exogenous surfactant to reactive oxygen species leads to less γ reduction, mainly due to oxidative modifications, and consequently impaired function, of SP-B and SP-C, although the PL are also affected.[171,308,345,424−429]

Many of the above mechanisms of inhibition can be overcome by the addition of SP-A.[345,422,425−430] It is likely that this is through the aforementioned formation of larger vesicles. The formation of larger aggregate bodies appears to promote enhanced surfactant activity in the presence of serum proteins through a process termed depletion-attraction[431,432] (see Zuo[13] for a review). With this process, large hydrated soluble molecules such as serum protein molecules are excluded from a depletion zone between large vesicles, when the hydrated vesicles are near the air−water interface. This results in an increased osmotic pressure arising from the depletion of soluble molecules from the surface region, which consequently drives the large vesicles toward the interface, enhancing adsorption. Both factors, a larger SASR and depletion-attraction, counteract surfactant inhibition due to serum proteins and other forms of inhibition.[430,433,434]

Interestingly, neutral and charged polymers, such as polyethylene glycol, chitosan, dextran, and hyaluronan, have been shown to enhance surfactant function using a similar depletion-attraction mechanism as described above.[176,211,432−434] As such, these compounds, when added

https://doi.org/10.1021/acs.chemrev.3c00146
Chem. Rev. 2023, 123, 13209−13290

to surfactant, can overcome serum protein and cholesterol inhibition. Considering the difficulty in producing synthetic variants of full length, oligomeric human SP-A, these polymers may be useful as additives to exogenous pulmonary surfactant in certain circumstances. Some success has been reported with dextran and hyaluronan in some animal injury models.[435,436] Unexpectedly, in others, such as with polyethylene glycol, lung injury worsened.[437] Consequently, further careful investigation, including effects on long-term surfactant recycling, is still required. Nevertheless, this approach appears to have therapeutic potential. The observation that brief exposure to hyaluronan fortifies surfactant, even after reisolation, is particularly intriguing.[434] Other factors, such as the possibility that surfactant PL headgroup dehydration may be involved in the ability of polymers to enhance surfactant function, require further investigation.[240] However, the endogenous alveolar glycocalyx also contains these types of molecules, specifically hyaluronan. Although little is known about the role of the glycocalyx in surfactant function, a recent study demonstrated that shedding of the glycocalyx led to surfactant impairment.[438,439] This could be related to the size of the hyaluronan fragments. It is tempting to speculate that the alveolar glycocalyx supportive effects on surfactant function involve a similar mechanism to that described for the polymer additives.

An intriguing form of inhibition is that by cholesterol, since it is one of the main constituents of endogenous surfactant. During development of the therapeutic surfactants BLES and Curosurf, it was noted that removing most or all of the neutral lipid fraction improved activity. Cholesterol is also removed during the manufacture of Survanta, but Infasurf maintains the full complement (Table 1). Other observations show a similar dichotomy. Studies with a surfactant-like PL mixture (DPPC:POPC:POPG, 50:25:15 wt %) show excellent surface activity during cycling with 1% porcine SP-B, similar to that of native porcine surfactant (i.e., $\gamma_{min} \sim 2$ mN/m; $\gamma_{max} \sim 30$ mN/m, with a surface area reduction of ~25%).[264,322] However, inclusion of either 5 or 10 wt % cholesterol markedly impeded this performance.[413,440] In contrast, adding 1 or 2 wt % SP-C to the PL mixture with the cholesterol reduced the surface area reduction required to attain low γ. Here, however, with or without cholesterol, very high γ_{max} was observed. Interestingly, these deleterious effects of physiological amounts of cholesterol were abolished by the simultaneous inclusion of both hydrophobic proteins. Thus, in the presence of physiological levels of cholesterol, neither hydrophobic protein alone could impart the necessary biophysical activity. It has also been observed that physiological amounts of cholesterol further exacerbated the deleterious effects of oxidation on surfactant function *in vitro*.[441]

A further important observation is that increasing cholesterol to supraphysiological levels, over 10 wt %, markedly interferes with surface activity during compression.[218,433,440] This could be due to interference with the stability of the hydrophobic protein-dependent neck-like attachment structures connecting the monolayers to the underlying bilayers. Unlike serum protein inhibition, the deleterious effects of high cholesterol are not reversed by multiple compression−decompression cycles.[376,442,443] As with other forms of inhibition, SP-A appears to counteract the effect of high cholesterol. Furthermore, cholesterol mediated inhibition of surfactant can be overcome using the cholesterol scavenger β-methyl cyclodextrin.[441,444]

In addition to inhibition by endogenous materials, surfactant can also be inhibited by inhaled aerosols and particles. In general, only small amounts of particles may reach the alveolar surface and interact with surfactant, with large material trapped in mucus and/or deposited in smaller airways.[445] Surfactant inhibitory effects of nanoparticles, which may be inhaled in a variety of circumstances, have been reported.[29,189−192,414,446] Nanoparticles vary in size, composition, properties, and uses; as such, it is impossible to generalize the effects of these materials on the surfactant system. Nevertheless, a negative impact on surfactant has been reported for some nanoparticles. For example, it has been shown that gold or titanium dioxide nanoparticles are capable of inhibiting both adsorption and γ reduction.[447,448] Similarly, several studies have demonstrated that some of the chemicals inhaled during the inhalation of e-cigarette vapor can impact surfactant function. In particular, inhalation of menthol flavoured vapor was shown to cause significantly impaired function of surfactant.[196,197] As vaping continues to increase in popularity, and nanotechnology continues to evolve, further studies on the impact on inhalation of these compounds on surfactant, and potential mechanisms to counteract this effect, are required.

6.8. Brief Synopsis of Surface Tension Reduction

Overall, although the majority of evidence suggests that a surface film enriched in DPPC and/or DPPC:cholesterol is responsible for reducing the γ to values near-zero, a number of potential mechanisms by which this surface film is generated have been proposed. Nevertheless, enticing new evidence suggests that adsorption-driven lipid sorting is responsible for an enriched surface film during the adsorption process at high concentrations. This mechanism, which is dependent on the previously suggested adsorption structures, involves DPPC enrichment without the need for compression-driven removal of non-DPPC compounds. This process is concentration dependent and, at low concentrations, can be enhanced by SP-A.

7. AN UPDATED MODEL OF SURFACTANT FUNCTION

In view of certain ambiguities with respect to the manner by which pulmonary surfactant forms a surface film capable of reducing γ to the low values required to stabilize the lung at end-expiration, we will in the following attempt to meld much of the current evidence into a cohesive model.

7.1. A New Perspective on Lung Surfactant Function

The information presented in Sections 5 and 6 indicates that current models for surfactant function do not fully explain all experimental data. Specifically, recent rheological and GIXD results are consistent with a DPPC-enriched monolayer being present at the end of adsorption and with purification increasing with higher initial bulk surfactant concentrations. It also appears undeniable that the adsorbed monolayers are functionally connected to reservoirs. Any model must account for these observations. Based on this we provide an updated perspective on lung surfactant function in healthy individuals namely:

- Pulmonary surfactant adsorbs rapidly to the air−water surface to *form a monolayer highly enriched in DPPC and cholesterol*. This process is termed adsorption-driven lipid sorting.

https://doi.org/10.1021/acs.chemrev.3c00146
Chem. Rev. 2023, 123, 13209−13290

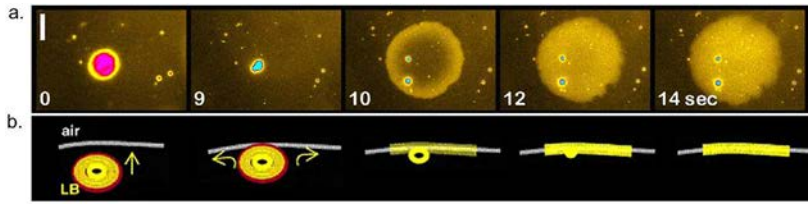

Figure 22. Inverted interfacial fluorescence microscopy images of an adsorbing lamellar body (LB) (a), and an interpretive description of the events occurring during this adsorption (b). The lipids within the lamellar body are noncovalently stained with the fluorescent dye FM 1−43. Once the lamellar body contacts the surface (9 s), there is a very rapid extrusion of fluorescent lipid onto the surface. The lamellar body contents spread at the interface until all or virtually all of the vesicular material is on the surface, forming a large, roughly circular surface patch. The nature of the two spots with bright circumferences is not known but could be membranous remnants surrounding the proteinaceous core observed within lamellar bodies. Note that it requires only ∼5 s to progress from the initial air contact to virtually complete lamellar body content insertion into the interface. Adapted with permission from ref 145. Copyright 2010 Elsevier.

- During the alveolar surface area reduction induced by exhalation, γ is reduced to low values. This is a consequence of the low compressibility of the DPPC:cholesterol film and occurs with *little or no change* in monolayer composition.
- Deep inhalations and sighs can induce temporary changes in monolayer composition, followed by compression-driven lipid sorting to restore the DPPC:cholesterol film.

7.1.1. Adsorption-Driven Lipid Sorting. There is strong biophysical evidence that at high concentrations of pulmonary surfactant, the initial rapid adsorption process leads to a monolayer film enriched in DPPC and cholesterol as the primary components. This process is facilitated by unsaturated PLs and the surfactant proteins SP-B and SP-C. With isolated lamellar bodies and high concentrations of natural surfactant, adsorbed films can attain very low γ with only ∼15% area reduction, similar to pure DPPC. It is also considered that there are SP-B and SP-C, and possibly combined, adsorption complexes, which act to catalyze formation of the enriched monolayer film along with an associated reservoir.

While the surfactant concentrations in the alveolar space in neonatal lungs at birth are hard to measure, there is convincing evidence, as outlined in Section 8, that the concentrations are sufficiently high (perhaps ∼6 mg/mL) to support the concept of adsorption-driven lipid sorting *in vivo*. Note that lamellar bodies, that are the source of surfactant in neonatal lungs, have been shown to possess superior adsorption qualities even at low concentrations.

We therefore propose that *in vitro* and *in vivo*, the initial adsorption process leads to a monolayer, enriched in DPPC and cholesterol, but that likely contains other minor components, that can support γ approaching zero.

7.1.2. Normal Breathing. The consequence of initially forming a monolayer film that can attain low γ is that this monolayer film needs not change composition to sustain normal breathing. This is significant for two reasons: First, the monolayer is an elastically compressible film, which means that normal breathing requires minimal work. Second, the monolayer can respond dynamically more rapidly, since between ∼2 and ∼15 mN/m there is no significant exchange of material from the film to the underlying bilayers.

Postulate II of the classical model envisioned formation of a DPPC-rich monolayer by squeeze-out, which stabilized the lung during each exhalation−inhalation cycle. The classical model also predicted the potential loss of small amounts of monolayer material during exhalation, requiring the adsorption of "new" surfactant material during the subsequent inspiration.[354,355,393] Both these actions would be energetically and dynamically inefficient.

7.1.3. Deep Breaths. Notwithstanding the lack of a biophysical requirement for lipid exchange between the surface film, the surfactant reservoirs, or surfactant in the hypophase, alveolar surfactant continuously turns over. This turnover presumably preempts surfactant dysfunction due to lipid and protein oxidation or other modifications of the surfactant film occurring from inhaled deleterious material during normal breathing. Secretion of new surfactant occurs during a deep inhalation, when the surface area of the alveoli expands beyond the normal range sustained by the DPPC:cholesterol monolayer. Here additional material from the reservoirs, and/or the freshly secreted material, is recruited to cover the expanded surface. Presumably, during the subsequent exhalation, or deep sighs, there will be a compression-driven lipid squeeze-out, that expels the unsaturated PLs back to the reservoirs.

7.2. The Model for Adsorption-Driven Lipid Sorting

7.2.1. The Process of Forming the *de Novo* Film. We propose that there are four steps leading to adsorption-driven lipid sorting.

(1) Diffusion of secreted lamellar body structures to the clean air−water interface.

(2) Rapid, explosive transfer of all the components of one or more of the outer bilayers of the lamellar bodies or vesicles to the air−water interface to form part of a monolayer.

(3) Rapid formation of a surface completely covered with surfactant, possibly with the incompletely adsorbed surplus material remaining as reservoirs.

(4) Depletion of most of the unsaturated PLs from the surface into the subphase as the surface pressure in the monolayer increases, because of continuing adsorption of more surfactant material, with the surplus unsaturated material forming a new adsorption-driven surfactant reservoir.

The first step involves diffusion to the surface and orientation of the vesicle until a fusion structure contacts the air−water surface.[37,319,366] The second step starts when this adsorption structure interacts with the air−water interface, and there is a rapid "hemi-fusion" process (Figure 11) leading to the generation of a lipid monolayer.[26,37,175,366,449] Visual evidence for the rapid adsorption of isolated lamellar bodies to clean water surfaces has been reported and is shown in Figure 22. Using fluorescently labeled lipids, it was shown that adsorption occurs in an explosive process, that initiates

https://doi.org/10.1021/acs.chemrev.3c00146
Chem. Rev. 2023, 123, 13209−13290

monolayer creation in much less than a second. When the concentration of lamellar bodies is low, the entire lamellar body can dissipate in less than 5 s.[145]

The initial adsorption events appear to occur in fractions of a second. It appears possible that surfactant adsorption could be initiated when lipid molecules, from the outer leaflet of the outermost PL bilayer of pulmonary surfactant vesicles, reach the air−water surface *via* the previously hypothesized SP-B and/or SP-C adsorption structures (Figure 13e).[10,11,26,238]

Initially, the flow of PL molecules from the outer leaflet of the outermost bilayer onto the surface would reduce the intrinsic intramembrane lateral pressure within the lamellar bodies below its inherent value of ∼30 mN/m, promoting disintegration of the DPPC-enriched domains.[37,138−140,450] Additionally, the loss of outer leaflet material would create bilayer instability, leading to collapse of the outer bilayer onto the air−water surface. Although the mechanism remains unknown, rapid formation of a complete interfacial monolayer ensues. As shown in Figure 22a, all the fluorescently labeled lipid material in a lamellar body can be deposited onto the surface. Evidence suggests that SP-B- and SP-C-based interbilayer connections exist within lamellar bodies and clinical surfactant vesicles,[231,302,303] allowing lipids from all bilayers to flow onto the surface (Figure 13e).

The third step ensues when the concentration of lamellar bodies is high enough to form a complete monolayer during the rapid adsorption process. At this stage, it appears that there is excess membrane material remaining within the lamellar bodies that can form the SASR. Note that in addition considerable material will remain in the subphase, that is not associated with the surface.[451]

The fourth step arises once the surface is essentially completely covered with a monolayer and the surface pressure approaches equilibrium. At this point, only a small change in π is required to change the composition of the monolayer from a mixture of LO and LD phases to a monolayer highly enriched in DPPC and cholesterol. Such a change in composition during the adsorption process is equivalent to the compositional alteration observed during the compression process shown for a spread BLES film in Figure 17. Here a pressure difference of about 4 mN/m causes the formation of the DPPC-enriched monolayer with several bilayers containing mostly the unsaturated PLs. The adsorption-driven lipid sorting process is therefore essentially the same as the compression-driven squeeze-out process, except that in the former case the pressure increase is driven by the accumulation of more lipid at the surface, rather than a change in the surface area.

7.2.2. Possible Molecular Mechanisms for the Adsorption-Driven Lipid Sorting. We propose the following potential mechanisms for initiating the adsorption process.

When an isolated lamellar body or surfactant vesicle interacts with the surface, PLs will start to flow onto the surface. Since DPPC-rich domains are evident in surfactant bilayers at 37 °C,[263,452,453] the first lipid to flow will primarily be unsaturated PLs, presumably through the adsorption structures. Depletion of the outer leaflet of the outermost vesicular bilayer would rapidly cause instability, promoting the wholesale collapse of surfactant material, both saturated and unsaturated lipid, onto the interface. The spreading forces generated during the formation of an intact surface monolayer at equilibrium pressure would expel the more fluid components out of this interfacial layer by adsorption-promoted squeeze-out through the adsorption structures. This mechanism invokes the need for the SP-B and/or SP-C in destabilizing lipid bilayers at the interface by initiating the flow of fluid lipids.

Support for this interpretation of monolayer plus SASR formation has been reported for native isolated lamellar bodies[145,238,362−364] and for injected clinical pulmonary surfactant vesicles.[387,451] These studies and the recent CDS experiments confirm that adsorption occurs extremely quickly,[31] suggesting PL material from the subsurface bilayer can be expelled onto the surface with force.[31,240,364,454] It appears important to reiterate that with low concentrations the entire lamellar body can disintegrate during adsorption, and this can happen within ∼5 s.[145,363]

The driving forces for the depletion of unsaturated lipids would arise partly from the free energy associated with the intermolecular pressure forces within bilayers, which will promote continuous monolayer spreading to the equilibrium spreading pressure, and possibly beyond,[364] and from the energy generated through hydration of the PL headgroups. Highly dehydrated PL headgroups have been detected in lamellar bodies, and to a lesser extent in surfactant preparations.[238,362,363] It has also been reported that, on occasion, adsorbing lamellar bodies may generate γ below equilibrium.[364] In addition, the simultaneous collapse of many vesicles onto the air−water interface could create a combined lateral force that drives increasing π, explaining why a high concentration contributes to a highly effective adsorption-driven lipid sorting process.

The details of the processes involved in the collapse of the outermost regions of the lamellar bodies, or the surfactant vesicles, remain unknown. It has been suggested that interdigitation, which refers to the state where the acyl groups from opposing bilayer leaflets no longer interact end-to-end but form a thinner membrane since the fatty acids adopt a side-by-side configuration,[318,454−457] could act as an intermediate state in SP-C promoted adsorption.[316,318] In addition, it has been proposed that the collapsing bilayers could generate bicelles (bilayer:micelles), which are small patches composed of lipid bilayers with the unstable hydrophobic rims stabilized by amphipathic proteins such as SP-B or cone-shaped lipids such as PE, lyso-PC, or monoacyl-*bis*-glyerophosphate.[296,371] However, these discs are much too small to permit sufficient curvature to reform into closed bilayer vesicles. These concepts remain an important area for innovative investigation.

7.2.3. Potential Molecular Mechanisms for Formation of Surfactant Reservoirs. We propose that there are three closely related, potential mechanisms for forming attached reservoirs.

The first mechanism is based on the previously described evidence suggesting that there are surface-associated reservoirs, which retain both disaturated and unsaturated lipids, as outlined in Section 5.4.[25,172,358,387] Except at very low concentrations, there will be excess vesicular material that remains interconnected that could constitute a SASR. This would occur because adsorbing surfactant material from different secreted lamellar bodies or vesicles would cover the interface sufficiently quickly to limit the amount provided by each multilamellar vesicle. In addition, most of the lamellar bodies or surfactant vesicles injected into the subphase would be excluded from the adsorption process, and so would remain free, completely dissociated from the surface.[451] The key here is that due to its bulk, this surfactant reservoir would retain a

https://doi.org/10.1021/acs.chemrev.3c00146
Chem. Rev. 2023, 123, 13209−13290

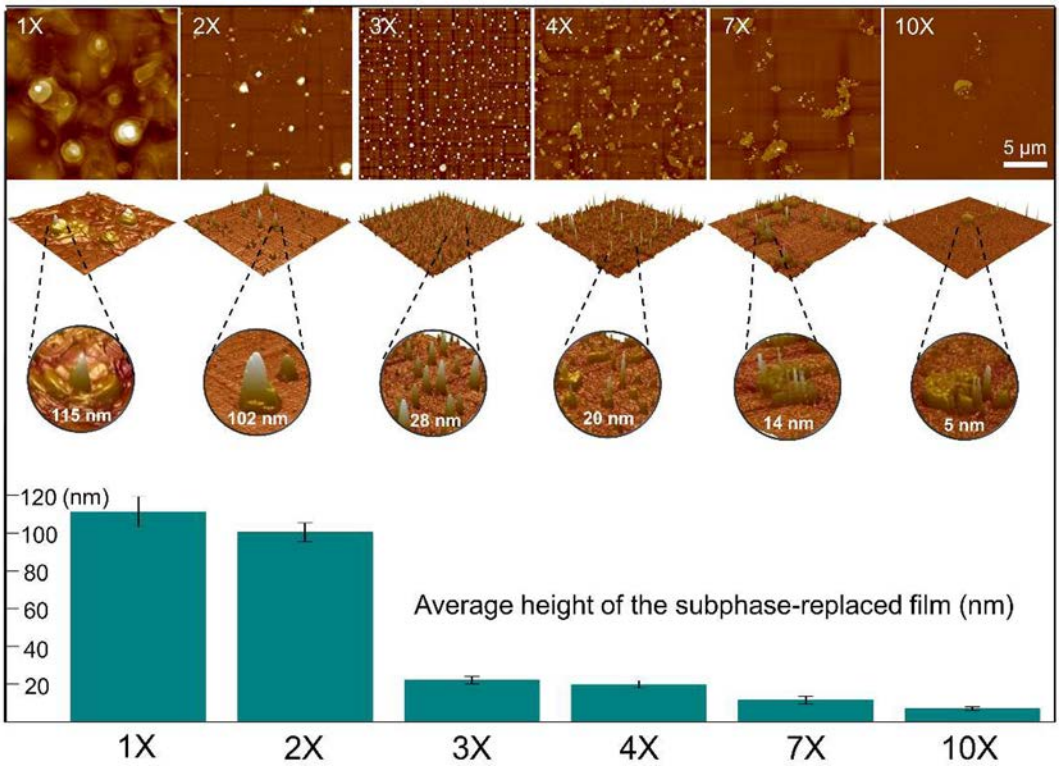

Figure 23. Lateral structure and topography of the subphase replaced Infasurf film with various replacing volumes from 1-fold (1×) to 10-fold (10×) of the original droplet volume. Also shown is a quantified height analysis of the subphase replaced Infasurf film with various replacing volumes. It was observed that 3-fold and 4-fold replacement volumes removed most of the larger surfactant structures, presumably vesicles of ∼110 nm height which may represent the SASR. With 3-fold or more volume replacements, smaller aggregates of ∼24 nm remain, which are interpreted to be adsorption-driven surfactant reservoirs. Most of these smaller aggregates are removed by the 10th wash. All AFM images have the same scanning size of 20 × 20 μm^2. Images in the first two columns have a z range of 100 nm, while the rest of the images have a z range of 20 nm. It is found that 3-fold and 4-fold replacement volumes are the optimized volumes, as they efficiently remove the large vesicles from the droplet and meanwhile preserve the adsorption-driven surfactant reservoirs of the adsorbed Infasurf film. Adapted with permission from ref 31. Copyright 2020 Cell Press.

composition similar to the bulk concentration of the initial surfactant, and hence is different from the DPPC-enriched monolayer.

In contrast to rapid expulsion of unsaturated PL-rich vesicles, the more condensed DPPC:cholesterol regions of the monolayer, present as LO domains, are too large to access the adsorption structures and should be sufficiently stable to be retained by the expanding monolayer, as π attains equilibrium. Thus, it is suggested that the SP-B- and/or SP-C-dependent adsorption structures on the SASR could permit retrograde flow of fluid lipid (i.e., desorption) back into the attached remnants of the adsorbing lamellar bodies or vesicles. Considering that surfactant contains ∼50% unstable lipid moieties,[25] approximately twice as much surfactant material must adsorb to form a complete monolayer composed entirely of the more stable elements. This mechanism would require that surfactant material is being adsorbed onto the surface at the same time that fluid material is being desorbed through the adsorption structures, which may be problematic.

The second mechanism is based on the observations that the adsorption-driven lipid sorting (as well as the compression-driven squeeze-out) leads to a surfactant reservoir, which would presumably contain mostly unsaturated lipid. Here, the more fluid areas of the monolayer initially formed would contain adsorption structures. As the adsorbing monolayers collide, π will rapidly increase the expulsion of unsaturated PLs through these structures into relatively small bilayer sac-like blebs (Figure 18), or multilamellar structures under the monolayer, as demonstrated by AFM (Figure 23).[31] Some unsaturated PLs could also form free vesicles, but this is less certain. The less fluid nano- and microdomains would be sequestered at the surface, allowing the monolayer to approach equilibrium. The small bilayer sac-like formations generated during this process would be similar to, and would possess properties much like, the multilayers observed with compression-driven squeeze-out of spread monolayers, i.e., the compression-driven surfactant reservoir, as described previously (Section 5.4). To differentiate, these new structures will be designated the adsorption-driven surfactant reservoir.

Evidence for this lipid propulsion stems from monolayer studies demonstrating the selective loss of fluid lipid during monolayer compression. Even with the slow Langmuir technique, high π is more readily attained with continuous, rather that quasistatic, area reduction.[357,358,393] This is in keeping with the fact that surfactant, adsorbed at higher bulk concentrations, requires less compression to attain high π during the first compression.[159,242,387]

In effect, this second mechanism is an extension of the previously described compression-driven process but involving two types of reservoirs. The adsorption structures act to catalyze the adsorption of part of the vesicular PL constituents onto the surface, but this is incomplete, resulting in remnants as the SASR (the originally proposed reservoir). In addition, the adsorption structures, contained within the collapsing

https://doi.org/10.1021/acs.chemrev.3c00146
Chem. Rev. 2023, 123, 13209−13290

vesicular layers that form the nascent monolayer, promote the desorption of fluid, unsaturated components into a second type of reservoir, the adsorption-driven surfactant reservoir. *In other words, while the very initial adsorption events are not selective, the following desorption process becomes selective for fluid components.* In both cases, DPPC:cholesterol enrichment of the surface monolayer, or DPPC in the case of Curosurf, would be sufficient to permit γ to fall from equilibrium to near-zero during the initial compression of 25% or less. Likewise, the lateral compression of the surfactant monolayer at the alveolar surface, generated during exhalation, can reduce γ to the low values required to stabilize the lung.[125,234]

Note, however, that while there is evidence for the existence of both types of surfactant reservoirs, it is not known whether they could functionally coexist in association with the same monolayer, since this would require three lipid structures with different compositions being at equilibrium—the SASR with a composition approximating the secreted lamellar bodies; the monolayer enriched in DPPC:cholesterol; and the adsorption-driven surfactant reservoir enriched in unsaturated lipids.

The third mechanism leads to formation of reservoirs containing primarily unsaturated PLs because of the enrichment of the surface monolayer with disaturated lipids and cholesterol. This is consistent with recent investigations from the laboratory of Zuo, using his most recent version of the CDS (see Section 4.2).[31] Examination of freshly adsorbed films by AFM reveals many multilayered vesicles of ∼100 nm, corresponding to 25-odd bilayers (Figure 23). Such vesicular material is consistent with the SASR concept proposed by Schürch, over 25 years ago.[172,234,358,387] However, these large vesicular structures can be removed by washing the adsorbed film with two or three replacement volumes. This observation brings into doubt the manner by which these large vesicular structures are attached to the surface film. In other words, these structures could be loosely adsorbed, rather than functionally connected by SP-B- or SP-C-dependent adsorption structures. The washed surfaces retained smaller, ∼24 nm high structures, corresponding to 6 bilayers, presumed to represent the adsorption-driven adsorption reservoirs containing unsaturated lipids. Further, this washed film is fully functional during repeated surface area cycles. Repeated washing, up to 10 replacement volumes, is required to remove enough of the smaller structures to hamper surfactant function. These observations would imply that the freshly adsorbed film is composed of a monolayer, with attached small adsorption-driven surfactant reservoirs composed of unsaturated PLs. In other words, there is no structural or functional need for a SASR.

Briefly, it is proposed that adsorption-driven lipid sorting arises through two continuous steps. First, there is lipid adsorption from the outer leaflets of the exterior layer from secreted lamellar bodies or surfactant multilamellar vesicles, which creates bilayer instability leading to collapse onto the interface. In the continuing process, the spreading monolayers arising from different lamellar bodies or vesicles collide with sufficient force to expel the more fluid constituents into monolayer associated bilayers. The required drive for this lipid sorting arises from intra-bilayer lateral pressure and from the rehydration of the surface PL.

We appreciate that these mechanisms are highly speculative and may appear counterintuitive. The first mechanism could be interpreted as suggesting that surfactant material is being transferred, both on and off the monolayer at the same time. The second mechanism implies the possibility of having two bilayers of differing composition being functionally associated with a monolayer through adsorption structures. The third mechanism indicates that the more traditional concept of the SASR being composed of the residues of non-fully adsorbed surfactant vesicles may be untenable. Nevertheless, each of these models conform with a considerable amount of theoretical and experimental evidence.

7.3. Consequences and Caveats Related to the Model

Following a summary of the key evidence supporting adsorption-driven lipid sorting, this section will present concerns and apparent gaps in the available experimental support.

When lipid extract surfactant labeled with ^{14}C-DPPC is injected under a clean surface to a final concentration of 0.3 mg/mL, γ attains equilibrium within minutes. This process is accelerated by SP-A.[376,458] Surface radioactivity, with or without SP-A, does not equilibrate until over an hour. Thus, only a very small fraction of the administered surfactant is present in the surface film.

As discussed earlier, increasing the bulk concentration results in a film with superior surfactant properties. This coincides with the view that multiplying the adsorption sites generates a better film by creating a more powerful spreading force to expulse the fluid PL. This is also consistent with the observation that adding SP-A or employing isolated lamellar bodies produces excellent films. Moreover, with low levels of lamellar bodies, the adsorption, i.e., γ reduction, initiates rapidly, but thereafter slows.[459] With many lamellar bodies, only the rapid phase will occur, thus eliminating the slower phase and maintaining a powerful spreading force. These observations indicate that a more rapid monolayer formation facilitates adsorption-driven lipid sorting. This is consistent with the rheological observations indicating a stiff DPPC-enriched monolayer at the end of adsorption.[31] As well, continuous dynamic cycling of surfactant yields better surface activity than quasi-static cycling.[171,264,322,334,358] This could be associated with subsequent squeeze-out occurring during further compressions, and again, refining improves with faster compression.

As shown by GIXD, adsorbing lipid extract surfactant vesicles (Infasurf) form surface unit structures containing DPPC:cholesterol, with basic crystalline units of varying sizes (Figure 20).[33] Increasing the bulk concentrations leads to an increase in these basic units, consistent with a more rigid film.

The rheological and GIXD results are consistent with a DPPC-enriched monolayer being present at the end of adsorption and with purification increasing with higher bulk surfactant concentrations. It also appears highly likely that the monolayer is functionally connected to surfactant reservoirs. As suggested above, any model should account for these observations.

Overall, it is proposed that as the monolayer starts to achieve equilibrium, sufficient backpressure would ensue promoting adsorption-driven lipid sorting. The connected underlying bilayers forming the SASR are important, as they both provide additional material during the initial adsorption stage and, at least theoretically, can accept the less stable components from the interface via the SP-B and SP-C adsorption structures during the later compressive stage. Evidence for this stems from EM of isolated lamellar bodies indicating membrane:-membrane interconnections, apparently due to SP-B and/or

https://doi.org/10.1021/acs.chemrev.3c00146
Chem. Rev. 2023, 123, 13209−13290

SP-C. In addition, bilayer bifurcations linking adjacent lamellae have been detected.[241,302,460]

In addition to rehydration, further force could be provided by the bending energy involved in producing curvature of the vesicular bilayers. As indicated above, the surface film in the alveoli is essentially flat, compared to vesicles. The bending energy released during the formation of stacked lipid membranes and relaxation of the curved structure could provide an additional force toward ejecting PLs onto the surface. It has been reported that single or a few lamellar body structures can adsorb onto an air−liquid interface with sufficient force to generate both LO and LD monolayer phases and a multilayered structure.[364] We suggest that with a high lamellar body content, the interface becomes primarily LO.

A potential difficulty with the model is that the mechanisms involved in bilayer collapse to form the monolayer are admittedly vague. In addition, the forces involved in the ejection of unsaturated PLs from the surface during adsorption are still ill-defined. The monolayer internal equilibrium π of ∼47 mN/m is higher than that of the internal membrane π of ∼30 mN/m, generating a pressure gradient.[138−140,450] More importantly, it has been argued that lamellar bodies are more highly dehydrated than natural surfactant, or extract surfactant, and this contributes to the superior activity.[242,362]

Another possible objection to this model is that the proposed acyl group exposure to water during the bilayer collapse may seem unlikely. This criticism may be overstated. Water interactions with hydrocarbons occur with short chained PLs and with detergent micelles, and this helps explain their rapid adsorption. These structures also have low critical micellar concentrations. DPPC preparations that are sonicated for long periods to produce small vesicles adsorb rapidly, presumably because the very high curvature induces defects allowing water penetration. This permeation would also apply to curved DPPC bilayer membranes, especially below 41 °C.[461] DPPC membranes are water permeable, and this is markedly reduced by cholesterol, which reduces the intramembranous free cavity density.[462] Thus, it appears that water hydrocarbon interactions can occur, but are energetically costly.[244]

The least evidence-supported proposition of the model may be the suggested collapse of partially delipidated bilayers to form a monolayer containing all of the lipid constituents. This step is critical in the formation of a DPPC-enriched monolayer. There does not seem to be any direct evidence for other explanations, such as SP-B- or SP-C-mediated selective DPPC transport. Both SP-B and SP-C reside in the fluid sections of monolayers[300,315] and bilayers.[294,301,453] It appears undeniable that DPPC somehow accesses the interface. Bilayer collapse onto the surface appears to be the most likely way of rapidly transporting DPPC to the surface.

It has been reported that the initial step in surfactant lipid absorption proceeds more rapidly when anionic PLs, such as DPPG or PG, are included and as the PL concentration is increased.[366] This step is dependent on the hydrophobic proteins, but surprisingly, the PL saturation state has little effect. The subsequent step proceeds more efficiently when unsaturated lipids are included and with higher PL surface concentrations, i.e., with higher π. With low PL concentrations, this can result in an acceleration during the late stage of adsorption.[377] This contrasts with detergents, such as sodium dodecyl sulfate, which adsorb to equilibrium with first-order kinetics.

It has also been suggested that unsaturated lipids may adsorb initially in an apoprotein-independent manner. The hydrophobic proteins, particularly SP-B, would then contribute to advancing this process.[319] However, the ability of antibodies against either SP-B or SP-C to block adsorption of isolated lamellar bodies appears to indicate an important role in initiation and that these small peptides are present close together at the periphery or may form a complex.[238]

The suggestion that DPPC or DPPC:cholesterol nano- and microdomains are formed in the monolayer, as high π is restored during adsorption, is conjectural, but seems logical. However, the proportion of these surface structures present at physiological temperatures is uncertain.[26,392] It is known that BLES and Infasurf films compressed to near-zero γ in the CBS can remain stable even at supraphysiological temperatures. In the case of BLES, low γ is maintained for hours. Lungs maintained at end compression *in situ* exhibit behavior consistent with a prolonged maintenance of low γ.[235,399] These observations are in agreement with the suggestion that the monolayer must be highly enriched in DPPC.

The ability of adsorbed surfactant to maintain low maximum and minimum γ during cycling has long been attributed to the presence of a functional SASR (Section 5.4).[172,358] It is therefore interesting to note that surface activity compatible with normal lung properties can be achieved in the absence of a SASR. Imaging of Langmuir−Blodgett deposits of adsorbed Infasurf films revealed that three subphase washes of these films removed essentially all of the larger membrane structures of ∼100 nm height, presumably the SASR (Figure 23). After 3 subphase washes, only smaller bilayer structures with a height of ∼24 nm remained. Nevertheless, despite the loss of the SASR, surface activity representative of good dynamic cycling was retained up to 10 subphase washes. This observation could be simply explained by the larger structures being more fragile and thus being able to break off during washing to yield smaller structures. However, this could also be interpreted as the larger structures being loosely associated, nonfunctional adsorbed surfactant, rather than a SASR.[31]

The observation that the presence of a SASR, as defined by Schürch, is not essential for dynamic cycling warrants a brief re-examination of this entity. This concept arose from observations that after the subphases of adsorbed surfactant films were extensively washed, adsorbed films could be expanded and then compressed to low tensions at a surface area several times larger than originally.[172,358] This led to the suggestion that surplus material was associated in a hydrophobic protein-dependent manner. These studies reinforced reconstitution investigations demonstrating that in addition to inducing monolayer formation, the hydrophobic proteins functioned to bind PL vesicles to the monolayer.[343,365] Cations, particularly divalent cations such as calcium, were found to be critical, even in the absence of the anionic PL PG. Rinsing with ethylenediaminetetraacetic acid (EDTA) abolished vesicle binding. In contrast to other studies, little effect of PL composition, such as including anionic lipids, was observed. These authors suggested that differences in adsorption due to PG, reported by others, might be explained by differences in vesicle size. Note that while consistent with a SASR, these findings could also be explained by loosely adsorbed vesicles, which were not bound by hydrophobic proteins.

The observation that extra DPPC can be incorporated into the surface monolayer during area expansion seems to conflict with the suggestion that the only reservoir associated with the

https://doi.org/10.1021/acs.chemrev.3c00146
Chem. Rev. 2023, 123, 13209−13290

monolayer is the small monolayer-associated blebs generated by the adsorption-driven surfactant reservoir.[31] These smaller monolayer-associated structures would contain very little disaturated lipid, certainly not the 4−5-fold complement which can be accessed during subsequent expansion. However, it could be that the washing procedures were inadequate to remove all free or nonfunctionally adsorbed vesicles. These could then adsorb when γ rose to equilibrium. Thus, once again, whether these vesicular remnants represent adsorption structure attached to the monolayer by hydrophobic proteins or are monolayer-associated vesicles is not clear, but both structures could readily be incorporated into the surface monolayer.

Yet another objection to the two-reservoir-dependent mechanism is that it could be argued that the simultaneous presence of large attached multilamellar vesicles as a SASR and small monolayer sacs is unlikely, because of the difference in the forces due to membrane bending. This interpretation would suggest that the large structures associated with the adsorbed films in Figure 23 are loosely adsorbed material and are not functionally attached. This is consistent with observations on the formation of supported lipid bilayers. With this latter procedure, vesicles adsorb and spontaneously rupture onto a substrate of glass, mica, silicone, or other materials. Here, attractive forces between the vesicle lipids and the substrate, such as van der Waals and electrostatic, are thought to induce vesicle deformation, resulting in rapid rupture due to vesicle:substrate interactions.[378−380,463] Subsequent bilayers can then adsorb onto the original substrate bound structure by vesicle:vesicle interactions. This could bring into question the coexistence of large vesicular remnants comprising the SASR, coexisting with the small sacs generated by adsorption-driven squeeze-out.

Yet, the greatest bending energy would be inherent in very small vesicles. However, isolated lamellar bodies and lipid extract surfactant vesicles, which are quite large, adsorb most readily. Also, it has been suggested that the positive curvature of the outer leaflet of a bilayer is compensated by the negative curvature associated with the inner leaflet.[26] Consequently, the contribution of forces derived from curvature may be limited. Pore formation can contribute to bilayer rupture, and this appears linked to high curvature necks or "worm-hole" formation.[384,385] However, in any event, the adsorption mechanism for surfactant vesicles does not require a curvature-induced bilayer pore, because both SP-B and SP-C readily promote vesicle leakage, presumably via the transmembrane neck-like structures.[10,26,290,326]

Examination of fixed lung tissue by EM reveals the presence of a bilayer, apparently covering the entire alveolar hypophase.[172,358,388,415] In some places flat stacked bilayer structures are also observed (see Figure 11 in Schürch et al.[358] for specific details). Assuming a composition similar to that of the secreted surfactant, the single bilayer would contain roughly the same amount of DPPC as the monolayer. Presumably the bilayer is attached to the monolayer by apoprotein-based adsorption structures. During deep breaths, this could supply additional lipid to the monolayer as the surface expanded. This could explain how surfactant accesses the monolayer with SP-A$^{-/-}$-deficient mice lacking tubular myelin.[464,465] It appears plausible that this bilayer, and the associated stacks, represents the remains of the SASR, but the possibility that it arises from fusion of the squeezed-out bilayer blebs cannot be discounted. In this latter case, these bilayers would mainly be unsaturated.

When the usual aqueous surfactant suspension is replaced by an alginate solution during surfactant adsorption at 1 mg/mL, the latter can be solidified by addition of calcium.[409] This enabled EM examination of the surface film. Alginate did not hamper biophysical properties. After osmium fixation, the adsorbed films appear similar to those observed with micrographs of fixed lungs.[358,409] Unilamellar vesicles were detected just under the surface films, but whether these associations are functional is not known. Not unexpectantly, spread DPPC monolayers did not stain with osmium. More rapid adsorption, for example with higher bulk concentrations, led to increased multilamellar formation. Film compression leading to low γ generated larger multilayers. Suspensions of DPPC:unsaturated PG formed distinct surface films with associated unilamellar vesicles but fewer multilamellar structures. Once again, whether the surface bilayer directly under the hypophase surface represents the SASR, or the recently observed adsorption-promoted surfactant reservoir, or both, is not clear.

7.4. Brief Synopsis of the New Model

Because of the complexity of the proposed formation of the monolayer and associated reservoirs, it may be helpful to highlight the key points:

(1) A partial monolayer forms when surfactant vesicles (or secreted lamellar bodies) interact with the interface, allowing mainly unsaturated PLs from the outer vesicular bilayer leaflet to initially gain the surface *via* SP-B/SP-C adsorption structures.

(2) The loss of PLs from the outer vesicular leaflet causes collapse of the vesicular content onto the surface causing all PLs to transfer to the surface, forming an expanding monolayer in a nonspecific process.

(3) As a complete monolayer is forming, the π increases, forcing the fluid lipids out of the monolayer, leaving a monolayer enriched in saturated lipids, mainly DPPC.

(4) The final monolayer will have reservoirs of surfactant functionally attached, and there are three possible scenarios:

   a. Vesicles that have not fully collapsed may remain attached. These would essentially have the original composition PLs and could provide access to lipids during breathing.

   b. Vesicles that have not fully collapsed may remain attached along with the newly formed adsorption-driven reservoirs of mostly unsaturated PLs arising from the enrichment of the monolayer in saturated lipids.

   c. Only newly formed reservoirs of mostly unsaturated PLs remain functionally attached to the monolayer, providing access to lipids during deep breaths.

In summary, it is proposed that a monolayer highly enriched in DPPC:cholesterol can be achieved rapidly during surfactant adsorption. Ambiguity exists as to whether this adsorption-driven lipid sorting involves a single or two distinct surfactant reservoirs. Assuming there are two distinct reservoirs, the first would correspond to the original SASR postulated by Schürch.[172,358,387] This reservoir is composed of remnants of the adsorbing vesicles which remain functionally attached to the monolayer. These provide material for the adsorbing

https://doi.org/10.1021/acs.chemrev.3c00146
Chem. Rev. 2023, 123, 13209−13290

monolayer and may accept desorbing fluid components. However, evidence for this SASR is highly circumstantial. The additional reservoir, consisting of small bilayer blebs, is formed by forces generated through the confluence of expanding material arising from multiple adsorption sites. These appear to be a likely depot for the desorbed fluid components.

Expanding this model to breathing *in vivo*, once the DPPC-enriched TC or LO phase monolayer is formed, we propose that it can be compressed and expanded with γ ranging between ∼2 and ∼20 mN/m, without any significant change in the monolayer composition. This occurs with a surface area reduction of only ∼15%. The role of the hydrophobic proteins and the unsaturated lipids in the reservoirs will arise if the surface is expanded beyond the point where γ is elevated above ∼23 mN/m, such as with a deep inhalation. It is envisaged that the unsaturated lipids will flow from the SASR or the smaller bilayer blebs onto the surface during this excessive expansion, followed by a compression-driven squeeze-out process to restore the DPPC-rich LO phase during exhalation.

8. WHAT DO PHYSIOLOGICAL AND PATHOPHYSIOLOGICAL STUDIES TEACH US ABOUT SURFACTANT FUNCTION?

Whereas the above sections mainly focus on the biophysics of the formation of a surface tension reducing film, this surfactant layer exists in a complex physiological environment. Crosstalk between our understanding of surfactant biophysics and pulmonary physiology is required to further enhance our understanding. For example, our model of adsorption-driven lipid sorting implies a requirement for high surfactant concentrations at birth. Conversely, physiological studies on surfactant have elucidated an important role for this material in host defense mechanisms. There likely exists an interconnectivity between these roles and surfactant's biophysical functions, which will be influenced by surfactant homeostasis. Furthermore, in various pathological states, surfactant's dysfunction may well be a significant contributing factor to disease initiation, progression, and severity. As such, this section will provide an overview of surfactant's contributions to pulmonary health and disease, starting with the neonatal lung leading to observations in the adult. Since the surfactant system in mammalian species is highly conserved, our knowledge in this area is the result of both animal studies and observations in humans.

8.1. Pulmonary Surfactant in the Neonatal Lung

When an infant is born, it must clear its lungs of fetal pulmonary fluid and establish normal breathing. As has been alluded to above, surfactant plays a particularly crucial role in these processes. As term approaches, the fetus synthesizes increasing amounts of surfactant in pulmonary Type II cells. Type II cell surfactant is stored as intracellular osmiophilic lamellar bodies.[9,116,466,467] These organelles possess a limiting membrane, which fuses with the plasma membrane during secretion to release the lamellar body.[239,460] Secreted lamellar bodies accumulate in the fetal pulmonary fluid during late gestation, although considerable amounts are lost to amniotic fluid, possibly during fetal breathing movements.[468,469] These breathing movements not only strengthen the muscles used in breathing but also serve to promote lung growth and maturation and act to mold the alveoli by thinning the alveolar walls.[470−473] From ∼24 weeks, the human fetus forms clusters of terminal air sacs, known as saccules, which have primary septa containing the capillaries necessary for gaseous exchange. As maturation progresses, secondary septa grow into the saccules to create alveoli. This greatly increases respiratory surface area. Although lung maturation, specifically the formation of alveoli, continues postnatally for several years, at term the lung structure and the available surfactant amounts are sufficiently matured to allow for the onset of air breathing.[81,474]

Since establishing an effective surfactant film at birth by adsorption-driven lipid sorting is dependent on the concentration of surfactant, knowing these values *prior to* the first breath would be very informative. We will first discuss the hurdles, assumptions, and calculations associated with generating an estimate of the surfactant concentration in the neonatal human lung. Subsequently, we will discuss the accumulation of surfactant during gestation, describe the implication of premature birth or other pathologies interfering with surfactant, and describe exogenous surfactant therapy in neonates.

8.1.1. The Concentration of Pulmonary Surfactant in the Human Lung at Birth. The surfactant concentrations throughout this review are normally expressed as mg/mL. This is because this parameter is almost universally used for therapy and for biophysical studies. However, directly translating or correlating these studies to the *in vivo* situation at birth is difficult, since there are several limitations to obtaining the concentration of surfactant in the lung at this time point.

(1) Obtaining surfactant by lung lavage near the time of birth is inefficient since each lavage procedure only removes a portion of the surfactant. For example, with humans, the initial lavage recovered accounts for only ∼30% of the surfactant recovered by five washes.[475] This likely reflects not only limited recovery but also surfactant secretion induced by stretching during expansion to TLC. Thus, the lung lavage procedure itself alters the amount of surfactant recovered. In addition, animal studies demonstrate that significant additional surfactant is released during the neonatal period.[469] In contrast, other animal studies have shown that delaying lavage after sacrifice can lead to a marked decrease in surfactant recovery.[476] Consequently, estimates of human fetal alveolar surfactant pool sizes are highly problematic.

(2) Animal studies have demonstrated a rapid increase in alveolar surfactant during labor and by secretion induced by lung expansion during the first few breaths. Further increases, in some cases up to 50% of the initial pool, can continue for hours after birth. Thus, measurements subsequent to the first few breaths are not truly reflective of pool sizes at birth.[469,477,478]

(3) During labor and after birth, infants rapidly clear lung liquid. This rapid fluid clearance makes it difficult to determine the exact volume and, therefore, impairs accurate assessment of surfactant concentration.

(4) When measured in physiological studies, surfactant levels are normally expressed as mg surfactant/kg bodyweight. Estimations of alveolar surfactant obtained by lavage employ total PL or total or disaturated PC, as determined by phosphorus assays. Disaturated PC is routinely isolated with alumina columns, after oxidation with osmium tetroxide to exclude other PLs.[479]

https://doi.org/10.1021/acs.chemrev.3c00146
Chem. Rev. 2023, 123, 13209−13290

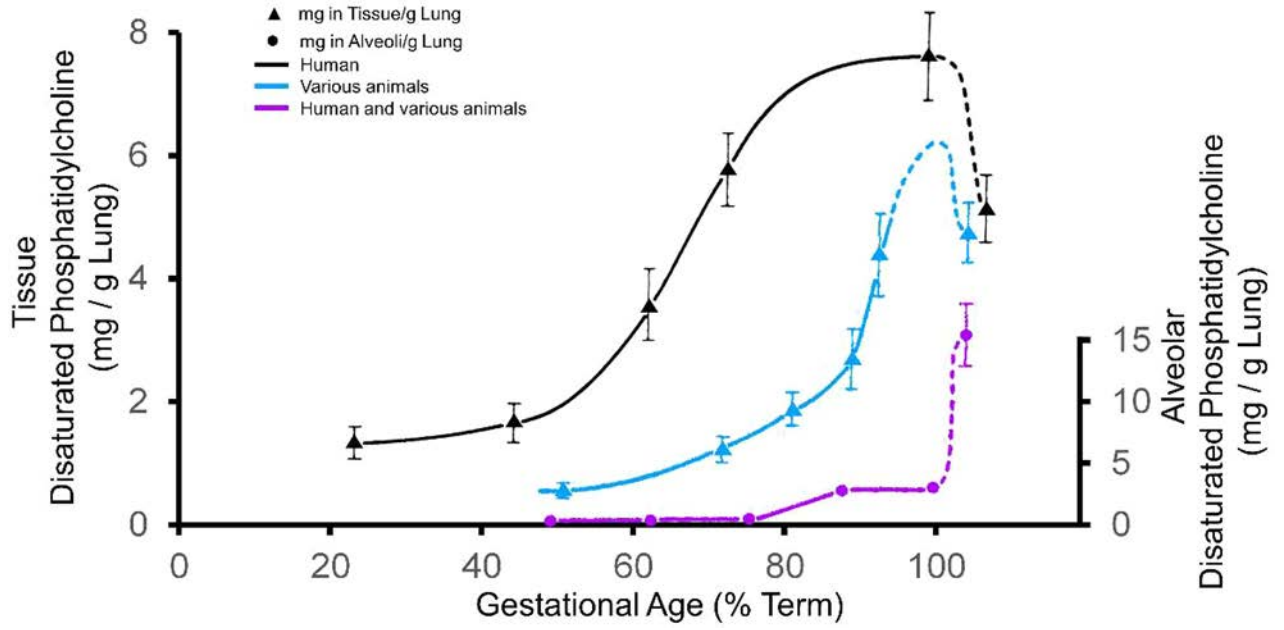

Figure 24. Tissue levels of disaturated phosphatidylcholine in the lungs of humans and other mammals as a function of gestational age. The dashes depict an extrapolation at birth: human lung (black triangles); rat, rabbit, lamb, and monkey lung (blue triangles). Alveolar levels for disaturated phosphatidylcholine for all species are also presented (purple circles). Adapted with permission from Jobe.[469] Copyright 1988 Elsevier.

Although this procedure tends to include small amounts of monenoic PC, it provides a rapid estimation of a critical factor for comparison.[480] While alveolar surfactant is easily isolated by lavage, lung tissue also contains disaturated PC in cellular caveolae and rafts and in erythrocytes. As a result, the amount of surfactant disaturated PC is not readily determined.[481] Although the surfactant within lung tissue can be isolated using appropriate gradient centrifugation, this procedure is only seldom employed.[482−486]

Despite the above hurdles, it is feasible to obtain an approximate estimate of the concentration of surfactant at term by combining a variety of different experimental observations and making some assumptions. An obvious, yet important, aspect to carefully consider is the specific units being used and the methodological limitations in reported published surfactant levels. Pulmonary surfactant levels have been reported as mg total surfactant, mg PL, mg PC, or mg disaturated PC and sometimes expressed per gram lung weight and at other times per kg bodyweight. Sometimes, different units are utilized within the same publication. Conversion of these units here considers disaturated PC to be 50% of the total PC in surfactant and PC to be 80% of the total amount of surfactant PL and estimates that PL represents approximately 80% of surfactant weight, i.e., disaturated PC would be about 32% of the total surfactant weight.

The second component required for obtaining estimates establishing surfactant concentrations at birth is data on the alveolar pool size at birth. Actual measurements are limited and generally involve time points hours, or even several days, after birth. Nevertheless, converting the reported values of ∼1.5 mg disaturated PC per g lung recovered from human infants near term, succumbing without RDS, leads to an estimated pool size of approximately 60 mg/kg bodyweight.[487−489]

A second method to obtain these values is through the use of a stable isotope tracer. Either DPPC or other surfactant compounds can be labeled and measured in tracheal aspirates of neonates on mechanical ventilation. This method applies the Fick diffusion principle[490,491] to obtain values for two compartments noted as an M_1 accessible (i.e., alveolar and airways), surfactant pool and an M_2 tissue-associated (i.e., Type II cell contained) surfactant pool.[492,493] This approach generated estimates of alveolar surfactant pool sizes between 30 and 45 mg/kg, values that are not far off those calculated above.[492,493]

The final estimate required is that of the alveolar fluid volume. As term approaches, labor-induced hormonal alterations induce the fetal lung to arrest fluid secretion and initiate adsorption. Uterine contractions and the compression generated during passage through the birth canal serve to further expel fluid. During labor, the fluid in the potential air spaces declines further. Prior to birth, over 90% of the blood coming from the umbilical cord bypasses the lungs, via the ductus arteriosus. Once the umbilical cord is clamped, due to changes in hemodynamic balance, most of the blood is diverted through the inflated lungs. This diversion is markedly enhanced by the changes in pulmonary surface forces induced by surfactant. Failure to induce these circulatory changes results in persistent pulmonary hypertension leading to fetal demise.[41]

After birth, additional fluid uptake is facilitated by the lowered γ.[494−497] The lung inflation promoted by the presence of sufficient surfactant greatly facilitates this change. This reduction in lung fluid during the neonatal period can continue over a period of hours. The exact lung volume in humans at birth is not known. However, in rabbits and lambs it has been determined to be ∼10 mL/kg, which appears to be a reasonable proxy for human values.[478]

Applying the above estimates of an alveolar pool of 60 mg/kg and an alveolar fluid volume of 10 mL/kg[478] results in an estimated surfactant concentration in term human neonates during the first breath of 6.0 mg/mL. These values, when tested in the biophysical assessments as described above, would result in rapid adsorption and adsorption-driven film

https://doi.org/10.1021/acs.chemrev.3c00146
Chem. Rev. 2023, 123, 13209−13290

purification. It is appreciated that the assumptions associated with this surfactant pool size estimation could feasibly have produced an overestimation. Nevertheless, should the endogenous pool size have been overestimated by 50% (and thus be 40 mg/kg, rather than 60 mg/kg) and the alveolar fluid volume have been underestimated by 50% (and thus be 15 mL/kg rather than 10 mL/kg), the resulting alveolar concentration would be ∼2.5 mg/mL. Considering that, at birth, surfactant is composed primarily of secreted lamellar bodies, which adsorb very quickly at low concentrations,[242] such values would clearly allow for rapid adsorption and film purification to occur.

8.1.2. Pulmonary Surfactant in the Fetal Lung. The high concentrations of surfactant at birth are a consequence of synthesis and secretion of surfactant in the lungs during the last trimester.[57,355,469,494,495] While variable amounts are secreted into the alveolar spaces as lamellar bodies during gestation, most of the surfactant remains as lamellar bodies within the Type II cells until close to birth.[241,467,498−500] The suggested alveolar levels of ∼60 mg/kg bodyweight in term infants[487−489] are somewhat lower than the alveolar pool sizes of ∼100 mg/kg bodyweight or more reported for laboratory animals at term.[57,469,499,501,502] Soon after birth the alveolar pools begin to fall, eventually reaching ∼4 mg/kg in adult humans.[475] These are similar to the levels reported for rat (∼5 mg/kg[503]) and rabbit (∼10 mg/kg[57]) alveolar surfactant. Interestingly, these adult values are also similar to the alveolar surfactant levels of ∼5 (1−10) mg/kg in infants with RDS, implying that the high surfactant concentrations are specifically required at birth.[469,494,495,499]

The observation that alveolar concentration at birth for human infants is ∼60 mg/kg bodyweight could be taken to imply a potential deficit compared to animals with ∼100 mg/kg bodyweight. However, when expressed as mg surfactant per g lung, this difference disappears (Figure 24).[469,489,494,495] In fact, while the levels of tissue disaturated PC *in utero*, expressed per g lung, increase dramatically at approximately 80−85% of gestation in mammalian species other than the human, this increase occurs in humans at ∼60% of gestation. These time points are relevant, because they are associated with the ability to establish air breathing and survive. Most animals delivered prematurely at 85−90% of term develop severe RDS and succumb.[504] In contrast, many human infants can establish regular breathing at 75% of term (30 weeks). In fact, only ∼20% of humans born between 30 and 32 weeks develop RDS, and infants can often establish regular breathing at 65% of term (28-week gestation) or less.[57,504]

The beneficial effects of the high surfactant levels at term can be illustrated by the difference in resting air volumes observed during the first few breaths of immature lamb fetuses (127 day gestation), compared to a mature fetus near term (140 day, term 147 day).[497] With the mature lamb, the first inflation initiates with an opening pressure of ∼20 cm H_2O, after which full volume is attained with little further pressure increase. On deflation, a resting air volume corresponding to ∼25% of the total inflatable volume is achieved. The second inflation commences immediately with very low pressure. Each of the next few succeeding inflations will promote a further ∼30% reduction of the remaining alveolar fluid, thereby increasing the surfactant concentration. Immature lungs also require ∼20 cm H_2O pressure to initiate inflation but, in contrast, completely deflate during decompression, thus requiring large opening pressures for each subsequent reinflation.[57,497]

Likewise, with ventilated premature rabbit pups, considerable opening pressures are required for inflation with the first 4 inflations, followed in each case by complete collapse on deflation. When exogenous surfactant is infused, lung volumes progressively increase by ∼25% and deflate by ∼25% less during the first 4 inflation−deflation cycles.[40,469,505] These observations are in keeping with the lung stability achieved by rabbit pups delivered at term, consistent with a low γ being established within a few breaths.[505] Following surfactant treatment of infants with RDS, normal breathing is promoted, and blood oxygen increases, usually within minutes.[56]

Taken together, the above considerations support the concept that due to the relatively high concentrations present, surfactant adsorption occurs rapidly at birth to generate γ at or near equilibrium during the first, or the first few, inhalations. Furthermore, very low tensions are attained during exhalation soon after birth. The physiological information available, taken together with the biophysical data, would suggest the hypophase surface is covered by a monolayer composed primarily of DPPC:cholesterol very soon after birth. Furthermore, this monolayer also contains the only partially defined adsorption structures, which maintain contact with the underlying SASR and adsorption-driven surfactant reservoir. The physiological significance of these reductions in surface tension includes a marked reduction in the resistance to flow within alveolar capillaries, thereby counteracting pulmonary hypertension and supporting increased blood oxygenation.[46,549]

8.1.3. Pathological Conditions Affecting the Surfactant System in Neonates. The primary condition in which surfactant contributes to a pathophysiology in neonates is prematurity. As discovered by Avery and Mead,[4] lung dysfunction due to prematurity is due to surfactant deficiency. Indeed, reported levels of pulmonary surfactant in infants dying from RDS range from 1 to 10 mg/kg, about 10-fold less than term,[469,494,495] and infants that do not develop serious RDS or are recovering can have 2−3 times this level. In this latter scenario, surfactant synthesis and secretion increase after preterm birth, such that adequate amounts are often available within 3−5 days.[469,499,502,506,507]

However, it must also be stressed that the problems faced by the lungs of premature infants go beyond surfactant deficiency. These lungs are very fragile and are prone to injury arising from oxygen-induced injury.[508−510] Optimal ventilatory practices for preventing pressure-related injury with these infants are still under investigation.[510,511] Serum leakage can occur at the bronchiolar−alveolar junction, where the airway radius is smallest. Repeated expansion−contraction cycles at this site of maximal pressure difference result in bronchiolar cell sloughing. Coagulation of the leaking serum protein forms hyaline membranes, also known as "bloodless clots", which can obstruct air flow.[512] This could explain why in premature macaques, and presumably, humans with RDS, TLC is reduced for the first few days, providing an additional respiratory burden.[513]

A less common, but severe pathology is that of hereditary SP-B deficiency.[110,112] This recessive condition leads to a complete absence of functional SP-B in affected infants. Despite delivery at term, the lack of SP-B causes a similar clinical presentation of lung dysfunction as marked prematurity. These symptoms are due to a lack of active surfactant, confirming the critical role that SP-B plays in surfactant function. Treatment with exogenous surfactant improves lung

https://doi.org/10.1021/acs.chemrev.3c00146
Chem. Rev. 2023, 123, 13209−13290

function acutely. However, this is not a long-term solution and until approaches to restore the genetic defect are feasible,[514] lung transplantation is the only therapeutic option for these patients (see Wert[110] and Hamvas[515] for reviews).

A third pathology at birth involving the surfactant system is meconium aspiration syndrome (MAS). In these infants, intestinal contents, voided into the amniotic fluid, due to stress, are aspirated into the lungs, where they interfere with surfactant function. This inhibition of surfactant function has been demonstrated *in vitro*. Since meconium consists of a broad variety of compounds, including bile acids, sterols, free unsaturated fatty acids, and proteins, including phospholipase A_2, this effect comprises the cumulation of the impact of these inhibitory agents. Consistent with the pathologies mentioned above, inhibition of surfactant contributes to severe lung injury. Infants with MAS can be treated with exogenous surfactant, with or without lung rinsing using dilute surfactant to remove some of the noxious materials. Recent investigations suggest lowering the body temperature of afflicted infants to ~33 °C can improve surfactant function[177] (see Autilio[516] for a further review).

8.1.4. Exogenous Surfactant Therapy in Neonates. Exogenous surfactant treatment for RDS has greatly improved mortality and morbidity with premature infants.[61] From a biophysical and clinical perspective, the currently available exogenous surfactants appear to be highly efficacious, despite differences in their source and composition. Further improvement of this therapy with the current preparations appears to be primarily related to other therapeutic aspects such as timing, method of administration, and dosing. For example, recently, less invasive interventions, such as LISA (Less Invasive Surfactant Administration), employing thin catheters have been introduced to avoid intubation injury, especially with very small infants.[517,518] Surfactant supplementation increases the alveolar pool considerably, buying the neonates time to begin supplying sufficient surfactant of their own to facilitate breathing.

Based on surfactant deficiency, it makes intuitive sense that in premature neonates, the rapid formation of a functional surface film by exogenous surfactant is paramount. This objective is achieved by using an appropriate composition and dose. Exogenous surfactant should contain those components that facilitate rapid adsorption and creation of a stable film. This means a high proportion of disaturated PLs (40−60 wt %) and sufficient unsaturated PL, PG, and the surfactant proteins SP-B and SP-C.[480,519,520] While cholesterol appears to enhance certain biophysical properties, whether this is an important ingredient of exogenous surfactant preparations remains debatable. In terms of the dosing, exogenous surfactants are usually administered at doses of ~100−200 mg/kg. These high levels are thought necessary to achieve effective spreading. It also appears that exogenous surfactant is not as effective as endogenous surfactant, possibly because of variable alveolar distribution.

Data from various comparisons suggest high dose Curosurf (200 mg/kg) treatment resulted in decreased ventilatory requirements and lower mortality, compared to a low dose (100 mg/kg) not only of Curosurf but also of either Alveofact, Infasurf, or Survanta. Thus this difference appears to be associated with the approximately 2-fold higher dose rather that differences in clinical surfactant efficacy.[521−523] Overall, the data from exogenous surfactant therapy for premature infants is consistent with the biophysical studies, demonstrating the crucial roles for hydrophobic surfactant proteins, DPPC and PG, and supports the concepts of concentration impacting the adsorbed film.

In terms of the overall therapy in the intensive care unit, premature infants demonstrating low circulatory oxygen are given nasal Continuous Positive Airway Pressure (CPAP) or Nasal Intermittent Positive Pressure Ventilation, and where needed supplementary oxygen is initiated.[517] Positive pressure ventilation prevents collapse at end expiration, thereby maintaining a larger FRC as indicated by the Young−Laplace relationship. Where positive airway pressure proves insufficient, mechanical ventilation is implemented, at which time clinical surfactants are administered. Occasionally retreatment is required. As a result of this approach, combined with additional therapies beyond the scope of this review, death due to RDS in infants of <1,500 g, without other serious complications, is rare in developed countries. It has been estimated that current practices have sufficed to reduce infant mortality in babies of <1,500 g by >95% compared to the 1960s.[61] Nevertheless, it is suggested that worldwide approximately one million infants succumb annually due to prematurity-associated causes, including RDS.

8.2. Pulmonary Surfactant in the Mature Lung

In contrast to the rapid changes occurring to surfactant during the end of gestation and at birth, once established, the pulmonary surfactant film covering the alveolar hypophase is maintained for life. The concentration of surfactant in the hypophase of human, rat, and rabbit lungs is estimated at 5−20 mg/mL. This is calculated in similar fashion as described for the neonate, based on pool size measurements,[57,475,503] lung surface area determinations,[388] and applying the average hypophase thickness of 0.2 μm measured for rat lung by Bastacky.[524] According to Weibel,[388] similar alveolar hypophase depths are observed in different species. Visualization of this extracellular surfactant via EM studies reveal that the alveolar surface is primarily covered with a trilayer, consisting of a monolayer overlying a PL bilayer, combined with significant areas containing 2 to 7 or more multilayers.[234,241,358,388] Based on the data obtained by Schürch's fluorocarbon microdroplet investigations on lungs *in situ* (Section 6.2), it appears that during quiet breathing, γ varies between ~2 and 15 mN/m. This variation could be accommodated by elastic expansion−compression cycles that would not require much material exchanges with the surfactant reservoirs[125,234,358] or the expenditure of much energy.

Despite the above assertion, studies in both human and animals demonstrate that this stable alveolar surfactant film is not a static feature. Rather, the surfactant is in constant flux to maintain the surface film.[525] This includes secretion of fresh surfactant from Type II cells as lamellar bodies, its incorporation into the surface film, displacement of spent surfactant from the film as small vesicles presumably during compression, the reuptake of these small vesicles by Type II cells for recycling and degradation (~25% each), as well as removal and hydrolysis of surfactant by alveolar and interstitial macrophages (~50%), and a small but significant loss to the airways (~3%).[20,502,526,527]

8.2.1. Pulmonary Surfactant Metabolism in the Normal Mature Lung. Pulmonary surfactant metabolism can be subdivided into intracellular synthesis, storage, secretion, and uptake for recycling and degradation. The biosynthesis of surfactant components has been reviewed in

https://doi.org/10.1021/acs.chemrev.3c00146
Chem. Rev. 2023, 123, 13209−13290

detail elsewhere.[527−529] Briefly, the available evidence documents distinct differences in the intracellular pathways for the biosynthesis of the various surfactant components. For example, PC and PG are synthesized in the endoplasmic reticulum of Type II cells and transferred directly to the intracellular lamellar inclusion bodies by a Golgi apparatus-independent pathway.[527,530] The ATP-Binding Cassette lipid transporter, ABCA3, localized on lamellar inclusion bodies is responsible for packing lipids into these lysosomal-related organelles.[531−534] Other ABCA transporters likely also contribute to lamellar body formation. SP-A and SP-D are transported to the Golgi, glycosylated, and then secreted constitutively. Secreted SP-A is taken up by Type II cells and partially rerouted through early endosomes and multivesicular bodies to lamellar inclusion bodies or degraded in lysosomes. SP-D is also taken up and degraded in Type II cells but is not routed to the lamellar bodies. SP-A and SP-D are also taken up and degraded by macrophages. SP-B and SP-C preproproteins are partially processed in the multivesicular bodies and then transported to nascent lamellar inclusions, where they are fully processed.[530,531]

Alveolar pulmonary surfactant homeostasis is still only partially understood. Current evidence indicates that lamellar body secretion occurs through constitutive and regulated pathways, involving cholinergic, adrenergic, and purinergic agonists.[279,531,535−537] Regulated secretion has been shown to involve three separate G-protein-coupled receptor (GPCR) mechanisms: the P2RY2 purinoreceptor pathway, the β_2 adrenergic receptor pathway, and the adenosine A_{2B} pathway. Activation of these pathways by extracellular agonists produces increases in second messengers, primarily calcium, inositol-trisphosphate, and/or cyclic AMP. This results in downstream protein kinase activity resulting in lamellar body exocytosis.

Importantly, it has become clear that the major single mechanism impacting alveolar levels operates through the mechanical stretch generated during ventilation. ATP derivatives can enhance surfactant secretion via $P2X_7$ purinergic receptors or piezo1 receptors on Type I cells.[538,539] For example, it was concluded that ATP release from alveolar Type I cells, arising from stretch stimulation of $P2X_7$ R receptors, activates P2Y2 receptors on Type II cells in a paracrine fashion, generating calcium signals resulting in surfactant secretion via protein kinase C.[539] The failure of $P2X_7$ $R^{-/-}$-deficient mutant mice to respond to hyperventilation by increasing surfactant secretion emphasizes the physiological significance of this route. Mixed culture and *in situ* studies reveal that stretch-induced calcium waves originating in Type I cells can spread to Type II cells *via* gap junctions to promote secretion.[540]

A pathway that negatively influences alveolar surfactant involves the orphan receptor (ligand unknown) guanidine protein receptor116 (GPR116), also known as $Adgrf_7$.[535,541] Mice bearing mutated, aberrant GPR116 progressively accumulate alveolar surfactant. This increase was accompanied by elevated surfactant synthesis, despite no alteration in the relevant PL synthesizing enzymes. At 30 weeks, the mice exhibit a 30-fold elevation in alveolar surfactant, foamy macrophages, neutrophilia, and epithelial cell destruction. The purinergic receptors, P2RY2 receptors, known to mediate surfactant secretion in an ATP-dependent manner, are induced, presumably as a compensatory mechanism. It thus appears that GPR116 functions as a molecular sensor of alveolar luminal pulmonary surfactant pool sizes and modulates these by tempering the surfactant secretion induced by the mechanical stretch provided during cyclical breathing.,

Further investigations indicate a complicated scenario by which GPR116 influences surfactant secretion.[541] Type II cell GPR116 holoprotein is proteolytically processed to yield an N-terminal fragment (NTF) and a large C-terminal fragment (CTF), consisting of an ectodomain attached to a 7-transmembrane domain (7TMD). The available data suggest that the NTF remains noncovalently associated with the CTF but can undergo dissociation or a conformational change during stretch. This dissociation frees the CTF ectodomain to fruitfully interact with the 7TMD segment, thereby resulting in coupling of the G proteins, G_Q−G_{11}. This coupling activates PI-specific phospholipase C leading to the formation of inositol triphosphate and diacylglycerol. The subsequent calcium influx, plus the diacylglycerol, promotes cytoskeletal F and G actin rearrangements which hamper stretch-induced surfactant secretion.[541,542] It has also been suggested that SP-D could interact with the GPR116 ectoprotein, thereby abrogating the negative influence on surfactant levels.

The seemingly paradoxical observation that calcium both induces secretion, *via* PKC activation, and hampers it, *via* cytoskeletal actin rearrangements, can be explained in several ways. Secretion may require compartmentalization and/or multiple simultaneous signals. Lamellar body extrusion appears to require long sustained intracellular calcium signals with the contribution of external calcium influx.[543]

Interestingly, SP-B lipid mixtures also promote lamellar body exocytosis by stimulating ATP release, calcium influx, and the activation of purogenic P2Y2 receptors.[347] These observations serve to link SP-B's role in LB formation and alveolar γ reduction to surfactant homeostasis.

Following secretion, material from the lamellar bodies interacts with separately secreted SP-A to generate tubular myelin. As mentioned above, studies with isolated lamellar bodies show rapid adsorption and unravelling at a clean air−liquid interface to form a surface film. In the lung, upon secretion, unravelling occurs within the hypophase. It has been pointed out that the pores through which the lamellar bodies are secreted are narrow relative to the diameter of the lamellar body and that this may contribute to structural, and possibly functional, rearrangements.[115] In addition, it is also clear that this secreted material interacts with separately secreted SP-A to generate tubular myelin. While it is clear that tubular myelin can adsorb to form a surface film, SP-$A^{-/-}$ KO mice demonstrate this form is not essential.[9,544] Consequently, the manner by which the freshly released surfactant penetrates the surface film and provides new monolayer material is still unresolved. Considering surfactant's ability to respread, it appears highly unlikely that sufficient "clear" space is created even during deep inhalations. However, DPPC-radiolabeled surfactant extract vesicles injected beneath either a DPPC or lipid extract surfactant spread monolayer at equilibrium do not exchange DPPC with the surface.[376] One possibility is that normally secreted lamellar bodies coalesce into the tubular myelin, which tends to accumulate in the deep niches around the Type II cells, as shown by EM (Figure 25).[9,415] This tubular myelin could then act as the source of the surface film. However, as indicated above, the specifics of this process require further clarification. This is especially evident considering that SP-$A^{-/-}$ animals, lacking tubular myelin, maintain a competent surface film and considering the

https://doi.org/10.1021/acs.chemrev.3c00146
Chem. Rev. 2023, 123, 13209−13290

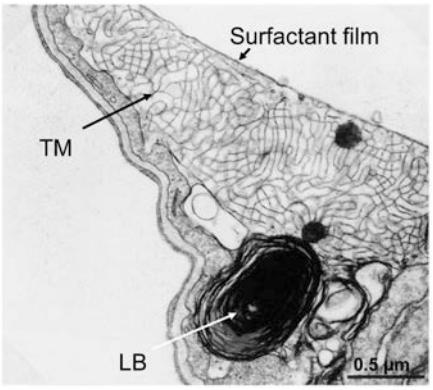

Figure 25. Tubular myelin overlying a secreted lamellar body in an alveolar corner niche. The surfactant film is primarily a monolayer over a single bilayer, with other areas covered by some stacked bilayers. This micrograph shows a freshly secreted lamellar body (LB) lying under tubular myelin (TM) figures. The tubular myelin extends from immediately under the surface film to the lamellar body and the alveolar epithelium. Two small lamellar body remnants are apparent. It is suggested that the secreted material from the lamellar bodies may react with separately secreted SP-A to feed into the tubular membranes. These structures, in turn, could eventually supply new surfactant material to the surface film. Reprinted with permission of the American Thoracic Society. Adapted with permission from ref 415. Copyright 1999 American Thoracic Society.

observation that isolated lamellar bodies only adsorb well when π is below ~25 mN/n (γ is above ~45 mN/m).[363]

The overall processes by which a relatively constant level of surfactant is maintained in the alveolar environment by Type II cells and macrophage degradation (~50% each) are also only partially understood. Surfactant Protein-A has regulatory roles in both the secretion and clearance of surfactant. High levels of SP-A reduce surfactant secretion.[16,20,95,545,546] Surfactant clearance by Type II cells proceeds by at least two mechanisms: a SP-A receptor-mediated clathrin-dependent pathway and a non-clathrin, actin-mediated pathway.[95] The SP-A receptor has been identified as P63(CKAP4). With SP-A deficiency, the actin-mediated pathway suffices to maintain surfactant levels under normal conditions. However, this mechanism proves inadequate with physiological challenges, such as hyperventilation and persistent exposure to secretagogues. The potential role of the SP-A receptor, P63(CKAP4), in surfactant secretion is not clear. Also, while other apparent receptors for SP-A are present in Type II cells, their roles in homeostasis are uncertain.[95]

Interestingly, the pool sizes of surfactant increase ~3-fold in SP-D-deficient *SFTPD*$^{-/-}$ mice, demonstrating an important role in surfactant homeostasis.[28,547] This elevation is due to a reduction in the uptake of surfactant vesicles by Type II cells, with little apparent effect on macrophages.[547,548] Adding SP-D to surfactant isolated from these animals produces numerous small particles containing several lamellae and unilamellar vesicles. This activity is related to the ability of SP-D to bind PI. In contrast, SP-D does not bind PG well, although SP-D has a small effect on surfactant uptake with PG-containing vesicles. Thus, the effect of SP-D on surfactant uptake is primarily due to the formation of small vesicles. Small vesicles are preferentially taken up by Type II cells, whereas surfactant form and size have only a minor effect on endocytosis by macrophages.[548,550]

While SP-D is secreted separately from lamellar bodies, immunochemical examination of newborn and adult ovine lungs reveals SP-D associates with lamellar bodies extracellularly. SP-D also interacts with loosely aggregated lamellar structures and small vesicles but not tubular myelin.[548]

The hydrophobic proteins SP-B and SP-C are secreted in lamellar bodies. After cellular uptake, these hydrophobic proteins are processed, as with surfactant lipids, by Type II cells and macrophages. The half-lives of these proteins differ from each other, and from that of DPPC, emphasizing the differences in metabolism.[464,494] The surfactant lipid constituents taken up by Type II cells are routed into endosomes, which then fuse with lysosomes. Some of the resulting organelles convert into multivesicular units which then transform into lamellar inclusion bodies. In newborns ~90% of surfactant DPPC is recycled in this manner, but this process declines to ~50% in the adult.[57,499] This alteration in surfactant levels seems to be related to increased uptake and degradation by Type II cells, but maturation of the macrophage system may also contribute.[548]

Some 30−50% percent of the airspace surfactant is taken up and catabolized by alveolar and interstitial macrophages.[102,548] Factors interfering with these processes result in large accumulations within the alveoli. Ablation of the genes involved in production and regulation of granulocyte-macrophage colony-stimulating factor (GM-CSF) results in impaired macrophage maturation and the development of pulmonary alveolar proteinosis (PAP).[99,551] This pulmonary disease manifests by the accumulation of sufficient surfactant in the lung to interfere with normal lung function. Primary PAP can also occur as an autoimmune disease due to antibodies against GM-CSF.[99,101,102,552] Secondary PAP is associated with a number of endogenous and environmental factors interfering with normal macrophage function. Congenital PAP can involve various mutations including some in the surfactant proteins. This condition is commonly associated with impaired cholesterol metabolism resulting in foamy macrophages.[101,102,552] Not surprisingly, individuals suffering from low effective GM-CSF levels are highly prone to bacterial and viral infections. During infection, phagocytosis and catabolism of surfactant by neutrophils also contribute to the reduction observed with ARDS.

The overall purpose of alveolar metabolism is to maintain the surface film. It is likely that during the normal breathing process, where approximately 10,000 L of air flow in and out of the lung per day, the surface film will be affected by inhaled particles and compounds, leading to the requirement for turnover. The turnover process likely involves deep inhalations above the regular tidal volume breathing. This deep inhalation accomplishes two things: it promotes surfactant secretion, and it produces surface area expansions allowing γ to rise above equilibrium, permitting small amounts of fresh material to access the surface. The source of how this additional surfactant material accesses the surface monolayer is not clear. It is feasible that the extra material represents mainly unsaturated PLs from the SASR or the adsorption-driven monolayer-associated PL blebs, which are subsequently squeezed out of the film during compression.

In summary, lamellar body secretion is regulated by lung expansion and a number of secretory and hormonal factors. In addition, the reuptake of this material by Type II cells and alveolar macrophages clearly plays an important role in maintaining steady state levels of surfactant in healthy mature

https://doi.org/10.1021/acs.chemrev.3c00146
Chem. Rev. 2023, 123, 13209−13290

lungs. Together, these complex processes maintain an alveolar pool size of surfactant of ∼4 mg/kg in adult humans.[475]

8.2.2. Surfactant Subtypes: Large and Small Aggregates. In addition to monitoring surfactant *via* its individual components, it should also be noted that experimentally many studies have explored the different structural forms or subtypes of surfactant isolated from bronchoalveolar lavage fluid. Whereas the literature contains different terminologies and isolation procedures for the different subtypes,[240,373,553] the most prevalent is that of large and small surfactant aggregates (LA and SA, respectively).[554−556] The usual protocol for obtaining these subfractions is to take the lavage fluid and, after a light spin to remove cells and debris, pellet the larger surfactant structures via centrifugation at 40,000*g* to 50,000*g* for 15 to 20 min to yield the LA subtype.[556,557] The surfactant remaining in the centrifuged supernatant consists of SA. While LA and SA have identical PL compositions, the lighter subtype has more neutral lipid and very little protein and seems to lack surfactant proteins.[499,548,558−561] More importantly, LA contain tubular myelin, other lamellar structures, and large lipid complexes, whereas the SA are small, mainly single-walled vesicles.

Significantly, a clear relationship exists between the subtypes obtained *ex vivo* and pulmonary physiology.[9,240,241,499,562] First, newborns are devoid of SA at birth, and these accumulate during the first few hours of respiration.[558,559] Second, studies with either radiolabelled or stable isotopes in either neonatal or adult lungs demonstrate a metabolic relationship in which the label first incorporates into LA and follows into the SA fraction.[558,563] Third, in adulthood, the relative levels of LA and SA are relatively constant, with the lighter subtypes accounting for a third to a half of the surfactant lipid depending on the species. Fourth, under various physiological conditions, including lung injuries, exercise, hyperventilation, and ischemia:reperfusion, the relative proportions of the subtypes change.[84,564−568] Specifically, increased relative amounts of SA are observed in lavage fluid with ARDS.[80]

The above data support the conclusions that SA are formed from LA, that a change in alveolar surface area (i.e., ventilation) promotes an increase in SA in lavage, and that the relative amounts correlate with certain physiological conditions. Together, these observations are consistent with a physiological significance of these experimentally separated subtypes. This overall conclusion is strongly supported by observations revealing that alterations in subtype profile observed within the alveoli by EM are reflected by the subtype's ratios measured in lavage.[241] Notable examples include ischemia:reperfusion,[415,569] hyperventilation,[570] and inflammatory asthma.[571]

In terms of surfactant function, it has been shown that the LA subtype is capable of reducing γ to near 0 mN/m, when tested using a surfactometer, and improves lung function in surfactant-deficient animals.[571,572] In contrast, the SA cannot reduce surface tension to low values, nor can this subfraction support normal lung function in premature rabbit pups.[573] It should also be noted that in many experimental studies, LA are isolated to determine the biophysical properties of natural surfactants; this includes studies of surfactant inhibition and the properties of surfactant in clinical conditions, as will be discussed later. Furthermore, several lavage-derived exogenous surfactants include a centrifugation step to eliminate the SA subfraction. Thus, from a pragmatic point of view, LA have been the main subtype utilized to understand the biophysics of natural surfactant.

Notwithstanding the above assertation of the relevance of LA and SA, the precise relationship between these lavage-derived subtypes and the structures present in the lung is difficult to define. One obvious complication is that the lavage procedure itself dilutes the hypophase liquid and it does not allow for isolation of the surface film. The manner in which the monolayer segregates in either LA or SA during the lavage and isolation procedure is not known. Electron microscopic examination of fixed lungs visualizes well organized lipid structures within the alveoli. It has been reported that the small (and sometimes not so small) unilamellar vesicles in the alveoli represent, in terms of volume fraction, one-third to one-half of the lipid structures.[415,569,571] Volume fraction is obtained by measuring the outer perimeter of the particular objects being examined. However, since the larger forms contain numerous lamellae, they will contain considerably more membranous material. This would indicate that, contrary to the LA/SA ratios assayed in lavage, the unilamellar vesicles account for only a small proportion of total surfactant in the alveolar space. Furthermore, many of these unilamellar vesicles have associated SP-A, and so differ from the small aggregates isolated with lavage.[574,575] However, whether the small unilamellar vesicles are as faithfully fixed as the larger forms is of potential concern, even with vascular fixation which is superior to bronchiolar fixative perfusion.

Furthermore, it is generally considered that the surfactant apoproteins are taken up by cells in association with small lipid vesicles.[527,531] Certainly, addition of SP-A, SP-C, or SP-D stimulates uptake of surfactant-like lipids by Type II cells. Addition of SP-B produces small discoid structures which could be taken up by alveolar cells. However, the isolated SA fraction appears to lack these surfactant proteins.[548,560,576] Additionally, the manner by which the surfactant small vesicles could be produced in the alveoli is not entirely clear. As mentioned above, it has been suggested that these particles are generated during repetitive compression:expansion of the surface monolayer (i.e., ventilation). However, vesicles generated from the surface monolayer might be expected to be enriched in DPPC. How such vesicles manage to penetrate through the virtually continuous bilayer and multilayer reservoirs remains unexplained. As noted, addition of SP-D to surfactant *in vitro* generates small vesicles.[548] Thus, despite its experimental and apparent physiological relevance, details regarding LA and SA as they relate to the *in vivo* behavior of surfactant clearly require further investigation.

In brief, although it is generally considered that the intra-alveolar, unilamellar vesicles are primarily responsible for transporting surfactant apoprotein to Type II cells and alveolar macrophages, these proteins appear absent from SA isolated by lavage. This contradicts the usual assumption that these SA are similar, if not identical, to the alveolar unilamellar vesicles. A potential explanation for this apparent discrepancy is that only a very small proportion of the total alveolar surfactant PLs is present as apoprotein-containing unilamellar vesicles. The disruption of parts of the surface film lacking apoproteins during lavage would generate numerous small vesicles. The alveolar small vesicles will be isolated along with the SA generated by lavage, but their overall mass and surfactant apoprotein content would be relatively small. As a result, the surfactant protein content of lavage SA becomes undetectable

https://doi.org/10.1021/acs.chemrev.3c00146
Chem. Rev. 2023, 123, 13209−13290

due to dilution by the large amount of SA lipid generated during lavage.

Notwithstanding the above, these observations do not conflict with the view that overall, the monolayer associated with the surface surfactant film created at birth is highly enriched in DPPC:cholesterol. There appears to be very little, if any, change in the composition of this monolayer during quiet breathing. With deep inhalations, additional material, probably unsaturated PLs, enter the monolayer. This material is likely largely expelled during expiration, restoring the original composition. Apparently, with repeated expansion:compression of the surface film, small unilamellar vesicles, with a lipid composition similar to that of the whole film and of freshly secreted lamellar bodies, are generated by an unknown mechanism.

8.2.3. Pathological Conditions Affecting the Surfactant System in Adults. The prototypic disease illustrating the importance of surfactant in the adult lung is ARDS.[85,577−580] The physiological lung dysfunctions that defines ARDS—reduced compliance and low blood oxygenation—are directly related to the biophysical function of surfactant. Further, analysis of surfactant function, using samples obtained from ARDS patients, demonstrates a significant inhibition of both adsorption and γ reduction. Nevertheless, our understanding of the specific mechanisms by which surfactant is impaired in ARDS is incomplete and, despite a strong physiological rationale, surfactant therapy for this syndrome has not yet proven successful in significantly reducing mortality.[15,581,582] Nevertheless, it is of specific relevance that significant clinical improvement can be achieved through limiting ventilation volumes, a practice known to maintain active surfactant levels in addition to limiting stretch-induced injury.[583−585]

Analysis of surfactant from patients with ARDS, or from animal models of the disease, shows reduced amounts of surfactant, as well as changes in PL profiles, reduced surfactant apoprotein content, and sometimes an increase in cholesterol. Whereas these compositional alterations, by themselves, may impact surfactant surface activity, this effect is enhanced by additional injurious factors impacting γ reduction, including reactive oxygen species, proteases, and serum protein influx. For example, it has been demonstrated that an increase in lysophospholipid, potentially due to increased phospholipase A2 activity in the injured lung, enhances the susceptibility of surfactant to protein inhibition, thereby impacting surfactant function both *in vitro* and *in vivo*.[258,586,587] Additionally, cholesterol, which is increased during injurious mechanical ventilation, further sensitizes surfactant to the negative effects of oxidation.[441]

In general, surfactant impairment in ARDS reflects the cumulative effects of several pathological processes, i.e., multiple hits, rather than a single insult alteration. This then leads to the altered biophysical properties of this material, which are detectable *in vitro*. The synthesis and turnover of surfactant components such as SP-B and SP-C can be altered, leading to lower levels.[588,589] Antibodies against these proteins can also interfere with surfactant function.[590] Large amounts of surfactant are taken up and degraded by invading neutrophils, further increasing the deficit.[591] One of the complicating factors translating these mechanisms to the *in vivo* situation is that measurements of inhibition include the formation of a surface film, whereas, as noted above in our model of surfactant function, within the lungs the surface film is generated during adsorption at birth and maintained throughout life. As such, a large knowledge gap exists in the mechanism by which an existing surface film is inactivated *in vivo*, versus the biophysical inhibition that is observed during and after the generation of a dysfunctional film.[428] It does appear that depressed film function leads to increased alveolar edema, rather than the reverse.[415]

A second, albeit rare, disease affecting the pulmonary surfactant in adult lungs is alveolar proteinosis. This is a disease characterized by surfactant accumulation within the alveolar space leading to difficulty in breathing. There are several causes of PAP, the most common including disruption of GM-CSF signaling through mutations or by anti-GMCSF antibodies leading to impaired surfactant catabolism by alveolar macrophages. In general, the lung architecture is intact.[99,279]

The pathogenesis of alveolar proteinosis demonstrates the importance of surfactant metabolism. Focusing on the role of GM-CSF, it was first observed that mice deficient in this cytokine developed the characteristics of PAP proteinosis. Subsequent discovery of neutralizing antibodies for GM-CSF in patients with alveolar proteinosis supported the role of this molecule. This accounts for the majority of proteinosis cases. Without GM-CSF, alveolar macrophages have limited catabolism of surfactant. This leads, over a period of months or longer, to an accumulation of surfactant that interferes with normal lung function. While disruption of GM-CSF signaling is the most common form of PAP, there are other less well-defined causes. These include associations with a number of various diseases, toxic inhalation exposures, and genetic mutations. Regardless of the cause, the primary process in the development of the disease is altered surfactant catabolism and, consequently, surfactant accumulation.

Although other therapies are being developed and tested, one of the main therapies for PAP, as noted above, is lung lavage.[102,552] This has provided researchers with large quantities of human surfactant material, which has been utilized to purify large quantities of the surfactant proteins for research. Unfortunately, it has been observed that, likely by virtue of retention in the lung for prolonged periods of time, these proteins have undergone a variety of modifications that cause them, in some case, to behave differently than proteins obtained from healthy lungs. For example, differences in SP-A function and structure have been reported among different isolations of SP-A from various alveolar proteinosis patients. It has also been shown that SP-D exists in large oligomeric structures in the lavage from alveolar proteinosis patients, as compared to normal. The fact that surfactant is altered during prolonged exposure to inhaled air provides evidence for the need for continued synthesis, secretion, and reuptake of surfactant.

Finally, changes to the surfactant system have been reported in other conditions and diseases. For example, surfactant dysfunction has been reported in post graft dysfunction after experimental lung transplantation, a condition with similarities to ARDS.[592,593] Surfactant alterations have also been observed with COPD,[594] with various forms of pulmonary fibrosis,[588,595] and with other respiratory diseases.

8.2.4. Exogenous Surfactant in the Mature Lung. As outlined above, surfactant dysfunction is associated with ARDS and there is a strong physiological rationale for exogenous surfactant administration in this syndrome. However, compared to the relatively straightforward, surfactant-deficient lung in RDS, treating the complex pathology of ARDS with

https://doi.org/10.1021/acs.chemrev.3c00146
Chem. Rev. 2023, 123, 13209−13290

surfactant has proven much more complicated. Although new trials focused on COVID-19-induced ARDS are ongoing[92−94] and results are eagerly anticipated, to date, clinical trials have not provided conclusive evidence to support use of this therapy in the ARDS population. This is despite many encouraging animal studies and a few, mainly pediatric, trials.[596] It is clear that translating the many encouraging ALI studies into successful clinical application has proven difficult.

The lack of clinical success in ARDS, despite promising animal studies, is not unique to exogenous surfactant; numerous promising therapies in animals have not translated into the clinical setting. These unfortunate findings relate to limitations of animal studies, with some suggestions that, for example, preclinical animal studies should be tested in a multicenter setting prior to clinical trials. Importantly, interpretation of negative clinical results should not be only interpreted with respect to the implementation of a therapy but also be used to enhance our understanding of the disease processes and improve experimental therapeutic approaches. With regard to exogenous surfactant, clinical trials in ARDS have yielded large amounts of new information to consider including: was an optimal surfactant preparation utilized; was significant applied surfactant lost due to coating of bronchi:bronchiolar surfaces; was the volume and dosing appropriate; and was the surfactant delivered at the right time.[79,89,597,598]

One example of an unsuccessful study was a large, blinded clinical trial with Venticute, a recombinant SP-C-based synthetic surfactant containing DPPC, POPG, and palmitic acid. This study demonstrated a highly significant improvement in oxygenation but failed to achieve a significant increase in survival.[599] Retrospective *post hoc* analysis of those patients with severe respiratory insufficiency, due to pneumonia or aspiration resulting from bacterial infection, had significantly reduced mortality.[88] A large follow-up trial, targeting these direct causation ARDS patients, proved completely unsuccessful. However, as in the very early attempts at treating RDS with aerosolized DPPC,[41,42] there were potential explanations for this failure. Examination of the material used for this trial revealed that it possessed a reduced ability to lower γ on a CBS. This was attributed to a newly introduced method for dispersing the surfactant prior to instillation, but it may have been due to the tendency of SP-C to generate irreversible beta-sheet aggregates.[87]

One of the main issues to consider in treating pulmonary insufficiency is that of surfactant inhibition. In ARDS, endogenous surfactant is inactivated, and it is likely that exogenous surfactant administered to the ARDS lungs will be exposed to similar inhibitory mechanisms. Considering SP-A's potential capacity to limit inhibition by serum proteins[295,426,427,430] and its ability to restore the activity of surfactant after exposure to reactive oxygen species,[425] it would appear that supplementing exogenous surfactant with this large hydrophilic protein could be advantageous. Limitations in obtaining sufficient quantities of full-length human SP-A, and justified concerns regarding immunological responses to other sources of this large hydrophobic protein, have traditionally curtailed this approach. However, advances in molecular genetic biotechnology have allowed synthesis of rhSP-A.[68,600] Future work on quantities produced, quality control, and the long-term stability is the next important step for this exciting research toward studies examining potential clinical applications.

It is also possible that the currently available exogenous surfactants are not sufficiently robust for ARDS. New synthetic surfactants that contain, for example, synthetic lipids that are resistant to phospholipases, or surfactant protein mimics resistant to proteases, appear worthwhile for investigation.[601,602] Whether polymer additives, as discussed above, will be able to replace the beneficial effects of SP-A, by counteracting protein inhibition, must still be determined.[436] Another strategy, either alone or in combination with exogenous surfactant, that has been suggested is to use β-methyl-dextrin to remove excess cholesterol, thereby improving the activity of the endogenous surfactant.[433,441,442,444] Importantly, these types of investigational strategies could benefit from a better insight into the mechanism of dysfunction in endogenous and exogenous surfactants within lungs with ARDS.

A further useful approach to evaluating the lack of success in clinical surfactant trials for ARDS is to carefully examine the specific conditions in which exogenous surfactant therapy was effective in animal studies. In this regard, a critical component of the therapy appears to be the early administration of the exogenous material. For example, exogenous surfactant has been shown to be effective in mitigating graft dysfunction in experimental lung transplantation. Transplantation is a unique scenario in this regard, as surfactant can be administered to the donor prior to the reperfusion.[569,593,603] Similarly, it was demonstrated that the damaging effects of mechanical ventilation could be mitigated by administration of aerosolized surfactant during the ventilation process.[604,605] To an extent, these studies correlate with the pediatric experience, which has shown that surfactant can limit damage but by itself does not reverse injury.

However, considering the extensive pathophysiology of ARDS, which, in addition to surfactant dysfunction, includes overwhelming inflammation, oxidative stress, and edema formation, it should also be considered that exogenous surfactant, by itself, will not be sufficient to improve outcomes. It seems more appropriate to use a combined approach in which, depending on the initial insult, the therapeutic surfactants could be used to also deliver protective agents. To present just a few examples, antivirals, antibiotics, antimicrobial peptides, and anti-inflammatory drugs could be administered, depending on the situation.[606−608] Solnatide, a drug capable of decreasing extravascular lung water, could readily be combined with aerosolized or bolus surfactant treatments with ARDS.[609] Limiting alveolar edema would increase endogenous and exogenous surfactant concentrations, thereby contributing to improved lung function.

In conclusion, the full spectrum of the therapeutic potential of exogenous surfactant in mature lungs has not yet been explored. Whereas initial trials for ARDS were negative, progress is being made to improve this therapy. The basis for this optimism is severalfold. First, progress in the understanding of surfactant function and dysfunction and our understanding of disease development and progression will improve targeted exogenous surfactant approaches. Second, improved surfactant nebulization methods developed in recent years will allow for early and less-invasive application, before ARDS is fully established.[604,605,610−614] This would have the potential to curtail the progress of multiorgan injury, the major cause of mortality, on an individualized basis.[615−617] Third, the development of more synthetic preparations can be optimized for specific applications such as delivering other therapeutics

https://doi.org/10.1021/acs.chemrev.3c00146
Chem. Rev. 2023, 123, 13209−13290

such as anti-inflammatory agents on an individualized basis.[66,520,618]

8.2.5. Surfactant Composition across Mammalian Species. While pulmonary surfactant compositions from different animal species are similar, small but significant differences had been documented. For example, there are changes in the relative amounts of PG and PI between different animal species and with development.[243,619−622] The levels of DPPC and disaturated PC, as a proportion of total PC species, can vary from ∼35% (bovine) to ∼60% of total (human, mouse, rat). The amount of cholesterol, relative to surfactant disaturated PL, is also known to vary considerably.[12,619,620,623−625] These differences in composition among species raise the question as to whether they represent optimized adaptations to a specific species' physiological circumstances or if they simple represent natural variations without functional significance.[12,620,626] Based on current literature, arguments can be made for both these viewpoints.

Several studies have shown that higher respiratory rates and smaller alveolar size correlate with lower relative values of DPPC.[243,619,620,627] These correlations are consistent with the suggestion that surfactant is optimized for specific species and/or circumstances. Adaptation of surfactant composition to physiological conditions has also been reported for hibernating animals such as the 13-lined ground squirrel (*Ictidomys tridecemlineatus*).[628,629] Surfactant from summer-active squirrels (37 °C) contains higher proportions of DPPC to total PC than that from hibernating (<5 °C) animals (∼55% versus ∼43%). A similar pattern was observed for disaturated PG (36% vs 28%). However, despite these changes in composition, the function of both surfactants was similar at either high or low temperatures. Interestingly, comparison of ground squirrel surfactant with pig surfactant revealed a better activity for pig surfactant at 37 °C but a superior activity of the squirrel surfactant at low temperatures 3−5 °C. These results were taken to indicate that 13-lined ground squirrels have developed a pulmonary surfactant, which functions adequately under both summer-active and hibernating conditions. Further, the hibernating form possesses sufficient functional flexibility to permit the hibernating animals to undergo arousal to warm temperatures, as occurs approximately every 7 days.

A number of investigations by the laboratory of Orgeig and Daniels have shown that heterothermic animals can undergo large alterations in surfactant cholesterol content, consistent with the notion that this sterol's levels are being modulated to enhance fluidity to compensate for the effects of lowed temperature.[630,631] For example, with the central Australian agamid lizard, *Ctenophorus nuchalis*, body temperature may vary from 13 to 45 °C, with the mean preferred body temperature being 37 °C. During a decrease in ambient temperature from 37 to 15 °C, surfactant cholesterol content increases ∼2.5-fold, relative to PLs. Such observations reinforced the concept of surfactant adaptation to temperature by elevating sterol. It should be pointed out that lizards have high levels of not very active surfactant. Since they possess faveolae, large air containing structures from ten to a thousand-fold bigger than alveoli, this is not critical. Such non-mammalian vertebrates also tend to have lower disaturated PC levels.[630,632]

Following this notion, a number of studies conducted with fat-tailed dunnarts (*Sminthopsis crassicaudata*) and bats (Gould's wattled bat, *Chalinolobus gouldii)* in torpor and in hibernating golden-mantled ground squirrels (*S. lateralis)* have found that cholesterol levels were increased in alveolar lavage from animals in the lower temperature states. Following from the nonmammalian studies, this has widely been taken as indicating that this elevated sterol content was important for increasing surfactant fluidity at the lower body temperatures,[174,624,632−635] implying an important role for cholesterol. However, with dunnarts the cholesterol content does not increase for hours after the temperature decrease, indicating this alteration may not be crucial.[635,636] More importantly, the early compositional analyses were conducted on aliquots of whole lung lavages. When the surfactant LA were pelleted by centrifugation, there was no difference in cholesterol content between active animals and those in torpor.[624,625] Surfactant isolated from Gould's bats at different temperatures varies between 2.0 and 2.5% PLs. Whether such an alteration in cholesterol levels, that are lower than the norm, has any significant effect on activity is unknown.[633] Consequently, there does not appear to be any consistent experimental evidence suggesting that alterations in cholesterol content serve to increase surfactant fluidity with low body temperatures in mammals.

An important line of evidence that supports the view that the functional significance of the variable composition among species is limited stems from surfactant supplementation experiments. The efficacy of bovine- or porcine-derived exogenous surfactants in treating not only premature neonates but also surfactant deficient rats, rabbits, and sheep clearly demonstrates the cross-species compatibility of surfactant. Nevertheless, it should be noted that a direct comparison of interspecies versus intraspecies surfactant administration over prolonged periods has, to our knowledge, not been reported.

It should also be noted that surfactant composition can be affected by diet. This implies that some variation among species may be related to dietary differences. More importantly, in experiments in which surfactant composition has been altered within one species, this has not led to either altered lung function or altered surfactant properties. For example, supplementing the diets of day-19 old rats with 2% trimyristin (14:03) for a week led to an increase in 16:0/14:0-PC from 10 to 45% total PC and of dimyristoyl-PC (14:0,14:0-PC) from 0 to 12%.[637] These increases were accompanied by compensatory decreases in DPPC of ∼25% and 16:0/16:1-PC of ∼5%. However, these relatively large alterations in PC molecular species failed to have significant effects on the respiratory functional activity or the surface behavior on the captive bubble.

Some seals (pinnipeds) and whales (cetaceans) often dive to such depths that most of the air is forced out of their lungs, and so the opposing alveolar walls contact each other.[638] On surfacing, surfactant facilitates the rapid separation of these walls, enhancing the uptake of oxygen. Studies have revealed that seal surfactant is less surface active than that of terrestrial mammals, possibly as a result of evolutionary alterations favoring compositions favorable to the special needs of these animals. It has been suggested that, in addition to seals and whales, this antiadhesive property of surfactant is critical to pulmonary function in a variety of other vertebrates, including lungfish, aquatic amphibians, lizards, and sea snakes.[108]

In addition, in general the generation of mice strains that synthesize and secrete normal humanized surfactant proteins appears to have little overall effect on surfactant function *in vivo*. In contrast, mutated forms of these human proteins can lead to distinct negative outcomes.[351,639−643]

https://doi.org/10.1021/acs.chemrev.3c00146
Chem. Rev. 2023, 123, 13209−13290

Consequently, in brief, the question of the significance of the functional relevance of variabilities in endogenous surfactant composition under healthy conditions remains largely unanswered. It is possible that some variability is relevant for other aspects of the surfactant system rather than its biophysics, such as its host defense mechanisms, metabolism, or lamellar body lipid uptake or secretion. It should also be appreciated that assessment of biophysical function *in vitro* may not reflect all features that impact surfactant biophysics *in vivo*. For example, the connectivity of the surface film between alveoli, the interaction of surfactant with the alveolar glycocalyx, breath to breath variations in terms of surface film compression:expansion, or surfactant recycling pathways could all be related to intra- or interspecies variations in surfactant composition.

Thus, in the context of the surfactant's biophysical function, it appears appropriate to speculate that in spite of the species variation, all surfactants have the ability to adsorb rapidly and form an initial monolayer, which is primarily composed of DPPC (or other disaturated PC) and cholesterol, approximately 3:1, with small amounts of other lipids under various biological conditions.

8.2.6. Host Defense Functions of Surfactant in the Mature Lung. In view of the observation that the respiratory surface defines the largest area exposed to the environment (~100 m^2), with the passage of some 10,000 L of air per day, it is obvious that the respiratory airways and alveoli experience very large amounts of various particulates. The lung must somehow dispose of these, while deciphering whether they are dangerous or not. Therefore, although not a major focus of this review, when discussing surfactant in lung physiology, it is clearly important to acknowledge the host defense functions of surfactant.[643,644] Since this material lines the entire respiratory surface, inhaled air with its many contaminants will continuously encounter the surface film. It is therefore not surprising that the surfactant system plays an important role in innate immunity. Surfactant also functions in adaptive immunity, which is delayed but strengthens with each subsequent challenge. In addition to defending the lung from injurious invaders, the surfactant system also plays a role in limiting responses to less dangerous materials in order to prevent self-injury.

A brief summation of this very complex area follows. The innate host defense system protects the pulmonary tract, in general, and the alveolar surfaces, in particular, from bacteria, viruses, and fungi. The immune system also clears infected, necrotic, and apoptotic cells. Studies related to these properties have largely focused on the large hydrophilic proteins SP-A and SP-D, although the hydrophobic components are also clearly involved. Several excellent reviews have been published focusing on the function of the collectins, SP-A and SP-D, which include extensive information on the broad ranging activities of these complex proteins.[97,98,645−647] It should also be noted that the location of these "surfactant proteins" is not limited to the lung.[648−650]

The collectins, SP-A and SP-D, interact with invading microorganisms *via* multiple noncovalent attachments with a number of complex glycoconjugates containing, for example, fucose, mannose, and *N*-acetyl-galactosamine, designated pathogen-associated molecular patterns (PAMPs). Since these collectins possess different specificities, they not only bind a large common cohort of microbes but also show selective interaction toward smaller differing groups of invaders. By binding to infective agents, SP-A and SP-D can neutralize them, reducing their ability to multiply or generate toxicity. For example, both collectins avidly bind Gram-negative bacterial lipopolysaccharide, neutralizing its activity. Further, the coating, and agglutination, of microorganisms opsonizes them, promoting interactions with immune cells, thereby facilitating phagocytosis and destruction. Initially, this primarily involves resident and the many recruited neutrophils, but macrophages, resident and evolved from recruited monocytes, also rapidly participate. Additional defense cells such as dendritic cells, mast cells, and natural T lymphocytes become involved later (see Casals,[17] Watson,[68] Whitsett,[551] and Arroyo[651] for further details).

Independent from directly interacting with pathogens, SP-A and D also impact inflammation. For example, SP-A and SP-D impact the formation of reactive oxygen species, which contribute to the intracellular and extracellular killing of pathogens. Additionally, neutrophils, and likely other immune cells, can extrude DNA forming complexes known as neutrophil extracellular traps. Both SP-A and SP-D bind to these and thereby augment microbial binding and killing.[68,652] The pulmonary collectins also play a role in clearance of infected, necrotic, and apoptotic cells, the removal of which supplants their ability to release potentially dangerous materials, designated damage-associated molecular patterns (DAMPs).

Innate immunology, although rapid, is limited in extent. SP-A and SP-D coordinate this initial defense with the adaptive system, which primarily involves antibody-directed protection. Certain cytokines, also known as chemokines, released at least in part by collectin activity, promote the longer range induction of acquired immunity. The two major cell types responsible are B-lymphocytes, which produce antibodies, and T-lymphocytes, which either help B-cells or function in cell-mediated immunity. The latter can involve humeral immunity where soluble antibodies interact with infective agents, neutralizing them and facilitating uptake by phagocytes. Cell mediated immunity occurs *via* T-lymphocytes and is important for defense against intracellular microbes. $CD4^+$ helper T lymphocytes assisted macrophage killing is enhanced by SP-D, as is the secretion of cytokines by these cells. As well, $CD8^+$ cytotoxic T-lymphocytes target host cells harboring intracellular pathogens, thereby eliminating reservoirs of infection.[28,67,98,653,654] Thus, the pulmonary collectins regulate the functions of innate immune cells and they react with antigen-presenting cells and T-cells. As such, they link the innate and adaptive immunity systems. It should also be recognized that while innate and adaptive immunity are essential for host defense, they comprise a double-edged sword, since these systems can contribute to pulmonary disease.

Hence, both SP-A and SP-D are known to play important roles in the resolution of damage. Notably, these hydrophilic surfactant proteins reduce airway inflammation by curtailing the activation and influx of $CD4^+$ T-lymphocytes, eosinophils, and mast cells. Aberrant expression of SP-D, in particular, appears to play an important role (see Noutsios,[105] Winkler,[106] and Ledford[655] for further details). Likewise, both complex proteins suppress inflammatory responses by inhibiting Toll-like receptor (TLR) signaling and the production of inflammatory cytokines in alveolar macrophages. SP-D down-regulates macrophage and dendritic cell antigen presentation, T-cell activation, and proliferation. This protein also has a major role in the downregulation of reactive oxygen species

https://doi.org/10.1021/acs.chemrev.3c00146
Chem. Rev. 2023, 123, 13209−13290

and metalloproteinases. Deficiency of SP-D has been shown to induce inflammation contributing to the development of emphysema.[656]

Furthermore, even in the absence of pathogens, SP-A influences the proteome of alveolar macrophages by contributing a calming effect toward nonharmful particulates.[17,657−660] For example, when bound to pathogens via its trimeric lectin headgroups, SP-A can interact with receptors, such as SIRPα, by its collagen-like regions promoting phagocytosis and proinflammatory signaling. However, when free, the trimeric headgroups can interact with immune cell calreticulin, thereby generating anti-inflammatory signaling.[661] Whereas the above information mainly pertains to animal studies, the findings for human SP-A are similar with one caveat: examination of SP-A in humans has demonstrated the presence of two variants, SP-A1 and SP-A2. Intriguingly, these variants not only have different responses in their host defense functions and their biophysical effects, but they are also associated with sex differences in terms of their response.[659,662,663]

From a global perspective, functions of SP-D, such as binding pathogens, enhancing phagocytosis, and modulating inflammation, considerably overlap with the characteristics of SP-A. However, the specific interactions with different pathogens, and their influences on inflammatory processes, are distinct.[664] As indicated earlier, unlike SP-A, which binds to DPPC, SP-D binds selectively to PI. This binding can also affect surfactant lipid morphology by generating distinct myelin-resembling structures in the presence of SP-B.[665] However, the association with surfactant appears to be weak, since only about 10% of the SP-D collected by lavage is associated with isolated large aggregates.[666] However, this latter property could be related to the lack of calcium in the lavage buffers.

The recent advances in the production of recombinant human SP-A (rhSP-A) and SP-D (rhSP-D) by molecular genetic biotechnology have renewed interest in examining potential clinical applications of these collectins.[68,98] A number of investigations have identified targets for novel therapies employing these complex recombinant proteins. One example is the ability of rhSP-D, in combination with a commercial clinical surfactant, to normalize the surfactant pools in prematurely delivered lambs.[664] Another notable finding is that the rhSP-D:clinical surfactant formulation can abolish inflammation in hyperventilated premature lambs by interacting and downregulating alveolar macrophages.[664] Interestingly, the full length rhSP-D addition rendered Survanta more resistant to plasma protein inhibition. Clinical trials using full length rhSP-D-supplemented surfactant are currently being conducted with the aim of limiting the incidence of bronchopulmonary dysplasia (BPD), a condition in premature infants due to aberrant lung development resulting from prolonged inflammation arising from elevated oxygenation and high ventilatory pressures.[667] Another ongoing clinical trial is examining the potential benefit of SP-D fortified surfactant in curtailing the harmful effects of viral infections, including COVID-19.[668]

The role of the hydrophobic components of surfactant in host defense is less well-defined. There is evidence that both SP-B and SP-C, in isolation, have immune functions. However, *in vivo* these proteins will always be associated with the lipids of surfactant. Consequently, to some extent these functions may reflect a physical barrier of the lipids rather than specific interactions, since the lipids can mute the bactericidal effects of SP-B-derived peptides.[669] Nevertheless, more recent data from knockout animals and findings of polymorphisms with SP-B and SP-C in respiratory disease suggest a significant role for the hydrophobic component of surfactant in maintaining clean and healthy respiratory surfaces.

As indicated earlier, the *SFTPB* gene product, a SP-B proprotein of ∼300 amino acids, contains three saposin-like protein domains. The surface active, 79 residue, hydrophobically mature SP-B, discussed in detail throughout this article, derives from the middle saposin-like protein domain and hence is sometimes designated as SP-B^{M} or SP-BM. In addition, there is a protein product of ∼81 amino acids coded by the N-terminal saposin-like domain, designated SP-B^{N}. Unlike SP-B^{M}, mature SP-B^{N} is slightly anionic and does not adhere to surfactant lipids. In keeping with its saposin-like nature, SP-B^{N} is bactericidal against both Gram-positive and Gram-negative bacterial, but only at low pH. Consequently, this soluble protein appears to contribute to lysosomal-related microbial killing by macrophages.[670−673] In addition to the mutations disrupting SP-B^{M} surface activity and requiring neonatal lung transplantation, numerous other *SFTPB* variants have been detected. Of particular note is a relatively common single nucleotide polymorphism involving a cytosine to tyrosine alteration (SP-B-C to SP-B-T) affecting the N-terminal saposin-like peptide, SP-B^{N}. This nucleotide replacement induces a threonine to isoleucine shift involving a potential glycosylation site in the proSP-B polypeptide.[674]

Investigations have been conducted with transgenic mice lacking endogenous SP-B expression but bearing the human SP-B-C or SP-B-T alleles. Under normal conditions, such mice are healthy and possess similar levels of surface-active SP-B^{M}. However, when challenged with *Pseudomonas aeruginosa, Klebsiella pneumomiae*, or *Staphylococcus aeruginosa*, the SP-B-C mice exhibited higher morbidity and mortality, greater bacterial burden, increased lung injury, and elevated cytokine levels.[671−673,675] Under normal conditions, no difference could be detected between the surface activities of LA surfactant from mice bearing the human SP-B-C or SP-B-T alleles or from WT mice. Surfactant from infected mice, on the other hand, demonstrated reduced activity, with SP-B-C LA being less active than SP-B-T LA, which was less active than LA from normal murine WT animals.

Several explanations are available. The relevant alteration could affect the glycosylation of proSP-B, thereby influencing its uptake into newly forming lamellar bodies. It was also proposed that this could be related to altered alveolar levels, due to differences in the uptake and degradation of these variants. It has also been observed that fragments of proSP-B, other than the mature surface-active peptide, can synergise with SP-A to mount an early response toward pathogens and this may differ between different variants.[670,673] It also appears that the cytokines released during infection downregulated SP-B biosynthesis through NF-κB signaling, and this response may differ among the two forms.[672,673]

It is notable that the SP-B-C allele is associated with an increased incidence of RDS and an elevated severity of ARDS.[676−678] These observations provide further strong evidence for an important relation between surfactant biophysical functions, host defense, and surfactant homeostasis.

Recent studies utilizing surface plasmon resonance indicate SP-B may interact directly with the angiotensin-converting

https://doi.org/10.1021/acs.chemrev.3c00146
Chem. Rev. 2023, 123, 13209−13290

enzyme 2 receptor, thereby providing steric hindrance toward infection by COVID-19 virus.[679] Patients bearing this pathogen demonstrate higher titers of anti-SP-B and anti-SP-C antibodies.

Similar to SP-B, whereas SP-C has been mainly examined for its ability to aid formation of a surface film, recent studies by a number of investigators have demonstrated altered innate immunity in mice either lacking or with mutant forms of SP-C. For example, *SFPC*$^{-/-}$ mice show enhance susceptibility to a number of pathogens, including *P. aeruginosa,* and to respiratory syncytial virus.[680−682] Furthermore, familial as well as idiopathic lung fibrosis and cystic fibrosis have also been associated with human SP-C mutations.[110,683−686]

Interestingly, whereas there is a clear segregation in the scientific literature between host defense functions and the γ reducing properties of surfactant lipids, there is increasing convincing evidence that these two functions are in fact intricately related. For example, PG, which is a critical component for the biophysical properties of surfactant, has been reported to be also involved in bacterial clearance in the lung.[154,687−689]

Linkage between biophysics and host defense has also been implied via SP-A and SP-D's association with surfactant lipids. As indicated earlier, SP-A binds to DPPC and is an integral component of tubular myelin structures. This collectin augments surface activity. Surfactant protein-A can also bind phosphatidylserine, abrogating this lipid's role in inducing apoptosis. Overall the association of SP-D with surfactant appears to be weak, since only about 10% of the SP-D collected by lavage is associated with the LA.[666] Surfactant protein-D binds selectively to PI and can affect surfactant lipid morphology by generating distinct myelin-like structures in the presence of SP-B and also fragments surfactant vesicles.[548,665,666] It has been suggested that these lipid interactions could contribute to host defense by localizing these proteins at the alveolar surface.[22,110,548,686]

To conclude, these interrelationships between biophysics and host defense functions of surfactant clearly imply that alterations in the biophysical properties of surfactant will not only impact lung physiology directly but also influence immune responses and inflammation within the lung. In particular, the two collectins, SP-A and SP-D, play critical roles in innate and adaptive host defense.[97,98,650,690] These collectins modulate the lung's immunogenic environment for host defense, while simultaneously blocking a potential overzealous inflammatory response which could easily lead to lung damage and impair gaseous exchange. Furthermore, strong evidence supports involvement of not only the hydrophobic surfactant proteins, SP-B and SP-C, but also the surfactant lipids.

8.2.7. Other Activities Related to Pulmonary Surfactant and Its Constituents. One aspect of surfactant's role in maintaining airway function is its apparent roles in asthma.[105,106,691,692] This is another example of the link between the innate and adaptive immune response systems. Exposure to inhaled allergens and pathogens triggers airway inflammation and subsequent bronchoconstriction, leading to episodes of airway narrowing. Surfactant activity can be impaired. Pulmonary surfactant components, particularly SP-A and SP-D, interact with a number of the immune cells, which orchestrate airway inflammatory responses to allergen-driven or pathogen-driven episodes. SP-A and SP-D have been shown to modulate eosinophil chemotaxis, inhibit eosinophil mediator release, and mediate macrophage clearance of apoptotic eosinophils.[693] While repeated allergenic challenges can result in airway remodelling, exasperating the condition, this response can be modulated by SP-D.[694]

An additional, but often overlooked, role of surfactant in the airways is to maintain patency of the smaller airways and at airway junctions. Surfactant keeps the airway hypophase thin, preventing the formation of menisci, especially at branch-points, thereby maintaining patency and allowing for maximal gaseous flow. This also restricts the formation of bubbles, which would hamper the delivery of fresh air to the alveoli.[165,695] Interestingly, high dietary cholesterol resulted in a lowering of patency, as assayed by a capillary surfactometer[696] In addition, surfactant plays an important role in promoting mucociliary clearance.[106,697]

It has long been known that infants succumbing to RDS display sloughed epithelial and damaged endothelial cells in their terminal bronchioles, leading to serum leakage.[40] This serum forms small "bloodless" clear clots, designated "Hyaline Membranes", that can limit passage of air into the air-exchange units. The narrowest section of the airways is at the terminal part of the bronchioles where they expand into the alveoli. The Young−Laplace equation for cylinders (eq 1, $\Delta P = \gamma/R$) asserts that this will be the point of maximal collapse pressure. Surfactant's ability to virtually abolish this collapse pressure likely constitutes its most important role in prevention of RDS.

The levels of certain surfactant components in serum or sputum have been used as markers for a number of human pathologies. Most investigations have targeted the collectins. Elevated serum SP-A can predict pulmonary damage due to smoking.[698] Increases in plasma or serum SP-A, SP-D, and SP-B have been observed with cardiovascular morbidity and mortality, interstitial pulmonary fibrosis, ARDS, small cell lung cancer, and acute and chronic kidney disease.[699−706]

Patients with either acute or chronic heart failure have lung function abnormalities stemming from pulmonary edema and defective gas exchange.[707] With acute cardiogenic pulmonary edema, SP-A, SP-D, and immature forms of SP-B are elevated in plasma, reflecting alveolar epithelial- capillary barrier disruption.[700,708] Immature SP-B refers to partially processed proSP-B. The release of immature SP-B is presumably related to high pulmonary capillary blood pressure.[709] This links the cardiopathologies directly to alterations in the alveolar capillary bed. Plasma immature SP-B levels correlate with depressed alveolar capillary gas exchange and so provide prognostic information.[710] With chronic heart failure there can also be increased connective tissue in the alveolar units as well as impaired gas exchange.[711]

Such alterations in plasma SP-B molecular forms can occur rapidly. Both immature and mature SP-B levels are elevated during cardiopulmonary bypass. Mature SP-B returns to normal within 48 h.[707] The utility of monitoring surfactant apoproteins is illustrated by clinical investigations, where patients with cardiomyopathy were treated with Levosimendan. This drug increases the heart's sensitivity to calcium, thereby supporting contractibility without elevations in cellular calcium.[712] During treatment, reductions in circulating SP-A, SP-D, and immature SP-B were noted, while mature SP-B increased.[707] The decrease in SP-D and immature SP-B indicates a reduction of inflammatory stress; conversely, increased mature SP-B suggests alveolar cell function restoration. Immature SP-B levels were significantly related to both cardiovascular related hospitalization and death.

https://doi.org/10.1021/acs.chemrev.3c00146
Chem. Rev. 2023, 123, 13209−13290

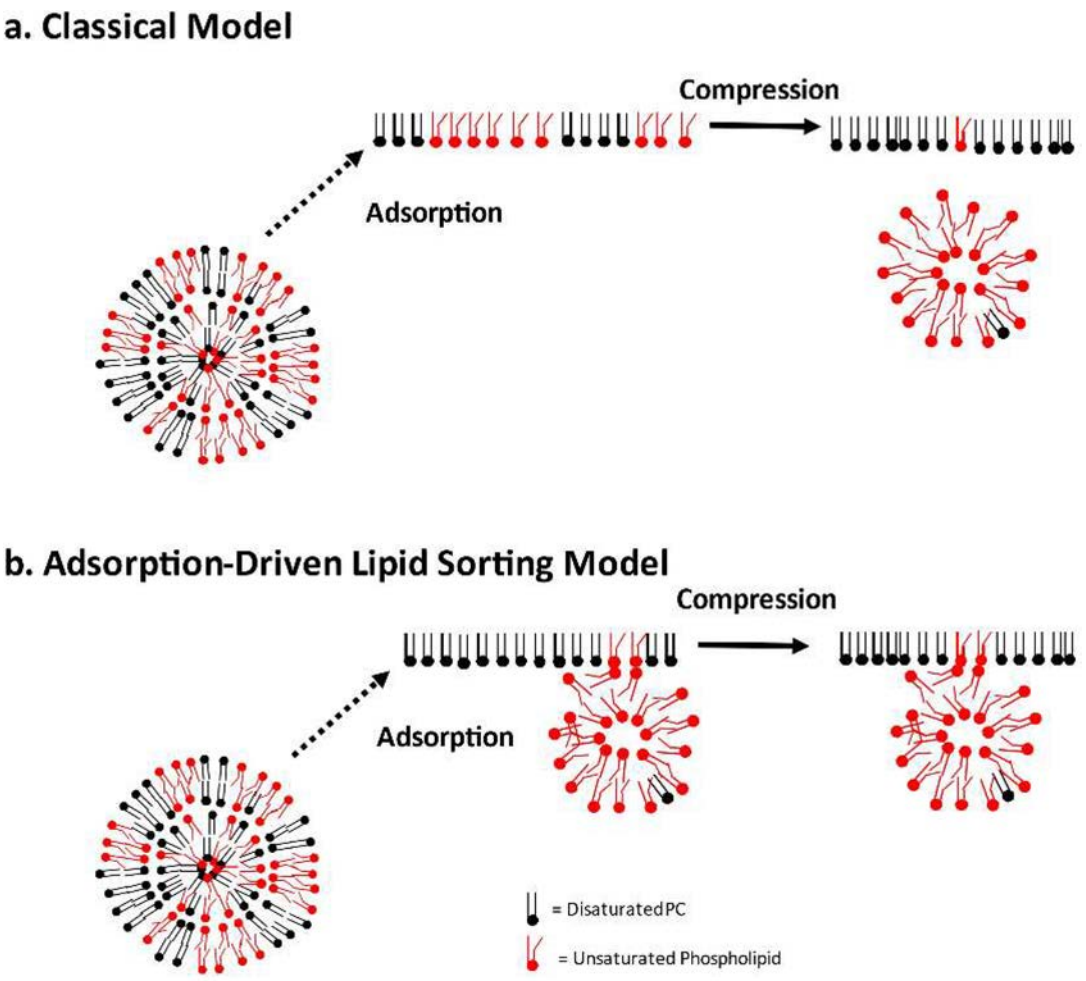

Figure 26. Comparison of the essential difference between the classical model and the adsorption-driven lipid sorting model presented in this review. (a) In the classical model, the surfactant vesicles with a nearly equimolar mixture of saturated (black) and unsaturated (red) lipids adsorb to form a monolayer with the same composition. During compression, the unsaturated lipids are gradually squeezed out, resulting in a smaller monolayer consisting mostly of saturated lipids that can attain a low surface tension and vesicles containing predominantly unsaturated PLs. During expansion to equilibrium γ, the surface film forms a mixed monolayer again but with less unsaturated lipid present than in the freshly adsorbed film. (b) In the adsorption-driven lipid sorting model, the surfactant vesicles adsorb to form a monolayer highly enriched in saturated lipids, while creating a surfactant reservoir with mostly unsaturated lipids. During the compression, there is no change in composition but a ∼15% decrease in surface area. During expansion to equilibrium γ, the surface area change is reversed with little or no change in composition.

Epithelial cells, including alveolar Type II cells, release small extracellular vesicles into the bloodstream.[713,714] These Type II cell-derived extracellular vesicles contain SP-C. Such increases in vesicular SP-C link various clinical diagnoses directly to pulmonary capillary disruption. Alterations in the level of such vascular vesicles can occur rapidly follow a challenge. For example, during the inflammatory stages of COVID-19, such extracellular vesicles can transfer viral genetic material and infect cardiomyocytes, thereby leading to heart failure.[714] It has been suggested that monitoring circulating vesicular SP-C could provide a convenient means to detect the possibility of imminent heart failure.

Chronic Obstructive Pulmonary Disease (COPD), or emphysema, represents one of the current leading causes of chronic morbidity and mortality.[715,716] While elevated alpha-1 antitrypsin is considered a prototypic biomarker for emphysema, it only accounts for 1−5% of this disease. Many different complex mechanisms underlie the initiation and progression of this multifactorial ailment.[717]

The levels of SP-D in serum and the levels of SP-A and SP-D in sputum are elevated in COPD patients.[717−721] In contrast, SP-D in bronchoalveolar lavage is reduced, especially during exasperations, indicating increased loss across the alveolar barrier. Chronic Obstructive Pulmonary Disease is common in smokers, and cigarette smoke has been shown to affect SP-D oligomerization, although whether this plays a major effect is not clear. Recent trials employing the phosphodiesterase-3 and -14 inhibitor ensifentrine, which spares cyclic AMP and cyclic GMP, have shown considerable promise in improving lung function and limiting exasperations.[722] The potential use of rhSP-D in limiting COPD progression has been suggested.

Studies in mice have led to the proposal that the appearance of SP-A in amniotic fluid, due to augmented production in the fetal lung near term, causes activation and migration of fetal amniotic fluid macrophages to the maternal uterus. Here the increased lectin level promotes increased production of IL-1β and activates NF-κB, leading to labor.[723] This SP-A-induced effect involves the TLR2 receptor on amniotic fluid macrophages. These novel findings suggest that expression of this pulmonary collectin acting via TLR2 serves a modulatory role in the timing of labor, thus connecting parturition with ample surfactant production.[724]

https://doi.org/10.1021/acs.chemrev.3c00146
Chem. Rev. 2023, 123, 13209−13290

8.3. Brief Synopsis of Physiological and Pathological Observations Related to Surfactant

The majority of research into the physiology of surfactant has focused on the time period around birth. Not only is this the time at which most dynamic changes to surfactant occur, it is also highly clinically significant, since birth without a functional surfactant system leads to direct lung failure. Despite extensive research, the exact alveolar amounts of surfactant at birth in humans are not precisely know and can only be approximately estimated. Nevertheless, these values are clearly much higher, on a per g lung and per kg birthweight basis, than in adults. This data, and corresponding data on surfactant treatment, indicate that high concentrations of surfactant are needed to establish air breathing. After birth, the surfactant system is relatively stable and undergoes active metabolism to maintain the film. The surfactant in these lungs not only maintains lung mechanics, but it also plays a role in the innate and adaptive host defense processes and in other activities. Disruption of the surfactant system in the mature lung contributes to lung injury in ARDS and in a number of other diseases. Surfactant components detected in the bloodstream can be indicative of a large number of maladies. However, due to the abundance of situations involved, clinical interpretation needs to be evaluated in terms of careful accompanying diagnoses and with the correlation of alterations in other circulating biomarkers.

9. PERSPECTIVES AND FUTURE CONSIDERATIONS

Our updated description of surfactant film establishment and maintenance is in approximate agreement with Postulate I of the classical model, proposed in the 1960s and 70s,[355,356,393,394,725] which states that the alveoli are stabilized by a monolayer, highly enriched in gel phase components, mainly DPPC, which reduces γ to low values near zero. The current interpretation would suggest that at the low γ arising during exhalation, the surface monolayer is highly enriched in the gel phase components, DPPC and cholesterol, ~3:1, likely with some other PC and PG disaturated PL. The monolayer is therefore primarily in the LO phase rather than the TC phase. The potential roles of non-DPPC disaturated PLs, particularly palmitoyl and myristoyl-PC, require further investigation. The monolayer likely also contains small pools of fluid PLs, mainly PG, but this is not certain. We consider it possible that the small pockets of the LE phase remaining could contribute to accommodating the SP-B and/or SP-C adsorption structures at the interface.

Importantly, in contrast to the classical model's suggestion of only a monolayer, it appears that the surface film could contain a SASR and an adsorption-driven surfactant reservoir. During the film expansion arising during quiet breathing, γ only rises to ~15 mN/m and so there is little need for additional material. Rather, the space between individual molecules or crystalline unit structures increases slightly to accommodate the extra space. With deep inhalations where γ exceeds 23 mN/m, additional small amounts of unsaturated and possibly disaturated PL can enter the interface, and this would most likely occur through the adsorption structures. Unsaturated PL could be largely, but not necessarily completely, eliminated during the next few exhalations or a deep sigh.

Postulate II of the classical model assumes that the lipid composition of the initial adsorbed surface monolayer, at equilibrium, is similar to the bulk surfactant. Monolayer refining then proceeds by a squeeze-out process during monolayer contraction. Our interpretation would suggest that this compositional equivalence likely initiates extremely early but as adsorption progresses adsorption-driven lipid sorting occurs to create a more stable film. This mechanism, which clearly conflicts with the classical model, is consistent with emerging data but must be further investigated.

In essence, the original classical model considered pulmonary surfactant function to consist of two independent actions, adsorption, to create the film, and squeeze-out, to generate monolayer enrichment in DPPC. The updated model proposed in this review postulates that these two processes occur as a single, connected, continuous event during monolayer formation. The difference between these two models is illustrated in Figure 26.

9.1. Notable Deficiencies in Our Current Appreciation of Pulmonary Surfactant Function

Whereas the above interpretation of surfactant function accommodates much of the accumulated data, there are specific details of the model, and indeed surfactant function in general, that require further experimental interrogation. Here we outline six major remaining directions, which will further test the validity and further explore the physiological and clinical implications of our experimental model of surfactant function. It should be noted that only six areas are selected out of a larger number of potential future directions, and we acknowledge author bias in the specific selection of the topics described.

9.1.1. Nature of the Proposed Adsorption Structures.

A considerable amount of our interpretation of surfactant function is dependent on the existence and nature of the proposed adsorption structures. These implied structures appear to explain many of the observations involving adsorption characteristics. The proposed involvement of nonbilayer hexagonal or cubic phases appears consistent with a number of experimental observations. The recent molecular dynamics simulations and EM evidence depicting SP-B based surface rings provide the best indication to date as to how natural lamellar bodies *in vivo*, and clinical surfactants *in vitro*, generate the surface film.

However, the precise mechanism(s) responsible for triggering natural, clinical, and lamellar body surfactant PLs unfolding at the air−water interface needs to be further elucidated. Except for the implied inclusion of PE, and possibly *bis*(monoacylglyero)phosphate, PL involvement in these curved structures must still be determined. The documented importance of PG interactions with SP-B in establishing the interfacial monolayer, and possibly its maintenance, requires further examination.

We find it intriguing that, although both SP-B and SP-C catalyze rapid adsorption to equilibrium and the ability to attain very low γ during lateral compression, only SP-B is essential for survival. Transgene-directed downregulation of SP-B leads to respiratory distress once SP-B levels have fallen to 25% of control.[726] This despite almost normal levels of SP-C. The amounts of PG in surfactant also decline. This is interesting in view of the observed functional relationship between PG and SP-B.[275,283,727] Thus, it is apparent that SP-B adsorption structures maintain a functional interfacial film in the absence of SP-C, but not the reverse. Elucidating the metabolic and biophysical basis of this difference could

https://doi.org/10.1021/acs.chemrev.3c00146
Chem. Rev. 2023, 123, 13209−13290

contribute much to our understanding of pulmonary surfactant function.

Much less is known about the mechanism whereby SP-C facilitates surfactant PL adsorption and γ reduction to low values, and this area deserves additional attention. Although certain synergistic properties suggest a common structure, we consider that present evidence does not yet fully support the implication that there are stable combined SP-B and SP-C containing adsorption structures contributing to alveolar stability. SP-B:SP-C stoichiometry supports this suggestion. Nevertheless, the possibility of combined SP-B and SP-C containing adsorption structures or the possibility that SP-C modifies the performance of the SP-B containing oligomeric rings clearly requires further investigation. As mentioned above, it is evident that SP-B containing structures alone are compatible with life. Additionally, how these hydrophobic proteins function to attach the monolayer-associated reservoirs requires further clarification. Indeed, are there both SASRs and adsorption-driven surfactant reservoirs? How do these interact to provide surface material during deep breaths and reincorporate the extra material during the subsequent exhalation? These areas remain a major gap in our ability to comprehend the relationship between surfactant function *in vitro* and *in vivo*.

9.1.2. Further Define the Role of Cholesterol in Surfactant Function. As noted throughout this review, the composition of the γ reducing monolayer appears to be either DPPC- or DPPC:cholesterol-enriched. The ambiguity about the role of cholesterol in the key structures of surfactant, especially *in vivo,* reflects a lack of understanding that exists with regard to the precise role of this neutral lipid.

Strong, evidence-based arguments can be made for the role of cholesterol in surfactant. All mammalian surfactants contain cholesterol, and in most cases, by weight this steroid is the third most abundant component after PC and PG (on a molar basis, cholesterol is usually present at approximately the same level as PG). Further, cholesterol impacts the phase behavior of lipid bi- and monolayers. Nevertheless DPPC:cholesterol films are quite stable and capable of reducing γ to near-zero values upon compression. Thus, cholesterol could contribute sufficient increased fluidity to enhance adsorption without hampering the ability to reduce γ to low values during compression. Exogenous surfactants containing cholesterol are effective both *in vitro* and *in vivo*. Consequently, its ubiquitous presence in surfactant and its impact on surface films would suggest an important functional role for cholesterol within surfactant.

Arguments contrasting the above are also supported by experimental data. For example, exogenous surfactants that contain no, or low amounts of, cholesterol are equally effective compared to the preparations containing cholesterol, although in practice the alveolar levels would be affected by endogenous sterol. DPPC films without cholesterol are highly stable and functional. While surfactant films enhance oxygen flux,[728] the cholesterol in such films would serve to reduce it somewhat.[686] Further, there is also strong evidence that high levels of cholesterol, such as observed in lung injury induced by mechanical ventilation, markedly impair surfactant function *in vitro* and *in vivo* by abrogating the 2D to 3D monolayer transition. Exogenous surfactants with lowered cholesterol could thus be advantageous in such situations where this sterol is abnormally high. Although this combined evidence does not preclude a role for cholesterol in surfactant, it certainly argues against it being essential. Clearly, further research is required to define the biophysical roles of this steroid.

9.1.3. Other Roles for Cholesterol and SP-C. As noted in the preceding two sections, large gaps remain in our understanding of the function of two of the main surfactant components, SP-C and cholesterol. However, this review mainly focused on γ reduction and, to a lesser extent, homeostasis and host defense. It is oft suggested that cholesterol contributes important biophysical properties to pulmonary surfactant. Theoretically, by increasing fluidity, cholesterol could promote adsorption of DPPC-containing PL mixtures. Whether this would extend to mixtures containing ~50% unsaturated PLs is not clear. We have not found any definite evidence for a clear role for cholesterol in promoting adsorption or γ reduction to low values with surfactant-like PL mixtures in the presence of both hydrophobic proteins. On the other hand, increased fluidity could theoretically hamper the ability of surfactant mixtures, despite containing high levels of disaturated lipids, to attain low γ during dynamic compression. It may be that an important role of SP-C is to counteract the dilatory effects of cholesterol on SP-B function.[322]

Interestingly, although most of the cholesterol in rat surfactant is derived from serum lipoproteins,[729] there are suggestions that lung-derived cholesterol can affect alveolar cholesterol when liver lipoprotein production is impaired.[730] Rapid changes in the disaturated PC:cholesterol ratio have been noted with alterations in total lung volume and the rate of breathing.[108,566,686,731] The source of the increased cholesterol or the manner by which alveolar cholesterol is rapidly decreased are not apparent, although macrophages could be involved. Recent evidence indicates the ABC lipid transporters are important in controlling pulmonary cholesterol homeostasis.[533]

It is also feasible that both SP-C and cholesterol serve non-biophysical functions. For example, evolutionary considerations would imply that, should cholesterol not be important, the ~7.5 wt % observed with most mammals would eventually be modified. Thus, it could be that the cholesterol in surfactant could play an intracellular role such as facilitating packing of surfactant lipids into lamellar bodies. Depleting cholesterol from Type II cell plasma membrane rafts interferes with lamellar body fusion and surfactant exocytosis.[732] Cholesterol could well have an, as yet undefined, role in homeostasis or host defense. Conversely, the potential role of cholesterol stabilizing drugs, such as statins, could prove beneficial with ARDS.[733] Furthermore, with some conditions, such as PAP, the alveolar cholesterol levels induce foamy macrophages with impaired activity.[101,102,552] Future studies on the role of cholesterol beyond γ reduction are clearly warranted.

The potential for an unanticipated role for SP-C appears to be supported by intriguing recent observations in genetically modified mice. SP-C-deficient mice are surfactant sufficient at birth and easily attain adulthood. However, with the specific genetic 129/Sv6 background, idiopathic pulmonary fibrosis (IPF), a form of interstitial lung diseases (ILDs) occurs in older animals.[110,686] This condition involves tissue scarring with increased collagen, heterogeneous overdistended air spaces, and reduced gaseous exchange. Idiopathic and familial lung fibrosis are also associated with a number of human SP-C mutations.[110,683,685,734,735] The 129/Sv6 strain and a number of other transgenic mice models exhibit abnormal Type II cell and alveolar macrophage signaling.[114,351,642,685,686,736] As well, proSP-C misfolding can induce endoplasmic reticulum

https://doi.org/10.1021/acs.chemrev.3c00146
Chem. Rev. 2023, 123, 13209−13290

stress.[114,351,737] There is also evidence for both alveolar instability during exhalation and overextension during inhalation. Aberrant Type II cell transdifferentiation into Type I cells can lead to Type II cell hyperplasia.[738] Further investigations to clarify these multiple bewildering observations are required.

Subsequently, as reviewed recently,[351] and beyond the scope of the current review, there appears to be a surprising and complex relationship between cholesterol and SP-C. This potential cholesterol/SP-C axis appears to be mainly evident in the development of pulmonary fibrosis. For example, the SP-C-deficient animals in the 129/Sv6 background, which exhibits elevated cholesterol adsorption, can display the presence of foamy macrophages within the lung airspaces.[351,686] Other altered processes involve effects of alveolar dynamics as well as impairment in lung repair mechanisms. Further elucidation of the proposed cholesterol/SP-C axis may not only explain the functional interaction of these two evolutionary conserved surfactant molecules, but it may also shine a light on the functional importance of each of these components individually.

9.1.4. Understanding the Mechanisms by Which Newly Secreted Surfactant Gets Incorporated into the Surface Film. The updated model suggests the presence of a monolayer film that does not change significantly during normal breathing. The apparent lack of material exchange from the film to the SASR, the adsorption-driven reservoirs, or the hypophase, other than potentially during deep breaths, may also have implications for our understanding of surfactant turnover. It is clear from studies with radioactive lipids, or stable isotopes, that surfactant is constantly synthesized, secreted, incorporated into the large membraneous forms, converted to the small unilamellar vesicles, and subsequently taken up either by Type II cells for recycling and degradation or by the alveolar macrophages for degradation. The build-up of surfactant in patients with, and animal models of, alveolar proteinosis provides further evidence of this process and its necessity. The detailed mechanisms by which this extracellular metabolism is regulated are still incompletely understood.

One of the specific questions that needs further study is what is the mechanism by which newly secreted surfactant material attains the hypophase surface, despite the presence of the SASR, the adsorption-driven surfactant reservoir, and the existing monolayer? Whereas several studies have shown how lamellar bodies rapidly adsorb to a clean interface, in a process that would likely occur in the neonate at birth, the fate of secreted lamellar bodies in a healthy mature lung is less clear. Electron microscopy reveals the unravelling of the lamellar bodies into tubular myelin-like structures underneath the surface film, but it is unknown how, or if, this freshly secreted material ultimately provides DPPC (and cholesterol) to the γ reducing monolayer. The difficulties in addressing this issue experimentally are that, first, *in vivo* studies with labeled surfactant involve lung lavage, which disrupts the film and does not allow one to examine the actual surface film; second, EM is limited by the fixing methods and only provides a static picture rather than dynamic views of metabolism; and third, *in vitro* studies are not performed in the time frames associated with this metabolic cycle. New methodologies likely need to be developed to address this question.

9.1.5. Elucidating the Mechanism by Which Surfactant Becomes Inactivated. Like our understanding of surfactant metabolism, the updated model of surfactant function also alters our thinking about the mechanisms by which surfactant is inhibited. Traditionally, many studies of surfactant inhibition have demonstrated this by the mixing of surfactant with the inhibitory component and subsequent testing on a surfactometer. In this scenario, surfactant inhibition can occur during the adsorption process, as well as during the expansion/compression cycles. In other words, most of, if not all of, the tested inhibitors impact surfactant adsorption. Correlating this to the *in vivo* scenario in which inhibition occurs by reducing the activity of the existing film is more difficult. For example, is a film of mostly disaturated lipids more resistant to inactivation than one with some unsaturated lipids? What is the effect of the adsorption structures in these processes?

9.1.6. New Exogenous Surfactants. Despite the success of surfactant treatment in neonates, there is still a need for alternative surfactant preparations. For example, making surfactant therapy available in underdeveloped regions will require an inexpensive product. With limited access to refrigeration, such a product should also be stable for prolonged periods at relatively high temperatures. Wholly synthetic surfactant preparations are attractive for several reasons. They may be more stable, they may become cheaper, they eliminate concern of using animal-derived substances, and importantly, they can be adapted to specific therapeutic conditions.

For RDS, synthetic surfactant preparations should closely mimic the properties of the currently available and successful modified natural surfactants. Thus, analogues of SP-B with DPPC, PG, and unsaturated PC appear to be essential components. A functional analogue of SP-C is also recommended. Despite cholesterol being suggested as an integral component of the surface-active film, inclusion of this material in an exogenous surfactant does not appear to be critical; in approximately half the currently available preparations, cholesterol is removed or reduced, without an apparent impact on efficacy.

The artificial surfactant CHF5633 constitutes an interesting step forward in the development of synthetic preparations. Although various aspects still require testing, this wholly synthetic preparation containing SP-B and SP-C analogues has been shown to be as effective as Curosurf in a lamb model of ARDS and in clinical trials with preterm babies.[62,65,739,740] Interestingly, the DPPC in CHF5633 was metabolized significantly more slowly in mice than was DPPC in Curosurf.[741] This difference was attributed to the larger dose of DPPC (2.5 vs 1.75 mg/mouse), which arose because CHF 5633 contains only two PLs.

In addition, a wholly synthetic surfactant containing the very active SP-B analogue BY-L or Super Mini-B and stable SP-C analogues formulated by Waring and associates[66,742,743] is being reviewed for clinical trials. The possibility of incorporating beneficial polymers should be investigated further. Progress has also been made in creating peptoid analogues of SP-B and SP-C. These "biomimics" are non-natural compounds in which the side chains are appended to the nitrogen of a polypeptide backbone rather than to a carbon molecule.[602] This creates a highly stable structure that is protease resistant. Each of these approaches to generate a functional synthetic surfactant are valuable areas for continued experimentation.[338,520,743]

Currently, clinical trials exploring the potential advantage of adding supplemental full length rhSP-D to clinical surfactants

https://doi.org/10.1021/acs.chemrev.3c00146
Chem. Rev. 2023, 123, 13209−13290

are being investigated with premature infants and the outcomes are eagerly awaited. Whether inclusion of the much less expensive shorter trimeric recombinant forms will prove sufficient in at least some situations must still be examined.

Surfactant administration has not yet been successful in reducing mortality with treatment of ARDS. However, this procedure could potentially have a greater impact on ARDS if used in combination with other therapeutics. The pathophysiology of ARDS is complex and extends well beyond surfactant dysfunction. Depending on the initial insult leading to the disease, agents such as antivirals, antibiotics, antimicrobial peptides, and perhaps anti-inflammatory drugs could be incorporated in the surfactant.[606−608] In this scenario, surfactant could improve lung function through its biophysical property of efficient spreading and simultaneously assist with the delivery of the incorporated drugs to the remote areas of the lung. An obvious but crucial aspect of this approach is to generate a drug-fortified surfactant preparation that maintains both the surfactant's biophysical properties as well as drug efficacy.[744,745] The development of synthetic surfactant customized for this type of therapeutic approach, rather than simply mixing various drugs with existing exogenous preparations, may prove optimal and represents an important future challenge for chemists engaged in surfactant research.

10. CONCLUSIONS

Our interpretation of the current literature led to a new model of surfactant function in which an adsorption-driven lipid sorting generating a monolayer enriched in stable lipid components represents a critical update of previous models, in which adsorption was fully dissociated from film purification. It is hoped that this will represent an initial framework to further define the molecular details of the generation and maintenance of the surfactant film. In this regard we provided a few examples of areas that, in the opinion of the authors, require further study to interrogate this new model further and to refine or expand our understanding of surfactant function. In addition to providing a better physiological understanding, such knowledge may ultimately help improve clinical outcomes in diseases in which surfactant is reduced or absent.

AUTHOR INFORMATION

Corresponding Authors

Fred Possmayer − *Department of Biochemistry and Department of Obstetrics/Gynaecology, Western University, London, Ontario N6A 3K7, Canada;* orcid.org/0000-0002-5173-3437; Email: fpossmay@uwo.ca

Yi Y. Zuo − *Department of Mechanical Engineering, University of Hawaii at Manon, Honolulu, Hawaii 96822, United States; Department of Pediatrics, John A. Burns School of Medicine, University of Hawaii, Honolulu, Hawaii 96826, United States;* orcid.org/0000-0002-3992-3238; Email: yzuo@hawaii.edu

Ruud A. W. Veldhuizen − *Department of Physiology & Pharmacology, Western University, London, Ontario N6A 5C1, Canada; Department of Medicine, Western University, London, Ontario N6A 3K7, Canada; Lawson Health Research Institute, London, Ontario N6A 4V2, Canada;* Email: rveldhui@uwo.ca

Nils O. Petersen − *Department of Chemistry, University of Alberta, Edmonton, Alberta T6G 2G2, Canada; Department of Chemistry, Western University, London, Ontario N6A 5B7, Canada;* Email: nils.petersen@ualberta.ca

Complete contact information is available at: https://pubs.acs.org/10.1021/acs.chemrev.3c00146

Author Contributions

CRediT: **Fred Possmayer** conceptualization, project administration, writing-original draft, writing-review & editing; **Yi Y. Zuo** conceptualization, funding acquisition, project administration, software, writing-original draft, writing-review & editing; **Ruud A. W. Veldhuizen** conceptualization, funding acquisition, project administration, writing-original draft, writing-review & editing; **Nils O. Petersen** conceptualization, formal analysis, project administration, writing-original draft, writing-review & editing.

Notes

The authors declare no competing financial interest.

Biographies

Fred Possmayer is a Professor Emeritus of Biochemistry and Obstetrics/Gynaecology at the University of Western Ontario (UWO, now Western University). After obtaining his PhD from UWO in 1965, he undertook postdoctoral studies at the Universität zu Köln, Germany, Rijksuniversiteit Utrecht, The Netherlands, and the University of California, Riverside, USA. In 1971, he returned to UWO as a faculty member in the Department of Biochemistry and the Department of Obstetrics and Gynaecology. His research involves phospholipid metabolism in brain and lung, the role of lipids in cell signaling, lipid−lipid and lipid−protein interactions in pulmonary surfactant, and the role of surfactant apoproteins in surfactant function *in vivo* and *in vitro*. His laboratory was involved in the development of the clinical surfactant BLES.

Yi Y. Zuo is a Professor in the Department of Mechanical Engineering at the University of Hawaii at Manoa and Adjunct Professor in the Department of Pediatrics in the John A. Burns School of Medicine. He received his PhD from the University of Toronto in 2006. He was a NSERC Postdoctoral Fellow at the University of Western Ontario between 2006 and 2008. His research focuses on colloid and surface science, biophysical study of pulmonary surfactant and tear film, and environmental science and technology related to nanoparticle and aerosol inhalation. He earned the NSF CAREER Award in 2013.

Ruud A. W. Veldhuizen is an Associate Professor in Medicine and Physiology & Pharmacology at Western University, Canada, and a Lawson Health Research Institute scientist. Following undergraduate studies at the Dr. Ing. Ghijssen Instituut and Utrecht University, he obtained a PhD in Biochemistry at Western University with Dr. Fred Possmayer. Subsequent postdoctoral fellowships with Drs. Jim Lewis (Western University), Henk Haagsman (Utrecht University), and Art Slustky (University of Toronto) led to the current faculty position. The general focus of research in Ruud's lab is pulmonary surfactant in health and disease. Current interests include the effect of vaping on surfactant as well as the impact of aging and exercise on lung injury. Over the years, his research has been supported by, among others, the Canadian Institute of Health Research, Natural Sciences and Engineering Research Council of Canada, the Ontario Thoracic Society, as well as internal funding from Lawson Health Research Institute and Western University.

Nils O. Petersen has been a Professor Emeritus of Chemistry and Biochemistry at the University of Western Ontario (UWO) from

2005 and Professor Emeritus of Chemistry at the University of Alberta (UofA) from 2015. He received an Honours BSc in Chemistry from UWO in 1972 and a PhD in Chemistry with a minor in Biology from California Institute of Technology in 1978. After postdoctoral fellowships at Cornell University and Washington University Medical School, he was a professor of chemistry at UWO for 24 years and then spent 10 years as Director General at the National Research Council, Canada, and Professor of Chemistry at UofA. His research interests focused on the biophysical properties of lipid membranes, cell membranes, and surfactants using spectroscopy (magnetic resonance and fluorescence) and imaging tools (confocal microscopy, atomic force microscopy, and time-of-flight secondary ion mass spectroscopy) to study the dynamics and distribution of membrane components.

ACKNOWLEDGMENTS

We thank Marc Possmayer for all the time and effort in assisting with graphic design and organizing references. We thank Kevin Keough for constructive comments on our manuscript. F.P. thanks Matthias Amrein, Lisa Cameron, Michael Dunn, Stephen Hall, Alan Jobe, Paul Kingma, Frank McCormack, Matthias Ochs, Alan Waring, Alastair Watson, and Joseph Zasadzinski for helpful discussions. We also thank Carrie Noble for designing and drawing the graphical abstract and students in the Veldhuizen lab for proofreading the manuscript. Y.Y.Z. was supported by National Science Foundation grant number CBET-2011317. R.A.W.V. was supported by Natural Sciences and Engineering Research Council of Canada grant number RGPIN 04745-2019.

LIST OF ABBREVIATIONS

A	Area
ADSA	Axisymmetric drop shape analysis
AFM	Atomic force microscopy
ALI	Acute lung injury
AMP	Adenosine monophosphate
ARDS	Acute respiratory distress syndrome
ATP	Adenosine triphosphate
CBS	Captive bubble surfactometry
CD	Cluster of differentiation
CDS	Constrained drop surfactometry
CL-ADSA	Closed loop-ADSA
CLSE	Calf lung surfactant extract (Infasurf)
COPD	Chronic obstructive pulmonary disease
COVID-19	Coronavirus disease 2019
CPAP	Continuous positive airway pressure
CTF	C-Terminal fragment
d	Periodic distance
DAMPs	Damage-associated molecular patterns
DOPG	Dioleoyl phosphatidylglycerol
DPPC	Dipalmitoyl phosphatidylcholine
DPPG	1,2-Dipalmitoyl-*sn*-glycero-3-phosphoglycerol, sodium salt
EDTA	Ethylenediaminetetraacetic acid
FRC	Functional residual capacity
G	Gibbs free energy
GIXD	Grazing incidence X-ray diffraction
GM-CSF	Granulocyte-macrophage-colony stimulating factor
GPR 116	Guanidine protein receptor 116
GPCR	Guanidine protein coupled receptor
GUV	Giant unilamellar vesicles
L	Perimeter
LA	Large aggregates
LD	Liquid-disordered
LE	Liquid-expanded
LISA	Less invasive surfactant administration
LO	Liquid-ordered
LPC	Lyso-phosphatidylcholine
MAS	Meconium aspiration syndrome
MD	Molecular dynamics
n	Number
NMR	Nuclear magnetic resonance
NTF	N-terminal fragment
P	Pressure
PAMPs	Pathogen-associated molecular patterns
PAP	Pulmonary alveolar proteinosis
PBS	Pulsating bubble surfactometry
PC	Phosphatidylcholine
PE	Phosphatidylethanolamine
PG	Phosphatidylglycerol
PI	Phosphatidylinositol
PLs	Phospholipids
POPC	Palmitoyl-oleoyl phosphatidylcholine
POPE	Palmitoyl-oleoyl phosphatidylethanolamine
POPG	Palmitoyl-oleoyl phosphatidylglycerol
PKC	Protein kinase C
P2RY2	Purinergic 2-receptor Y2
P2X7 R	Purinergic 2 X7 receptor
R	Radius
rhSP-A	Recombinant human SP-A
rhSP-D	Recombinant human SP-D
RDS	Respiratory distress syndrome
SA	Small aggregates
SASR	Surface-associated surfactant reservoir
SAXS	Small angle X-ray scattering
SIRPα	Signal-inhibitory regulatory protein α
SM	Sphingomyelin
SP-	Surfactant proteins
SP-B-C	Surfactant protein-B, cytosine allele
SP-BM	Middle saposin-like protein domain of proSP-B
SP-BN	N-Terminal saposin-like domain of proSP-B
SP-B-T	Surfactant protein-B, tyrosine allele
SFTPA	Surfactant protein A gene
SFTPB	Surfactant protein B gene
SFTPC	Surfactant protein C gene
SFTPD	Surfactant protein D gene
T	Temperature
T_m	Main transition temperature
TC	Tilted-condensed
TLC	Total lung capacity
TLR	Toll-like receptor
ToF-SIMS	Time-of-flight secondary ion mass spectrometry
TTF-1	Thyroid transcription factor-1
WAXS	Wide angle X-ray scattering
7-TMD	7-Transmembrane domain
λ	Lambda
γ	Surface tension
γ_o	Original surface tension
γ_{eq}	Equilibrium surface tension
π	Surface pressure
π_{eq}	Equilibrium spreading pressure
τ	Line tension

https://doi.org/10.1021/acs.chemrev.3c00146
Chem. Rev. 2023, 123, 13209−13290

REFERENCES

(1) von Neergaard, K. Neue Auffassungen Uber Einen Grundbegriff Der Atemmechanik. Die Retraktionskraft Der Lunge, Abhangig Von Der Oberflachenspannung in Den Alveolen. *Z. Gesamte Exp. Med.* **1929**, *66*, 373−394.

(2) Pattle, R. Properties, Function and Origin of the Alveolar Lining Layer. *Nature* **1955**, *175*, 1125−1126.

(3) Clements, J. A. Dependence of Pressure-Volume Characteristics of Lungs on Intrinsic Surface Active Material. *Am. J. Physiol.* **1956**, *187*, 592.

(4) Avery, M. E.; Mead, J. Surface Properties in Relation to Atelectasis and Hyaline Membrane Disease. *Am. J. Dis Child* **1959**, *97*, 517−523.

(5) Clements, J. A. Lung Surfactant: A Personal Perspective. *Annu. Rev. Physiol.* **1997**, *59*, 1−21.

(6) Brown, E. Isolation and Assay of Dipalmityl Lecithin in Lung Extracts. *Am. J. Physiol.* **1964**, *207*, 402−406.

(7) Possmayer, F. A Proposed Nomenclature for Pulmonary Surfactant-Associated Proteins. *Am. Rev. Respir. Dis.* **1988**, *138* (4), 990−998.

(8) Possmayer, F. The Role of Surfactant-Associated Proteins. *Am. Rev. Respir. Dis.* **1990**, *142* (4), 749−752.

(9) Goerke, J. Pulmonary Surfactant: Functions and Molecular Composition. *Biochim. Biophys. Acta* **1998**, *1408* (2−3), 79−89.

(10) Hawgood, S.; Derrick, M.; Poulain, F. Structure and Properties of Surfactant Protein B. *Biochim. Biophys. Acta* **1998**, *1408* (2−3), 150−160.

(11) Johansson, J.; Curstedt, T. Molecular Structures and Interactions of Pulmonary Surfactant Components. *Eur. J. Biochem.* **1997**, *244* (3), 675−693.

(12) Veldhuizen, R.; Nag, K.; Orgeig, S.; Possmayer, F. The Role of Lipids in Pulmonary Surfactant. *Biochim. Biophys. Acta* **1998**, *1408*, 90−108.

(13) Zuo, Y. Y.; Veldhuizen, R. A.; Neumann, A. W.; Petersen, N. O.; Possmayer, F. Current Perspectives in Pulmonary Surfactant–Inhibition, Enhancement and Evaluation. *Biochim. Biophys. Acta* **2008**, *1778* (10), 1947−1977.

(14) Postle, A. D.; Heeley, E. L.; Wilton, D. C. A Comparison of the Molecular Species Compositions of Mammalian Lung Surfactant Phospholipids. *Comp Biochem Physiol A Mol. Integr Physiol* **2001**, *129* (1), 65−73.

(15) Dushianthan, A.; Cusack, R.; Goss, V.; Postle, A. D.; Grocott, M. P. Clinical Review: Exogenous Surfactant Therapy for Acute Lung Injury/Acute Respiratory Distress Syndrome–Where Do We Go from Here? *Crit Care* **2012**, *16* (6), 238.

(16) McCormack, F.; Structure, X. Processing and Properties of Surfactant Protein A. *Biochim. Biophys. Acta* **1998**, *1408* (2−3), 109−131.

(17) Casals, C.; Campanero-Rhodes, M. A.; García-Fojeda, B.; Solís, D. The Role of Collectins and Galectins in Lung Innate Immune Defense. *Front Immunol* **2018**, *9*, 1998.

(18) Watson, A.; Phipps, M. J. S.; Clark, H. W.; Skylaris, C. K.; Madsen, J. Surfactant Proteins A and D: Trimerized Innate Immunity Proteins with an Affinity for Viral Fusion Proteins. *J. Innate Immun* **2018**, *11* (1), 13−28.

(19) Haagsman, H. P.; Hogenkamp, A.; van Eijk, M.; Veldhuizen, E. J. Surfactant Collectins and Innate Immunity. *Neonatology* **2008**, *93* (4), 288−294.

(20) Cañadas, O.; Olmeda, B.; Alonso, A.; Pérez-Gil, J. Lipid-Protein and Protein-Protein Interactions in the Pulmonary Surfactant System and Their Role in Lung Homeostasis. *Int. J. Mol. Sci.* **2020**, *21* (10), 3708.

(21) Cheng, O. Z.; Palaniyar, N. Net Balancing: A Problem in Inflammatory Lung Diseases. *Front Immunol* **2013**, *4*, 1.

(22) (a) McCormack, F. X.; Whitsett, J. A. The Pulmonary Collectins, SP-A and SP-D, Orchestrate Innate Immunity in the Lung. *J. Clin Invest* **2002**, *109* (6), 707−712. (b) Whitsett, J. A.; Weaver, T. E. Hydrophobic Surfactant Proteins in Lung Function and Disease. *N Engl J. Med.* **2002**, *347* (26), 2141−2148. (c) Whitsett, J. A.; Weaver, T. E. Hydrophobic Surfactant Proteins in Lung Function and Disease. *N Engl J. Med.* **2002**, *347* (26), 2141−2148.

(23) Whitsett, J. A.; Weaver, T. E. Hydrophobic Surfactant Proteins in Lung Function and Disease. *N Engl J. Med.* **2002**, *347* (26), 2141−2148.

(24) Perez-Gil, J.; Keough, K. M. W. Interfacial Properties of Surfactant Proteins. *Biochim. Biophys. Acta* **1998**, *1408* (2−3), 203−217.

(25) Possmayer, F.; Nag, K.; Rodriguez, K.; Qanbar, R.; Schürch, S. Surface Activity in Vitro: Role of Surfactant Proteins. *Comp Biochem Physiol A Mol. Integr Physiol* **2001**, *129* (1), 209−220.

(26) Rugonyi, S.; Biswas, S. C.; Hall, S. B. The Biophysical Function of Pulmonary Surfactant. *Respir Physiol Neurobiol* **2008**, *163* (1−3), 244−255.

(27) Casals, C.; Cañadas, O. Role of Lipid Ordered/Disordered Phase Coexistence in Pulmonary Surfactant Function. *Biochim Biophys Acta (BBA) - Biomembranes* **2012**, *1818* (11), 2550−2562.

(28) Kishore, U.; Greenhough, T. J.; Waters, P.; Shrive, A. K.; Ghai, R.; Kamran, M. F.; Bernal, A. L.; Reid, K. B. M.; Madan, T.; Chakraborty, T. Surfactant Proteins SP-A and SP-D: Structure, Function and Receptors. *Molecular Immunology* **2006**, *43* (9), 1293−1315.

(29) Valle, R. P.; Wu, T.; Zuo, Y. Y. Biophysical Influence of Airborne Carbon Nanomaterials on Natural Pulmonary Surfactant. *ACS Nano* **2015**, *9* (5), 5413−5421.

(30) Zuo, Y. Y.; Chen, R.; Wang, X.; Yang, J.; Policova, Z.; Neumann, A. W. Phase Transitions in Dipalmitoylphosphatidylcholine Monolayers. *Langmuir* **2016**, *32* (33), 8501−8506.

(31) Xu, L.; Yang, Y.; Zuo, Y. Y. Atomic Force Microscopy Imaging of Adsorbed Pulmonary Surfactant Films. *Biophys. J.* **2020**, *119* (4), 756−766.

(32) Picardi, M. V.; Cruz, A.; Orellana, G.; Perez-Gil, J. Phospholipid Packing and Hydration in Pulmonary Surfactant Membranes and Films as Sensed by Laurdan. *Biochim. Biophys. Acta* **2011**, *1808* (3), 696−705.

(33) Andreev, K.; Martynowycz, M. W.; Kuzmenko, I.; Bu, W.; Hall, S. B.; Gidalevitz, D. Structural Changes in Films of Pulmonary Surfactant Induced by Surfactant Vesicles. *Langmuir* **2020**, *36* (45), 13439−13447.

(34) Baoukina, S.; Monticelli, L.; Amrein, M.; Tieleman, D. P. The Molecular Mechanism of Monolayer-Bilayer Transformations of Lung Surfactant from Molecular Dynamics Simulations. *Biophys. J.* **2007**, *93* (11), 3775−3782.

(35) Baoukina, S.; Monticelli, L.; Risselada, H. J.; Marrink, S. J.; Tieleman, D. P. The Molecular Mechanism of Lipid Monolayer Collapse. *Proc. Natl. Acad. Sci. U. S. A.* **2008**, *105* (31), 10803−10808.

(36) Baoukina, S.; Tieleman, D. P. Computer Simulations of Lung Surfactant. *Biochim. Biophys. Acta* **2016**, *1858* (10), 2431−2440.

(37) Bai, X.; Xu, L.; Tang, J. Y.; Zuo, Y. Y.; Hu, G. Adsorption of Phospholipids at the Air-Water Surface. *Biophys. J.* **2019**, *117* (7), 1224−1233.

(38) Comroe, J. H., Jr. *Retrospectroscope: Insights into Medical Discovery*; Von Gehr Press, 1977.

(39) Comroe, J. H., Jr. Premature Science and Immature Lungs. Part III. The Attack on Immature Lungs. *Am. Rev. Respir. Dis.* **1977**, *116* (3), 497−518.

(40) Comroe, J. H., Jr. Premature Science and Immature Lungs. Part II. Chemical Warfare and the Newly Born. *Am. Rev. Respir. Dis.* **1977**, *116* (2), 311−323.

(41) Chu, J.; Clements, J. A.; Cotton, E. K.; Klaus, M. H.; Sweet, A. Y.; Tooley, W. H.; Bradley, B. L.; Brandorff, L. C. Neonatal Pulmonary Ischemia. I. Clinical and Physiological Studies. *Pediatrics* **1967**, *40* (4), 709−782.

(42) Robillard, E.; Alarie, Y.; Dagenais-Perusse, P.; Baril, E.; Guilbeault, A. Microaerosol Administration of Synthetic Beta-Gamma-Dipalmitoyl-L-Alpha-Lecithin in the Respiratory Distress Syndome: A Preliminary Report. *Can. Med. Assoc J.* **1964**, *90* (2), 55−57.

https://doi.org/10.1021/acs.chemrev.3c00146
Chem. Rev. 2023, 123, 13209−13290

(43) Enhörning, G.; Grossmann, G.; Robertson, B. Pharyngeal Deposition of Surfactant in the Premature Rabbit Fetus. *Biol. neonate* **2004**, *22* (1), 126−132.
(44) Enhörning, G.; Robertson, B. Lung Expansion in the Premature Rabbit Fetus after Tracheal Deposition of Surfactant. *Pediatrics* **1972**, *50* (1), 58−66.
(45) Enhörning, G. Expansion of the Lungs in the New-Born and Its Effect on Pulmonary Circulation. *Acta Obstet Gynecol Scand* **1969**, *48* (S3), 72−74.
(46) Enhörning, G.; Robertson, B. Expansion Patterns in the Premature Rabbit after Tracheal Deposition of Surfactant. *Acta Pathol. Microbiol. Scandanavia A* **1971**, *79* (6), 682.
(47) Comroe, J. H., Jr. Premature Science and Immature Lungs. Part I. Some Premature Discoveries. *Am. Rev. Respir. Dis.* **1977**, *116* (1), 127−135.
(48) Metcalfe, I. L.; Burgoyne, R.; Enhorning, G. Surfactant Supplementation in the Preterm Rabbit: Effects of Applied Volume on Compliance and Survival. *Pediatr. Res.* **1982**, *16* (10), 834−839.
(49) Metcalfe, I. L.; Pototschnik, R.; Burgoyne, R.; Enhorning, G. Lung Expansion and Survival in Rabbit Neonates Treated with Surfactant Extract. *J. Appl. Physiol.* **1982**, *53* (4), 838−843.
(50) Fujiwara, T.; Maeta, H.; Chida, S.; Morita, T.; Watabe, Y.; Abe, T. Artificial Surfactant Therapy in Hyaline-Membrane Disease. *Lancet* **1980**, *315* (8159), 55−59.
(51) Metcalfe, I. L.; Enhorning, G.; Possmayer, F. Pulmonary Surfactant-Associated Proteins: Their Role in the Expression of Surface Activity. *J. Appl. Physiol.* **1980**, *49* (1), 34−41.
(52) Kwong, M. S.; Egan, E. A.; Notter, R. H.; Shapiro, D. L. Double-Blind Clinical Trial of Calf Lung Surfactant Extract for the Prevention of Hyaline Membrane Disease in Extremely Premature Infants. *Pediatrics* **1985**, *76* (4), 585−592.
(53) Robertson, B. European Multicenter Trials of Curosurf for Treatment of Neonatal Respiratory Distress Syndrome. *Lung* **1990**, *168* (1), 860−863.
(54) Phibbs, R. H.; Ballard, R. A.; Clements, J. A.; Heilbron, D. C.; Phibbs, C. S.; Schlueter, M. A.; Sniderman, S. H.; Tooley, W. H.; Wakeley, A. Initial Clinical Trial of EXOSURF, a Protein-Free Synthetic Surfactant, for the Prophylaxis and Early Treatment of Hyaline Membrane Disease. *Pediatrics* **1991**, *88* (1), 1−9.
(55) Morley, C. J. Surfactant Substitution in the Newborn by Application of Artificial Surfactant. *J. Perinat Med.* **1987**, *15* (5), 469−478.
(56) Smyth, J. A.; Metcalfe, I. L.; Duffty, P.; Possmayer, F.; Bryan, M. H.; Enhorning, G. Hyaline Membrane Disease Treated with Bovine Surfactant. *Pediatrics* **1983**, *71* (6), 913−917.
(57) Jobe, A.; Ikegami, M. Surfactant for the Treatment of Respiratory Distress Syndrome. *Am. Rev. Respir. Dis.* **1987**, *136* (5), 1256−1275.
(58) Clements, J. A.; Avery, M. E. Lung Surfactant and Neonatal Respiratory Distress Syndrome. *Am. J. Respir Crit Care Med.* **1998**, *157* (4 Pt 2), S59−66.
(59) Robertson, B.; Halliday, H. L. Principles of Surfactant Replacement. *Biochim. Biophys. Acta* **1998**, *1408* (2−3), 346−361.
(60) McPherson, C.; Wambach, J. A. Prevention and Treatment of Respiratory Distress Syndrome in Preterm Neonates. *Neonatal network: NN* **2018**, *37* (3), 169−177.
(61) Kamath, B. D.; MacGuire, E. R.; McClure, E. M.; Goldenberg, R. L.; Jobe, A. H. Neonatal Mortality From Respiratory Distress Syndrome: Lessons for Low-Resource Countries. *Pediatrics* **2011**, *127* (6), 1139−1146.
(62) Mikolka, P.; Curstedt, T.; Feinstein, R.; Larsson, A.; Grendar, M.; Rising, A.; Johansson, J. Impact of Synthetic Surfactant CHF5633 with SP-B and SP-C Analogues on Lung Function and Inflammation in Rabbit Model of Acute Respiratory Distress Syndrome. *Physiol Rep* **2021**, *9* (1), No. e14700.
(63) Echaide, M.; Autilio, C.; Arroyo, R.; Perez-Gil, J. Restoring Pulmonary Surfactant Membranes and Films at the Respiratory Surface. *Biochim Biophys Acta (BBA) - Biomembranes* **2017**, *1859* (9, Part B), 1725−1739.
(64) Zhang, H.; Fan, Q.; Wang, Y. E.; Neal, C. R.; Zuo, Y. Y. Comparative Study of Clinical Pulmonary Surfactants Using Atomic Force Microscopy. *Biochim. Biophys. Acta* **2011**, *1808*, 1832−1842.
(65) Ramanathan, R.; Biniwale, M.; Sekar, K.; Hanna, N.; Golombek, S.; Bhatia, J.; Naylor, M.; Fabbri, L.; Varoli, G.; Santoro, D.; Del Buono, D.; Piccinno, A.; Dammann, C. E. Synthetic Surfactant CHF5633 Compared with Poractant Alfa in the Treatment of Neonatal Respiratory Distress Syndrome: A Multicenter, Double-Blind, Randomized, Controlled Clinical Trial. *J. Pediatr.* **2020**, *225*, 90−96. .
(66) Walther, F. J.; Chan, H.; Smith, J. R.; Tauber, M.; Waring, A. J. Aerosol, Chemical and Physical Properties of Dry Powder Synthetic Lung Surfactant for Noninvasive Treatment of Neonatal Respiratory Distress Syndrome. *Sci. Rep* **2021**, *11* (1), 16439.
(67) Arroyo, R.; Echaide, M.; Wilmanowski, R.; Martín-González, A.; Batllori, E.; Galindo, A.; Rosenbaum, J. S.; Moreno-Herrero, F.; Kingma, P. S.; Pérez-Gil, J. Structure and Activity of Human Surfactant Protein D from Different Natural Sources. *Am. J. Physiol Lung Cell Mol. Physiol* **2020**, *319* (1), L148−L158.
(68) Watson, A.; Sørensen, G. L.; Holmskov, U.; Whitwell, H. J.; Madsen, J.; Clark, H. Generation of Novel Trimeric Fragments of Human SP-A and SP-D after Recombinant Soluble Expression in E. coli. *Immunobiology* **2020**, *225* (4), No. 151953.
(69) Curstedt, T.; Halliday, H. L.; Hallman, M.; Saugstad, O. D.; Speer, C. P. 30 Years of Surfactant Research - from Basic Science to New Clinical Treatments for the Preterm Infant. *Neonatology* **2015**, *107* (4), 314−317.
(70) Halliday, H. L. History of Surfactant from 1980. *Biol. Neonate* **2005**, *87* (4), 317−322.
(71) Gerber, A. N. Glucocorticoids and the Lung. *Glucocorticoid Signaling* **2015**, *872*, 279−298.
(72) Ashbaugh, D. G.; Bigelow, D. B.; Petty, T. L.; Levine, B. E. Acute Respiratory Distress in Adults. *Lancet* **1967**, *290* (7511), 319−323.
(73) Ranieri, V. M.; Rubenfeld, G. D.; Thompson, B. T.; Ferguson, N. D.; Caldwell, E.; Fan, E.; Camporota, L.; Slutsky, A. S. Acute Respiratory Distress Syndrome: The Berlin Definition. *JAMA* **2012**, *307* (23), 2526−2533.
(74) Dushianthan, A.; Goss, V.; Cusack, R.; Grocott, M. P.; Postle, A. D. Altered Molecular Specificity of Surfactant Phosphatidycholine Synthesis in Patients with Acute Respiratory Distress Syndrome. *Respir Res.* **2014**, *15* (1), 128.
(75) Frerking, I.; Gunther, A.; Seeger, W.; Pison, U. Pulmonary Surfactant: Functions, Abnormalities and Therapeutic Options. *Intensive Care Med.* **2001**, *27* (11), 1699−1717.
(76) Gregory, T. J.; Longmore, W. J.; Moxley, M. A.; Whitsett, J. A.; Reed, C. R.; Fowler, A. A., 3rd; Hudson, L. D.; Maunder, R. J.; Crim, C.; Hyers, T. M. Surfactant Chemical Composition and Biophysical Activity in Acute Respiratory Distress Syndrome. *J. Clin Invest* **1991**, *88* (6), 1976−1981.
(77) Markart, P.; Ruppert, C.; Wygrecka, M.; Colaris, T.; Dahal, B.; Walmrath, D.; Harbach, H.; Wilhelm, J.; Seeger, W.; Schmidt, R.; et al. Patients with ARDS Show Improvement but Not Normalisation of Alveolar Surface Activity with Surfactant Treatment: Putative Role of Neutral Lipids. *Thorax* **2007**, *62* (7), 588−594.
(78) Seeds, M. C.; Grier, B. L.; Suckling, B. N.; Safta, A. M.; Long, D. L.; Waite, B. M.; Morris, P. E.; Hite, R. D. Secretory Phospholipase A2-Mediated Depletion of Phosphatidylglycerol in Early Acute Respiratory Distress Syndrome. *Am. J. Med. Sci.* **2012**, *343* (6), 446−451.
(79) Lewis, J. F.; Veldhuizen, R. A. The Future of Surfactant Therapy During ALI/ARDS. *Semin Respir Crit Care Med.* **2006**, *27* (4), 377−388.
(80) Gunther, A.; Ruppert, C.; Schmidt, R.; Markart, P.; Grimminger, F.; Walmrath, D.; Seeger, W. Surfactant Alteration and Replacement in Acute Respiratory Distress Syndrome. *Respir Res.* **2001**, *2* (6), 353−364.

https://doi.org/10.1021/acs.chemrev.3c00146
Chem. Rev. 2023, 123, 13209−13290

(81) Whitsett, J. A.; Kalin, T. V.; Xu, Y.; Kalinichenko, V. V. Building and Regenerating the Lung Cell by Cell. *Physiol. Rev.* **2019**, *99* (1), 513−554.
(82) Rubenfeld, G. D.; Caldwell, E.; Peabody, E.; Weaver, J.; Martin, D. P.; Neff, M.; Stern, E. J.; Hudson, L. D. Incidence and Outcomes of Acute Lung Injury. *New England Journal of Medicine* **2005**, *353* (16), 1685−1693.
(83) Bellani, G.; Laffey, J. G.; Pham, T.; Fan, E.; Brochard, L.; Esteban, A.; Gattinoni, L.; van Haren, F.; Larsson, A.; McAuley, D. F.; et al. Epidemiology, Patterns of Care, and Mortality for Patients with Acute Respiratory Distress Syndrome in Intensive Care Units in 50 Countries. *JAMA* **2016**, *315* (8), 788−800.
(84) Veldhuizen, R. A.; McCaig, L. A.; Akino, T.; Lewis, J. F. Pulmonary Surfactant Subfractions in Patients with the Acute Respiratory Distress Syndrome. *Am. J. Respir Crit Care Med.* **1995**, *152* (6 Pt 1), 1867−1871.
(85) Lewis, J. F.; Veldhuizen, R. The Role of Exogenous Surfactant in the Treatment of Acute Lung Injury. *Annu. Rev. Physiol.* **2003**, *65*, 613−642.
(86) Brower, R. G.; Fessler, H. E. Another "Negative" Trial of Surfactant. Time to Bury This Idea? *Am. J. Respir Crit Care Med.* **2011**, *183* (8), 966−968.
(87) Spragg, R. G.; Taut, F. J.; Lewis, J. F.; Schenk, P.; Ruppert, C.; Dean, N.; Krell, K.; Karabinis, A.; Günther, A. Recombinant Surfactant Protein C-Based Surfactant for Patients with Severe Direct Lung Injury. *Am. J. Respir Crit Care Med.* **2011**, *183* (8), 1055−1061.
(88) Taut, F. J.; Rippin, G.; Schenk, P.; Findlay, G.; Wurst, W.; Häfner, D.; Lewis, J. F.; Seeger, W.; Günther, A.; Spragg, R. G. A Search for Subgroups of Patients with ARDS Who May Benefit from Surfactant Replacement Therapy: A Pooled Analysis of Five Studies with Recombinant Surfactant Protein-C Surfactant (Venticute). *Chest* **2008**, *134* (4), 724−732.
(89) Grotberg, J. B.; Filoche, M.; Willson, D. F.; Raghavendran, K.; Notter, R. H. Did Reduced Alveolar Delivery of Surfactant Contribute to Negative Results in Adults with Acute Respiratory Distress Syndrome? *Am. J. Respir Crit Care Med.* **2017**, *195* (4), 538−540.
(90) Goligher, E. C.; Ranieri, V. M.; Slutsky, A. S. *Is Severe COVID-19 Pneumonia a Typical or Atypical Form of ARDS? And Does It Matter?*; Springer: 2021; Vol. *47*, pp 83−85.
(91) Matthay, M. A.; Leligdowicz, A.; Liu, K. D. Biological Mechanisms of COVID-19 Acute Respiratory Distress Syndrome. *Am. J. Respir Crit Care Med.* **2020**, *202* (11), 1489−1491.
(92) Veldhuizen, R. A. W.; Zuo, Y. Y.; Petersen, N. O.; Lewis, J. F.; Possmayer, F. The COVID-19 Pandemic: A Target for Surfactant Therapy? *Expert Rev. Respir Med.* **2021**, *15*, 597−608.
(93) Piva, S.; DiBlasi, R. M.; Slee, A. E.; Jobe, A. H.; Roccaro, A. M.; Filippini, M.; Latronico, N.; Bertoni, M.; Marshall, J. C.; Portman, M. A. Surfactant Therapy for COVID-19 Related ARDS: A Retrospective Case-Control Pilot Study. *Respir Res.* **2021**, *22* (1), 20.
(94) Ruaro, B.; Confalonieri, P.; Pozzan, R.; Tavano, S.; Mondini, L.; Baratella, E.; Pagnin, A.; Lerda, S.; Geri, P.; Biolo, M.; et al. Severe COVID-19 ARDS Treated by Bronchoalveolar Lavage with Diluted Exogenous Pulmonary Surfactant as Salvage Therapy: In Pursuit of the Holy Grail? *J. Clin Med.* **2022**, *11* (13), 3577.
(95) Bates, S. P63 (CKAP4) as an SP-A Receptor: Implications for Surfactant Turnover. *Cellular Physiology and Biochemistry* **2010**, *25* (1), 41−54.
(96) Hallman, M. The Surfactant System Protects Both Fetus and Newborn. *Neonatology* **2013**, *103* (4), 320−326.
(97) Seaton, B. A.; Crouch, E. C.; McCormack, F. X.; Head, J. F.; Hartshorn, K. L.; Mendelsohn, R. Review: Structural Determinants of Pattern Recognition by Lung Collectins. *Innate Immun* **2010**, *16* (3), 143−150.
(98) Watson, A.; Madsen, J.; Clark, H. W. SP-A and SP-D: Dual Functioning Immune Molecules with Antiviral and Immunomodulatory Properties. *Front Immun* **2021**, *11*, No. 622598.
(99) Ataya, A.; Knight, V.; Carey, B. C.; Lee, E.; Tarling, E. J.; Wang, T. The Role of GM-CSF Autoantibodies in Infection and Autoimmune Pulmonary Alveolar Proteinosis: A Concise Review. *Front Immun* **2021**, *12*, No. 752856.
(100) Lenz, D.; Stahl, M.; Seidl, E.; Schöndorf, D.; Brennenstuhl, H.; Gesenhues, F.; Heinzmann, T.; Longerich, T.; Mendes, M. I.; Prokisch, H. Rescue of Respiratory Failure in Pulmonary Alveolar Proteinosis Due to Pathogenic MARS1 Variants. *Pediatric Pulmonology* **2020**, *55* (11), 3057−3066.
(101) Trapnell, B. C.; Nakata, K.; Bonella, F.; Campo, I.; Griese, M.; Hamilton, J.; Wang, T.; Morgan, C.; Cottin, V.; McCarthy, C. Pulmonary Alveolar Proteinosis. *Nature Reviews Disease Primers* **2019**, *5* (1), 16.
(102) Huang, X.; Cao, M.; Xiao, Y. Alveolar Macrophages in Pulmonary Alveolar Proteinosis: Origin, Function, and Therapeutic Strategies. *Front Immun* **2023**, *14*, No. 1195988.
(103) Hristova, V. A.; Watson, A.; Chaerkady, R.; Glover, M. S.; Ackland, J.; Angerman, B.; Belfield, G.; Belvisi, M. G.; Burke, H.; Cellura, D.; Clark, H. W.; Etal, D.; Freeman, A.; Heinson, A. I.; Hess, S.; Hühn, M.; Hall, E.; Mackay, A.; Madsen, J.; McCrae, C.; Muthas, D.; Novick, S.; Ostridge, K.; Öberg, L.; Platt, A.; Postle, A. D.; Spalluto, C. M.; Vaarala, O.; Wang, J.; Staples, K. J.; Wilkinson, T. M. A. MICA II Study group. Multiomics Links Global Surfactant Dysregulation with Airflow Obstruction and Emphysema in COPD. *ERJ. Open Res.* **2023**, *9* (3), 00378-02022.
(104) Choi, Y.; Jang, J.; Park, H.-S. Pulmonary Surfactants: A New Therapeutic Target in Asthma. *Curr. Allergy Asthma Rep* **2020**, *20* (11), 70.
(105) Noutsios, G. T.; Floros, J. Childhood Asthma: Causes, Risks, and Protective Factors; a Role of Innate Immunity. *Swiss Med. Wkly* **2014**, *144*, w14036.
(106) Winkler, C.; Hohlfeld, J. M. Surfactant and Allergic Airway Inflammation. *Swiss Med. Wkly* **2013**, *143*, w13818.
(107) Fessler, M. B. The Intracellular Cholesterol Landscape: Dynamic Integrator of the Immune Response. *Trends Immunol* **2016**, *37* (12), 819−830.
(108) Orgeig, S.; Morrison, J. L.; Daniels, C. B. Evolution, Development, and Function of the Pulmonary Surfactant System in Normal and Perturbed Environments. *Compr Physiol* **2015**, *6* (1), 363−422.
(109) Osorio, F.; Lambrecht, B.; Janssens, S. The UPR and Lung Disease. *Semin Immunopathol* **2013**, *35* (3), 293−306.
(110) Wert, S. E.; Whitsett, J. A.; Nogee, L. M. Genetic Disorders of Surfactant Dysfunction. *Pediatr Dev Pathol* **2009**, *12* (4), 253−274.
(111) Nogee, L. M. Genetic Causes of Surfactant Protein Abnormalities. *Curr. Opin Pediatr* **2019**, *31* (3), 330−339.
(112) Hamvas, A.; Cole, F. S.; Nogee, L. M. Genetic Disorders of Surfactant Proteins. *Neonatology* **2007**, *91* (4), 311−317.
(113) Gower, W. A.; Nogee, L. M. Surfactant Dysfunction. *Paediatr Respir Rev.* **2011**, *12* (4), 223−229.
(114) Katzen, J.; Beers, M. F. Contributions of Alveolar Epithelial Cell Quality Control to Pulmonary Fibrosis. *J. Clin Invest* **2020**, *130* (10), 5088−5099.
(115) Dietl, P.; Haller, T. Exocytosis of Lung Surfactant: From the Secretory Vesicle to the Air-Liquid Interface. *Annu. Rev. Physiol Review of Physiology* **2005**, *67*, 595−621.
(116) Dietl, P.; Haller, T. Exocytosis of Lung Surfactant: From the Secretory Vesicle to the Air-Liquid Interface. *Annu. Rev. Physiol.* **2005**, *67*, 595−621.
(117) Guttentag, S. H.; Akhtar, A.; Tao, J.-Q.; Atochina, E.; Rusiniak, M. E.; Swank, R. T.; Bates, S. R. Defective Surfactant Secretion in a Mouse Model of Hermansky-Pudlak Syndrome. *Am. J. Respir. Cell Mol. Biol.* **2005**, *33* (1), 14−21.
(118) Osanai, K. Rab38 Mutation and the Lung Phenotype. *Int. J. Mol. Sci.* **2018**, *19* (8), 2203.
(119) Buccoliero, R.; Ginzburg, L.; Futerman, A. H. Elevation of Lung Surfactant Phosphatidylcholine in Mouse Models of Sandhoff and of Niemann-Pick A Disease. *J. Inherit Metab Dis* **2004**, *27* (5), 641−648.
(120) Griese, M.; Brasch, F.; Aldana, V. R.; Cabrera, M. M.; Goelnitz, U.; Ikonen, E.; Karam, B. J.; Liebisch, G.; Linder, M. D.;

Lohse, P.; Meyer, W.; Schmitz, G.; Pamir, A.; Ripper, J.; Rolfs, A.; Schams, A.; Lezana, F. J. Respiratory Disease in Niemann-Pick Type C2 Is Caused by Pulmonary Alveolar Proteinosis. *Clin Genetics* **2010**, *77* (2), 119−130.
(121) Pfrieger, F. W. The Niemann-Pick Type Diseases - A Synopsis of Inborn Errors in Sphingolipid and Cholesterol Metabolism. *Prog. Lipid Res.* **2023**, *90*, No. 101225.
(122) Li, W.; Hao, C.-J.; Hao, Z.-H.; Ma, J.; Wang, Q.-C.; Yuan, Y.-F.; Gong, J.-J.; Chen, Y.-Y.; Yu, J.-Y.; Wei, A.-H. New Insights into the Pathogenesis of Hermansky-Pudlak Syndrome. *Pigment Cell Melanoma Res.* **2022**, *35* (3), 290−302.
(123) Petersen, N. O. *Foundations for Nanoscience and Nanotechnology*; CRC Press, 2017.
(124) Prange, H. D. Laplace's Law and the Alveolus: A Misconception of Anatomy and a Misapplication of Physics. *Adv. Physiol Educ* **2003**, *27* (1−4), 34−40.
(125) Bachofen, H.; Schürch, S. Alveolar Surface Forces and Lung Architecture. *Comp Biochem Physiol A Mol. Integr Physiol* **2001**, *129* (1), 183−193.
(126) Clements, J. A. Surface Phenomena in Relation to Pulmonary Function. *Physiologist* **1962**, *5* (1), 11−28.
(127) Morgan, T. E. Pulmonary Surfactant. *N Engl J. Med.* **1971**, *284* (21), 1185−1193.
(128) Mead, J.; Whittenberger, J. L.; Radford, E. P. Surface Tension as a Factor in Pulmonary Volume-Pressure Hysteresis. *J. Appl. Physiol.* **1957**, *10* (2), 191−196.
(129) Marchand, A.; Weijs, J. H.; Snoeijer, J. H.; Andreotti, B. Why Is Surface Tension a Force Parallel to the Interface? *Am. J. Physics* **2011**, *79* (10), 999−1008.
(130) Smith, G. S.; Sirota, E. B.; Safinya, C. R.; Clark, N. A. Structure of the L Beta Phases in a Hydrated Phosphatidylcholine Multimembrane. *Phys. Rev. Lett.* **1988**, *60* (9), 813−816.
(131) Tristram-Nagle, S.; Zhang, R.; Suter, R. M.; Worthington, C. R.; Sun, W. J.; Nagle, J. F. Measurement of Chain Tilt Angle in Fully Hydrated Bilayers of Gel Phase Lecithins. *Biophys. J.* **1993**, *64* (4), 1097−1109.
(132) Katsaras, J. X-Ray Diffraction Studies of Oriented Lipid Bilayers. *Biochemistry and Cell Biology* **1995**, *73* (5−6), 209−218.
(133) Davis, J. H.; Clair, J. J.; Juhasz, J. Phase Equilibria in DOPC/DPPC-D62/Cholesterol Mixtures. *Biophys. J.* **2009**, *96* (2), 521−539.
(134) McConnell, H. M.; Moy, V. T. Shapes of Finite Two-Dimensional Lipid Domains. *J. Phys. Chem.* **1988**, *92* (15), 4520−4525.
(135) Keller, S. L.; McConnell, H. M. Stripe Phases in Lipid Monolayers near a Miscibility Critical Point. *Phys. Rev. Lett.* **1999**, *82* (7), 1602−1605.
(136) Honerkamp-Smith, A. R.; Cicuta, P.; Collins, M. D.; Veatch, S. L.; den Nijs, M.; Schick, M.; Keller, S. L. Line Tensions, Correlation Lengths, and Critical Exponents in Lipid Membranes near Critical Points. *Biophys. J.* **2008**, *95* (1), 236−246.
(137) Honerkamp-Smith, A. R.; Veatch, S. L.; Keller, S. L. An Introduction to Critical Points for Biophysicists; Observations of Compositional Heterogeneity in Lipid Membranes. *Biochim. Biophys. Acta* **2009**, *1788* (1), 53−63.
(138) Marsh, D. Lateral Pressure in Membranes. *Biochim. Biophys. Acta* **1996**, *1286* (3), 183−223.
(139) Demel, R. A.; Geurts van Kessel, W. S.; Zwaal, R. F.; Roelofsen, B.; van Deenen, L. L. Relation between Various Phospholipase Actions on Human Red Cell Membranes and the Interfacial Phospholipid Pressure in Monolayers. *Biochim. Biophys. Acta* **1975**, *406* (1), 97−107.
(140) Seelig, A. Local Anesthetics and Pressure: A Comparison of Dibucaine Binding to Lipid Monolayers and Bilayers. *Biochim. Biophys. Acta* **1987**, *899* (2), 196−204.
(141) Kaganer, V. M.; Mohwald, H.; Dutta, P. Structure and phase transitions in Langmuir monolayers. *Rev Mod Phys* **1999**, *71*, 779−819.
(142) Miyoshi, T.; Kato, S. Detailed Analysis of the Surface Area and Elasticity in the Saturated 1,2-Diacylphosphatidylcholine/Cholesterol Binary Monolayer System. *Langmuir* **2015**, *31* (33), 9086−9096.
(143) McConnell, H. Complexes in Ternary Cholesterol-Phospholipid Mixtures. *Biophys. J.* **2005**, *88* (4), L23−25.
(144) Ipsen, J. H.; Karlstrom, G.; Mourtisen, O. G.; Wennerstrom, H.; Zuckermann, M. J. Phase Equilibria in the Phosphatidylcholine-Cholesterol System. *Biochim. Biophys. Acta* **1987**, *905* (1), 162−172.
(145) Possmayer, F.; Hall, S. B.; Haller, T.; Petersen, N. O.; Zuo, Y. Y.; Bernardino de la Serna, J.; Postle, A. D.; Veldhuizen, R. A. W.; Orgeig, S. Recent Advances in Alveolar Biology: Some New Looks at the Alveolar Interface. *Respir. Physiol. Neurobiol.* **2010**, *173*, S55−64.
(146) Veatch, S. L.; Keller, S. L. Seeing Spots: Complex Phase Behavior in Simple Membranes. *Biochim. Biophys. Acta* **2005**, *1746* (3), 172−185.
(147) Silvius, J. R. Role of Cholesterol in Lipid Raft Formation: Lessons from Lipid Model Systems. *Biochim. Biophys. Acta* **2003**, *1610* (2), 174−183.
(148) Stottrup, B. L.; Stevens, D. S.; Keller, S. L. Miscibility of Ternary Mixtures of Phospholipids and Cholesterol in Monolayers, and Application to Bilayer Systems. *Biophys. J.* **2005**, *88* (1), 269−276.
(149) Perez-Gil, J. Structure of Pulmonary Surfactant Membranes and Films: The Role of Proteins and Lipid-Protein Interactions. *Biochim. Biophys. Acta* **2008**, *1778* (7−8), 1676−1695.
(150) Miyoshi, T.; Lönnfors, M.; Peter Slotte, J.; Kato, S. A Detailed Analysis of Partial Molecular Volumes in DPPC/Cholesterol Binary Bilayers. *Biochim. Biophys. Acta* **2014**, *1838* (12), 3069−3077.
(151) Abdelsalam, M.; Cheifetz, I. M. Goal-Directed Therapy for Severely Hypoxic Patients with Acute Respiratory Distress Syndrome: Permissive Hypoxemia. *Respir Care* **2010**, *55* (11), 1483−1490.
(152) Adachi, H.; Hayashi, H.; Sato, H.; Dempo, K.; Akino, T. Characterization of Phospholipids Accumulated in Pulmonary-Surfactant Compartments of Rats Intratracheally Exposed to Silica. *Biochem. J.* **1989**, *262* (3), 781−786.
(153) Bachofen, H.; Schürch, S.; Urbinelli, M.; Weibel, E. R. Relations among Alveolar Surface Tension, Surface Area, Volume, and Recoil Pressure. *J. Appl. Physiol (1985)* **1987**, *62* (5), 1878−1887.
(154) Agudelo, C. W.; Samaha, G.; Garcia-Arcos, I. Alveolar Lipids in Pulmonary Disease. A Review. *Lipids in Health and Disease* **2020**, *19*, DOI: 10.1186/s12944-020-01278-8.
(155) Clements, J. Surface Tension of Lung Extracts. *Proc. Soc. Exp Biol. Med.* **1957**, *95*, 170−172.
(156) Brown, E. S.; Johnson, R. P.; Clements, J. A. Pulmonary Surface Tension. *J. Appl. Physiol.* **1959**, *14*, 717−720.
(157) Clements, J. A.; Hustead, R. F.; Johnson, R. P.; Gribetz, I. Pulmonary Surface Tension and Alveolar Stability. *J. Appl. Physiol.* **1961**, *16* (3), 444−450.
(158) Oliveira, O. N.; Caseli, L.; Ariga, K. The Past and the Future of Langmuir and Langmuir−Blodgett Films. *Chem. Rev.* **2022**, *122* (6), 6459−6513.
(159) Autilio, C.; Echaide, M.; Cruz, A.; Garcia-Mouton, C.; Hidalgo, A.; Da Silva, E.; De Luca, D.; Sørli, J. B.; Perez-Gil, J. Molecular and Biophysical Mechanisms behind the Enhancement of Lung Surfactant Function during Controlled Therapeutic Hypothermia. *Sci. Rep.* **2021**, *11* (1), 728.
(160) Parra, E.; Pérez-Gil, J. Composition, Structure and Mechanical Properties Define Performance of Pulmonary Surfactant Membranes and Films. *Chem. Phys. Lipids* **2015**, *185*, 153−175.
(161) Adams, F. H.; Enhörning, G. Surface Properties of Lung Extracts. *Acta Physiologica Scandanavia* **1966**, *68* (1), 23−27.
(162) Robertson, B.; Enhörning, G.; Malmquist, E. Quantitative Determination of Pulmonary Surfactant with Pulsating Bubble. *Scandanavia J. Clin Lab Invest* **1972**, *29* (1), 45−49.
(163) Enhorning, G. Pulsating Bubble Technique for Evaluating Pulmonary Surfactant. *J. Appl. Physiol.* **1977**, *43* (2), 198−203.
(164) Enhorning, G. The Surface Tension OF Amniotic Fluid. *Am. J. Obstet Gynecol* **1964**, *88*, 519−523.

(165) Enhorning, G. Pulmonary Surfactant Function Studied with the Pulsating Bubble Surfactometer (PBS) and the Capillary Surfactometer (CS). *Comp Biochem Physiol A Mol. Integr Physiol* **2001**, *129* (1), 221−226.
(166) Schürch, S.; Bachofen, H.; Goerke, J.; Possmayer, F. A Captive Bubble Method Reproduces the in Situ Behavior of Lung Surfactant Monolayers. *J. Appl. Physiol.* **1989**, *67* (6), 2389−2396.
(167) Schoel, W. M.; Schürch, S.; Goerke, J. The Captive Bubble Method for the Evaluation of Pulmonary Surfactant: Surface Tension, Area, and Volume Calculations. *Biochim. Biophys. Acta* **1994**, *1200* (3), 281−290.
(168) Zuo, Y. Y.; Ding, M.; Bateni, A.; Hoorfar, M.; Neumann, A. W. Improvement of Interfacial Tension Measurement Using a Captive Bubble in Conjunction with Axisymmetric Drop Shape Analysis (ADSA). *Colloids and Surfaces a-Physicochemical and Engineering Aspects* **2004**, *250* (1−3), 233−246.
(169) Zuo, Y. Y.; Ding, M.; Li, D.; Neumann, A. W. Further Development of Axisymmetric Drop Shape Analysis-Captive Bubble for Pulmonary Surfactant Related Studies. *Biochim. Biophys. Acta* **2004**, *1675* (1−3), 12−20.
(170) Yang, J.; Yu, K.; Zuo, Y. Y. Accuracy of Axisymmetric Drop Shape Analysis in Determining Surface and Interfacial Tensions. *Langmuir* **2017**, *33* (36), 8914−8923.
(171) Schürch, S.; Bachofen, H.; Goerke, J.; Green, F. Surface Properties of Rat Pulmonary Surfactant Studied with the Captive Bubble Method: Adsorption, Hysteresis. *Stability. Biochim Biophys Acta* **1992**, *1103* (1), 127−136.
(172) Schürch, S.; Qanbar, R.; Bachofen, H.; Possmayer, F. The Surface -Associated Surfactant Reservoir in the Alveolar Lining. *Biol. Neonate* **2004**, *67*, 61−76.
(173) Putz, G.; Walch, M.; Van Eijk, M.; Haagsman, H. P. A Spreading Technique for Forming Film in a Captive Bubble. *Biophys. J.* **1998**, *75* (5), 2229−2239.
(174) Codd, J. R.; Schürch, S.; Daniels, C. B.; Orgeig, S. Torpor-Associated Fluctuations in Surfactant Activity in Gould's Wattled Bat. *Biochim. Biophys. Acta* **2002**, *1580* (1), 57−66.
(175) Zuo, Y. Y.; Gitiafroz, R.; Acosta, E.; Policova, Z.; Cox, P. N.; Hair, M. L.; Neumann, A. W. Effect of Humidity on the Adsorption Kinetics of Lung Surfactant at Air-Water Interfaces. *Langmuir* **2005**, *21* (23), 10593−10601.
(176) Zuo, Y. Y.; Alolabi, H.; Shafiei, A.; Kang, N.; Policova, Z.; Cox, P. N.; Acosta, E.; Hair, M. L.; Neumann, A. W. Chitosan Enhances the in Vitro Surface Activity of Dilute Lung Surfactant Preparations and Resists Albumin-Induced Inactivation. *Pediatr. Res.* **2006**, *60* (2), 125−130.
(177) Autilio, C.; Echaide, M.; De Luca, D.; Pérez-Gil, J. Controlled Hypothermia May Improve Surfactant Function in Asphyxiated Neonates with or without Meconium Aspiration Syndrome. *PLoS One* **2018**, *13* (2), No. e0192295.
(178) Yu, L. M. Y.; Lu, J. J.; Chan, Y. W.; Ng, A.; Zhang, L.; Hoorfar, M.; Policova, Z.; Grundke, K.; Neumann, A. W. Constrained Sessile Drop as a New Configuration to Measure Low Surface Tension in Lung Surfactant Systems. *J. Appl. Physiol (1985)* **2004**, *97* (2), 704−715.
(179) Li, G.; Xu, X.; Zuo, Y. Y. Langmuir-Blodgett Transfer from the Oil-Water Interface. *J. Colloid Interface Sci.* **2023**, *630* (Pt B), 21−27.
(180) Li, G.; Xu, X.; Zuo, Y. Y. Phase Transitions of the Pulmonary Surfactant Film at the Perfluorocarbon-Water Interface. *Biophys. J.* **2023**, *122*, 1772−1780.
(181) Li, G.; Xu, X.; Zuo, Y. Y. Biophysical Function of Pulmonary Surfactant in Liquid Ventilation. *Biophys. J.* **2023**, *122*, 3099−3107.
(182) Yu, K.; Yang, J.; Zuo, Y. Y. Automated Droplet Manipulation Using Closed-Loop Axisymmetric Drop Shape Analysis. *Langmuir* **2016**, *32* (19), 4820−4826.
(183) Yu, K.; Yang, J.; Zuo, Y. Y. Droplet Oscillation as an Arbitrary Waveform Generator. *Langmuir* **2018**, *34* (24), 7042−7047.
(184) Yang, J.; Yu, K.; Tsuji, T.; Jha, R.; Zuo, Y. Y. Determining the Surface Dilational Rheology of Surfactant and Protein Films with a Droplet Waveform Generator. *J. Colloid Interface Sci.* **2019**, *537*, 547−553.
(185) Xu, L.; Bosiljevac, G.; Yu, K.; Zuo, Y. Y. Melting of the Dipalmitoylphosphatidylcholine Monolayer. *Langmuir* **2018**, *34* (15), 4688−4694.
(186) Xu, L.; Zuo, Y. Y. Reversible Phase Transitions in the Phospholipid Monolayer. *Langmuir* **2018**, *34* (29), 8694−8700.
(187) Banaschewski, B. J. H.; Veldhuizen, E. J. A.; Keating, E.; Haagsman, H. P.; Zuo, Y. Y.; Yamashita, C. M.; Veldhuizen, R. A. W. Antimicrobial and Biophysical Properties of Surfactant Supplemented with an Antimicrobial Peptide for Treatment of Bacterial Pneumonia. *Antimicrob. Agents Chemother.* **2015**, *59* (6), 3075−3083.
(188) Xu, X.; Li, G.; Sun, B.; Zuo, Y. Y. S2 Subunit of SARS-CoV-2 Spike Protein Induces Domain Fusion in Natural Pulmonary Surfactant Monolayers. *J. Phys. Chem. Lett.* **2022**, *13* (35), 8359−8364.
(189) Valle, R. P.; Huang, C. L.; Loo, J. S. C.; Zuo, Y. Y. Increasing Hydrophobicity of Nanoparticles Intensifies Lung Surfactant Film Inhibition and Particle Retention. *ACS Sustainable Chem. Eng.* **2014**, *2* (7), 1574−1580.
(190) Chen, Y.; Yang, Y.; Xu, B.; Wang, S.; Li, B.; Ma, J.; Gao, J.; Zuo, Y. Y.; Liu, S. Mesoporous Carbon Nanomaterials Induced Pulmonary Surfactant Inhibition, Cytotoxicity, Inflammation and Lung Fibrosis. *J. Environ. Sci. (China)* **2017**, *62*, 100−114.
(191) Yang, Y.; Wu, Y.; Ren, Q.; Zhang, L. G.; Liu, S.; Zuo, Y. Y. Biophysical Assessment of Pulmonary Surfactant Predicts the Lung Toxicity of Nanomaterials. *Small Methods* **2018**, *2* (4), No. 1700367.
(192) Yang, Y.; Xu, L.; Dekkers, S.; Zhang, L. G.; Cassee, F. R.; Zuo, Y. Y. Aggregation State of Metal-Based Nanomaterials at the Pulmonary Surfactant Film Determines Biophysical Inhibition. *Environ. Sci. Technol.* **2018**, *52* (15), 8920−8929.
(193) Wu, Y.; Guo, Y.; Song, H.; Liu, W.; Yang, Y.; Liu, Y.; Sang, N.; Zuo, Y. Y.; Liu, S. Oxygen Content Determines the Bio-Reactivity and Toxicity Profiles of Carbon Black Particles. *Ecotoxicol Environ. Saf* **2018**, *150*, 207−214.
(194) Sorli, J. B.; Huang, Y.; Da Silva, E.; Hansen, J. S.; Zuo, Y. Y.; Frederiksen, M.; Norgaard, A. W.; Ebbehoj, N. E.; Larsen, S. T.; Hougaard, K. S. Prediction of Acute Inhalation Toxicity Using in Vitro Lung Surfactant Inhibition. *ALTEX* **2018**, *35* (1), 26−36.
(195) Da Silva, E.; Vogel, U.; Hougaard, K. S.; Pérez-Gil, J.; Zuo, Y. Y.; Sørli, J. B. An Adverse Outcome Pathway for Lung Surfactant Function Inhibition Leading to Decreased Lung Function. *Curr. Res. Toxicol* **2021**, *2*, 225−236.
(196) Xu, L.; Yang, Y.; Simien, J. M.; Kang, C.; Li, G.; Xu, X.; Haglund, E.; Sun, R.; Zuo, Y. Y. Menthol in Electronic Cigarettes Causes Biophysical Inhibition of Pulmonary Surfactant. *Am. J. Physiol Lung Cell Mol. Physiol* **2022**, *323* (2), L165−L177.
(197) Graham, E.; McCaig, L.; Shui-Kei Lau, G.; Tejura, A.; Cao, A.; Zuo, Y. Y.; Veldhuizen, R. E-Cigarette Aerosol Exposure of Pulmonary Surfactant Impairs Its Surface Tension Reducing Function. *PLoS One* **2022**, *17* (11), No. e0272475.
(198) Li, C.; Xu, L.; Zuo, Y. Y.; Yang, P. Tuning Protein Assembly Pathways through Superfast Amyloid-Like Aggregation. *Biomater Sci.* **2018**, *6* (4), 836−841.
(199) Xu, X.; Li, G.; Zuo, Y. Y. Biophysical Properties of Tear Film Lipid Layer I. Surface Tension and Surface Rheology. *Biophys. J.* **2022**, *121* (3), 439−450.
(200) Xu, X.; Kang, C.; Sun, R.; Zuo, Y. Y. Biophysical Properties of Tear Film Lipid Layer II. Polymorphism of FAHFA. *Biophys. J.* **2022**, *121* (3), 451−458.
(201) Xu, X.; Li, G.; Zuo, Y. Y. Effect of Model Tear Film Lipid Layer on Water Evaporation. *Invest Ophthalmol Vis Sci.* **2023**, *64* (1), 13.
(202) Schenk, H. J.; Espino, S.; Romo, D. M.; Nima, N.; Do, A. Y.; Michaud, J. M.; Papahadjopoulos-Sternberg, B.; Yang, J.; Zuo, Y. Y.; Steppe, K.; et al. Xylem Surfactants Introduce a New Element to the Cohesion-Tension Theory. *Plant Physiol* **2017**, *173* (2), 1177−1196.

https://doi.org/10.1021/acs.chemrev.3c00146
Chem. Rev. 2023, 123, 13209−13290

(203) Yang, J.; Michaud, J. M.; Jansen, S.; Schenk, H. J.; Zuo, Y. Y. Dynamic Surface Tension of Xylem Sap Lipids. *Tree Physiol* **2020**, *40* (4), 433−444.
(204) Nag, K.; Rich, N. H.; Boland, C.; Keough, K. M. W. Design and Construction of an Epifluorescence Microscopic Surface Balance for the Study of Lipid Monolayer Phase Transitions. *Rev. Sci. Instrum.* **1990**, *61*, 3425−3430.
(205) Discher, B. M.; Maloney, K. M.; Schief, W. R., Jr.; Grainger, D. W.; Vogel, V.; Hall, S. B. Lateral Phase Separation in Interfacial Films of Pulmonary Surfactant. *Biophys. J.* **1996**, *71* (5), 2583−2590.
(206) Nag, K.; Perez-Gil, J.; Ruano, M. L.; Worthman, L. A.; Stewart, J.; Casals, C.; Keough, K. M. Phase Transitions in Films of Lung Surfactant at the Air-Water Interface. *Biophys. J.* **1998**, *74* (6), 2983−2995.
(207) Cruz, A.; Vazquez, L.; Velez, M.; Perez-Gil, J. Effect of Pulmonary Surfactant Protein SP-B on the Micro- and Nanostructure of Phospholipid Films. *Biophys. J.* **2004**, *86* (1 Pt 1), 308−320.
(208) Cruz, A.; Vazquez, L.; Velez, M.; Perez-Gil, J. Influence of a Fluorescent Probe on the Nanostructure of Phospholipid Membranes: Dipalmitoylphosphatidylcholine Interfacial Monolayers. *Langmuir* **2005**, *21* (12), 5349−5355.
(209) Zhang, H.; Wang, Y. E.; Fan, Q.; Zuo, Y. Y. On the Low Surface Tension of Lung Surfactant. *Langmuir* **2011**, *27* (13), 8351−8358.
(210) Zuo, Y. Y.; Keating, E.; Zhao, L.; Tadayyon, S. M.; Veldhuizen, R. A.; Petersen, N. O.; Possmayer, F. Atomic Force Microscopy Studies of Functional and Dysfunctional Pulmonary Surfactant Films. I. Micro- and Nanostructures of Functional Pulmonary Surfactant Films and the Effect of SP-A. *Biophys. J.* **2008**, *94* (9), 3549−3564.
(211) Zuo, Y. Y.; Tadayyon, S. M.; Keating, E.; Zhao, L.; Veldhuizen, R. A.; Petersen, N. O.; Amrein, M. W.; Possmayer, F. Atomic Force Microscopy Studies of Functional and Dysfunctional Pulmonary Surfactant Films, II: Albumin-Inhibited Pulmonary Surfactant Films and the Effect of SP-A. *Biophys. J.* **2008**, *95* (6), 2779−2791.
(212) Amrein, M.; von Nahmen, A.; Sieber, M. A Scanning Force- and Fluorescence Light Microscopy Study of the Structure and Function of a Model Pulmonary Surfactant. *European Biophys Journal* **1997**, *26* (5), 349−357.
(213) von Nahmen, A.; Schenk, M.; Sieber, M.; Amrein, M. The Structure of a Model Pulmonary Surfactant as Revealed by Scanning Force Microscopy. *Biophys. J.* **1997**, *72*, 463−469.
(214) Zasadzinski, J. A.; Viswanathan, R.; Madsen, L.; Garnaes, J.; Schwartz, D. K. Langmuir-Blodgett Films. *Science* **1994**, *263* (5154), 1726−1733.
(215) Benninghoven, A. Chemical Analysis of Inorganic and Organic Surfaces and Thin Films by Static Time-of-Flight Secondary Ion Mass Spectrometry (Tof-SIMS). *Angewandte Chemie International Edition in English* **1994**, *33* (10), 1023−1043.
(216) Bourdos, N.; Kollmer, F.; Benninghoven, A.; Ross, M.; Sieber, M.; Galla, H. J. Analysis of Lung Surfactant Model Systems with Time-of-Flight Secondary Ion Mass Spectrometry. *Biophys. J.* **2000**, *79* (1), 357−369.
(217) Harbottle, R. R.; Nag, K.; McIntyre, N. S.; Possmayer, F.; Petersen, N. O. Molecular Organization Revealed by Time-of-Flight Secondary Ion Mass Spectrometry of a Clinically Used Extracted Pulmonary Surfactant. *Langmuir* **2003**, *19*, 3698−3704.
(218) Keating, E.; Rahman, L.; Francis, J.; Petersen, A.; Possmayer, F.; Veldhuizen, R.; Petersen, N. O. Effect of Cholesterol on the Biophysical and Physiological Properties of a Clinical Pulmonary Surfactant. *Biophys. J.* **2007**, *93* (4), 1391−1401.
(219) Keating, E.; Waring, A. J.; Walther, F. J.; Possmayer, F.; Veldhuizen, R. A.; Petersen, N. O. A Tof-SIMS Study of the Lateral Organization of Lipids and Proteins in Pulmonary Surfactant Systems. *Biochim. Biophys. Acta* **2011**, *1808* (3), 614−621.
(220) Keating, E.; Zuo, Y. Y.; Tadayyon, S. M.; Petersen, N. O.; Possmayer, F.; Veldhuizen, R. A. A Modified Squeeze-out Mechanism for Generating High Surface Pressures with Pulmonary Surfactant. *Biochim. Biophys. Acta* **2012**, *1818* (5), 1225−1234.
(221) Katsaras, J.; Yang, D. S.; Epand, R. M. Fatty-Acid Chain Tilt Angles and Directions in Dipalmitoyl Phosphatidylcholine Bilayers. *Biophys. J.* **1992**, *63* (4), 1170−1175.
(222) You, S. S.; Heffern, C. T. R.; Dai, Y.; Meron, M.; Henderson, J. M.; Bu, W.; Xie, W.; Lee, K. Y. C.; Lin, B. Liquid Surface X-Ray Studies of Gold Nanoparticle−Phospholipid Films at the Air/Water Interface. *J. Physical Chem. B* **2016**, *120* (34), 9132−9141.
(223) Kiselev, M. A.; Lombardo, D. Structural Characterization in Mixed Lipid Membrane Systems by Neutron and X-Ray Scattering. *Biochim. Biophys. Acta (BBA) - General Subjects* **2017**, *1861* (1, Part B), 3700−3717.
(224) Kjaer, K. Some Simple Ideas on X-Ray Reflection and Grazing-Incidence Diffraction from Thin Surfactant Films. *Physica B: Condensed Matter* **1994**, *198* (1), 100−109.
(225) Behyan, S.; Borozenko, O.; Khan, A.; Faral, M.; Badia, A.; DeWolf, C. Nanoparticle-Induced Structural Changes in Lung Surfactant Membranes: An X-Ray Scattering Study. *Environmental Science: Nano* **2018**, *5* (5), 1218−1230.
(226) Kinnun, J. J.; Scott, H. L.; Bolmatov, D.; Collier, C. P.; Charlton, T. R.; Katsaras, J. Biophysical Studies of Lipid Nanodomains Using Different Physical Characterization Techniques. *Biophys. J.* **2023**, *122* (6), 931−949.
(227) Günther, H. *NMR Spectroscopy: Basic Principles, Concepts and Applications in Chemistry*; Wiley, 2013.
(228) Lindblom, G.; Gröbner, G. NMR on Lipid Membranes and Their Proteins. *Curr. Opin. Colloid Interface Sci.* **2006**, *11* (1), 24−29.
(229) Petersen, N. O.; Chan, S. I. More on the Motional State of Lipid Bilayer Membranes: Interpretation of Order Parameters Obtained from Nuclear Magnetic Resonance Experiments. *Biochemistry* **1977**, *16* (12), 2657−2667.
(230) Chan, S. I.; Bocian, D. F.; Petersen, N. O. Nuclear Magnetic Resonance Studies of the Phospholipid Bilayer Membrane. In *Membrane Spectroscopy*; Grell, E., Ed.; Molecular Biology Biochemistry and Biophysics; Springer-Verlag, 1980; pp 1−50.
(231) Hu, G. Q.; Jiao, B.; Shi, X. H.; Valle, R. P.; Fan, Q. H.; Zuo, Y. Y. Physicochemical Properties of Nanoparticles Regulate Translocation across Pulmonary Surfactant Monolayer and Formation of Lipoprotein Corona. *ACS Nano* **2013**, *7* (12), 10525−10533.
(232) Hu, Q.; Bai, X.; Hu, G.; Zuo, Y. Y. Unveiling the Molecular Structure of Pulmonary Surfactant Corona on Nanoparticles. *ACS Nano* **2017**, *11* (7), 6832−6842.
(233) Tian, F.; Lin, X.; Valle, R. P.; Zuo, Y. Y.; Gu, N. Poly(Amidoamine) Dendrimer as a Respiratory Nanocarrier: Insights from Experiments and Molecular Dynamics Simulations. *Langmuir* **2019**, *35* (15), 5364−5371.
(234) Schürch, S.; Bachofen, H.; Possmayer, F. Surface Activity in Situ, in Vivo, and in the Captive Bubble Surfactometer. *Comp Biochem Physiol A Mol. Integr Physiol* **2001**, *129* (1), 195−207.
(235) Schürch, S. Surface Tension at Low Lung Volumes: Dependence on Time and Alveolar Size. *Respir Physiol* **1982**, *48*, 339−355.
(236) Schürch, S.; Goerke, J.; Clements, J. A. Direct Determination of Surface Tension in the Lung. *Proc. Natl. Acad. Sci. U. S. A.* **1976**, *73* (12), 4698−4702.
(237) Schürch, S.; Goerke, J.; Clements, J. A. Direct Determination of Volume- and Time-Dependence of Alveolar Surface Tension in Excised Lungs. *Proc. Natl. Acad. Sci. U. S. A.* **1978**, *75* (7), 3417−3421.
(238) Hobi, N.; Giolai, M.; Olmeda, B.; Miklavc, P.; Felder, E.; Walther, P.; Dietl, P.; Frick, M.; Pérez-Gil, J.; Haller, T. A Small Key Unlocks a Heavy Door: The Essential Function of the Small Hydrophobic Proteins SP-B and SP-C to Trigger Adsorption of Pulmonary Surfactant Lamellar Bodies. *Biochimica et Biophysica Acta (BBA) - Molecular Cell Research* **2016**, *1863* (8), 2124−2134.
(239) Dietl, P.; Liss, B.; Felder, E.; Miklavc, P.; Wirtz, H. Lamellar Body Exocytosis by Cell Stretch or Purinergic Stimulation: Possible

https://doi.org/10.1021/acs.chemrev.3c00146
Chem. Rev. 2023, 123, 13209−13290

Physiological Roles, Messengers and Mechanisms. *Cellular Physiology and Biochemistry* **2010**, *25* (1), 1−12.
(240) Castillo-Sánchez, J. C.; Cruz, A.; Pérez-Gil, J. Structural Hallmarks of Lung Surfactant: Lipid-Protein Interactions, Membrane Structure and Future Challenges. *Arch. Biochem. Biophys.* **2021**, *703*, No. 108850.
(241) Ochs, M. The Closer We Look the More We See? Quantitative Microscopic Analysis of the Pulmonary Surfactant System. *Cellular Physiology and Biochemistry* **2010**, *25* (1), 27−40.
(242) Castillo-Sánchez, J. C.; Roldán, N.; García-Álvarez, B.; Batllori, E.; Galindo, A.; Cruz, A.; Pérez-Gil, J. The Highly Packed and Dehydrated Structure of Preformed Unexposed Human Pulmonary Surfactant Isolated from Amniotic Fluid. *Am. J. Physiol Lung Cell Mol. Physiol* **2022**, *322* (2), L191−L203.
(243) Bernhard, W.; Mottaghian, J.; Gebert, A.; Rau, G. A.; von der Hardt, H.; Poets, C. F. Commercial versus Native Surfactants. Surface Activity, Molecular Components, and the Effect of Calcium. *Am. J. Respir Crit Care Med.* **2000**, *162* (4 Pt 1), 1524−33.
(244) Tanford, C. Interfacial Free Energy and the Hydrophobic Effect. *Proc. Natl. Acad. Sci. U. S. A.* **1979**, *76* (9), 4175−4176.
(245) Cullis, P. R.; Hope, M. J.; Tilcock, C. P. Lipid Polymorphism and the Roles of Lipids in Membranes. *Chem. Phys. Lipids* **1986**, *40* (2−4), 127−144.
(246) Zuo, J.; Chen, Z.; Zhou, Y.; Liu, Z.; Zhou, C.; Xu, S.; Cheng, J.; Wen, X.; Pi, P. Superwetting Charged Copper Foams with Long Permeation Channels for Ultrafast Emulsion Separation and Surfactant Removal. *Journal of Materials Chemistry A* **2021**, *9* (22), 13170−13181.
(247) Perkins, W. R.; Dause, R. B.; Parente, R. A.; Minchey, S. R.; Neuman, K. C.; Gruner, S. M.; Taraschi, T. F.; Janoff, A. S. Role of Lipid Polymorphism in Pulmonary Surfactant. *Science* **1996**, *273* (5273), 330−332.
(248) Yu, S.-H.; Harding, P. G. R.; Possmayer, F. Artificial Pulmonary Surfactant. *Biochimica et Biophysica Acta (BBA) - Biomembranes* **1984**, *776* (1), 37−47.
(249) Chavarha, M.; Khoojinian, H.; Schulwitz, L. E.; Biswas, S. C.; Rananavare, S. B.; Hall, S. B. Hydrophobic Surfactant Proteins Induce a Phosphatidylethanolamine to Form Cubic Phases. *Biophys. J.* **2010**, *98* (8), 1549−1557.
(250) Chavarha, M.; Loney, R. W.; Kumar, K.; Rananavare, S. B.; Hall, S. B. Differential Effects of the Hydrophobic Surfactant Proteins on the Formation of Inverse Bicontinuous Cubic Phases. *Langmuir* **2012**, *28* (48), 16596−16604.
(251) Chavarha, M.; Loney, R. W.; Rananavare, S. B.; Hall, S. B. Hydrophobic Surfactant Proteins Strongly Induce Negative Curvature. *Biophys. J.* **2015**, *109* (1), 95−105.
(252) Biswas, S. C.; Rananavare, S. B.; Hall, S. B. Effects of Gramicidin-A on the Adsorption of Phospholipids to the Air-Water Interface. *Biochim. Biophys. Acta* **2005**, *1717* (1), 41−49.
(253) Ridolfi, A.; Humphreys, B.; Caselli, L.; Montis, C.; Nylander, T.; Berti, D.; Brucale, M.; Valle, F. Nanoscale Structural and Mechanical Characterization of Thin Bicontinuous Cubic Phase Lipid Films. *Colloids Surf. B Biointerfaces* **2022**, *210*, No. 112231.
(254) Tenchov, B.; MacDonald, R. C.; Siegel, D. P. Inverted Bicontinuous Cubic Phases in Unsaturated PC/Cholesterol Mixtures: A Dual Role for Cholesterol in Fusion and Raft Formation? *Biophys. J.* **2005**, *88*, 68A−68A.
(255) Demurtas, D.; Guichard, P.; Martiel, I.; Mezzenga, R.; Hébert, C.; Sagalowicz, L. Direct Visualization of Dispersed Lipid Bicontinuous Cubic Phases by Cryo-Electron Tomography. *Nat. Commun.* **2015**, *6* (1), 8915.
(256) Tenchov, B. G.; MacDonald, R. C.; Siegel, D. P. Cubic Phases in Phosphatidylcholine-Cholesterol Mixtures: Cholesterol as Membrane Fusogen. *Biophys. J.* **2006**, *91* (7), 2508−2516.
(257) Tran, N.; Kurian, J.; Bhatt, A.; McKenna, R.; Long, J. R. Entropic Anomaly Observed in Lipid Polymorphisms Induced by Surfactant Peptide SP-B(1−25). *J. Physical Chem. B* **2017**, *121* (39), 9102−9112.
(258) Biswas, S. C.; Rananavare, S. B.; Hall, S. B. Differential Effects of Lysophosphatidylcholine on the Adsorption of Phospholipids to an Air/Water Interface. *Biophys. J.* **2007**, *92* (2), 493−501.
(259) Cockcroft, S. Mammalian Lipids: Structure, Synthesis and Function. *Essays in Biochemistry* **2021**, *65* (5), 813−845.
(260) Schoop, V.; Martello, A.; Eden, E. R.; Höglinger, D. Cellular Cholesterol and How to Find It. *Biochim Biophys Acta (BBA) - Molecular and Cell Biology of Lipids* **2021**, *1866* (9), 158989.
(261) Quinn, P. J.; Wolf, C. Thermotropic and Structural Evaluation of the Interaction of Natural Sphingomyelins with Cholesterol. *Biochim Biophys Acta (BBA) - Biomembranes* **2009**, *1788* (9), 1877−1889.
(262) Kim, K.; Choi, S. Q.; Zell, Z. A.; Squires, T. M.; Zasadzinski, J. A. Effect of Cholesterol Nanodomains on Monolayer Morphology and Dynamics. *Proc. Natl. Acad. Sci. U. S. A.* **2013**, *110* (33), E3054−3060.
(263) Bernardino de la Serna, J.; Perez-Gil, J.; Simonsen, A. C.; Bagatolli, L. A. Cholesterol Rules: Direct Observation of the Coexistence of Two Fluid Phases in Native Pulmonary Surfactant Membranes at Physiological Temperatures. *J. Biol. Chem.* **2004**, *279* (39), 40715−40722.
(264) Baumgart, F.; Ospina, O. L.; Mingarro, I.; Rodriguez-Crespo, I.; Perez-Gil, J. Palmitoylation of Pulmonary Surfactant Protein SP-C Is Critical for Its Functional Cooperation with SP-B to Sustain Compression/Expansion Dynamics in Cholesterol-Containing Surfactant Films. *Biophys. J.* **2010**, *99* (10), 3234−3243.
(265) Curstedt, T.; Jornvall, H.; Robertson, B.; Bergman, T.; Berggren, P. Two Hydrophobic Low-Molecular-Mass Protein Fractions of Pulmonary Surfactant. Characterization and Biophysical Activity. *Eur. J. Biochem.* **1987**, *168*, 255−262.
(266) Phizackerley, P. J.; Town, M. H.; Newman, G. E. Hydrophobic Proteins of Lamellated Osmiophilic Bodies Isolated from Pig Lung. *Biochem. J.* **1979**, *183* (3), 731−736.
(267) Possmayer, F.; Yu, S. H.; Weber, J. M.; Harding, P. G. Pulmonary Surfactant. *Can. J. Biochem Cell Biol.* **1984**, *62* (11), 1121−1133.
(268) Ross, G. F.; Notter, R. H.; Meuth, J.; Whitsett, J. A. Phospholipid Binding and Biophysical Activity of Pulmonary Surfactant-Associated Protein (SAP)-35 and Its Non-Collagenous COOH-Terminal Domains. *J. Biol. Chem.* **1986**, *261* (30), 14283−14291.
(269) Suzuki, Y. Effect of Protein, Cholesterol, and Phosphatidylglycerol on the Surface Activity of the Lipid-Protein Complex Reconstituted from Pig Pulmonary Surfactant. *J. Lipid Res.* **1982**, *23* (1), 62−69.
(270) Suzuki, Y.; Curstedt, T.; Grossmann, G.; Kobayashi, T.; Nilsson, R.; Nohara, K.; Robertson, B. The Role of the Low-Molecular Weight (Less Than or Equal to 15,000 Da) Apoproteins of Pulmonary Surfactant. *Eur. J. Respir Dis* **1986**, *69* (5), 336−345.
(271) Takahashi, A.; Fujiwara, T. Proteolipid in Bovine Lung Surfactant: Its Role in Surfactant Function. *Biochem. Biophys. Res. Commun.* **1986**, *135* (2), 527−532.
(272) Warr, R. G.; Hawgood, S.; Buckley, D. I.; Crisp, T. M.; Schilling, J.; Benson, B. J.; Ballard, P. L.; Clements, J. A.; White, R. T. Low Molecular Weight Human Pulmonary Surfactant Protein (SP5): Isolation, Characterization and cDNA and Amino Acid Sequences. *Proc. Natl. Acad. Sci. U. S. A.* **1987**, *84*, 7915−7919.
(273) Whitesst, J. A.; Ohning, B. L.; Ross, G.; Meuth, J.; Weaver, T.; Holm, B. A.; Shapiro, D. L.; Notter, R. H. Hydrophobic Surfactant-Associated Protein in Whole Lung Surfactant and Its Importance for Biophysical Activity in Lung Surfactant Extracts Used for Replacement Therapy. *Pediatr. Res.* **1986**, *20* (5), 460−467.
(274) Yu, S. H.; Possmayer, F. Reconstitution of Surfactant Activity by Using the 6 Kda Apoprotein Associated with Pulmonary Surfactant. *Biochem. J.* **1986**, *236* (1), 85−89.
(275) Yu, S. H.; Possmayer, F. Comparative Studies on the Biophysical Activities of the Low-Molecular- Weight Hydrophobic Proteins Purified from Bovine Pulmonary Surfactant. *Biochim. Biophys. Acta* **1988**, *961* (3), 337−350.

https://doi.org/10.1021/acs.chemrev.3c00146
Chem. Rev. 2023, 123, 13209−13290

(276) Olmeda, B.; García-Álvarez, B.; Pérez-Gil, J. Structure-Function Correlations of Pulmonary Surfactant Protein SP-B and the Saposin-like Family of Proteins. *European biophys journal* **2013**, *42* (2−3), 209−222.
(277) Waring, A. J.; Walther, F. J.; Gordon, L. M.; Hernandez-Juviel, J. M.; Hong, T.; Sherman, M. A.; Alonso, C.; Alig, T.; Braun, A.; Bacon, D.; Zasadzinski, J. A. The Role of Charged Amphipathic Helices in the Structure and Function of Surfactant Protein B. *J. Pept Res.* **2005**, *66* (6), 364−374.
(278) Whitsett, J. A.; Nogee, L. M.; Weaver, T. E.; Horowitz, A. D. Human Surfactant Protein B: Structure, Function, Regulation, and Genetic Disease. *Physiol Rev.* **1995**, *75* (4), 749−757.
(279) Whitsett, J. A.; Wert, S. E.; Weaver, T. E. Diseases of Pulmonary Surfactant Homeostasis. *Annu. Rev. Pathol* **2015**, *10*, 371−393.
(280) Gerson, K. D.; Foster, C. D.; Zhang, P.; Zhang, Z.; Rosenblatt, M. M.; Guttentag, S. H. Pepsinogen C Proteolytic Processing of Surfactant Protein B. *J. Biol. Chem.* **2008**, *283* (16), 10330−10338.
(281) Perez-Gil, J.; Weaver, T. E. Pulmonary Surfactant Pathophysiology: Current Models and Open Questions. *Physiology (Bethesda)* **2010**, *25* (3), 132−141.
(282) Zaltash, S.; Griffiths, W. J.; Beck, D.; Duan, C. X.; Weaver, T. E.; Johansson, J. Membrane Activity of (Cys48Ser) Lung Surfactant Protein B Increases with Dimerisation. *Biol. Chem.* **2001**, *382* (6), 933−939.
(283) Taneva, S.; Keough, K. M. Cholesterol Modifies the Properties of Surface Films of Dipalmitoylphosphatidylcholine Plus Pulmonary Surfactant-Associated Protein B or C Spread or Adsorbed at the Air-Water Interface. *Biochemistry* **1997**, *36* (4), 912−922.
(284) Rodriguez-Capote, K.; Nag, K.; Schürch, S.; Possmayer, F. Surfactant Protein Interactions with Neutral and Acidic Phospholipid Films. *Am. J. Physiol Lung Cell Mol. Physiol* **2001**, *281* (1), L231−242.
(285) Liekkinen, J.; Enkavi, G.; Javanainen, M.; Olmeda, B.; Pérez-Gil, J.; Vattulainen, I. Pulmonary Surfactant Lipid Reorganization Induced by the Adsorption of the Oligomeric Surfactant Protein B Complex. *Journal of molecular biology* **2020**, *432* (10), 3251−3268.
(286) Loney, R. W.; Brandner, B.; Dagan, M. P.; Smith, P. N.; Roche, M.; Fritz, J. R.; Hall, S. B.; Tristram-Nagle, S. A. Changes in Membrane Elasticity Caused by the Hydrophobic Surfactant Proteins Correlate Poorly with Adsorption of Lipid Vesicles. *Soft Matter* **2021**, *17* (12), 3358−3366.
(287) Hoffman, A. M.; Shifren, A.; Mazan, M. R.; Gruntman, A. M.; Lascola, K. M.; Nolen-Walston, R. D.; Kim, C. F.; Tsai, L.; Pierce, R. A.; Mecham, R. P.; et al. Matrix Modulation of Compensatory Lung Regrowth and Progenitor Cell Proliferation in Mice. *American Journal of Physiology Lung Cell Mol. Physiol* **2010**, *298* (2), L158−168.
(288) Korfhagen, T. R.; Glasser, S. W.; Wert, S. E.; Bruno, M. D.; Daugherty, C. C.; McNeish, J. D.; Stock, J. L.; Potter, S. S.; Whitsett, J. A. Cis-Acting Sequences from a Human Surfactant Protein Gene Confer Pulmonary-Specific Gene Expression in Transgenic Mice. *Proc. Natl. Acad. Sci. U. S. A.* **1990**, *87* (16), 6122−6126.
(289) Pérez-Gil, J.; Keogh, K. Structural Similarities between Myelin and Hydrophobic Surfactant Associated Proteins: Protein Motifs for Interacting with Bilayers. *Journal of theoretical biology* **1994**, *169* (3), 221−229.
(290) Johansson, J. Structure and Properties of Surfactant Protein C. *Biochim. Biophys. Acta* **1998**, *1408* (2−3), 161−172.
(291) Olafson, R. W.; Rink, U.; Kielland, S.; Yu, S.-H.; Chung, J.; Harding, P. G. R.; Possmayer, F. Protein Sequence Analysis Studies on the Low Molecular Weight Hydrophobic Proteins Associated with Bovine Pulmonary Surfactant. *Biochem Biophysl Res. Commun.* **1987**, *148* (3), 1406−1411.
(292) Serrano, A. G.; Perez-Gil, J. Protein-Lipid Interactions and Surface Activity in the Pulmonary Surfactant System. *Chem. Phys. Lipids* **2006**, *141* (1−2), 105−118.
(293) Pastrana, B.; Mautone, A. J.; Mendelsohn, R. Fourier Transform Infrared Studies of Secondary Structure and Orientation of Pulmonary Surfactant SP-C and Its Effect on the Dynamic Surface Properties of Phospholipids. *Biochemistry* **1991**, *30* (41), 10058−10064.
(294) Loney, R. W.; Panzuela, S.; Chen, J.; Yang, Z.; Fritz, J. R.; Dell, Z.; Corradi, V.; Kumar, K.; Tieleman, D. P.; Hall, S. B.; et al. Location of the Hydrophobic Surfactant Proteins, SP-B and Sp-C, in Fluid-Phase Bilayers. *J. Phys. Chem. B* **2020**, *124* (31), 6763−6774.
(295) Venkitaraman, A. R.; Hall, S. B.; Whitsett, J. A.; Notter, R. H. Enhancement of Biophysical Activity of Lung Surfactant Extracts and Phospholipid-Apoprotein Mixtures by Surfactant Protein A. *Chem. Phys. Lipids* **1990**, *56* (2−3), 185−194.
(296) Morrow, M. R.; Perez-Gil, J.; Simatos, G.; Boland, C.; Stewart, J.; Absolom, D.; Sarin, V.; Keough, K. M. Pulmonary Surfactant-Associated Protein SP-B Has Little Effect on Acyl Chains in Dipalmitoylphosphatidylcholine Dispersions. *Biochemistry* **1993**, *32* (16), 4397−4402.
(297) Plasencia, I.; Rivas, L.; Keough, K. M. W.; Marsh, D.; Pérez-Gil, J. The N-Terminal Segment of Pulmonary Surfactant Lipopeptide SP-C Has Intrinsic Propensity to Interact with and Perturb Phospholipid Bilayers. *Biochem. J.* **2004**, *377* (1), 183−193.
(298) Plasencia, I.; Keough, K. M. W.; Perez-Gil, J. Interaction of the N-Terminal Segment of Pulmonary Surfactant Protein SP-C with Interfacial Phospholipid Films. *Biochim Biophys Acta (BBA) - Biomembranes* **2005**, *1713* (2), 118−128.
(299) Roldan, N.; Goormaghtigh, E.; Pérez-Gil, J.; Garcia-Alvarez, B. Palmitoylation as a Key Factor to Modulate SP-C−Lipid Interactions in Lung Surfactant Membrane Multilayers. *Biochim Biophys Acta (BBA) - Biomembranes* **2015**, *1848* (1, Part A), 184−191.
(300) Nag, K.; Perez-Gil, J.; Cruz, A.; Keough, K. M. Fluorescently Labeled Pulmonary Surfactant Protein C in Spread Phospholipid Monolayers. *Biophys. J.* **1996**, *71* (1), 246−256.
(301) Liekkinen, J.; Olżyńska, A.; Cwiklik, L.; Bernardino de la Serna, J.; Vattulainen, I.; Javanainen, M. Surfactant Proteins SP-B and SP-C in Pulmonary Surfactant Monolayers: Physical Properties Controlled by Specific Protein-Lipid Interactions. *Langmuir* **2023**, *39* (12), 4338−4350.
(302) Bernardino de la Serna, J.; Vargas, R.; Picardi, V.; Cruz, A.; Arranz, R.; Valpuesta, J. M.; Mateu, L.; Pérez-Gil, J. Segregated Ordered Lipid Phases and Protein-Promoted Membrane Cohesivity Are Required for Pulmonary Surfactant Films to Stabilize and Protect the Respiratory Surface. *Faraday Discuss.* **2013**, *161*, 535−548; discussion 563−89. .
(303) Serrano, A. G.; Ryan, M.; Weaver, T. E.; Perez-Gil, J. Critical Structure-Function Determinants within the N-Terminal Region of Pulmonary Surfactant Protein SP-B. *Biophys. J.* **2006**, *90* (1), 238−249.
(304) Cabré, E. J.; Martínez-Calle, M.; Prieto, M.; Fedorov, A.; Olmeda, B.; Loura, L. M. S.; Pérez-Gil, J. Homo- and Hetero-Oligomerization of Hydrophobic Pulmonary Surfactant Proteins SP-B and SP-C in Surfactant Phospholipid Membranes. *J. Biol. Chem.* **2018**, *293* (24), 9399−9411.
(305) Olmeda, B.; García-Álvarez, B.; Gómez, M. J.; Martínez-Calle, M.; Cruz, A.; Pérez-Gil, J. A Model for the Structure and Mechanism of Action of Pulmonary Surfactant Protein B. *FASEB J.* **2015**, *29* (10), 4236−4247.
(306) Roldan, N.; Nyholm, T. K. M.; Slotte, J. P.; Pérez-Gil, J.; García-Álvarez, B. Effect of Lung Surfactant Protein SP-C and SP-C-Promoted Membrane Fragmentation on Cholesterol Dynamics. *Biophys. J.* **2016**, *111* (8), 1703−1713.
(307) Yu, S.-H.; Possmayer, F. Effect of Pulmonary Surfactant Protein B (SP-B) and Calcium on Phospholipid Adsorption and Squeeze-out of Phosphatidylglycerol from Binary Phospholipid Monolayers Containing Dipalmitoylphosphatidylcholine. *Biochim. Biophys. Acta* **1992**, *1126*, 26−34.
(308) Manzanares, D.; Rodriguez-Capote, K.; Liu, S.; Haines, T.; Ramos, Y.; Zhao, L.; Doherty-Kirby, A.; Lajoie, G.; Possmayer, F. Modification of Tryptophan and Methionine Residues Is Implicated in the Oxidative Inactivation of Surfactant Protein B. *Biochemistry* **2007**, *46* (18), 5604−5615.

https://doi.org/10.1021/acs.chemrev.3c00146
Chem. Rev. 2023, 123, 13209−13290

(309) Ryan, M. A.; Qi, X.; Serrano, A. G.; Ikegami, M.; Perez-Gil, J.; Johansson, J.; Weaver, T. E. Mapping and Analysis of the Lytic and Fusogenic Domains of Surfactant Protein B. *Biochemistry* **2005**, *44* (3), 861−872.
(310) Martínez-Calle, M.; Parra-Ortiz, E.; Cruz, A.; Olmeda, B.; Pérez-Gil, J. Towards the Molecular Mechanism of Pulmonary Surfactant Protein SP-B: At the Crossroad of Membrane Permeability and Interfacial Lipid Transfer. *Journal of molecular biology* **2021**, *433* (3), No. 166749.
(311) Martinez-Calle, M.; Prieto, M.; Olmeda, B.; Fedorov, A.; Loura, L. M. S.; Pérez-Gil, J. Pulmonary Surfactant Protein SP-B Nanorings Induce the Multilamellar Organization of Surfactant Complexes. *Biochim Biophys Acta. Biomembranes* **2020**, *1862* (6), No. 183216.
(312) Creuwels, L. A.; Demel, R. A.; van Golde, L. M.; Benson, B. J.; Haagsman, H. P. Effect of Acylation on Structure and Function of Surfactant Protein C at the Air-Liquid Interface. *J. Biol. Chem.* **1993**, *268* (35), 26752−26758.
(313) Oosterlaken-Dijksterhuis, M. A.; van Eijk, M.; van Golde, L. M. G.; Haagsman, H. P. Lipid Mixing Is Mediated by the Hydrophobic Surfactant Protein SP-B but Not by SP-C. *Biochim Biophys Acta (BBA) - Biomembranes* **1992**, *1110* (1), 45−50.
(314) Brockman, J. M.; Wang, Z.; Notter, R. H.; Dluhy, R. A. Effect of Hydrophobic Surfactant Proteins SP-B and SP-C on Binary Phospholipid Monolayers: II. Infrared External Reflectance-Absorption Spectroscopy. *Biophys. J.* **2003**, *84* (1), 326−340.
(315) Nag, K.; Taneva, S. G.; Perez-Gil, J.; Cruz, A.; Keough, K. M. Combinations of Fluorescently Labeled Pulmonary Surfactant Proteins SP-B and SP-C in Phospholipid Films. *Biophys. J.* **1997**, *72* (6), 2638−2650.
(316) Plasencia, I.; Baumgart, F.; Andreu, D.; Marsh, D.; Pérez-Gil, J. Effect of Acylation on the Interaction of the N-Terminal Segment of Pulmonary Surfactant Protein SP-C with Phospholipid Membranes. *Biochim Biophys Acta (BBA) - Biomembranes* **2008**, *1778* (5), 1274−1282.
(317) Gonzalez-Horta, A.; Andreu, D.; Morrow, M. R.; Perez-Gil, J. Effects of Palmitoylation on Dynamics and Phospholipid-Bilayer-Perturbing Properties of the N-Terminal Segment of Pulmonary Surfactant Protein SP-C as Shown by 2H-NMR. *Biophys. J.* **2008**, *95* (5), 2308−2317.
(318) Roldan, N.; Pérez-Gil, J.; Morrow, M. R.; García-Álvarez, B. Divide & Conquer: Surfactant Protein SP-C and Cholesterol Modulate Phase Segregation in Lung Surfactant. *Biophys J. l* **2017**, *113* (4), 847−859.
(319) Klenz, U.; Saleem, M.; Meyer, M. C.; Galla, H. J. Influence of Lipid Saturation Grade and Headgroup Charge: A Refined Lung Surfactant Adsorption Model. *Biophys. J.* **2008**, *95* (2), 699−709.
(320) Krüger, P.; Baatz, J. E.; Dluhy, R. A.; Lösche, M. Effect of Hydrophobic Surfactant Protein SP-C on Binary Phospholipid Monolayers. Molecular Machinery at the Air/Water Interface. *Biophys. Chem.* **2002**, *99* (3), 209−228.
(321) Barriga, A.; Morán-Lalangui, M.; Castillo-Sánchez, J. C.; Mingarro, I.; Pérez-Gil, J.; García-Álvarez, B. Role of Pulmonary Surfactant Protein Sp-C Dimerization on Membrane Fragmentation: An Emergent Mechanism Involved in Lung Defense and Homeostasis. *Biochim Biophys Acta Biomembr* **2021**, *1863* (6), No. 183572.
(322) Gomez-Gil, L.; Schürch, D.; Goormaghtigh, E.; Perez-Gil, J. Pulmonary Surfactant Protein SP-C Counteracts the Deleterious Effects of Cholesterol on the Activity of Surfactant Films under Physiologically Relevant Compression-Expansion Dynamics. *Biophys. J.* **2009**, *97* (10), 2736−2745.
(323) Diemel, R. V.; Snel, M. M. E.; van Golde, L. M. G.; Putz, G.; Haagsman, H. P.; Batenburg, J. J. Effects of Cholesterol on Surface Activity and Surface Topography of Spread Surfactant Films. *Biochemistry* **2002**, *41* (50), 15007−15016.
(324) Korolainen, H.; Lolicato, F.; Enkavi, G.; Pérez-Gil, J.; Kulig, W.; Vattulainen, I. Dimerization of the Pulmonary Surfactant Protein C in a Membrane Environment. *PLoS One* **2022**, *17* (4), No. e0267155.
(325) Roldan, N.; Cruz, A.; Sanz, A.; Bruix, M.; Pérez-Gil, J.; Garcia-Alvarez, B. Delivery of Lung Surfactant SP-C Based Nanostructures to Respiratory Air-Liquid Interfacial Films. *Biophys. J.* **2017**, *112* (3), 389a−390a.
(326) Parra, E.; Moleiro, L. H.; López-Montero, I.; Cruz, A.; Monroy, F.; Pérez-Gil, J. A Combined Action of Pulmonary Surfactant Proteins SP-B and SP-C Modulates Permeability and Dynamics of Phospholipid Membranes. *Biochem. J.* **2011**, *438* (3), 555−564.
(327) Baatz, J. E.; Smyth, K. L.; Whitsett, J. A.; Baxter, C.; Absolom, D. R. Structure and Functions of a Dimeric Form of Surfactant Protein SP-C: A Fourier Transform Infrared and Surfactometry Study. *Chem. Phys. Lipids* **1992**, *63* (1), 91−104.
(328) Vandenbussche, G.; Clercx, A.; Curstedt, T.; Johansson, J.; Jörnvall, H.; Ruysschaert, J.-M. Structure and Orientation of the Surfactant-Associated Protein C in a Lipid Bilayer. *Eur. J. Biochem.* **1992**, *203* (1−2), 201−209.
(329) Qanbar, R.; Possmayer, F. On the Surface Activity of Surfactant-Associated Protein C (SP-C): Effects of Palmitoylation and Ph. *Biochim. Biophys. Acta* **1995**, *1255* (3), 251−259.
(330) Wang, Z.; Gurel, O.; Baatz, J. E.; Notter, R. H. Acylation of Pulmonary Surfactant Protein-C Is Required for Its Optimal Surface Active Interactions with Phospholipids. *J. Biol. Chem.* **1996**, *271* (32), 19104−19109.
(331) Lukovic, D.; Cruz, A.; Gonzalez-Horta, A.; Almlen, A.; Curstedt, T.; Mingarro, I.; Pérez-Gil, J. Interfacial Behavior of Recombinant Forms of Human Pulmonary Surfactant Protein SP-C. *Langmuir* **2012**, *28* (20), 7811−7825.
(332) Lukovic, D.; Plasencia, I.; Taberner, F. J.; Salgado, J.; Calvete, J. J.; Pérez-Gil, J.; Mingarro, I. Production and Characterisation of Recombinant Forms of Human Pulmonary Surfactant Protein C (SP-C): Structure and Surface Activity. *Biochim Biophys Acta (BBA) - Biomembranes* **2006**, *1758* (4), 509−518.
(333) Walther, F. J.; Waring, A. J.; Hernández-Juviel, J. M.; Ruchala, P.; Wang, Z.; Notter, R. H.; Gordon, L. M. Surfactant Protein C Peptides with Salt-Bridges ("ion-Locks") Promote High Surfactant Activities by Mimicking the α-Helix and Membrane Topography of the Native Protein. *PeerJ.* **2014**, *2*, No. e485.
(334) Schürch, D.; Ospina, O. L.; Cruz, A.; Perez-Gil, J. Combined and Independent Action of Proteins SP-B and SP-C in the Surface Behavior and Mechanical Stability of Pulmonary Surfactant Films. *Biophys. J.* **2010**, *99* (10), 3290−3299.
(335) Glasser, S. W.; Burhans, M. S.; Korfhagen, T. R.; Na, C. L.; Sly, P. D.; Ross, G. F.; Ikegami, M.; Whitsett, J. A. Altered Stability of Pulmonary Surfactant in SP-C-Deficient Mice. *Proc. Natl. Acad. Sci. U. S. A.* **2001**, *98* (11), 6366−6371.
(336) Dluhy, R. A.; Shanmukh, S.; Leapard, J. B.; Krüger, P.; Baatz, J. E. Deacylated Pulmonary Surfactant Protein SP-C Transforms from A-Helical to Amyloid Fibril Structure Via a PH-Dependent Mechanism: An Infrared Structural Investigation. *Biophys. J.* **2003**, *85* (4), 2417−2429.
(337) Johansson, J.; Weaver, T. E.; Tjernberg, L. O. Proteolytic Generation and Aggregation of Peptides from Transmembrane Regions: Lung Surfactant Protein C and Amyloid B-Peptide. *Cellular and Molecular Life Sciences CMLS* **2004**, *61* (3), 326−335.
(338) Johansson, J.; Curstedt, T. Synthetic Surfactants with SP-B and SP-C Analogues to Enable Worldwide Treatment of Neonatal Respiratory Distress Syndrome and Other Lung Diseases. *Journal of internal medicine* **2019**, *285* (2), 165−186.
(339) Szyperski, T.; Wüthrich, K.; Vandenbussche, G.; Ruysschaert, J.-M.; Curstedt, T.; Johansson, J. Pulmonary Surfactant-Associated Polypeptide C in a Mixed Organic Solvent Transforms from a Monomeric A-Helical State into Insoluble B-Sheet Aggregates. *Protein Sci.* **1998**, *7* (12), 2533−2540.
(340) Wüstneck, N.; Wüstneck, R.; Perez-Gil, J.; Pison, U. Effects of Oligomerization and Secondary Structure on the Surface Behavior of Pulmonary Surfactant Proteins SP-B and SP-C. *Biophys. J.* **2003**, *84* (3), 1940−1949.

https://doi.org/10.1021/acs.chemrev.3c00146
Chem. Rev. 2023, 123, 13209−13290

(341) Almlén, A.; Stichtenoth, G.; Linderholm, B.; Haegerstrand-Björkman, M.; Robertson, B.; Johansson, J.; Curstedt, T. Surfactant Proteins B and C Are Both Necessary for Alveolar Stability at End Expiration in Premature Rabbits with Respiratory Distress Syndrome. *J. Appl. Physiol (1985)* **2008**, *104* (4), 1101−1108.
(342) Almlén, A.; Walther, F. J.; Waring, A. J.; Robertson, B.; Johansson, J.; Curstedt, T. Synthetic Surfactant Based on Analogues of SP-B and SP-C Is Superior to Single-Peptide Surfactants in Ventilated Premature Rabbits. *Neonatology* **2010**, *98* (1), 91−99.
(343) Oosterlaken-Dijksterhuis, M. A.; Haagsman, H. P.; van Golde, L. M. G.; Demel, R. A. Interaction of Lipid Vesicles with Monomolecular Layers Containing Lung Surfactant Proteins SP-B or SP-C. *Biochemistry* **1991**, *30*, 8276−8281.
(344) Parra, E.; Alcaraz, A.; Cruz, A.; Aguilella, V. M.; Pérez-Gil, J. Hydrophobic Pulmonary Surfactant Proteins SP-B and SP-C Induce Pore Formation in Planar Lipid Membranes: Evidence for Proteolipid Pores. *Biophys. J.* **2013**, *104* (1), 146−155.
(345) Rodriguez-Capote, K.; McCormack, F. X.; Possmayer, F. Pulmonary Surfactant Protein-A (SP-A) Restores the Surface Properties of Surfactant after Oxidation by a Mechanism That Requires the Cys6 Interchain Disulfide Bond and the Phospholipid Binding Domain. *J. Biol. Chem.* **2003**, *278* (23), 20461−20474.
(346) Taneva, S.; Keough, K. M. Pulmonary Surfactant Proteins SP-B and SP-C in Spread Monolayers at the Air-Water Interface: III. Proteins SP-B Plus SP-C with Phospholipids in Spread Monolayers. *Biophys. J.* **1994**, *66* (4), 1158−1166.
(347) Martínez-Calle, M.; Olmeda, B.; Dietl, P.; Frick, M.; Pérez-Gil, J. Pulmonary Surfactant Protein SP-B Promotes Exocytosis of Lamellar Bodies in Alveolar Type II Cells. *FASEB J.* **2018**, *32* (8), 4600−4611.
(348) Plasencia, I.; Cruz, A.; Casals, C.; Pérez-Gil, J. Superficial Disposition of the N-Terminal Region of the Surfactant Protein SP-C and the Absence of Specific SP-B-SP-C Interactions in Phospholipid Bilayers. *Biochem. J.* **2001**, *359* (Pt 3), 651−659.
(349) Fritz, J. R.; Loney, R. W.; Hall, S. B.; Tristram-Nagle, S. Suppression of L(A)/L(B) Phase Coexistence in the Lipids of Pulmonary Surfactant. *Biophys. J.* **2021**, *120* (2), 243−253.
(350) Yu, S. H.; Chung, W.; Olafson, R. W.; Harding, P. G.; Possmayer, F. Characterization of the Small Hydrophobic Proteins Associated with Pulmonary Surfactant. *Biochim. Biophys. Acta* **1987**, *921* (3), 437−448.
(351) Sehlmeyer, K.; Ruwisch, J.; Roldan, N.; Lopez-Rodriguez, E. Alveolar Dynamics and Beyond - The Importance of Surfactant Protein C and Cholesterol in Lung Homeostasis and Fibrosis. *Front physiol* **2020**, *11*, 386.
(352) Curstedt, T.; Johansson, J. Different Effects of Surfactant Proteins B and C - Implications for Development of Synthetic Surfactants. *Neonatology* **2010**, *97* (4), 367−372.
(353) Curstedt, T.; Calkovska, A.; Johansson, J. New Generation Synthetic Surfactants. *Neonatology* **2013**, *103* (4), 327−330.
(354) Bangham, A. D. Lung Surfactant: How It Does and Does Not Work. *Lung* **1987**, *165* (1), 17−25.
(355) Clements, J. A. Functions of the Alveolar Lining. *Am. Rev. Respir. Dis.* **1977**, *115* (6 Pt 2), 67−71.
(356) King, R. J.; Clements, J. A. Surface Active Materials from Dog Lung. II. Composition and Physiological Correlations. *Am. J. Physiol.* **1972**, *223* (3), 715−726.
(357) Notter, R. H.; Holcomb, H.; Mavis, R. D. Dynamic Surface Properties of Phosphatidylglycerol-Dipalmitoylphosphatidylcholine Mixed Films. *Chem. Phys. Lipids* **1980**, *27*, 305−319.
(358) Schürch, S.; Green, F. H.; Bachofen, H. Formation and Structure of Surface Films: Captive Bubble Surfactometry. *Biochim. Biophys. Acta* **1998**, *1408* (2−3), 180−202.
(359) Young, S. L.; Fram, E. K.; Larson, E. W. Three-Dimensional Reconstruction of Tubular Myelin. *Exp Lung Res.* **1992**, *18* (4), 497−504.
(360) Hassett, R. J.; Engleman, W.; Kuhn, C. Extramembranous Particles in Tubular Myelin from Rat Lung. *Journal of Ultrastructure Research* **1980**, *71* (1), 60−67.
(361) Palaniyar, N.; Ikegami, M.; Korfhagen, T.; Whitsett, J.; McCormack, F. X. Domains of Surfactant Protein A That Affect Protein Oligomerization, Lipid Structure and Surface Tension. *Comp Biochem Physiol A Mol. Integr Physiol* **2001**, *129* (1), 109−127.
(362) Cerrada, A.; Haller, T.; Cruz, A.; Pérez-Gil, J. Pneumocytes Assemble Lung Surfactant as Highly Packed/Dehydrated States with Optimal Surface Activity. *Biophys. J.* **2015**, *109* (11), 2295−2306.
(363) Haller, T.; Dietl, P.; Stockner, H.; Frick, M.; Mair, N.; Tinhofer, I.; Ritsch, A.; Enhorning, G.; Putz, G. Tracing Surfactant Transformation from Cellular Release to Insertion into an Air-Liquid Interface. *Am. J. Physiol Lung Cell Mol. Physiol* **2004**, *286* (5), L1009−15.
(364) Ravasio, A.; Olmeda, B.; Bertocchi, C.; Haller, T.; Perez-Gil, J. Lamellar Bodies Form Solid Three-Dimensional Films at the Respiratory Air-Liquid Interface. *J. Biol. Chem.* **2010**, *285* (36), 28174−28182.
(365) Oosterlaken-Dijksterhuis, M. A.; Haagsman, H. P.; van Golde, L. M.; Demel, R. A. Characterization of Lipid Insertion into Monomolecular Layers Mediated by Lung Surfactant Proteins SP-B and SP-C. *Biochemistry* **1991**, *30* (45), 10965−10971.
(366) Walters, R. W.; Jenq, R. R.; Hall, S. B. Distinct Steps in the Adsorption of Pulmonary Surfactant to an Air- Liquid Interface. *Biophys. J.* **2000**, *78* (1), 257−266.
(367) Weber, M. J.; Possmayer, F. Calcium Interactions in Pulmonary Surfactant. *Biochim Biophys Acta (BBA) - Lipids and Lipid Metabolism* **1984**, *796* (1), 83−91.
(368) Wustneck, R.; Perez-Gil, J.; Wustneck, N.; Cruz, A.; Fainerman, V. B.; Pison, U. Interfacial Properties of Pulmonary Surfactant Layers. *Adv. Colloid Interface Sci.* **2005**, *117* (1−3), 33−58.
(369) Vollhardt, D. Nucleation in Monolayers. *Adv. Colloid Interface Sci.* **2006**, *123*−*126*, 173−188.
(370) Lettau, M.; Timm, S.; Dittmayer, C.; Lopez-Rodriguez, E.; Ochs, M. The Ultrastructural Heterogeneity of Lung Surfactant Revealed by Serial Section Electron Tomography: Insights into the 3-D Architecture of Human Tubular Myelin. *American Journal of Physiology Lung Cellular and Molecular Physiology* **2022**, *322* (6), L873−L881.
(371) Williams, M. C.; Hawgood, S.; Hamilton, R. L. Changes in Lipid Structure Produced by Surfactant Proteins SP-A, SP-B, and SP-C. *Am. J. Respir. Cell Mol. Biol.* **1991**, *5* (1), 41−50.
(372) Goerke, J. Lung Surfactant. *Biochim Biophys Acta (BBA) - Reviews on Biomembranes* **1974**, *344* (3), 241−261.
(373) Putz, G.; Goerke, J.; Clements, J. A. Surface Activity of Rabbit Pulmonary Surfactant Subfractions at Different Concentrations in a Captive Bubble. *J. Appl. Physiol.* **1994**, *77* (2), 597−605.
(374) Suzuki, Y.; Fujita, Y.; Kogishi, K. Reconstitution of Tubular Myelin from Synthetic Lipids and Proteins Associated with Pig Pulmonary Surfactant. *Am. Rev. Respir. Dis.* **1989**, *140*, 75−81.
(375) Ikegami, M.; Jobe, A. H.; Whitsett, J.; Korfhagen, T. Tolerance of SP-A-Deficient Mice to Hyperoxia or Exercise. *J. Appl. Physiol (1985)* **2000**, *89* (2), 644−648.
(376) Yu, S. H.; Possmayer, F. Effect of Pulmonary Surfactant Protein A and Neutral Lipid on Accretion and Organization of Dipalmitoylphosphatidylcholine in Surface Films. *J. Lipid Res.* **1996**, *37* (6), 1278−1288.
(377) Loney, R. W.; Anyan, W. R.; Biswas, S. C.; Rananavare, S. B.; Hall, S. B. The Accelerated Late Adsorption of Pulmonary Surfactant. *Langmuir* **2011**, *27* (8), 4857−4866.
(378) Jackman, J. A.; Cho, N.-J. Supported Lipid Bilayer Formation: Beyond Vesicle Fusion. *Langmuir* **2020**, *36* (6), 1387−1400.
(379) Richter, L.; Vollhardt, D. Force Measuring Methods for Determination of Surface Tension of Liquids: A Comparison. *Tenside Surfactants Detergents* **2006**, *43* (5), 256−261.
(380) Hamai, C.; Cremer, P. S.; Musser, S. M. Single Giant Vesicle Rupture Events Reveal Multiple Mechanisms of Glass-Supported Bilayer Formation. *Biophys. J.* **2007**, *92* (6), 1988−1999.
(381) Hamai, C.; Yang, T.; Kataoka, S.; Cremer, P. S.; Musser, S. M. Effect of Average Phospholipid Curvature on Supported Bilayer

https://doi.org/10.1021/acs.chemrev.3c00146
Chem. Rev. 2023, 123, 13209−13290

Formation on Glass by Vesicle Fusion. *Biophys. J.* **2006**, *90* (4), 1241−1248.
(382) Lind, T. K.; Cárdenas, M. Understanding the Formation of Supported Lipid Bilayers via Vesicle Fusion-A Case That Exemplifies the Need for the Complementary Method Approach (Review). *Biointerphases* **2016**, *11* (2), No. 020801.
(383) Schief, W. R.; Antia, M.; Discher, B. M.; Hall, S. B.; Vogel, V. Liquid-Crystalline Collapse of Pulmonary Surfactant Monolayers. *Biophys. J.* **2003**, *84* (6), 3792−3806.
(384) Alam Shibly, S. U.; Ghatak, C.; Sayem Karal, M. A.; Moniruzzaman, M.; Yamazaki, M. Experimental Estimation of Membrane Tension Induced by Osmotic Pressure. *Biophys. J.* **2016**, *111* (10), 2190−2201.
(385) Lipowsky, R. Multispherical Shapes of Vesicles Highlight the Curvature Elasticity of Biomembranes. *Adv. Colloid Interface Sci.* **2022**, *301*, No. 102613.
(386) Katsaras, J.; Pencer, J.; Nieh, M.-P.; Abraham, T.; Kučerka, N.; Harroun, T. A. Neutron and X-Ray Scattering from Isotropic and Aligned Membranes. *Structure and Dynamics of Membranous Interfaces*; John Wiley & Sons, Ltd, 2008; pp 107−134.
(387) Schürch, S.; Schürch, D.; Curstedt, T.; Robertson, B. Surface Activity of Lipid Extract Surfactant in Relation to Film Area Compression and Collapse. *J. Appl. Physiol.* **1994**, *77* (2), 974−986.
(388) Weibel, E. R. Morphological Basis of Alveolar-Capillary Gas Exchange. *Physiol Rev.* **1973**, *53* (2), 419−495.
(389) Yu, S. H.; Possmayer, F. Dipalmitoylphosphatidylcholine and Cholesterol in Monolayers Spread from Adsorbed Films of Pulmonary Surfactant. *J. Lipid Res.* **2001**, *42* (9), 1421−1429.
(390) Hall, S. B.; Venkitaraman, A. R.; Whitsett, J. A.; Holm, B. A.; Notter, R. H. Importance of Hydrophobic Apoproteins as Constituents of Clinical Exogenous Surfactants. *Am. Rev. Respir. Dis.* **1992**, *145* (1), 24−30.
(391) Wang, L.; Cai, P.; Galla, H. J.; He, H.; Flach, C. R.; Mendelsohn, R. Monolayer-Multilayer Transitions in a Lung Surfactant Model: IR Reflection-Absorption Spectroscopy and Atomic Force Microscopy. *European Biophys J.* **2005**, *34* (3), 243−254.
(392) Piknova, B.; Schram, V.; Hall, S. B. Pulmonary Surfactant: Phase Behavior and Function. *Curr. Opin Struct Biol.* **2002**, *12* (4), 487−494.
(393) Watkins, J. C. The Surface Properties of Pure Phospholipids in Relation to Those of Lung Extracts. *Biochim. Biophys. Acta* **1968**, *152* (2), 293−306.
(394) Bangham, A. D.; Morley, C. J.; Phillips, M. C. The Physical Properties of an Effective Lung Surfactant. *Biochim. Biophys. Acta* **1979**, *573* (3), 552−556.
(395) Zuo, Y. Y.; Possmayer, F. How Does Pulmonary Surfactant Reduce Surface Tension to Very Low Values? *J. Appl. Physiol.* **2007**, *102* (5), 1733−1734.
(396) Lee, K. Y. Collapse Mechanisms of Langmuir Monolayers. *Annu. Rev. Phys. Chem.* **2008**, *59*, 771−791.
(397) Fleming, B. D.; Keough, K. M. W. Surface Respreading after Collapse of Monolayers Containing Major Lipids of Pulmonary Surfactant. *Chem. Phys. Lipids.* **1988**, *49*, 81−86.
(398) Yan, W.; Biswas, S. C.; Laderas, T. G.; Hall, S. B. The Melting of Pulmonary Surfactant Monolayers. *J. Appl. Physiol.* **2007**, *102* (5), 1739−1745.
(399) Horie, T.; Hildebrandt, J. Dynamic Compliance, Limit Cycles, and Static Equilibria of Excised Cat Lung. *J. Appl. Physiol.* **1971**, *31* (3), 423−430.
(400) Inoue, H.; Inoue, C.; Hildebrandt, J. Temperature and Surface Forces in Excised Rabbit Lungs. *J. Appl. Physiol.* **1981**, *51* (4), 823−829.
(401) Tarczy-Hornoch, P.; Hildebrandt, J.; Mates, E. A.; Standaert, T. A.; Lamm, W. J.; Hodson, W. A.; Jackson, J. C. Effects of Exogenous Surfactant on Lung Pressure-Volume Characteristics During Liquid Ventilation. *J. Appl. Physiol.* **1996**, *80* (5), 1764−1771.
(402) de la Serna, J. B.; Oradd, G.; Bagatolli, L. A.; Simonsen, A. C.; Marsh, D.; Lindblom, G.; Perez-Gil, J. Segregated Phases in Pulmonary Surfactant Membranes Do Not Show Coexistence of Lipid Populations with Differentiated Dynamic Properties. *Biophys. J.* **2009**, *97* (5), 1381−1389.
(403) Bernardino de la Serna, J.; Hansen, S.; Berzina, Z.; Simonsen, A. C.; Hannibal-Bach, H. K.; Knudsen, J.; Ejsing, C. S.; Bagatolli, L. A. Compositional and Structural Characterization of Monolayers and Bilayers Composed of Native Pulmonary Surfactant from Wild Type Mice. *Biochim. Biophys. Acta* **2013**, *1828* (11), 2450−2459.
(404) Discher, B. M.; Schief, W. R.; Vogel, V.; Hall, S. B. Phase Separation in Monolayers of Pulmonary Surfactant Phospholipids at the Air-Water Interface: Composition and Structure. *Biophys. J.* **1999**, *77* (4), 2051−2061.
(405) Discher, B. M.; Maloney, K. M.; Grainger, D. W.; Sousa, C. A.; Hall, S. B. Neutral Lipids Induce Critical Behavior in Interfacial Monolayers of Pulmonary Surfactant. *Biochemistry* **1999**, *38* (1), 374−383.
(406) Piknova, B.; Schief, W. R.; Vogel, V.; Discher, B. M.; Hall, S. B. Discrepancy between Phase Behavior of Lung Surfactant Phospholipids and the Classical Model of Surfactant Function. *Biophys. J.* **2001**, *81* (4), 2172−2180.
(407) Pocivavsek, L.; Frey, S. L.; Krishan, K.; Gavrilov, K.; Ruchala, P.; Waring, A. J.; Walther, F. J.; Dennin, M.; Witten, T. A.; Lee, K. Y. Lateral Stress Relaxation and Collapse in Lipid Monolayers. *Soft Matter* **2008**, *4*, 2019−2029.
(408) Ding, J.; Takamoto, D. Y.; von Nahmen, A.; Lipp, M. M.; Lee, K. Y.; Waring, A. J.; Zasadzinski, J. A. Effects of Lung Surfactant Proteins, SP-B and SP-C, and Palmitic Acid on Monolayer Stability. *Biophys. J.* **2001**, *80* (5), 2262−2272.
(409) Bachofen, H.; Gerber, U.; Gehr, P.; Amrein, M.; Schürch, S. Structures of Pulmonary Surfactant Films Adsorbed to an Air-Liquid Interface in Vitro. *Biochim. Biophys. Acta* **2005**, *1720* (1−2), 59−72.
(410) Bi, X.; Taneva, S.; Keough, K. M. W.; Mendelsohn, R.; Flach, C. R. Thermal Stability and DPPC/Ca2+ Interactions of Pulmonary Surfactant SP-A from Bulk-Phase and Monolayer IR Spectroscopy. *Biochemistry* **2001**, *40* (45), 13659−13669.
(411) Crane, J. M.; Hall, S. B. Rapid Compression Transforms Interfacial Monolayers of Pulmonary Surfactant. *Biophys. J.* **2001**, *80* (4), 1863−1872.
(412) Smith, E. C.; Crane, J. M.; Laderas, T. G.; Hall, S. B. Metastability of a Supercompressed Fluid Monolayer. *Biophys. J.* **2003**, *85* (5), 3048−3057.
(413) Zhang, H.; Wang, Y. E.; Neal, C. R.; Zuo, Y. Y. Differential Effects of Cholesterol and Budesonide on Biophysical Properties of Clinical Surfactant. *Pediatr. Res.* **2012**, *71* (4), 316−323.
(414) Fan, Q.; Wang, Y. E.; Zhao, X.; Loo, J. S.; Zuo, Y. Y. Adverse Biophysical Effects of Hydroxyapatite Nanoparticles on Natural Pulmonary Surfactant. *ACS Nano* **2011**, *5* (8), 6410−6416.
(415) Ochs, M.; Nenadic, I.; Fehrenbach, A.; Albes, J. M.; Wahlers, T.; Richter, J.; Fehrenbach, H. Ultrastructural Alterations in Intraalveolar Surfactant Subtypes after Experimental Ischemia and Reperfusion. *Am. J. Respir Crit Care Med.* **1999**, *160* (2), 718−724.
(416) Al-Saiedy, M.; Tarokh, A.; Nelson, S.; Hossini, K.; Green, F.; Ling, C.-C.; Prenner, E. J.; Amrein, M. The Role of Multilayers in Preventing the Premature Buckling of the Pulmonary Surfactant. *Biochimica et Biophysica Acta (BBA) - Biomembranes* **2017**, *1859* (8), 1372−1380.
(417) Pocivavsek, L.; Gavrilov, K.; Cao, K. D.; Chi, E. Y.; Li, D.; Lin, B.; Meron, M.; Majewski, J.; Lee, K. Y. Glycerol-Induced Membrane Stiffening: The Role of Viscous Fluid Adlayers. *Biophys. J.* **2011**, *101* (1), 118−127.
(418) Sachan, A. K.; Zasadzinski, J. A. Interfacial Curvature Effects on the Monolayer Morphology and Dynamics of a Clinical Lung Surfactant. *Proc. Natl. Acad. Sci. U. S. A.* **2018**, *115* (2), E134−E143.
(419) Girard, M.; Bereau, T. Induced Asymmetries in Membranes. *Biophys. J.* **2023**, *122* (11), 2092−2098.
(420) Kumar, K.; Chavarha, M.; Loney, R. W.; Weiss, T. M.; Rananavare, S. B.; Hall, S. B. The L(Γ) Phase of Pulmonary Surfactant. *Langmuir* **2018**, *34* (22), 6601−6611.
(421) Keough, K. How Thin Can Glass Be? New Ideas, New Approaches. *Biophys. J.* **2003**, *85* (5), 2785−2786.

https://doi.org/10.1021/acs.chemrev.3c00146
Chem. Rev. 2023, 123, 13209−13290

(422) Nag, K.; Rodriguez-Capote, K.; Panda, A. K.; Frederick, L.; Hearn, S. A.; Petersen, N. O.; Schürch, S.; Possmayer, F. Disparate Effects of Two Phosphatidylcholine Binding Proteins, C-Reactive Protein and Surfactant Protein A, on Pulmonary Surfactant Structure and Function. *Am. J. Physiol Lung Cell Mol. Physiol* **2004**, *287* (6), L1145−1153.
(423) Saenz, A.; López-Sánchez, A.; Mojica-Lázaro, J.; Martínez-Caro, L.; Nin, N.; Bagatolli, L. A.; Casals, C. Fluidizing Effects of C-Reactive Protein on Lung Surfactant Membranes: Protective Role of Surfactant Protein A. *FASEB J.* **2010**, *24* (10), 3662−3673.
(424) Bailey, T. C.; Da Silva, K. A.; Lewis, J. F.; Rodriguez-Capote, K.; Possmayer, F.; Veldhuizen, R. A. W. Physiological and Inflammatory Response to Instillation of an Oxidized Surfactant in a Rat Model of Surfactant Deficiency. *J. Appl. Physiol (1985)* **2004**, *96* (5), 1674−1680.
(425) Bailey, T. C.; Maruscak, A. A.; Petersen, A.; White, S.; Lewis, J. F.; Veldhuizen, R. A. Physiological Effects of Oxidized Exogenous Surfactant in Vivo: Effects of High Tidal Volume and Surfactant Protein A. *Am. J. Physiol Lung Cell Mol. Physiol* **2006**, *291* (4), L703−709.
(426) Casals, C. Role of Surfactant Protein A (SP-A)/Lipid Interactions for SP-A Functions in the Lung. *Pediatr. Pathol. Mol. Med.* **2001**, *20* (4), 249−268.
(427) Cockshutt, A. M.; Weitz, J.; Possmayer, F. Pulmonary Surfactant-Associated Protein A Enhances the Surface Activity of Lipid Extract Surfactant and Reverses Inhibition by Blood Proteins in Vitro. *Biochemistry* **1990**, *29* (36), 8424−8429.
(428) Holm, B. A.; Wang, Z.; Notter, R. H. Multiple Mechanisms of Lung Surfactant Inhibition. *Pediatr. Res.* **1999**, *46* (1), 85−93.
(429) Milos, S.; Hiansen, J. Q.; Banaschewski, B.; Zuo, Y. Y.; Yao, L.-J.; McCaig, L. A.; Lewis, J.; Yamashita, C. M.; Veldhuizen, R. A. W. The Effect of Diet-Induced Serum Hypercholesterolemia on the Surfactant System and the Development of Lung Injury. *Biochem Biophys Rep* **2016**, *7*, 180−187.
(430) Hiansen, J. Q.; Keating, E.; Aspros, A.; Yao, L. J.; Bosma, K. J.; Yamashita, C. M.; Lewis, J. F.; Veldhuizen, R. A. Cholesterol-Mediated Surfactant Dysfunction Is Mitigated by Surfactant Protein A. *Biochim. Biophys. Acta* **2015**, *1848* (3), 813−820.
(431) Zasadzinski, J. A.; Alig, T. F.; Alonso, C.; de la Serna, J. B.; Perez-Gil, J.; Taeusch, H. W. Inhibition of Pulmonary Surfactant Adsorption by Serum and the Mechanisms of Reversal by Hydrophilic Polymers: Theory. *Biophys. J.* **2005**, *89* (3), 1621−1629.
(432) Zasadzinski, J. A.; Stenger, P. C.; Shieh, I.; Dhar, P. Overcoming Rapid Inactivation of Lung Surfactant: Analogies between Competitive Adsorption and Colloid Stability. *Biochim. Biophys. Acta* **2010**, *1798* (4), 801−828.
(433) Gunasekara, L. C.; Pratt, R. M.; Schoel, W. M.; Gosche, S.; Prenner, E. J.; Amrein, M. W. Methyl-Beta-Cyclodextrin Restores the Structure and Function of Pulmonary Surfactant Films Impaired by Cholesterol. *Biochim. Biophys. Acta* **2010**, *1798* (5), 986−994.
(434) Lopez-Rodriguez, E.; Cruz, A.; Richter, R. P.; Taeusch, H. W.; Pérez-Gil, J. Transient Exposure of Pulmonary Surfactant to Hyaluronan Promotes Structural and Compositional Transformations into a Highly Active State. *J. Biol. Chem.* **2013**, *288* (41), 29872−29881.
(435) Calkovska, A.; Some, M.; Linderholm, B.; Curstedt, T.; Robertson, B. Therapeutic Effects of Exogenous Surfactant Enriched with Dextran in Newborn Rabbits with Respiratory Failure Induced by Airway Instillation of Albumin. *Pulm Pharmacol Ther* **2008**, *21* (2), 393−400.
(436) Lu, K. W.; Taeusch, H. W.; Clements, J. A. Hyaluronan with Dextran Added to Therapeutic Lung Surfactants Improves Effectiveness in Vitro and in Vivo. *Exp Lung Res.* **2013**, *39* (4−5), 191−200.
(437) Campbell, H.; Bosma, K.; Brackenbury, A.; McCaig, L.; Yao, L. J.; Veldhuizen, R.; Lewis, J. Polyethylene Glycol (PEG) Attenuates Exogenous Surfactant in Lung-Injured Adult Rabbits. *Am. J. Respir Crit Care Med.* **2002**, *165* (4), 475−480.
(438) Ochs, M.; Hegermann, J.; Lopez-Rodriguez, E.; Timm, S.; Nouailles, G.; Matuszak, J.; Simmons, S.; Witzenrath, M.; Kuebler, W. M. On Top of the Alveolar Epithelium: Surfactant and the Glycocalyx. *Int. J. Mol. Sci.* **2020**, *21* (9), 3075.
(439) Rizzo, A. N.; Haeger, S. M.; Oshima, K.; Yang, Y.; Wallbank, A. M.; Jin, Y.; Lettau, M.; McCaig, L. A.; Wickersham, N. E.; McNeil, J. B.; Zakharevich, I.; McMurtry, S. A.; Langouët-Astrié, C. J.; Kopf, K. W.; Voelker, D. R.; Hansen, K. C.; Shaver, C. M.; Kerchberger, V. E.; Peterson, R. A.; Kuebler, W. M.; Ochs, M.; Veldhuizen, R. A.; Smith, B. J.; Ware, L. B.; Bastarache, J. A.; Schmidt, E. P. Alveolar Epithelial Glycocalyx Degradation Mediates Surfactant Dysfunction and Contributes to Acute Respiratory Distress Syndrome. *JCI Insight* **2022**, *7* (2), No. e154573.
(440) Gunasekara, L.; Schürch, S.; Schoel, W. M.; Nag, K.; Leonenko, Z.; Haufs, M.; Amrein, M. Pulmonary Surfactant Function Is Abolished by an Elevated Proportion of Cholesterol. *Biochim. Biophys. Acta* **2005**, *1737* (1), 27−35.
(441) Al-Saiedy, M.; Gunasekara, L.; Green, F.; Pratt, R.; Chiu, A.; Yang, A.; Dennis, J.; Pieron, C.; Bjornson, C.; Winston, B.; Amrein, M. Surfactant Dysfunction in ARDS and Bronchiolitis Is Repaired with Cyclodextrins. *Military medicine* **2018**, *183* (suppl_1), 207−215.
(442) Gunasekara, L.; Schoel, W. M.; Schürch, S.; Amrein, M. W. A Comparative Study of Mechanisms of Surfactant Inhibition. *Biochim. Biophys. Acta* **2008**, *1778* (2), 433−444.
(443) Leonenko, Z.; Gill, S.; Baoukina, S.; Monticelli, L.; Doehner, J.; Gunasekara, L.; Felderer, F.; Rodenstein, M.; Eng, L. M.; Amrein, M. An Elevated Level of Cholesterol Impairs Self-Assembly of Pulmonary Surfactant into a Functional Film. *Biophys. J.* **2007**, *93* (2), 674−683.
(444) Gunasekara, L.; Al-Saiedy, M.; Green, F.; Pratt, R.; Bjornson, C.; Yang, A.; Michael Schoel, W.; Mitchell, I.; Brindle, M.; Montgomery, M.; Keys, E.; Dennis, J.; Shrestha, G.; Amrein, M. Pulmonary Surfactant Dysfunction in Pediatric Cystic Fibrosis: Mechanisms and Reversal with a Lipid-Sequestering Drug. *J. Cyst Fibros* **2017**, *16* (5), 565−572.
(445) Zuo, Y. Y.; Uspal, W. E.; Wei, T. Airborne Transmission of COVID-19: Aerosol Dispersion, Lung Deposition, and Virus-Receptor Interactions. *ACS Nano* **2020**, *14* (12), 16502−16524.
(446) Xu, Y.; Li, S.; Luo, Z.; Ren, H.; Zhang, X.; Huang, F.; Zuo, Y. Y.; Yue, T. Role of Lipid Coating in the Transport of Nanodroplets across the Pulmonary Surfactant Layer Revealed by Molecular Dynamics Simulations. *Langmuir* **2018**, *34* (30), 9054−9063.
(447) Bakshi, M. S.; Zhao, L.; Smith, R.; Possmayer, F.; Petersen, N. O. Metal Nanoparticle Pollutants Interfere with Pulmonary Surfactant Function in Vitro. *Biophys. J.* **2008**, *94* (3), 855−868.
(448) Schleh, C.; Mühlfeld, C.; Pulskamp, K.; Schmiedl, A.; Nassimi, M.; Lauenstein, H. D.; Braun, A.; Krug, N.; Erpenbeck, V. J.; Hohlfeld, J. M. The Effect of Titanium Dioxide Nanoparticles on Pulmonary Surfactant Function and Ultrastructure. *Respir Res.* **2009**, *10* (1), 90.
(449) Baoukina, S.; Tieleman, D. P. Lung Surfactant Protein SP-B Promotes Formation of Bilayer Reservoirs from Monolayer and Lipid Transfer between the Interface and Subphase. *Biophys. J.* **2011**, *100* (7), 1678−1687.
(450) Baoukina, S.; Marrink, S. J.; Tieleman, D. P. Lateral Pressure Profiles in Lipid Monolayers. *Faraday Discuss.* **2010**, *144*, 393−409. Discussion 445−381.
(451) Yu, S. H.; Possmayer, F. Lipid Compositional Analysis of Pulmonary Surfactant Monolayers and Monolayer-Associated Reservoirs. *J. Lipid Res.* **2003**, *44* (3), 621−629.
(452) Bagatolli, L. A. To See or Not to See: Lateral Organization of Biological Membranes and Fluorescence Microscopy. *Biochim. Biophys. Acta* **2006**, *1758* (10), 1541−1556.
(453) Nag, K.; Pao, J. S.; Harbottle, R. R.; Possmayer, F.; Petersen, N. O.; Bagatolli, L. A. Segregation of Saturated Chain Lipids in Pulmonary Surfactant Films and Bilayers. *Biophys. J.* **2002**, *82* (4), 2041−2051.
(454) Katsaras, J.; Jeffrey, K. R. Evidence of the Hydration Force in Gel Phase Lipid Multibilayers. *Europhys. Lett.* **1997**, *38* (1), 43.

https://doi.org/10.1021/acs.chemrev.3c00146
Chem. Rev. 2023, 123, 13209−13290

(455) Knight, C.; Rahmani, A.; Morrow, M. R. Effect of an Anionic Lipid on the Barotropic Behavior of a Ternary Bicellar Mixture. *Langmuir* **2016**, *32* (40), 10259−10267.
(456) Rahmani, A.; Knight, C.; Morrow, M. R. Response to Hydrostatic Pressure of Bicellar Dispersions Containing an Anionic Lipid: Pressure-Induced Interdigitation. *Langmuir* **2013**, *29* (44), 13481−13490.
(457) Singh, H.; Emberley, J.; Morrow, M. R. Pressure Induces Interdigitation Differently in DPPC and DPPG. *European Biophys Journal* **2008**, *37* (6), 783−792.
(458) Yu, S.-H.; McCormack, F. X.; Voelker, D. R.; Possmayer, F. Interactions of Pulmonary Surfactant Protein SP-A with Monolayers of Dipalmitoylphosphatidylcholine and Cholesterol: Roles of SP-A Domains. *J. Lipid Res.* **1999**, *40* (5), 920−929.
(459) Bertocchi, C.; Ravasio, A.; Bernet, S.; Putz, G.; Dietl, P.; Haller, T. Optical Measurement of Surface Tension in a Miniaturized Air-Liquid Interface and Its Application in Lung Physiology. *Biophys. J.* **2005**, *89* (2), 1353−1361.
(460) Vanhecke, D.; Herrmann, G.; Graber, W.; Hillmann-Marti, T.; Mühlfeld, C.; Studer, D.; Ochs, M. Lamellar Body Ultrastructure Revisited: High-Pressure Freezing and Cryo-Electron Microscopy of Vitreous Sections. *Histochem Cell Biol.* **2010**, *134* (4), 319−326.
(461) Davoudi, S.; Ghysels, A. Defining Permeability of Curved Membranes in Molecular Dynamics Simulations. *Biophys. J.* **2023**, *122* (11), 2082−2091.
(462) Saito, H.; Shinoda, W. Cholesterol Effect on Water Permeability through DPPC and PSM Lipid Bilayers: A Molecular Dynamics Study. *J. Phys. Chem. B* **2011**, *115* (51), 15241−15250.
(463) Jackman, J. A.; Cho, N.-J. Supported Lipid Bilayer Formation: Beyond Vesicle Fusion. *Langmuir* **2020**, *36* (6), 1387−1400.
(464) Ikegami, M.; Jobe, A. H. Surfactant Protein Metabolism in Vivo. *Biochim. Biophys. Acta* **1998**, *1408* (2−3), 218−225.
(465) Ikegami, M.; Elhalwagi, B. M.; Palaniyar, N.; Dienger, K.; Korfhagen, T.; Whitsett, J. A.; McCormack, F. X. The Collagen-Like Region of Surfactant Protein A (SP-A) Is Required for Correction of Surfactant Structural and Functional Defects in the SP-A Null Mouse. *J. Biol. Chem.* **2001**, *276* (42), 38542−38548.
(466) Macklin, C. The Pulmonary Alveolar Mucoid Film and the Pneumonocytes. *Lancet* **1954**, *263*, 1099−1104.
(467) Williams, M. C. Conversion of Lamellar Body Membranes into Tubular Myelin in Alveoli of Fetal Rat Lungs. *J. Cell Biol.* **1977**, *72* (2), 260−277.
(468) Hallman, M.; Pohjavuori, M.; Järvenpää, A. L.; Bry, K.; Merritt, T. A.; Pesonen, E. Human Surfactant in the Treatment of Respiratory Distress Syndrome. A Spectrum of Clinical Responses. *Eur. Respir J. Suppl* **1989**, *3*, 77S−80S.
(469) Jobe, A. The Role of Surfactant in Neonatal Adaptation. *Semin. Perinatol.* **1988**, *12* (2), 113−123.
(470) Harding, R.; Hooper, S. B. Regulation of Lung Expansion and Lung Growth before Birth. *J. Appl. Physiol (1985)* **1996**, *81* (1), 209−224.
(471) Liggins, G.; Kitterman, J. Development of the Fetal Lung. In *The Fetus and Independent Life*; Pitman, 1981; Vol. *86*, pp 308−330.
(472) Liggins, G. C.; Howie, R. N. A Controlled Trial of Antepartum Glucocorticoid Treatment for Prevention of the Respiratory Distress Syndrome in Premature Infants. *Pediatrics* **1972**, *50* (4), 515−525.
(473) Vilos, G. A.; Liggins, G. C. Intrathoracic Pressures in Fetal Sheep. *J. Dev. Physiol.* **1982**, *4* (4), 247−256.
(474) Mullassery, D.; Smith, N. P. Lung Development. *Semin Pediatr Surg* **2015**, *24* (4), 152−155.
(475) Rebello, C. M.; Jobe, A. H.; Eisele, J. W.; Ikegami, M. Alveolar and Tissue Surfactant Pool Sizes in Humans. *Am. J. Respir Crit Care Med.* **1996**, *154* (3 Pt 1), 625−628.
(476) Egberts, J.; Sietaram, M. A. Postmortem Effects on the Yield and Composition of Alveolar Surfactant from Rat Lungs. *Respiration* **2004**, *57* (4), 254−258.
(477) Faridy, E. E.; Thliveris, J. Rate of Secretion of Lung Surfactant before and after Birth. *Respir Physiol* **1987**, *68* (3), 269−277.
(478) Hillman, N. H.; Kallapur, S. G.; Jobe, A. H. Physiology of Transition from Intrauterine to Extrauterine Life. *Clinics in Perinatology* **2012**, *39* (4), 769−783.
(479) Mason, R. J.; Nellenbogen, J.; Clements, J. A. Isolation of Disaturated Phosphatidylcholine with Osmium Tetroxide. *J. Lipid Res.* **1976**, *17* (3), 281−284.
(480) Holm, B. A.; Wang, Z.; Egan, E. A.; Notter, R. H. Content of Dipalmitoyl Phosphatidylcholine in Lung Surfactant: Ramifications for Surface Activity. *Pediatr. Res.* **1996**, *39* (5), 805−811.
(481) Nanjundan, M.; Possmayer, F. Pulmonary Phosphatidic Acid Phosphatase and Lipid Phosphate Phosphohydrolase. *Am. J. Physiol Lung Cell Mol. Physiol* **2003**, *284* (1), L1−23.
(482) Doyle, I. R.; Barr, H. A.; Nicholas, T. E. Distribution of Surfactant Protein a in Rat Lung. *Am. J. Respir. Cell Mol. Biol.* **1994**, *11* (4), 405−415.
(483) Frosolono, M.; Charms, B.; Pawlowski, R.; Slivka, S. Isolation, Characterization, and Surface Chemistry of a Surface-Active Fraction from Dog Lung. *J. Lipid Res.* **1970**, *11* (5), 439−457.
(484) Katyal, S.; Estes, L.; Lombardi, B. Method for the Isolation of Surfactant from Homogenates and Lavages of Lung of Adult, Newborn, and Fetal Rats. *Laboratory Investigation: A Journal of technical methods and pathology* **1977**, *36* (6), 585−592.
(485) Oulton, M.; Fraser, M.; Dolphin, M.; Yoon, R.; Faulkner, G. Quantification of Surfactant Pool Sizes in Rabbit Lung During Perinatal Development. *J. Lipid Res.* **1988**, *27* (6), 602−612.
(486) Sanders, R. L.; Hassett, R. J.; Vatter, A. E. Isolation of Lung Lamellar Bodies and Their Conversion to Tubular Myelin Figures in Vitro. *Anat Rec* **1980**, *198* (3), 485−501.
(487) Adams, F. H.; Fujiwara, T.; Emmanouilides, G. C.; Räihä, N. Lung Phospholipids of Human Fetuses and Infants with and without Hyaline Membrane Disease. *J. Pediatr* **1970**, *77* (5), 833−841.
(488) Adams, F. H. Origin of Fetal Lung Fluid. *J. Pediatr* **1965**, *67* (5), 1036−1037.
(489) Clements, J. A.; Tooley, W. H. Kinetics of Surface-Active Material in the Fetal Lung. In *Development of the Lung*; Hodson, W. A., Ed.; Marcel Dekker, 1977; pp 349−366.
(490) Torresin, M.; Zimmermann, L. J.; Cogo, P. E.; Cavicchioli, P.; Badon, T.; Giordano, G.; Zacchello, F.; Sauer, P. J.; Carnielli, V. P. Exogenous Surfactant Kinetics in Infant Respiratory Distress Syndrome: A Novel Method with Stable Isotopes. *Am. J. Respir Crit Care Med.* **2000**, *161* (5), 1584−1589.
(491) Hallman, M.; Merritt, T. A.; Pohjavuori, M.; Gluck, L. Effect of Surfactant Substitution on Lung Effluent Phospholipids in Respiratory Distress Syndrome: Evaluation of Surfactant Phospholipid Turnover, Pool Size, and the Relationship to Severity of Respiratory Failure. *Pediatr. Res.* **1986**, *20* (12), 1228−1235.
(492) Cogo, P. E.; Simonato, M.; Mariatoffolo, G.; Stefanutti, G.; Chierici, M.; Cobelli, C.; Ori, C.; Carnielli, V. P. Dexamethasone Therapy in Preterm Infants Developing Bronchopulmonary Dysplasia: Effect on Pulmonary Surfactant Disaturated-Phosphatidylcholine Kinetics. *Pediatr. Res.* **2008**, *63* (4), 433−437.
(493) Cogo, P.; Baritussio, A.; Rosso, F.; Gucciardi, A.; Moretti, V.; Badon, T.; Duner, E.; Zimmernann, L.; Carnielli, V. P. Surfactant-Associated Protein B Kinetics in Vivo in Newborn Infants by Stable Isotopes. *Pediatr. Res.* **2005**, *57* (4), 519−522.
(494) Carnielli, V. P.; Giorgetti, C.; Simonato, M.; Vedovelli, L.; Cogo, P. Neonatal Respiratory Diseases in the Newborn Infant: Novel Insights from Stable Isotope Tracer Studies. *Neonatology* **2016**, *109* (4), 325−333.
(495) Carnielli, V. P.; Zimmermann, L. J. I.; Hamvas, A.; Cogo, P. E. Pulmonary Surfactant Kinetics of the Newborn Infant: Novel Insights from Studies with Stable Isotopes. *J. Perinatol* **2009**, *29 Suppl 2*, S29−37.
(496) Enhörning, G.; Adams, F. H.; Norman, A. Effect of Lung Expansion on the Fetal Lamb Circulation. *Acta Paediatrica Scandinavica* **1966**, *55* (5), 441−451.
(497) Strang, L. B. The Lungs at Birth. *Arch Dis Child* **1965**, *40* (214), 575−582.

https://doi.org/10.1021/acs.chemrev.3c00146
Chem. Rev. 2023, 123, 13209−13290

(498) Gluck, L. Surfactant: 1972. *Pediatr Clin North Am.* **1972**, *19* (2), 325−331.
(499) Jobe, A. H. Pulmonary Surfactant Therapy. *N. Engl. J. Med.* **1993**, *328* (12), 861−868.
(500) Zimmermann, L.; Janssen, D.; Tibboel, D.; Hamvas, A.; Carnielli, V. Surfactant Metabolism in the Neonate. *Neonatology* **2005**, *87* (4), 296−307.
(501) Jackson, J. C.; Palmer, S.; Truog, W. E.; Standaert, T. A.; Murphy, J. H.; Hodson, W. A. Surfactant Quantity and Composition During Recovery from Hyaline Membrane Disease. *Pediatr. Res.* **1986**, *20* (12), 1243−1247.
(502) Jobe, A. H.; Ikegami, M. Biology of Surfactant. *Clinics in Perinatology* **2001**, *28* (3), 655−669, vii−viii. .
(503) Malloy, J. L.; Veldhuizen, R. A.; Lewis, J. F. Effects of Ventilation on the Surfactant System in Sepsis-Induced Lung Injury. *J. Appl. Physiol.* **2000**, *88* (2), 401−408.
(504) Hallman, M.; Glumoff, V.; Rämet, M. Surfactant in Respiratory Distress Syndrome and Lung Injury. *Comp Biochem Physiol A Mol. Integr Physiol* **2001**, *129* (1), 287−294.
(505) Lachmann, B.; Grossmann, G.; Nilsson, R.; Robertson, B. Lung Mechanics During Spontaneous Ventilation in Premature and Fullterm Rabbit Neonates. *Respir Physiol* **1979**, *38* (3), 283−302.
(506) Ikegami, M.; Rebello, C. M.; Jobe, A. H. Surfactant Inhibition by Plasma: Gestational Age and Surfactant Treatment Effects in Preterm Lambs. *J. Appl. Physiol.* **1996**, *81* (6), 2517−2522.
(507) Jobe, A. H. Mechanisms to Explain Surfactant Responses. *Neonatology* **2006**, *89* (4), 298−302.
(508) Kothe, T. B.; Kemp, M. W.; Schmidt, A.; Royse, E.; Salomone, F.; Clarke, M. W.; Musk, G. C.; Jobe, A. H.; Hillman, N. H. Surfactant plus Budesonide Decreases Lung and Systemic Inflammation in Mechanically Ventilated Preterm Sheep. *Am. J. Physiol Lung Cell Mol. Physiol* **2019**, *316* (5), L888−L893.
(509) Walther, F. J.; David-Cu, R.; Lopez, S. L. Antioxidant-Surfactant Liposomes Mitigate Hyperoxic Lung Injury in Premature Rabbits. *Am. J. Physiol.* **1995**, *269* (5 Pt 1), L613−617.
(510) Tingay, D. G.; Fatmous, M.; Kenna, K.; Dowse, G.; Douglas, E.; Sett, A.; Perkins, E. J.; Sourial, M.; Pereira-Fantini, P. M. Inflating Pressure and Not Expiratory Pressure Initiates Lung Injury at Birth in Preterm Lambs. *Am. J. Respir. Crit. Care Med.* **2023**, *208*, 589.
(511) Davies, I. M.; Polglase, G. R. Inflating or Overinflation? New Evidence for Lung Injury at Birth. *Am. J. Respir Crit Care Med.* **2023**, *208* (5), 517−518.
(512) Gitlin, D.; Craig, J. M. The Nature of the Hyaline Membrane in Asphyxia of the Newborn. *Pediatrics* **1956**, *17* (1), 64−71.
(513) Jackson, J. C.; Standaert, T. A.; Truog, W. E.; Murphy, J. H.; Palmer, S.; Chi, E. Y.; Woodrum, D. E.; Watchko, J.; Hodson, W. A. Changes in Lung Volume and Deflation Stability in Hyaline Membrane Disease. *J. Appl. Physiol.* **1985**, *59* (6), 1783−1789.
(514) Kang, M. H.; van Lieshout, L. P.; Xu, L.; Domm, J. M.; Vadivel, A.; Renesme, L.; Mühlfeld, C.; Hurskainen, M.; Mižíková, I.; Pei, Y.; van Vloten, J. P.; Thomas, S. P.; Milazzo, C.; Cyr-Depauw, C.; Whitsett, J. A.; Nogee, L. M.; Wootton, S. K.; Thébaud, B. A Lung Tropic AAV Vector Improves Survival in a Mouse Model of Surfactant B Deficiency. *Nat. Commun.* **2020**, *11* (1), 3929.
(515) Hamvas, A. Inherited Surfactant Protein-B Deficiency and Surfactant Protein-C Associated Disease: Clinical Features and Evaluation. *Semin Perinatol* **2006**, *30* (6), 316−326.
(516) Autilio, C.; Echaide, M.; Shankar-Aguilera, S.; Bragado, R.; Amidani, D.; Salomone, F.; Pérez-Gil, J.; De Luca, D. Surfactant Injury in the Early Phase of Severe Meconium Aspiration Syndrome. *Am. J. Respir. Cell Mol. Biol.* **2020**, *63* (3), 327−337.
(517) Herting, E.; Kribs, A.; Härtel, C.; von der Wense, A.; Weller, U.; Hoehn, T.; Vochem, M.; Möller, J.; Wieg, C.; Roth, B.; Göpel, W. Two-Year Outcome Data Suggest That Less Invasive Surfactant Administration (LISA) Is Safe. Results from the Follow-up of the Randomized Controlled AMV (Avoid Mechanical Ventilation) Study. *European journal of pediatrics* **2020**, *179* (8), 1309−1313.
(518) Härtel, C.; Glaser, K.; Speer, C. P. The Miracles of Surfactant: Less Invasive Surfactant Administration, Nebulization, and Carrier of Topical Drugs. *Neonatology* **2021**, *118* (2), 225−234.
(519) Mulrooney, N.; Champion, Z.; Moss, T. J.; Nitsos, I.; Ikegami, M.; Jobe, A. H. Surfactant and Physiologic Responses of Preterm Lambs to Continuous Positive Airway Pressure. *Am. J. Respir Crit Care Med.* **2005**, *171* (5), 488−493.
(520) Pérez-Gil, J. A Recipe for a Good Clinical Pulmonary Surfactant. *Biomedical Journal* **2022**, *45* (4), 615−628.
(521) Dizdar, E. A.; Sari, F. N.; Aydemir, C.; Oguz, S. S.; Erdeve, O.; Uras, N.; Dilmen, U. A Randomized, Controlled Trial of Poractant Alfa Versus Beractant in the Treatment of Preterm Infants with Respiratory Distress Syndrome. *Am. J. Perinatol* **2012**, *29* (2), 95−100.
(522) Singh, N.; Halliday, H. L.; Stevens, T. P.; Suresh, G.; Soll, R.; Rojas-Reyes, M. X. Comparison of Animal-Derived Surfactants for the Prevention and Treatment of Respiratory Distress Syndrome in Preterm Infants. *Cochrane database of systematic reviews* **2015**, *2015* (12), No. CD010249.
(523) Ramanathan, R.; Rasmussen, M. R.; Gerstmann, D. R.; Finer, N.; Sekar, K. A Randomized, Multicenter Masked Comparison Trial of Poractant Alfa (Curosurf) versus Beractant (Survanta) in the Treatment of Respiratory Distress Syndrome in Preterm Infants. *Am. J. Perinatol* **2004**, *21* (3), 109−119.
(524) Bastacky, J.; Lee, C. Y.; Goerke, J.; Koushafar, H.; Yager, D.; Kenaga, L.; Speed, T. P.; Chen, Y.; Clements, J. A. Alveolar Lining Layer Is Thin and Continuous: Low-Temperature Scanning Electron Microscopy of Rat Lung. *J. Appl. Physiol.* **1995**, *79* (5), 1615−1628.
(525) Wright, J. R.; Hawgood, S. Pulmonary Surfactant Metabolism. *Clin Chest Med.* **1989**, *10* (1), 83−93.
(526) Gurel, O.; Ikegami, M.; Chroneos, Z. C.; Jobe, A. H. Macrophage and Type II Cell Catabolism of SP-A and Saturated Phosphatidylcholine in Mouse Lungs. *Am. J. Physiol Lung Cell Mol. Physiol* **2001**, *280* (6), L1266−1272.
(527) Olmeda, B.; Martínez-Calle, M.; Pérez-Gil, J. Pulmonary Surfactant Metabolism in the Alveolar Airspace: Biogenesis, Extracellular Conversions, Recycling. *Annals of Anatomy - Anatomischer Anzeiger: official organ of the Anatomische Gesellschaft* **2017**, *209*, 78−92.
(528) Goss, V.; Hunt, A. N.; Postle, A. D. Regulation of Lung Surfactant Phospholipid Synthesis and Metabolism. *Biochim. Biophys. Acta* **2013**, *1831* (2), 448−458.
(529) Batenburg, J. J. Surfactant Phospholipids: Synthesis and Storage. *Am. J. Physiol Lung Cell Mol. Physiol* **1992**, *262* (4), L367−L385.
(530) Osanai, K.; Oikawa, R.; Higuchi, J.; Kobayashi, M.; Tsuchihara, K.; Iguchi, M.; Jongsu, H.; Toga, H.; Voelker, D. R. A Mutation in Rab38 Small GTPase Causes Abnormal Lung Surfactant Homeostasis and Aberrant Alveolar Structure in Mice. *Am. J. Path* **2008**, *173* (5), 1265−1274.
(531) Andreeva, A. V.; Kutuzov, M. A.; Voyno-Yasenetskaya, T. A. Regulation of Surfactant Secretion in Alveolar Type II Cells. *Am. J. Physiol Lung Cell Mol. Physiol* **2007**, *293* (2), L259−271.
(532) Beers, M. F.; Mulugeta, S. The Biology of the ABCA3 Lipid Transporter in Lung Health and Disease. *Cell Tissue Res.* **2017**, *367* (3), 481−493.
(533) Chai, A. B.; Ammit, A. J.; Gelissen, I. C. Examining the Role of ABC Lipid Transporters in Pulmonary Lipid Homeostasis and Inflammation. *Respir Res.* **2017**, *18* (1), 41.
(534) Rindler, T. N.; Stockman, C. A.; Filuta, A. L.; Brown, K. M.; Snowball, J. M.; Zhou, W.; Veldhuizen, R.; Zink, E. M.; Dautel, S. E.; Clair, G.; Ansong, C.; Xu, Y.; Bridges, J. P.; Whitsett, J. A. Alveolar Injury and Regeneration Following Deletion of ABCA3. *JCI Insight* **2017**, *2* (24), e97381. .
(535) Bridges, J. P.; Ludwig, M.-G.; Mueller, M.; Kinzel, B.; Sato, A.; Xu, Y.; Whitsett, J. A.; Ikegami, M. Orphan G Protein−Coupled Receptor GPR116 Regulates Pulmonary Surfactant Pool Size. *Am. J. Respir. Cell Mol. Biol.* **2013**, *49* (3), 348−357.

https://doi.org/10.1021/acs.chemrev.3c00146
Chem. Rev. 2023, 123, 13209−13290

(536) Wright, J. R.; Dobbs, L. G. Regulation of Pulmonary Surfactant Secretion and Clearance. *Annu. Rev. Physiol.* **1991**, *53*, 395−414.
(537) Wirtz, H.; Schmidt, M. Ventilation and Secretion of Pulmonary Surfactant. *Clinical Investigator* **1992**, *70* (1), 3−13.
(538) Diem, K.; Fauler, M.; Fois, G.; Hellmann, A.; Winokurow, N.; Schumacher, S.; Kranz, C.; Frick, M. Mechanical Stretch Activates Piezo1 in Caveolae of Alveolar Type I Cells to Trigger ATP Release and Paracrine Stimulation of Surfactant Secretion from Alveolar Type II Cells. *FASEB J.* **2020**, *34* (9), 12785−12804.
(539) Mishra, A. New Insights of P2 × 7 Receptor Signaling Pathway in Alveolar Functions. *J. Biomed Sci.* **2013**, *20* (1), 26.
(540) Ashino, Y.; Ying, X.; Dobbs, L. G.; Bhattacharya, J. [Ca(2+)](I) Oscillations Regulate Type II Cell Exocytosis in the Pulmonary Alveolus. *Am. J. Physiol Lung Cell Mol. Physiol* **2000**, *279* (1), L5−13.
(541) Brown, K.; Filuta, A.; Ludwig, M.-G.; Seuwen, K.; Jaros, J.; Vidal, S.; Arora, K.; Naren, A. P.; Kandasamy, K.; Parthasarathi, K.; Offermanns, S.; Mason, R. J.; Miller, W. E.; Whitsett, J. A.; Bridges, J. P. Epithelial Gpr116 Regulates Pulmonary Alveolar Homeostasis via Gq/11 Signaling. *JCI Insight* **2017**, *2* (11), e93700. .
(542) Islam, M. N.; Gusarova, G. A.; Monma, E.; Das, S. R.; Bhattacharya, J. F-Actin Scaffold Stabilizes Lamellar Bodies During Surfactant Secretion. *Am. J. Physiol Lung Cell Mol. Physiol* **2014**, *306* (1), L50−L57.
(543) Frick, M.; Eschertzhuber, S.; Haller, T.; Mair, N.; Dietl, P. Secretion in Alveolar Type II Cells at the Interface of Constitutive and Regulated Exocytosis. *Am. J. Respir. Cell Mol. Biol.* **2001**, *25* (3), 306−315.
(544) Korfhagen, T. R.; LeVine, A. M.; Whitsett, J. A. Surfactant Protein A (SP-A) Gene Targeted Mice. *Biochim. Biophys. Acta* **1998**, *1408* (2−3), 296−302.
(545) Hawgood, S.; Poulain, F. R. The Pulmonary Collectins and Surfactant Metabolism. *Annu. Rev. Physiol.* **2001**, *63* (1), 495−519.
(546) Kuroki, Y.; McCormack, F. X.; Ogasawara, Y.; Mason, R. J.; Voelker, D. R. Epitope Mapping for Monoclonal Antibodies Identifies Functional Domains of Pulmonary Surfactant Protein A That Interact with Lipids. *J. Biol. Chem.* **1994**, *269* (47), 29793−29800.
(547) Korfhagen, T. R.; Sheftelyevich, V.; Burhans, M. S.; Bruno, M. D.; Ross, G. F.; Wert, S. E.; Stahlman, M. T.; Jobe, A. H.; Ikegami, M.; Whitsett, J. A.; et al. Surfactant Protein-D Regulates Surfactant Phospholipid Homeostasis in Vivo. *J. Biol. Chem.* **1998**, *273* (43), 28438−28443.
(548) Ikegami, M. Surfactant Catabolism. *Respirology* **2006**, *11*, S24−7.
(549) Ikegami, M.; Weaver, T. E.; Grant, S. N.; Whitsett, J. A. Pulmonary Surfactant Surface Tension Influences Alveolar Capillary Shape and Oxygenation. *Am. J. Respir. Cell Mol. Biol.* **2009**, *41* (4), 433−439.
(550) Miles, P. R.; Ma, J. Y.; Bowman, L. Degradation of Pulmonary Surfactant Disaturated Phosphatidylcholines by Alveolar Macrophages. *J. Appl. Physiol (1985)* **1988**, *64* (6), 2474−2481.
(551) Whitsett, J.; Review, A. The Intersection of Surfactant Homeostasis and Innate Host Defense of the Lung: Lessons from Newborn Infants. *Innate Immun* **2010**, *16* (3), 138−142.
(552) Alkalai, J.; Iwata, A.; Lee, E.; Tarling, E. J.; Wang, T. Pulmonary Alveolar Proteinosis: An Overview and Emerging Therapeutics. **2023**. *touchREVIEWS in Respiratory & Pulmonary Diseases.* **2023**, *8* (1), 21−27.
(553) Wright, J. R.; Benson, B. J.; Williams, M. C.; Georke, J.; Clements, J. A. Protein Composition of Rabbit Alveolar Surfactant Subfractions. *Biochim. Biophys. Acta* **1984**, *791* (3), 320−332.
(554) Gross, N. J. Extracellular Metabolism of Pulmonary Surfactant: The Role of a New Serine Protease. *Annu. Rev. Physiol.* **1995**, *57*, 135−150.
(555) Gross, N. J.; Kellam, M.; Young, J.; Krishnasamy, S.; Dhand, R. Separation of Alveolar Surfactant into Subtypes. A Comparison of Methods. *Am. J. Respir Crit Care Med.* **2000**, *162* (2 Pt 1), 617−622.
(556) Veldhuizen, R.; Possmayer, F. Phospholipid Metabolism in Lung Surfactant. *Subcell Biochem* **2004**, *37*, 359−388.
(557) Lewis, J. F.; Ikegami, M.; Jobe, A. H. Altered Surfactant Function and Metabolism in Rabbits with Acute Lung Injury. *J. Appl. Physiol (1985)* **1990**, *69* (6), 2303−2310.
(558) Bruni, R.; Baritussio, A.; Quaglino, D.; Gabelli, C.; Benevento, M.; Ronchetti, I. P. Postnatal Transformations of Alveolar Surfactant in the Rabbit: Changes in Pool Size, Pool Morphology and Isoforms of the 32−38 Kda Apolipoprotein. *Biochim Biophys Acta (BBA)-Lipids and Lipid Metabolism* **1988**, *958* (2), 255−267.
(559) Baritussio, A.; Alberti, A.; Quaglino, D.; Pettenazzo, A.; Dalzoppo, D.; Sartori, L.; Pasquali-Ronchetti, I. SP-A, SP-B, and SP-C in Surfactant Subtypes around Birth: Reexamination of Alveolar Life Cycle of Surfactant. *Am. J. Physiol.* **1994**, *266* (4 Pt 1), L436−447.
(560) Putman, E.; Creuwels, L. A.; van Golde, L. M.; Haagsman, H. P. Surface Properties, Morphology and Protein Composition of Pulmonary Surfactant Subtypes. *Biochem. J.* **1996**, *320* (2), 599−605.
(561) Ueda, T.; Ikegami, M.; Jobe, A. Surfactant Subtypes. In Vitro Conversion, in Vivo Function, and Effects of Serum Proteins. *Am. J. Respir Crit Care Med.* **1994**, *149* (5), 1254−1259.
(562) Gross, N. J.; Bublys, V.; J, D. A.; Brown, C. L. The Role of Alpha 1-Antitrypsin in the Control of Extracellular Surfactant Metabolism. *Am. J. Physiol.* **1995**, *268* (3 Pt 1), L438−445.
(563) Baritussio, A. G.; Magoon, M. W.; Goerke, J.; Clements, J. A. Precursor-Product Relationship between Rabbit Type II Cell Lamellar Bodies and Alveolar Surface-Active Material. Surfactant Turnover Time. *Biochim. Biophys. Acta* **1981**, *666* (3), 382−393.
(564) Maruscak, A. A.; Vockeroth, D. W.; Girardi, B.; Sheikh, T.; Possmayer, F.; Lewis, J. F.; Veldhuizen, R. A. Alterations to Surfactant Precede Physiological Deterioration during High Tidal Volume Ventilation. *Am. J. Physiol Lung Cell Mol. Physiol* **2008**, *294* (5), L974−83.
(565) Gross, N. J. Surfactant Subtypes in Experimental Lung Damage: Radiation Pneumonitis. *Am. J. Physiol.* **1991**, *260* (4 Pt 1), L302−310.
(566) Doyle, I. R.; Morton, S.; Crockett, A. J.; Barr, H. A.; Davidson, K. G.; Jones, M. J.; Jones, M. E.; Nicholas, T. E. Composition of Alveolar Surfactant Changes with Training in Humans. *Respirology* **2000**, *5* (3), 211−220.
(567) Nicholas, T. E.; Power, J. H.; Barr, H. A. Surfactant Homeostasis in the Rat Lung during Swimming Exercise. *J. Appl. Physiol.-Respir. Environ. Exerc. Physiol.* **1982**, *53* (6), 1521−1528.
(568) Veldhuizen, R. A.; Inchley, K.; Hearn, S. A.; Lewis, J. F.; Possmayer, F. Degradation of Surfactant-Associated Protein B (SP-B) During in Vitro Conversion of Large to Small Surfactant Aggregates. *Biochem. J.* **1993**, *295* (Pt 1), 141−147.
(569) Mühlfeld, C.; Becker, L.; Bussinger, C.; Vollroth, M.; Nagib, R.; Schaefer, I.-M.; Knudsen, L.; Richter, J.; Madershahian, N.; Wahlers, T. Exogenous Surfactant in Ischemia/Reperfusion: Effects on Endogenous Surfactant Pools. *J. Heart Lung Transplant.* **2010**, *29* (3), 327−334.
(570) Savov, J.; Silbajoris, R.; Young, S. L. Mechanical Ventilation of Rat Lung: Effect on Surfactant Forms. *Am. J. Physiol.* **1999**, *277* (2), L320−326.
(571) Schmiedl, A.; Hoymann, H.-G.; Ochs, M.; Menke, A.; Fehrenbach, A.; Krug, N.; Tschernig, T.; Hohlfeld, J. M. Increase of Inactive Intra-Alveolar Surfactant Subtypes in Lungs of Asthmatic Brown Norway Rats. *Virchows Arch* **2003**, *442* (1), 56−65.
(572) Brackenbury, A. M.; Malloy, J. L.; McCaig, L. A.; Yao, L. J.; Veldhuizen, R. a. W.; Lewis, J. F. Evaluation of Alveolar Surfactant Aggregates in Vitro and in Vivo. *Eur. Respir. J.* **2002**, *19* (1), 41−46.
(573) Yamada, T.; Ikegami, M.; Jobe, A. H. Effects of Surfactant Subfractions on Preterm Rabbit Lung Function. *Pediatr. Res.* **1990**, *27* (6), 592−598.
(574) Ochs, M.; Johnen, G.; Muller, K.-M.; Wahlers, T.; Hawgood, S.; Richter, J.; Brasch, F. Intracellular and Intraalveolar Localization of Surfactant Protein A (SP-A) in the Parenchymal Region of the Human Lung. *Am. J. Respir. Cell Mol. Biol.* **2002**, *26* (1), 91−98.

https://doi.org/10.1021/acs.chemrev.3c00146
Chem. Rev. 2023, 123, 13209−13290

(575) (575) Savov, J.; Wright, J. R.; Young, S. L. Incorporation of Biotinylated SP-A into Rat Lung Surfactant Layer, Type II Cells, and Clara Cells. *Am. J. Physiol Lung Cell Mol. Physiol* **2000**, *279* (1), L118−126.
(576) Baritussio, A.; Benevento, M.; Pettenazzo, A.; Bruni, R.; Santucci, A.; Dalzoppo, D.; Barcaglioni, P.; Crepaldi, G. The Life Cycle of a Low-Molecular-Weight Protein of Surfactant (SP-C) in 3-Day-Old Rabbits. *Biochim. Biophys. Acta* **1989**, *1006* (1), 19−25.
(577) Matthay, M. A.; Zemans, R. L.; Zimmerman, G. A.; Arabi, Y. M.; Beitler, J. R.; Mercat, A.; Herridge, M.; Randolph, A. G.; Calfee, C. S. Acute Respiratory Distress Syndrome. *Nature reviews. Disease primers* **2019**, *5* (1), 18.
(578) Bosma, K. J.; Taneja, R.; Lewis, J. F. Pharmacotherapy for Prevention and Treatment of Acute Respiratory Distress Syndrome: Current and Experimental Approaches. *Drugs* **2010**, *70* (10), 1255−1282.
(579) Maruscak, A.; Lewis, J. F. Exogenous Surfactant Therapy for ARDS. *Expert Opin Investig Drugs* **2006**, *15* (1), 47−58.
(580) Smith, B. J.; Roy, G. S.; Cleveland, A.; Mattson, C.; Okamura, K.; Charlebois, C. M.; Hamlington, K. L.; Novotny, M. V.; Knudsen, L.; Ochs, M.; Hite, R. D.; Bates, J. H. T. Three Alveolar Phenotypes Govern Lung Function in Murine Ventilator-Induced Lung Injury. *Front physiol* **2020**, *11*, 660.
(581) Meng, H.; Sun, Y.; Lu, J.; Fu, S.; Meng, Z.; Scott, M.; Li, Q. Exogenous Surfactant May Improve Oxygenation but Not Mortality in Adult Patients with Acute Lung Injury/Acute Respiratory Distress Syndrome: A Meta-Analysis of 9 Clinical Trials. *Journal of Cardiothoracic and Vascular Anesthesia* **2012**, *26* (5), 849−856.
(582) Willson, D. F.; Notter, R. H. The Future of Exogenous Surfactant Therapy. *Respiratory Care* **2011**, *56* (9), 1369−1388.
(583) Fan, E.; Brodie, D.; Slutsky, A. S. Acute Respiratory Distress Syndrome: Advances in Diagnosis and Treatment. *JAMA* **2018**, *319* (7), 698−710.
(584) Veldhuizen, R. A.; Tremblay, L. N.; Govindarajan, A.; van Rozendaal, B. A.; Haagsman, H. P.; Slutsky, A. S. Pulmonary Surfactant Is Altered during Mechanical Ventilation of Isolated Rat Lung. *Crit Care Med.* **2000**, *28* (7), 2545−2551.
(585) Veldhuizen, R. A. W.; Slutsky, A. S.; Joseph, M.; McCaig, L. Effects of Mechanical Ventilation of Isolated Mouse Lungs on Surfactant and Inflammatory Cytokines. *Eur. Respir. J.* **2001**, *17* (3), 488−494.
(586) Cockshutt, A. M.; Possmayer, F. Lysophosphatidylcholine Sensitizes Lipid Extracts of Pulmonary Surfactant to Inhibition by Serum Proteins. *Biochim. Biophys. Acta* **1991**, *1086* (1), 63−71.
(587) Hite, R. D.; Seeds, M. C.; Jacinto, R. B.; Grier, B. L.; Waite, B. M.; Bass, D. A. Lysophospholipid and Fatty Acid Inhibition of Pulmonary Surfactant: Non-Enzymatic Models of Phospholipase A2 Surfactant Hydrolysis. *Biochim. Biophys. Acta* **2005**, *1720* (1−2), 14−21.
(588) Mulugeta, S.; Beers, M. F. Surfactant Protein C: Its Unique Properties and Emerging Immunomodulatory Role in the Lung. *Microbes Infect* **2006**, *8* (8), 2317−2323.
(589) Simonato, M.; Baritussio, A.; Ori, C.; Vedovelli, L.; Rossi, S.; Massara, L. D.; Rizzi, S.; Carnielli, V. P.; Cogo, P. E. Disaturated-Phosphatidylcholine and Surfactant Protein-B Turnover in Human Acute Lung Injury and in Control Patients. *Respir Res.* **2011**, *12* (1), 36.
(590) Sinnberg, T.; Lichtensteiger, C.; Ali, O. H.; Pop, O. T.; Jochum, A.-K.; Risch, L.; Brugger, S. D.; Velic, A.; Bomze, D.; Kohler, P.; Vernazza, P.; Albrich, W. C.; Kahlert, C. R.; Abdou, M.-T.; Wyss, N.; Hofmeister, K.; Niessner, H.; Zinner, C.; Gilardi, M.; Tzankov, A.; Röcken, M.; Dulovic, A.; Shambat, S. M.; Ruetalo, N.; Buehler, P. K.; Scheier, T. C.; Jochum, W.; Kern, L.; Henz, S.; Schneider, T.; Kuster, G. M.; Lampart, M.; Siegemund, M.; Bingisser, R.; Schindler, M.; Schneiderhan-Marra, N.; Kalbacher, H.; McCoy, K. D.; Spengler, W.; Brutsche, M. H.; Maček, B.; Twerenbold, R.; Penninger, J. M.; Matter, M. S.; Flatz, L. Pulmonary Surfactant Proteins Are Inhibited by Immunoglobulin A Autoantibodies in Severe COVID-19. *Am. J. Respir Crit Care Med.* **2023**, *207* (1), 38−49.
(591) Malloy, J. L.; Wright, J. R. In Vivo Clearance of Surfactant Lipids During Acute Pulmonary Inflammation. *Respir Res.* **2004**, *5* (1), 8.
(592) Kermeen, F.; McNeil, K.; Fraser, J.; McCarthy, J.; Ziegenfuss, M.; Mullany, D.; Dunning, J.; Hopkins, P. Resolution of Severe Ischemia−Reperfusion Injury Post−Lung Transplantation after Administration of Endobronchial Surfactant. *J. Heart Lung Transplant* **2007**, *26* (8), 850−856.
(593) Nakajima, D.; Liu, M.; Ohsumi, A.; Kalaf, R.; Iskender, I.; Hsin, M.; Kanou, T.; Chen, M.; Baer, B.; Coutinho, R.; Maahs, L.; Behrens, P.; Azad, S.; Martinu, T.; Waddell, T. K.; Lewis, J. F.; Post, M.; Veldhuizen, R. A. W.; Cypel, M.; Keshavjee, S. Lung Lavage and Surfactant Replacement During Ex Vivo Lung Perfusion for Treatment of Gastric Acid Aspiration-Induced Donor Lung Injury. *J. Heart Lung Transplant* **2017**, *36* (5), 577−585.
(594) Olortegui-Rodriguez, J. J.; Soriano-Moreno, D. R.; Benites-Bullón, A.; Pelayo-Luis, P. P.; Huaringa-Marcelo, J. Prevalence and Incidence of Chronic Obstructive Pulmonary Disease in Latin America and the Caribbean: A Systematic Review and Meta-Analysis. *BMC Pulm Med.* **2022**, *22* (1), 273.
(595) Schmidt, R.; Meier, U.; Markart, P.; Grimminger, F.; Velcovsky, H.; Morr, H.; Seeger, W.; Gunther, A. Altered Fatty Acid Composition of Lung Surfactant Phospholipids in Interstitial Lung Disease. *Am. J. Physiol Lung Cell Mol. Physiol* **2002**, *283* (5), L1079−L1085.
(596) Willson, D. F.; Thomas, N. J.; Markovitz, B. P.; Bauman, L. A.; DiCarlo, J. V.; Pon, S.; Jacobs, B. R.; Jefferson, L. S.; Conaway, M. R.; Egan, E. A. Pediatric Acute Lung Injury and Sepsis Investigators, for the. Effect of Exogenous Surfactant (Calfactant) in Pediatric Acute Lung InjuryA Randomized Controlled Trial. *JAMA* **2005**, *293* (4), 470−476.
(597) Raghavendran, K.; Willson, D.; Notter, R. H. Surfactant Therapy for Acute Lung Injury and Acute Respiratory Distress Syndrome. *Crit Care Clin* **2011**, *27* (3), 525−559.
(598) Willson, D. F.; Thomas, N. J.; Tamburro, R.; Truemper, E.; Truwit, J.; Conaway, M.; Traul, C.; Egan, E. E. Pediatric Calfactant in Acute Respiratory Distress Syndrome Trial. *Pediatr Crit Care Med.* **2013**, *14* (7), 657−665.
(599) Spragg, R. G.; Lewis, J. F.; Walmrath, H. D.; Johannigman, J.; Bellingan, G.; Laterre, P. F.; Witte, M. C.; Richards, G. A.; Rippin, G.; Rathgeb, F.; et al. Effect of Recombinant Surfactant Protein C-Based Surfactant on the Acute Respiratory Distress Syndrome. *N Engl J. Med.* **2004**, *351* (9), 884−892.
(600) Rynkiewicz, M. J.; Wu, H.; Cafarella, T. R.; Nikolaidis, N. M.; Head, J. F.; Seaton, B. A.; McCormack, F. X. Differential Ligand Binding Specificities of the Pulmonary Collectins Are Determined by the Conformational Freedom of a Surface Loop. *Biochemistry* **2017**, *56* (31), 4095−4105.
(601) Chang, Y.; Wang, Z.; Schwan, A. L.; Wang, Z.; Holm, B. A.; Baatz, J. E.; Notter, R. H. Surface Properties of Sulfur-and Ether-Linked Phosphonolipids with and without Purified Hydrophobic Lung Surfactant Proteins. *Chem. Physics Lipids* **2005**, *137* (1−2), 77−93.
(602) Czyzewski, A. M.; McCaig, L. M.; Dohm, M. T.; Broering, L. A.; Yao, L. J.; Brown, N. J.; Didwania, M. K.; Lin, J. S.; Lewis, J. F.; Veldhuizen, R.; Barron, A. E. Effective in Vivo Treatment of Acute Lung Injury with Helical, Amphipathic Peptoid Mimics of Pulmonary Surfactant Proteins. *Sci. Rep.* **2018**, *8* (1), 6795.
(603) Novick, R. J.; Possmayer, F.; Veldhuizen, R. A.; Menkis, A. H.; McKenzie, F. N. Surfactant Analysis and Replacement Therapy: A Future Tool of the Lung Transplant Surgeon? *Annu. Thorac Surg* **1991**, *52* (5), 1194−1200.
(604) Daniher, D.; McCaig, L.; Ye, Y.; Veldhuizen, R.; Lewis, J.; Ma, Y.; Zhu, J. Protective Effects of Aerosolized Pulmonary Surfactant Powder in a Model of Ventilator-Induced Lung Injury. *Int. J. Pharm.* **2020**, *583*, No. 119359.
(605) Cummings, J. J.; Gerday, E.; Minton, S.; Katheria, A.; Albert, G.; Flores-Torres, J.; Famuyide, M.; Lampland, A.; Guthrie, S.; Kuehn, D.; Weitkamp, J. H.; Fort, P.; Abu Jawdeh, E. G.; Ryan, R. M.;

https://doi.org/10.1021/acs.chemrev.3c00146
Chem. Rev. 2023, 123, 13209−13290

Martin, G. C.; Swanson, J. R.; Mulrooney, N.; Eyal, F.; Gerstmann, D.; Kumar, P.; Wilding, G. E.; Egan, E. A. Aerosolized Calfactant for Newborns With Respiratory Distress: A Randomized Trial. *Pediatrics* **2020**, *146* (5), DOI: 10.1542/peds.2019-3967.

(606) Younis, U. S.; Chu, H. W.; Kraft, M.; Ledford, J. G. A 20-Mer Peptide Derived from the Lectin Domain of SP-A2 Decreases Tumor Necrosis Factor Alpha Production during Mycoplasma Pneumoniae Infection. *Infection and immunity* **2020**, *88* (9), DOI: 10.1128/IAI.00099-20.

(607) Carcaterra, M.; Caruso, C. Alveolar Epithelial Cell Type II as Main Target of SARS-CoV-2 Virus and COVID-19 Development via NF-Kb Pathway Deregulation: A Physio-Pathological Theory. *Medical hypotheses* **2021**, *146*, No. 110412.

(608) Chaudhary, R.; Garg, J.; Houghton, D. E.; Murad, M. H.; Kondur, A.; Chaudhary, R.; Wysokinski, W. E.; McBane, R. D., 2nd. Thromboinflammatory Biomarkers in COVID-19: Systematic Review and Meta-Analysis of 17,052 Patients. *Mayo Clin Proc. Innov Qual Outcomes* **2021**, *5* (2), 388−402.

(609) Horie, S.; McNicholas, B.; Rezoagli, E.; Pham, T.; Curley, G.; McAuley, D.; O'Kane, C.; Nichol, A.; Dos Santos, C.; Rocco, P. R. M.; Bellani, G.; Laffey, J. G. Emerging Pharmacological Therapies for ARDS: COVID-19 and Beyond. *Intensive Care Med.* **2020**, *46* (12), 2265−2283.

(610) Dani, C.; Talosi, G.; Piccinno, A.; Ginocchio, V. M.; Balla, G.; Lavizzari, A.; Stranak, Z.; Gitto, E.; Martinelli, S.; Plavka, R.; Krolak-Olejnik, B.; Lista, G.; Spedicato, F.; Ciurlia, G.; Santoro, D.; Sweet, D.; CURONEB Study Group.. A Randomized, Controlled Trial to Investigate the Efficacy of Nebulized Poractant Alfa in Premature Babies with Respiratory Distress Syndrome. *J. Pediatr* **2022**, *246*, 40−47.e5.

(611) Minocchieri, S.; Knoch, S.; Schoel, W. M.; Ochs, M.; Nelle, M. Nebulizing Poractant Alfa versus Conventional Instillation: Ultrastructural Appearance and Preservation of Surface Activity. *Pediatr Pulmonol* **2014**, *49* (4), 348−356.

(612) Postle, A. D.; Clark, H. W.; Fink, J.; Madsen, J.; Koster, G.; Panchal, M.; Djukanovic, R.; Brealey, D.; Grocott, M. P. W.; Dushianthan, A. Rapid Phospholipid Turnover after Surfactant Nebulization in Severe COVID-19 Infection: A Randomized Clinical Trial. *Am. J. Respir Crit Care Med.* **2022**, *205* (4), 471−473.

(613) Walther, F. J.; Waring, A. J.; Otieno, M.; DiBlasi, R. M. Efficacy, Dose-Response, and Aerosol Delivery of Dry Powder Synthetic Lung Surfactant Treatment in Surfactant-Deficient Rabbits and Premature Lambs. *Respir Res.* **2022**, *23* (1), 78.

(614) Walther, F. J.; Waring, A. J. Aerosol Delivery of Lung Surfactant and Nasal CPAP in the Treatment of Neonatal Respiratory Distress Syndrome. *Front Pediatr* **2022**, *10*, No. 923010.

(615) Loganathan, S.; Kuppusamy, M.; Wankhar, W.; Gurugubelli, K. R.; Mahadevappa, V. H.; Lepcha, L.; Choudhary, A. K. Angiotensin-Converting Enzyme 2 (ACE2): COVID 19 Gate Way to Multiple Organ Failure Syndromes. *Respir Physiol Neurobiol* **2021**, *283*, No. 103548.

(616) Nair, A. B.; Cohen, M. J.; Flori, H. R. Clinical Characteristics, Major Morbidity, and Mortality in Trauma-Related Pediatric Acute Respiratory Distress Syndrome. *Pediatric Crit Care Med.* **2020**, *21* (2), 122−128.

(617) Villar, J.; Zhang, H.; Slutsky, A. S. Lung Repair and Regeneration in ARDS: Role of Pecam1 and Wnt Signaling. *Chest* **2019**, *155* (3), 587−594.

(618) Pioselli, B.; Salomone, F.; Mazzola, G.; Amidani, D.; Sgarbi, E.; Amadei, F.; Murgia, X.; Catinella, S.; Villetti, G.; De Luca, D.; et al. Pulmonary Surfactant: A Unique Biomaterial with Life-Saving Therapeutic Applications. *Curr. Med. Chem.* **2022**, *29* (3), 526−590.

(619) Bernhard, W.; Hoffmann, S.; Dombrowsky, H.; Rau, G. A.; Kamlage, A.; Kappler, M.; Haitsma, J. J.; Freihorst, J.; von der Hardt, H.; Poets, C. F. Phosphatidylcholine Molecular Species in Lung Surfactant: Composition in Relation to Respiratory Rate and Lung Development. *Am. J. Respir. Cell Mol. Biol.* **2001**, *25* (6), 725−731.

(620) Bernhard, W.; Schmiedl, A.; Koster, G.; Orgeig, S.; Acevedo, C.; Poets, C. F.; Postle, A. D. Developmental Changes in Rat Surfactant Lipidomics in the Context of Species Variability. *Pediatric pulmonology* **2007**, *42* (9), 794−804.

(621) Egberts, J.; Beintema-Dubbeldam, A.; de Boers, A. Phosphatidylinositol and Not Phosphatidylglycerol Is the Important Minor Phospholipid in Rhesus-Monkey Surfactant. *Biochim. Biophys. Acta* **1987**, *919* (1), 90−92.

(622) Rau, G. A.; Vieten, G.; Haitsma, J. J.; Freihorst, J.; Poets, C.; Ure, B. M.; Bernhard, W. Surfactant in Newborn Compared with Adolescent Pigs: Adaptation to Neonatal Respiration. *Am. J. Respir. Cell Mol. Biol.* **2004**, *30* (5), 694−701.

(623) Jiao, X.; Keating, E.; Tadayyon, S.; Possmayer, F.; Zuo, Y. Y.; Veldhuizen, R. A. Atomic Force Microscopy Analysis of Rat Pulmonary Surfactant Films. *Biophys Chem.* **2011**, *158* (2−3), 119−125.

(624) Lang, C. J.; Postle, A. D.; Orgeig, S.; Possmayer, F.; Bernhard, W.; Panda, A. K.; Jurgens, K. D.; Milsom, W. K.; Nag, K.; Daniels, C. B. Dipalmitoylphosphatidylcholine Is Not the Major Surfactant Phospholipid Species in All Mammals. *Am. J. Physiol Regul Integr Comp Physiol* **2005**, *289* (5), R1426−39.

(625) Orgeig, S.; Bernhard, W.; Biswas, S. C.; Daniels, C. B.; Hall, S. B.; Hetz, S. K.; Lang, C. J.; Maina, J. N.; Panda, A. K.; Perez-Gil, J.; Possmayer, F.; Veldhuizen, R. A.; Yan, W. The Anatomy, Physics, and Physiology of Gas Exchange Surfaces: Is There a Universal Function for Pulmonary Surfactant in Animal Respiratory Structures? *Integrative and Comparative Biology* **2007**, *47* (4), 610−627.

(626) Daniels, C. B.; Orgeig, S. Pulmonary Surfactant: The Key to the Evolution of Air Breathing. *Physiology* **2003**, *18*, 151−157.

(627) Ridsdale, R.; Roth-Kleiner, M.; D'Ovidio, F.; Unger, S.; Yi, M.; Keshavjee, S.; Tanswell, A. K.; Post, M. Surfactant Palmitoylmyristoylphosphatidylcholine Is a Marker for Alveolar Size During Disease. *Am. J. Respir Crit Care Med.* **2005**, *172* (2), 225−232.

(628) Suri, L. N.; McCaig, L.; Picardi, M. V.; Ospina, O. L.; Veldhuizen, R. A.; Staples, J. F.; Possmayer, F.; Yao, L. J.; Perez-Gil, J.; Orgeig, S. Adaptation to Low Body Temperature Influences Pulmonary Surfactant Composition Thereby Increasing Fluidity While Maintaining Appropriately Ordered Membrane Structure and Surface Activity. *Biochim. Biophys. Acta* **2012**, *1818* (7), 1581−1589.

(629) Suri, L. N.; Cruz, A.; Veldhuizen, R. A.; Staples, J. F.; Possmayer, F.; Orgeig, S.; Perez-Gil, J. Adaptations to Hibernation in Lung Surfactant Composition of 13-Lined Ground Squirrels Influence Surfactant Lipid Phase Segregation Properties. *Biochim. Biophys. Acta* **2013**, *1828* (8), 1707−1714.

(630) Daniels, C. B.; Orgeig, S.; Smits, A. W. The Composition and Function of Reptilian Pulmonary Surfactant. *Respir Physiol* **1995**, *102* (2−3), 121−135.

(631) Daniels, C. B.; Barr, H. A.; Power, J. H.; Nicholas, T. E. Body Temperature Alters the Lipid Composition of Pulmonary Surfactant in the Lizard Ctenophorus Nuchalis. *Exp Lung Res.* **1990**, *16* (5), 435−449.

(632) Orgeig, S.; Daniels, C. B. The Roles of Cholesterol in Pulmonary Surfactant: Insights from Comparative and Evolutionary Studies. *Comp Biochem Physiol A Mol. Integr Physiol* **2001**, *129* (1), 75−89.

(633) Codd, J. R.; Daniels, C. B.; Orgeig, S. Thermal Cycling of the Pulmonary Surfactant System in Small Heterothermic Mammals. *Life in the Cold*; Springer, 2000; pp 187−197.

(634) Daniels, C. B.; Orgeig, S. The Comparative Biology of Pulmonary Surfactant: Past, Present and Future. *Comp Biochem Physiol A Mol. Integr Physiol* **2001**, *129* (1), 9−36.

(635) Langman, C.; Orgeig, S.; Daniels, C. B. Alterations in Composition and Function of Surfactant Associated with Torpor in Sminthopsis Crassicaudata. *Am. J. Physiol.* **1996**, *271* (2 Pt 2), R437−445.

(636) Lopatko, O. V.; Orgeig, S.; Palmer, D.; Schürch, S.; Daniels, C. B. Alterations in Pulmonary Surfactant after Rapid Arousal from Torpor in the Marsupial Sminthopsis Crassicaudata. *J. Appl. Physiol.* **1999**, *86* (6), 1959−1970.

(637) Schipke, J.; Jütte, D.; Brandenberger, C.; Autilio, C.; Perez-Gil, J.; Bernhard, W.; Ochs, M.; Mühlfeld, C. Dietary Carbohydrates and

Fat Induce Distinct Surfactant Alterations in Mice. *Am. J. Respir. Cell Mol. Biol.* **2021**, *64* (3), 379−390.
(638) Foot, N. J.; Orgeig, S.; Daniels, C. B. The Evolution of a Physiological System: The Pulmonary Surfactant System in Diving Mammals. *Respir Physiol Neurobiol* **2006**, *154* (1−2), 118−138.
(639) Beck, D. C.; Na, C. L.; Whitsett, J. A.; Weaver, T. E. Ablation of a Critical Surfactant Protein B Intramolecular Disulfide Bond in Transgenic Mice. *J. Biol. Chem.* **2000**, *275* (5), 3371−3376.
(640) Weaver, T. E.; Beck, D. C. Use of Knockout Mice to Study Surfactant Protein Structure and Function. *Biol. Neonate* **1999**, *76 Suppl 1*, 15−18.
(641) Bridges, J. P.; Weaver, T. E. Use of Transgenic Mice to Study Lung Morphogenesis and Function. *ILAR Journal* **2006**, *47* (1), 22−31.
(642) Venosa, A.; Katzen, J.; Tomer, Y.; Kopp, M.; Jamil, S.; Russo, S. J.; Mulugeta, S.; Beers, M. F. Epithelial Expression of an Interstitial Lung Disease-Associated Mutation in Surfactant Protein-C Modulates Recruitment and Activation of Key Myeloid Cell Populations in Mice. *J. Immunol* **2019**, *202* (9), 2760−2771.
(643) Whitsett, J. A.; Wert, S. E.; Xu, Y. Genetic Disorders of Surfactant Homeostasis. *Biol. Neonate* **2005**, *87* (4), 283−287.
(644) Han, S.; Mallampalli, R. K. The Role of Surfactant in Lung Disease and Host Defense against Pulmonary Infections. *Annals of the American Thoracic Society* **2015**, *12* (5), 765−774.
(645) Casals, C.; García-Fojeda, B.; Minutti, C. M. Soluble Defense Collagens: Sweeping up Immune Threats. *Molecular Immunology* **2019**, *112*, 291−304.
(646) Depicolzuane, L.; Phelps, D. S.; Floros, J. Surfactant Protein-A Function: Knowledge Gained From SP-A Knockout Mice. *Front Pediatr* **2022**, *9*, No. 799693.
(647) Hsieh, I.-N.; De Luna, X.; White, M. R.; Hartshorn, K. L. The Role and Molecular Mechanism of Action of Surfactant Protein D in Innate Host Defense Against Influenza A Virus. *Front Immunol* **2018**, *9*, 1368.
(648) King, S. D.; Chen, S.-Y. Recent Progress on Surfactant Protein A: Cellular Function in Lung and Kidney Disease Development. *Am. J. Physiol Cell Physiol* **2020**, *319* (2), C316−C320.
(649) Qin, Y.; Liu, J.; Liu, J.; Hu, F. Collectins in Urinary Tract and Kidney Diseases. *Int. Urol Nephrol* **2018**, *50* (4), 695−703.
(650) Ujma, S.; Horsnell, W. G. C.; Katz, A. A.; Clark, H. W.; Schäfer, G. Non-Pulmonary Immune Functions of Surfactant Proteins A and D. *J. Innate Immun* **2017**, *9* (1), 3−11.
(651) Arroyo, R.; Grant, S. N.; Colombo, M.; Salvioni, L.; Corsi, F.; Truffi, M.; Ottolina, D.; Hurst, B.; Salzberg, M.; Prosperi, D.; Kingma, P. S. Full-Length Recombinant hSP-D Binds and Inhibits SARS-CoV-2. *Biomolecules* **2021**, *11* (8), 1114.
(652) Palaniyar, N.; Nadesalingam, J.; Clark, H.; Shih, M. J.; Dodds, A. W.; Reid, K. B. Nucleic Acid Is a Novel Ligand for Innate, Immune Pattern Recognition Collectins Surfactant Proteins A and D and Mannose-Binding Lectin. *J. Biol. Chem.* **2004**, *279* (31), 32728−32736.
(653) Jäkel, A.; Clark, H.; Reid, K. B. M.; Sim, R. B. The Human Lung Surfactant Proteins A (SP-A) and D (SP-D) Interact with Apoptotic Target Cells by Different Binding Mechanisms. *Immunobiology* **2010**, *215* (7), 551−558.
(654) Kuroki, Y.; Takahashi, M.; Nishitani, C. Pulmonary Collectins in Innate Immunity of the Lung. *Cell Microbiol* **2007**, *9* (8), 1871−1879.
(655) Ledford, J. G.; Pastva, A. M.; Wright, J. R. Review: Collectins Link Innate and Adaptive Immunity in Allergic Airway Disease. *Innate Immun* **2010**, *16* (3), 183−190.
(656) Nandy, D.; Sharma, N.; Senapati, S. Systematic Review and Meta-Analysis Confirms Significant Contribution of Surfactant Protein D in Chronic Obstructive Pulmonary Disease. *Front Genetics* **2019**, *10*, 339.
(657) Borron, P.; Veldhuizen, R. A.; Lewis, J. F.; Possmayer, F.; Caveney, A.; Inchley, K.; McFadden, R. G.; Fraher, L. J. Surfactant Associated Protein-A Inhibits Human Lymphocyte Proliferation and IL-2 Production. *Am. J. Respir. Cell Mol. Biol.* **1996**, *15* (1), 115−121.
(658) Borron, P.; McCormack, F. X.; Elhalwagi, B. M.; Chroneos, Z. C.; Lewis, J. F.; Zhu, S.; Wright, J. R.; Shepherd, V. L.; Possmayer, F.; Inchley, K.; et al. Surfactant Protein A Inhibits T Cell Proliferation Via Its Collagen-Like Tail and a 210-Kda Receptor. *Am. J. Physiol.* **1998**, *275* (4), L679−686.
(659) Floros, J.; Thorenoor, N.; Tsotakos, N.; Phelps, D. S. Human Surfactant Protein SP-A1 and SP-A2 Variants Differentially Affect the Alveolar Microenvironment, Surfactant Structure, Regulation and Function of the Alveolar Macrophage, and Animal and Human Survival Under Various Conditions. *Front Immunol* **2021**, *12*, No. 681639.
(660) Pandit, H.; Thakur, G.; Koippallil Gopalakrishnan, A. R.; Dodagatta-Marri, E.; Patil, A.; Kishore, U.; Madan, T. Surfactant Protein D Induces Immune Quiescence and Apoptosis of Mitogen-Activated Peripheral Blood Mononuclear Cells. *Immunobiology* **2016**, *221* (2), 310−322.
(661) Jakel, A.; Qaseem, A. S.; Kishore, U.; Sim, R. B. Ligands and Receptors of Lung Surfactant Proteins SP-A and SP-D. *Front Biosci (Landmark Ed)* **2013**, *18* (3), 1129−1140.
(662) Lopez-Rodriguez, E.; Boden, C.; Echaide, M.; Perez-Gil, J.; Kolb, M.; Gauldie, J.; Maus, U. A.; Ochs, M.; Knudsen, L. Surfactant Dysfunction During Overexpression of TGF-B1 Precedes Profibrotic Lung Remodeling in Vivo. *Am. J. Physiol Lung Cell Mol. Physiol* **2016**, *310* (11), L1260−1271.
(663) Phelps, D. S.; Chinchilli, V. M.; Yang, L.; Shearer, D.; Weisz, J.; Zhang, X.; Floros, J. The Alveolar Macrophage Toponome of Female SP-A Knockout Mice Differs from That of Males before and after SP-A1 Rescue. *Sci. Rep* **2022**, *12* (1), 5039.
(664) Sato, A.; Whitsett, J. A.; Scheule, R. K.; Ikegami, M. Surfactant Protein-D Inhibits Lung Inflammation Caused by Ventilation in Premature Newborn Lambs. *Am. J. Respir Crit Care Med.* **2010**, *181* (10), 1098−1105.
(665) Poulain, F. R.; Akiyama, J.; Allen, L.; Brown, C.; Chang, R.; Goerke, J.; Dobbs, L.; Hawgood, S. Ultrastructure of Phospholipid Mixtures Reconstituted with Surfactant Proteins B and D. *Am. J. Respir. Cell Mol. Biol.* **1999**, *20* (5), 1049−1058.
(666) Ikegami, M.; Na, C.-L.; Korfhagen, T. R.; Whitsett, J. A. Surfactant Protein D Influences Surfactant Ultrastructure and Uptake by Alveolar Type II Cells. *Am. J. Physiol Lung Cell Mol. Physiol* **2005**, *288* (3), L552−561.
(667) Thébaud, B.; Goss, K. N.; Laughon, M.; Whitsett, J. A.; Abman, S. H.; Steinhorn, R. H.; Aschner, J. L.; Davis, P. G.; McGrath-Morrow, S. A.; Soll, R. F.; Jobe, A. H. Bronchopulmonary Dysplasia. *Nature reviews. Disease primers* **2019**, *5* (1), 78.
(668) Salzberg, M. O. Clinical Safety Study on AT-100 in Treating Adults with Severe COVID-19 Infection or Severed Community Acquired Pneumonia. Clinicaltrials.Gov Identifier: Nct04659122. 2020.
(669) Ryan, M. A.; Akinbi, H. T.; Serrano, A. G.; Perez-Gil, J.; Wu, H.; McCormack, F. X.; Weaver, T. E. Antimicrobial Activity of Native and Synthetic Surfactant Protein B Peptides. *J. Immunol* **2006**, *176* (1), 416−425.
(670) Coya, J. M.; Akinbi, H. T.; Sáenz, A.; Yang, L.; Weaver, T. E.; Casals, C. Natural Anti-Infective Pulmonary Proteins: In Vivo Cooperative Action of Surfactant Protein SP-A and the Lung Antimicrobial Peptide SP-BN. *J. Immunol* **2015**, *195* (4), 1628−1636.
(671) Xu, Y.; Ge, L.; Abdel-Razek, O.; Jain, S.; Liu, Z.; Hong, Y.; Nieman, G.; Johnson, F.; Golub, L. M.; Cooney, R. N.; Wang, G. Differential Susceptibility of Human SP-B Genetic Variants on Lung Injury Caused by Bacterial Pneumonia and the Effect of a Chemically Modified Curcumin. *Shock* **2016**, *45* (4), 375−384.
(672) Yang, L.; Johansson, J.; Ridsdale, R.; Willander, H.; Fitzen, M.; Akinbi, H. T.; Weaver, T. E. Surfactant Protein B Propeptide Contains a Saposin-Like Protein Domain with Antimicrobial Activity at Low Ph. *J. Immunol* **2010**, *184* (2), 975−983.
(673) Yang, F.; Zhang, J.; Yang, Y.; Ruan, F.; Chen, X.; Guo, J.; Abdel-Razek, O.; Zuo, Y. Y.; Wang, G. Regulatory Roles of Human Surfactant Protein B Variants on Genetic Susceptibility to

https://doi.org/10.1021/acs.chemrev.3c00146
Chem. Rev. 2023, 123, 13209−13290

Pseudomonas Aeruginosa Pneumonia-Induced Sepsis. *Shock* **2020**, *54* (4), 507−519.
(674) Wang, G.; Christensen, N. D.; Wigdahl, B.; Guttentag, S. H.; Floros, J. Differences in N-Linked Glycosylation between Human Surfactant Protein-B Variants of the C or T Allele at the Single-Nucleotide Polymorphism at Position 1580: Implications for Disease. *Biochem. J.* **2003**, *369* (Pt 1), 179−184.
(675) Ge, L.; Liu, X.; Chen, R.; Xu, Y.; Zuo, Y. Y.; Cooney, R. N.; Wang, G. Differential Susceptibility of Transgenic Mice Expressing Human Surfactant Protein B Genetic Variants to Pseudomonas Aeruginosa Induced Pneumonia. *Biochem. Biophys. Res. Commun.* **2016**, *469* (2), 171−175.
(676) Dahmer, M. K.; O'cain, P.; Patwari, P. P.; Simpson, P.; Li, S.-H.; Halligan, N.; Quasney, M. W. The Influence of Genetic Variation in Surfactant Protein B on Severe Lung Injury in African American Children. *Crit Care Med.* **2011**, *39* (5), 1138−1144.
(677) Hamvas, A.; Heins, H. B.; Guttentag, S. H.; Wegner, D. J.; Trusgnich, M. A.; Bennet, K. W.; Yang, P.; Carlson, C. S.; An, P.; Cole, F. S. Developmental and Genetic Regulation of Human Surfactant Protein B in Vivo. *Neonatology* **2009**, *95* (2), 117−124.
(678) Lin, Z.; Pearson, C.; Chinchilli, V.; Pietschmann, S. M.; Luo, J.; Pison, U.; Floros, J. Polymorphisms of Human SP-A, SP-B, and SP-D Genes: Association of SP-B Thr131Ile with ARDS. *Clin Genet* **2000**, *58* (3), 181−191.
(679) Waring, A. J.; Jung, G. C.-L.; Sharma, S. K.; Walther, F. J. Lung Surfactant Protein B Peptide Mimics Interact with the Human ACE2 Receptor. *Int. J. Mol. Sci.* **2023**, *24* (13), 10837.
(680) Glasser, S. W.; Senft, A. P.; Maxfield, M. D.; Ruetschilling, T. L.; Baatz, J. E.; Page, K.; Korfhagen, T. R. Genetic Replacement of Surfactant Protein-C Reduces Respiratory Syncytial Virus Induced Lung Injury. *Respir Res.* **2013**, *14* (1), 19.
(681) Glasser, S. W.; Witt, T. L.; Senft, A. P.; Baatz, J. E.; Folger, D.; Maxfield, M. D.; Akinbi, H. T.; Newton, D. A.; Prows, D. R.; Korfhagen, T. R. Surfactant Protein C-Deficient Mice Are Susceptible to Respiratory Syncytial Virus Infection. *Am. J. Physiol Lung Cell Mol. Physiol* **2009**, *297* (1), L64−72.
(682) Glasser, S. W.; Senft, A. P.; Maxfield, M. D.; Ruetschilling, T. L.; Baatz, J. E.; Page, K.; Korfhagen, T. R. Genetic Replacement of Surfactant Protein-C Reduces Respiratory Syncytial Virus Induced Lung Injury. *Respiratory research* **2013**, *14* (1), 19.
(683) Hawkins, A.; Guttentag, S. H.; Deterding, R.; Funkhouser, W. K.; Goralski, J. L.; Chatterjee, S.; Mulugeta, S.; Beers, M. F. A Non-Brichos SFTPC Mutant (SP-C I73T) Linked to Interstitial Lung Disease Promotes a Late Block in Macroautophagy Disrupting Cellular Proteostasis and Mitophagy. *Am. J. Physiol Lung Cell Mol. Physiol* **2015**, *308* (1), L33−L47.
(684) Lin, Z.; Thorenoor, N.; Wu, R.; DiAngelo, S. L.; Ye, M.; Thomas, N. J.; Liao, X.; Lin, T. R.; Warren, S.; Floros, J. Genetic Association of Pulmonary Surfactant Protein Genes, SFTPA1, SFTPA2, SFTPB, SFTPC, and SFTPD With Cystic Fibrosis. *Front Immunol* **2018**, *9*, 2256.
(685) Nureki, S.-I.; Tomer, Y.; Venosa, A.; Russo, S.; Katzen, J.; Mulugeta, S.; Kadota, J.; Beers, M. Ontogeny of Osteopontin Expression in a Non-Brichos Mutant Surfactant Protein C Mouse Model of Idiopathic Pulmonary Fibrosis. *C72. Pulmonary Fibrosis: Mechanisms and Models*; American Thoracic Society, 2018; p A5758.
(686) Ruwisch, J.; Sehlmeyer, K.; Roldan, N.; Garcia-Alvarez, B.; Perez-Gil, J.; Weaver, T. E.; Ochs, M.; Knudsen, L.; Lopez-Rodriguez, E. Air Space Distension Precedes Spontaneous Fibrotic Remodeling and Impaired Cholesterol Metabolism in the Absence of Surfactant Protein C. *Am. J. Respir. Cell Mol. Biol.* **2020**, *62* (4), 466−478.
(687) Numata, M.; Voelker, D. R. Anti-Inflammatory and Anti-Viral Actions of Anionic Pulmonary Surfactant Phospholipids. *Biochim Biophys Acta Mol. Cell Biol. Lipids* **2022**, *1867* (6), No. 159139.
(688) Voelker, D. R.; Numata, M. Phospholipid Regulation of Innate Immunity and Respiratory Viral Infection. *J. Biol. Chem.* **2019**, *294* (12), 4282−4289.
(689) Numata, M.; Kandasamy, P.; Voelker, D. R. The Anti-Inflammatory and Antiviral Properties of Anionic Pulmonary Surfactant Phospholipids. *Immunol Rev.* **2023**, *317*, 166.
(690) Forbes, L. R.; Haczku, A. SP-D and Regulation of the Pulmonary Innate Immune System in Allergic Airway Changes. *Clin. Exp. Allergy* **2010**, *40* (4), 547−562.
(691) Enhorning, G. Surfactant in Airway Disease. *Chest* **2008**, *133* (4), 975−980.
(692) Qaseem, A. S.; Sonar, S.; Mahajan, L.; Madan, T.; Sorensen, G. L.; Shamji, M. H.; Kishore, U. Linking Surfactant Protein SP-D and Il-13: Implications in Asthma and Allergy. *Molecular immunology* **2013**, *54* (1), 98−107.
(693) Ledford, J. G.; Addison, K. J.; Foster, M. W.; Que, L. G. Eosinophil-Associated Lung Diseases. A Cry for Surfactant Proteins A and D Help? *Am. J. Respir. Cell Mol. Biol.* **2014**, *51* (5), 604−614.
(694) Principe, S.; Benfante, A.; Battaglia, S.; Maitland-van der Zee, A. H.; Scichilone, N. The Potential Role of SP-D as an Early Biomarker of Severity of Asthma. *Journal of Breath Research* **2021**, *15* (4), No. 041001.
(695) Enhorning, G.; Duffy, L. C.; Welliver, R. C. Pulmonary Surfactant Maintains Patency of Conducting Airways in the Rat. *Am. J. Respir Crit Care Med.* **1995**, *151* (2 Pt 1), 554−556.
(696) McCrae, K. C.; Weltman, B.; Alyward, S.; Shaw, R. A.; Sowa, M. G.; Unruh, H. W.; Rand, T. G.; Thliveris, J. A.; Scott, J. E. The Effect of Elevated Dietary Cholesterol on Pulmonary Surfactant Function in Adolescent Mice. *Pediatr Pulmonol* **2008**, *43* (5), 426−434.
(697) Macklin, C. C. Pulmonary Sumps, Dust Accumulations, Alveolar Fluid and Lymph Vessels. *Cells Tissues Organs* **2004**, *23* (1), 1−33.
(698) Mazur, W.; Toljamo, T.; Ohlmeier, S.; Vuopala, K.; Nieminen, P.; Kobayashi, H.; Kinnula, V. Elevation of Surfactant Protein A in Plasma and Sputum in Cigarette Smokers. *Eur. Respir. J.* **2011**, *38* (2), 277−284.
(699) Brankovic, M.; Akkerhuis, K. M.; Mouthaan, H.; Constantinescu, A.; Caliskan, K.; van Ramshorst, J.; Germans, T.; Umans, V.; Kardys, I. Utility of Temporal Profiles of New Cardio-Renal and Pulmonary Candidate Biomarkers in Chronic Heart Failure. *International Journal of cardiology* **2019**, *276*, 157−165.
(700) De Pasquale, C. G.; Arnolda, L. F.; Doyle, I. R.; Aylward, P. E.; Chew, D. P.; Bersten, A. D. Plasma Surfactant Protein-B: A Novel Biomarker in Chronic Heart Failure. *Circulation* **2004**, *110* (9), 1091−1096.
(701) Greene, K. E.; King, T. E.; Kuroki, Y.; Bucher-Bartelson, B.; Hunninghake, G. W.; Newman, L. S.; Nagae, H.; Mason, R. J. Serum Surfactant Proteins-A and -D as Biomarkers in Idiopathic Pulmonary Fibrosis. *Eur. Respir. J.* **2002**, *19* (3), 439−446.
(702) Imtiazul, I. M.; Asma, R.; Lee, J.-H.; Cho, N.-J.; Park, S.; Song, H.-Y.; Gil, H.-W. Change of Surfactant Protein D and a after Renal Ischemia Reperfusion Injury. *PloS one* **2019**, *14* (12), No. e0227097.
(703) Kinder, B. W.; Brown, K. K.; McCormack, F. X.; Ix, J. H.; Kervitsky, A.; Schwarz, M. I.; King, T. E., Jr Serum Surfactant Protein-A Is a Strong Predictor of Early Mortality in Idiopathic Pulmonary Fibrosis. *Chest* **2009**, *135* (6), 1557−1563.
(704) Magrì, D.; Brioschi, M.; Banfi, C.; Schmid, J. P.; Palermo, P.; Contini, M.; Apostolo, A.; Bussotti, M.; Tremoli, E.; Sciomer, S. Circulating Plasma Surfactant Protein Type B as Biological Marker of Alveolar-Capillary Barrier Damage in Chronic Heart Failure. *Circulation: Heart Failure* **2009**, *2* (3), 175−180.
(705) Yamaguchi, H.; Soda, H.; Nakamura, Y.; Takasu, M.; Tomonaga, N.; Nakano, H.; Doi, S.; Nakatomi, K.; Nagashima, S.; Takatani, H. Serum Levels of Surfactant Protein D Predict the Anti-Tumor Activity of Gefitinib in Patients with Advanced Non-Small Cell Lung Cancer. *Cancer Chemotherapy and Pharmacology* **2011**, *67*, 331−338.
(706) Yoshikawa, T.; Otsuka, M.; Chiba, H.; Ikeda, K.; Mori, Y.; Umeda, Y.; Nishikiori, H.; Kuronuma, K.; Takahashi, H. Surfactant Protein A as a Biomarker of Outcomes of Anti-Fibrotic Drug Therapy

https://doi.org/10.1021/acs.chemrev.3c00146
Chem. Rev. 2023, 123, 13209−13290

in Patients with Idiopathic Pulmonary Fibrosis. *BMC Pulmonary Medicine* **2020**, *20* (1), 27.
(707) Campodonico, J.; Mapelli, M.; Spadafora, E.; Ghilardi, S.; Agostoni, P.; Banfi, C.; Sciomer, S. Surfactant Proteins Changes after Acute Hemodynamic Improvement in Patients with Advanced Chronic Heart Failure Treated with Levosimendan. *Respir Physiol Neurobiol* **2018**, *252*−*253*, 47−51.
(708) Gargiulo, P.; Banfi, C.; Ghilardi, S.; Magrì, D.; Giovannardi, M.; Bonomi, A.; Salvioni, E.; Battaia, E.; Filardi, P. P.; Tremoli, E.; et al. Surfactant-Derived Proteins as Markers of Alveolar Membrane Damage in Heart Failure. *PloS one* **2014**, *9* (12), e115030.
(709) De Pasquale, C. G. Surfactant Protein-B in Chronic Heart Failure: An Insight to the Alveolocapillary Barrier. *Rev. Esp Cardiol* **2009**, *62* (2), 117−119.
(710) Magrì, D.; Banfi, C.; Maruotti, A.; Farina, S.; Vignati, C.; Salvioni, E.; Morosin, M.; Brioschi, M.; Ghilardi, S.; Tremoli, E.; Agostoni, P. Plasma Immature Form of Surfactant Protein Type B Correlates with Prognosis in Patients with Chronic Heart Failure. A Pilot Single-Center Prospective Study. *Int. J. Cardiol* **2015**, *201*, 394−399.
(711) Nugent, K.; Dobbe, L.; Rahman, R.; Elmassry, M.; Paz, P. Lung Morphology and Surfactant Function in Cardiogenic Pulmonary Edema: A Narrative Review. *J. Thorac Dis* **2019**, *11* (9), 4031−4038.
(712) Papp, Z.; Édes, I.; Fruhwald, S.; De Hert, S. G.; Salmenperä, M.; Leppikangas, H.; Mebazaa, A.; Landoni, G.; Grossini, E.; Caimmi, P. Levosimendan: Molecular Mechanisms and Clinical Implications: Consensus of Experts on the Mechanisms of Action of Levosimendan. *International Journal of Cardiology* **2012**, *159* (2), 82−87.
(713) McVey, M. J.; Maishan, M.; Blokland, K. E. C.; Bartlett, N.; Kuebler, W. M. Extracellular Vesicles in Lung Health, Disease, and Therapy. *Am. J. Physiol Lung Cell Mol. Physiol* **2019**, *316* (6), L977−L989.
(714) Rudiansyah, M.; Terefe, E. M.; Opulencia, M. J. C.; Abdelbasset, W. K.; Bokov, D. O.; El-Sehrawy, A. A.; Baymakov, S.; Hammid, A. T.; Shirvaliloo, M.; Akhavan-Sigari, R. Type 2 Alveolar Epithelial Cell-Derived Circulating Extracellular Vesicle-Encapsulated Surfactant Protein C as a Mediator of Cardiac Inflammation in COVID-19. *Inflamm Res.* **2022**, *71* (9), 1003−1009.
(715) Chen, S.; Kuhn, M.; Prettner, K.; Yu, F.; Yang, T.; Bärnighausen, T.; Bloom, D. E.; Wang, C. The Global Economic Burden of Chronic Obstructive Pulmonary Disease for 204 Countries and Territories in 2020−50: A Health-Augmented Macroeconomic Modelling Study. *Lancet Glob Health* **2023**, *11* (8), e1183−e1193.
(716) Lin, C.-H.; Cheng, S.-L.; Chen, C.-Z.; Chen, C.-H.; Lin, S.-H.; Wang, H.-C. Current Progress of COPD Early Detection: Key Points and Novel Strategies. *Int. J. Chron Obstruct Pulmon Dis* **2023**, *18*, 1511−1524.
(717) Tesfaigzi, Y.; Curtis, J. L.; Petrache, I.; Polverino, F.; Kheradmand, F.; Adcock, I. M.; Rennard, S. I. Does COPD Originate from Different Cell Types? *Am. J. Respir. Cell Mol. Biol.* **2023**, DOI: 10.1165/rcmb.2023-0175PS.
(718) Lin, X.; Wu, Z.; Fan, Y.; Chi, M.; Wang, X.; Zhang, X.; Sun, D. Correlation Analysis of Surfactant Protein A and Surfactant Protein D with Lung Function in Exhaled Breath Condensate from Lung Cancer Patients with and without COPD. *Molecular Medicine Reports* **2017**, *16* (4), 4948−4954.
(719) Ohlmeier, S.; Vuolanto, M.; Toljamo, T.; Vuopala, K.; Salmenkivi, K.; Myllärniemi, M.; Kinnula, V. L. Proteomics of Human Lung Tissue Identifies Surfactant Protein A as a Marker of Chronic Obstructive Pulmonary Disease. *J. Proteome Res.* **2008**, *7* (12), 5125−5132.
(720) Ozyurek, B. A.; Ulasli, S. S.; Bozbas, S. S.; Bayraktar, N.; Akcay, S. Value of Serum and Induced Sputum Surfactant Protein-D in Chronic Obstructive Pulmonary Disease. *Multidiscip Respir Med.* **2013**, *8* (1), 36.
(721) Winkler, C.; Atochina-Vasserman, E. N.; Holz, O.; Beers, M. F.; Erpenbeck, V. J.; Krug, N.; Roepcke, S.; Lauer, G.; Elmlinger, M.; Hohlfeld, J. M. Comprehensive Characterisation of Pulmonary and Serum Surfactant Protein D in COPD. *Respir. Res.* **2011**, *12* (1), 29.
(722) Anzueto, A.; Barjaktarevic, I. Z.; Siler, T. M.; Rheault, T.; Bengtsson, T.; Rickard, K.; Sciurba, F. Ensifentrine, a Novel Phosphodiesterase 3 and 4 Inhibitor for the Treatment of Chronic Obstructive Pulmonary Disease: Randomized, Double-Blind, Placebo-Controlled, Multicenter Phase III Trials (the ENHANCE Trials). *Am. J. Respir Crit Care Med.* **2023**, *208* (4), 406−416.
(723) Condon, J.; Jeyasuria, P.; Faust, J.; Mendelson, C. R. Surfactant protein secreted by the maturing mouse fetal lung acts as a hormone that signals the initiation of parturition. *Proc. Natl. Acad. Sci. U. S. A.* **2004**, *101*, 4978−4983.
(724) Montalbano, A. P.; Hawgood, S.; Mendelson, C. R. Mice Deficient in Surfactant Protein A (SP-A) and SP-D or in TLR2Manifest Delayed Parturition and Decreased Expression of Inflammatory and Contractile Genes. *Endocrinology* **2013**, *154* (1), 483−498.
(725) Hildebran, J. N.; Goerke, J.; Clements, J. A. Pulmonary Surface Film Stability and Composition. *J. Appl. Physiol.* **1979**, *47* (3), 604−611.
(726) Melton, K. R.; Nesslein, L. L.; Ikegami, M.; Tichelaar, J. W.; Clark, J. C.; Whitsett, J. A.; Weaver, T. E. SP-B Deficiency Causes Respiratory Failure in Adult Mice. *Am. J. Physiol Lung Cell Mol. Physiol* **2003**, *285* (3), L543−549.
(727) Rose, D.; Rendell, J.; Lee, D.; Nag, K.; Booth, V. Molecular Dynamics Simulations of Lung Surfactant Lipid Monolayers. *Biophys. Chem.* **2008**, *138* (3), 67−77.
(728) Olmeda, B.; Villen, L.; Cruz, A.; Orellana, G.; Perez-Gil, J. Pulmonary Surfactant Layers Accelerate O(2) Diffusion through the Air-Water Interface. *Biochim. Biophys. Acta* **2010**, *1798* (6), 1281−1284.
(729) Hass, M. A.; Longmore, W. J. Surfactant Cholesterol Metabolism of the Isolated Perfused Rat Lung. *Biochim. Biophys. Acta* **1979**, *573* (1), 166−174.
(730) Davidson, K. G.; Acton, S. M.; Barr, H. A.; Nicholas, T. E. Effect of Lowering Serum Cholesterol on the Composition of Surfactant in Adult Rat Lung. *Am. J. Physiol.* **1997**, *272* (1 Pt 1), L106−114.
(731) Orgeig, S.; Barr, H. A.; Nicholas, T. E. Effect of Hyperpnea on the Cholesterol to Disaturated Phospholipid Ratio in Alveolar Surfactant of Rats. *Exp Lung Res.* **1995**, *21* (1), 157−174.
(732) Chintagari, N. R.; Jin, N.; Wang, P.; Narasaraju, T. A.; Chen, J.; Liu, L. Effect of Cholesterol Depletion on Exocytosis of Alveolar Type II Cells. *Am. J. Respir. Cell Mol. Biol.* **2006**, *34* (6), 677−687.
(733) Gowdy, K. M.; Fessler, M. B. Emerging Roles for Cholesterol and Lipoproteins in Lung Disease. *Pulm Pharmacol Ther* **2013**, *26* (4), 430−437.
(734) Avital, A.; Hevroni, A.; Godfrey, S.; Cohen, S.; Maayan, C.; Nusair, S.; Nogee, L. M.; Springer, C. Natural History of Five Children with Surfactant Protein C Mutations and Interstitial Lung Disease. *Pediatric pulmonology* **2014**, *49* (11), 1097−1105.
(735) Saenz, A.; Presto, J.; Lara, P.; Akinyi-Oloo, L.; Garcia-Fojeda, B.; Nilsson, I.; Johansson, J.; Casals, C. Folding and Intramembraneous Brichos Binding of the Prosurfactant Protein C Transmembrane Segment. *J. Biol. Chem.* **2015**, *290* (28), 17628−17641.
(736) Venosa, A.; Katzen, J.; Tomer, Y.; Kopp, M.; Jamil, S.; Russo, S. J.; Mulugeta, S.; Beers, M. F. Epithelial Expression of an Interstitial Lung Disease-Associated Mutation in Surfactant Protein-C Modulates Recruitment and Activation of Key Myeloid Cell Populations in Mice. *J. Immunol* **2019**, *202* (9), 2760−2771.
(737) Katzen, J.; Wagner, B. D.; Venosa, A.; Kopp, M.; Tomer, Y.; Russo, S. J.; Headen, A. C.; Basil, M. C.; Stark, J. M.; Mulugeta, S.; et al. An SFTPC Brichos Mutant Links Epithelial ER Stress and Spontaneous Lung Fibrosis. *JCI Insight* **2019**, *4* (6), No. e126125.
(738) Sitaraman, S.; Martin, E. P.; Na, C.-L.; Zhao, S.; Green, J.; Deshmukh, H.; Perl, A.-K. T.; Bridges, J. P.; Xu, Y.; Weaver, T. E. Surfactant Protein C Mutation Links Postnatal Type 2 Cell Dysfunction to Adult Disease. *JCI Insight* **2021**, *6* (14), DOI: 10.1172/jci.insight.142501.

(739) Sweet, D. G.; Turner, M. A.; Straňák, Z.; Plavka, R.; Clarke, P.; Stenson, B. J.; Singer, D.; Goelz, R.; Fabbri, L.; Varoli, G.; Piccinno, A.; Santoro, D.; Speer, C. P. A First-in-Human Clinical Study of a New SP-B and SP-C Enriched Synthetic Surfactant (CHF5633) in Preterm Babies with Respiratory Distress Syndrome. *Archives of Disease in Childhood - Fetal and Neonatal Edition* **2017**, *102* (6), F497−F503.
(740) Jeon, G. W. Surfactant Preparations for Preterm Infants with Respiratory Distress Syndrome: Past, Present, and Future. *Korean Journal of Pediatrics* **2019**, *62* (5), 155−161.
(741) Madsen, J.; Panchal, M. H.; Mackay, R. A.; Echaide, M.; Koster, G.; Aquino, G.; Pelizzi, N.; Perez-Gil, J.; Salomone, F.; Clark, H. W.; et al. Metabolism of a Synthetic Compared with a Natural Therapeutic Pulmonary Surfactant in Adult Mice. *J. Lipid Res.* **2018**, *59* (10), 1880−1892.
(742) Notter, R. H.; Gupta, R.; Schwan, A. L.; Wang, Z.; Shkoor, M. G.; Walther, F. J. Synthetic Lung Surfactants Containing SP-B and SP-C Peptides plus Novel Phospholipase-Resistant Lipids or Glycerophospholipids. *PeerJ.* **2016**, *4*, No. e2635.
(743) Walther, F. J.; Gordon, L. M.; Waring, A. J. Advances in Synthetic Lung Surfactant Protein Technology. *Expert Rev. Respir Med.* **2019**, *13* (6), 499−501.
(744) Baer, B.; Souza, L. M. P.; Pimentel, A. S.; Veldhuizen, R. A. W. New Insights into Exogenous Surfactant as a Carrier of Pulmonary Therapeutics. *Biochemical pharmacology* **2019**, *164*, 64−73.
(745) Guagliardo, R.; Pérez-Gil, J.; De Smedt, S.; Raemdonck, K. Pulmonary Surfactant and Drug Delivery: Focusing on the Role of Surfactant Proteins. *J. Controlled Release* **2018**, *291*, 116−126.

https://doi.org/10.1021/acs.chemrev.3c00146
Chem. Rev. 2023, 123, 13209−13290